Universidad Autónoma de Madrid
Faculty of Medicine
Department of Biochemistry

Characterization of genomic patterns that predict long-term metabolic side effects of antipsychotic treatments

Doctoral Thesis

Mónica Ruíz Rosario

Madrid, 2022

This Doctoral Thesis was funded by the Horizon 2020 Marie Sklodowska-Curie Innovative Training Network Program of the European Union (ITN-TREATMENT, consortium agreement 721236).

"Nada te turbe, nada te espante"

Santa Teresa de Ávila

DEDICATORIA

A mis papás **Alicia Rosario** y **Alfonso Ruiz** que siempre han caminado conmigo. Gracias por enseñarme lo que significa el amor. Gracias porque sin importar lo pequeño, grande o loco de cada uno de mis sueños, ustedes los han tomado como propios y me han enseñado a siempre seguir adelante.

A mis hermanos **Juan Carlos** y **Julio César** por darle alegría a mi vida. Por su apoyo y amor incondicionales.

A mi novio **Alfonso Rojas** por comprenderme, amarme y acompañarme.

A **mis amigos**, por estar presentes, apoyarme y compartir conmigo los buenos y malos momentos.

AGRADECIMIENTOS

Agradezco al **Dr. Juan Cruz Cigudosa**, por permitirme ser parte de este proyecto. Por confiar en mí y dedicar tiempo para compartir conmigo conocimientos y experiencias. Por el apoyo recibido durante la realización de esta investigación y por los acertados aportes a la corrección de este manuscrito.

A **NIMGenetics** y su equipo por permitirme realizar esta investigación dentro de la empresa y proporcionarme los recursos necesarios. Especialmente a la **Dra. Beatriz Maroto**, que llevó a cabo las gestiones necesarias para ser partícipes de la financiación otorgada por el proyecto europeo TREATMENT, al **Dr. Javier Botet** y el **Dr. Antonio Gomez** por su aportación al diseño del proyecto y solución de problemas durante la realización del mismo, a **Gemma Benito** y **Patricia Sánchez** por su contribución en la puesta a punto y desarrollo de protocolos de laboratorio, a **David Rubio** por la aportación de ideas y ayuda en el contraste de las mismas.

A los miembros del consorcio **TREATMENT**. Especialmente a la **Dra. Dora Kolle**r y el **Dr. Francisco Abad** por la aportación de muestras de sangre de voluntarios sanos, a la **Dra. Ángela Valderde**, la **Dra. María Monsalve**, la **Dra. Diana Grajales**, **Vítor Ferreira**, **Ramazán Yildiz** y **Gaurangkumar Patel** por la aportación de muestras de islotes pancreáticos e hígado de ratón.

ABSTRACT

Aripiprazole and olanzapine are atypical antipsychotics used mainly for schizophrenia treatment. Being schizophrenia a chronic disorder, it requires lifelong medication that subsequently triggers metabolic Adverse Drug Reactions (ADRs). Therefore, the project's main objective was to contribute to evaluating short- and long-term antipsychotic drug responses and their impact on the development of metabolic diseases.

An open, controlled, randomized, crossover clinical trial in healthy volunteers was carried out to evaluate the short-term effect (5 days) of olanzapine and aripiprazole. Blood samples were collected before and after each treatment, making 48 samples. Mice models were treated with short (5-days) and long-term (6 months) aripiprazole and olanzapine schemes. Liver and pancreatic islets were isolated. Total RNA was extracted from the blood and tissue samples and processed with Illumina TruSeq Stranded RNASeq technology. Differential expression analyses were performed, and differentially expressed genes were queried against KEGG and Gene Ontology databases to perform Gene Set Enrichment Analyses. A machine learning approach was used to train a model to classify the volunteers' samples according to their response to the treatments and, therefore, to predict the appearance of metabolic side effects. Feature selection strategies such as F-score and Random Forest were used to select the most relevant features for the classification of the samples.

The analysis of the different models allowed us to propose that olanzapine-induced metabolic disarrangements may be explained by PEPCK signalling repression from low-grade inflammation that may occur due to TLR4 signalling activation. Although aripiprazole may induce inflammatory signalling, it seems to activate compensation mechanisms such as promoting fatty acid synthesis to avoid metabolic disarrangements.

Differential response of the human volunteers to the treatments was identified, which may be at least partially attributed to polymorphisms in *PPARGC1*, which prevented the volunteers from activating aripiprazole's compensatory phenotypes. Stratification of the volunteers according to their response was possible, which may allow the development of a predictive pharmacogenomic test for the patients' response shortly after the beginning of the treatment, a step forward to personalized medicine.

RESUMEN

Aripiprazol y olanzapina son antipsicóticos atípicos que se utilizan principalmente para el tratamiento de la esquizofrenia. La esquizofrenia un trastorno crónico que requiere medicación a lo largo de toda la vida, lo que desencadena la aparición de reacciones metabólicas adversas. Debido a esto, el objetivo del presente proyecto es evaluar los efectos a corto y largo plazo de los fármacos antipsicóticos, así como su impacto en el desarrollo de enfermedades metabólicas.

Se llevó a cabo un ensayo clínico abierto, controlado, aleatorizado y cruzado en voluntarios sanos para evaluar el efecto a corto plazo (5 días) de olanzapina y aripiprazol. Se recolectaron muestras de sangre antes y después de cada tratamiento (48 en total). Se trataron modelos murinos con esquemas de aripiprazol y olanzapina a corto (5 días) y largo plazo (6 meses). Se aislaron muestras de islotes pancreáticos e hígado. Se extrajo ARN total de las muestras de sangre y tejido y se procesaron con la tecnología Illumina TruSeq Stranded RNASeq. Se realizaron análisis de expresión diferencial y los genes diferencialmente expresados se sometieron a análisis de enriquecimiento de grupos de genes. Se entrenó un modelo para clasificar las muestras de los voluntarios según su respuesta a los tratamientos para predecir la aparición de efectos secundarios metabólicos. Se utilizaron estrategias de selección de características como F-score y Random Forest para seleccionar las características más relevantes para la clasificación de las muestras.

El análisis en voluntarios sanos nos permitió proponer que los trastornos metabólicos inducidos por olanzapina podrían estar ligados a la represión de la señalización de PEPCK debida a un estado de inflamación de bajo grado producido por la activación de la señalización de TLR4. Aripiprazol, sin embargo, podría activar mecanismos de compensación contra el estado inflamatorio producido por el tratamiento, disminuyendo así los efectos metabólicos negativos del mismo.

Se identificó una respuesta diferencial de los voluntarios a los tratamientos, atribuible parcialmente a polimorfismos en *PPARGC1* que podrían bloquear los fenotipos compensatorios de aripiprazol. La estratificación de los voluntarios según su respuesta supone un paso adelante hacia la medicina personalizada ya que permitiría desarrollar un test predictivo individualizado de la respuesta de los pacientes poco después del inicio del tratamiento.

INDEX

INDEX OF TABLES AND FIGURES

ABBREVIATIONS

abn: Abnormalities

Actc1: Actin, alpha, cardiac muscle 1

ADRs: Adverse Drug Reactions

AMPK1: AMP-activated protein kinase

AN: Arcuate nucleus

ANS: Autonomous nervous system

ARVC: Arrhythmogenic right ventricular cardiomyopathy

ATP: Adenosine-triphosphate

Atp1a3: ATPase, Na+/K+ transporting, alpha 3 polypeptide

Atp1a4: ATPase, Na+/K+ transporting, alpha 4 polypeptide

BAT: Brown adipose tissue

BCL: Base Call

BMI: Body Mass Index

CAC: Citric acid cycle

Cacna1h: Calcium channel, voltage-dependent, T type, alpha 1H subunit

Cacng7: Calcium channel, voltage-dependent, gamma subunit 7

CAT: Catalase

cDNA: complementary DNA

Cfd: Complement factor D

CNS: Central nervous system

COX: Cyclooxygenase

Cox6a2: Cytochrome c oxidase subunit 6A2

CSN: Central Nervous System

CXCL5: C-X-C motif chemokine 5

CYP1A1: CYP450 isoform 1A1

Dagla: Diacylglycerol lipase, alpha

DAT: Dopamine transporter

DCM: Dilated cardiomyopathy

DCs: Dendritic cells

DEGs: Differentially Expressed Genes

DRD2: Dopamine Receptor D2

ds-cDNA: Double-stranded cDNA

EPS: Extrapyramidal symptoms

ETC: Electron Transport Chain

FABP: Fatty acid-binding protein

FAO: Fatty acid oxidation

FDR: False Discovery Rate

FFA: free fatty acid

FGAs: First-generation antipsychotics

FOXO1: Forkhead Box O1

FPKM: Fragments per kilobase of exon per million reads mapped

FPKMs: Fragments per kilobase of transcript per million fragments mapped

Fst: Follistatin

G3P: Glyceraldehyde 3-phosphate

GABA: Gamma-aminobutyric acid

$GABA_A$: Gamma-aminobutyric acid type A

Got1: Glutamic-oxaloacetic transaminase 1

GPx: Glutathione peroxidase

GSH-Px: Glutathione peroxidase

H2-Oa: Histocompatibility 2, O region alpha locus

HDL: High-Density Lipoprotein

HGO: Glucose production/output

IFN-γ: Interferon- γ

IGF-1: Insulin-like growth factor 1

IL: Interleukin

iNOS: Inducible nitric oxide synthase

INSIG: Insulin-induced gene

IR: Insulin receptor

IRS: Insulin receptor substrate

IRS: Insulin receptor substrate

Irs4: Insulin receptor substrate 4

LC n-3: Long-chain omega-3

LDL: Low-density lipoprotein

LDs: Lipid droplets

LPS: Lipopolysaccharide

MCP-1: Monocyte chemotactic protein-1

MDD: Major depressive disorder

MetS: Metabolic syndrome

MODY: maturity-onset diabetes of the young

MQs: Macrophages

mtDNA: Mitochondrial DNA

Myl2: Myosin, light polypeptide 2

NAFLD: Nonalcoholic fatty liver disease

NES: Normalized Enrichment Score

NMDAR: N-methyl-D-aspartate-glutamatergic receptor

NO: Nitric oxide

NPY: neuropeptide Y

Nr4a1: Nuclear receptor subfamily 4, group A, member 1

OAA: Oxaloacetate

Opa-1: Optic atrophy protein-1

Pabpc1l: Poly(A) binding protein, cytoplasmic 1-like

PBMC: Peripheral Blood Mononuclear Cells

PCA: Principal Component Analysis

Pdgfra: Alpha polypeptide gene

PDK1: 3-phosphoinositide-dependent protein kinase-1

PEP: Phosphoenolpyruvate

PGE2: Prostaglandin E2

PI3K: Phosphatidylinositol 3-kinase

PIP3: phosphatidylinositol (3,4,5)-triphosphate

PLA2G2F: Phospholipase A2 Group IIF

PLIN: Perilipin

Pnlip: Pancreatic lipase

POMC: Pro-opiomelanocortin neurons

PPARG: peroxisome proliferator-activated receptor gamma

PPARGC1: peroxisome proliferator-activated receptor gamma co-activator 1

PPARs: Peroxisome proliferator-activated receptors

Ptgs2: Prostaglandin-endoperoxide synthase 2

ROS: Oxygen species

SCAP: cleavage activating protein

SCFAs: Short-chain fatty acids

sd3b5: Hydroxy-delta-5-steroid dehydrogenase, 3 beta- and steroid delta-isomerase 5

SGAs: Second-generation antipsychotics

sIL-2R: Soluble interleukin-2 receptors

SOD: Superoxide dismutase

SOD: Superoxide dismutase

SREBPs: Sterol regulatory element-binding proteins

sTNFR: Soluble TNF receptor

T0: Time zero

T2DM: Type 2 diabetes mellitus

TGF: Transforming growth factor

TNF- α: Tumour necrosis factor-alpha

VST: Variance Stabilizing Transformation

VTA: Ventral tegmental area

WAT: White adipose tissue

α-MSH: α-melanocyte-stimulating hormone

1. INTRODUCTION

Schizophrenia is a severe mental disorder with a worldwide prevalence of approximately 1% (Lin et al. 2016) and a median lifetime prevalence of 4,0 per 1000 individuals (Belbasis et al. 2018). It is a complex, heterogeneous behavioural and cognitive syndrome (Owen, M. J., Sawa, A., Mortensen 2016) characterized by groups of symptoms such as hallucinations, delusions and cognitive impairments (Lin et al. 2016). Most cases start during adolescence and early adulthood (Lin et al. 2016). Furthermore, 50% of the diagnosed individuals have intermittent but long-term psychiatric problems and about 20% present chronic symptoms and disability (Owen, M. J., Sawa, A., Mortensen 2016). Schizophrenia ranked among the world's top 10 causes of disability-adjusted life years (DALYs) (Ringen et al. 2014), and its diagnosis also associates with premature mortality. Schizophrenia patients show a higher suicide risk, comorbid health disorders prevalence (Piotrowski et al. 2017), and 15-20 years shorter average life expectancy than the general population (Ringen et al. 2014). Due to schizophrenia affecting working-age people, it has become a highly significant concern for public health and society's economic development and welfare.

Over 2 million of Adverse Drug Reactions (ADRs) occur annually with an impact on society of €79 billion and 197,000 deaths, as informed by the European Commission Scientific Project Officer at the 2012 EnCePP Meeting. Being among them schizophrenia a chronic and disabling disorder, that requires long-life medication which, in addition to representing a high cost to the health service, triggers ADRs, like metabolic diseases. Within this context, it is important to notice that, although the death rate in the early stages of this disorder is predominantly due to suicide, later in life, it becomes principally due to cardio-metabolic disturbances (Belbasis et al. 2018).

Therefore, metabolic syndrome (MetS) is a leading cause of morbidity and mortality in schizophrenia patients, with a double prevalence rate than nonpsychiatric populations (Riordan, Antonini, and Murphy 2011). The metabolic syndrome is conceived as a set of metabolic irregularities that may include central obesity, insulin resistance, hypertension, hypertriglyceridemia, hypercholesterolemia, and reduced high-density lipoprotein (HDL) and cholesterol concentrations (Wang et al. 2020). It has been shown to 5-fold increase the risk of developing type 2 diabetes and double the risk for cardiovascular disease (Wang et al. 2020). Insulin resistance and abdominal obesity are associated with the development of metabolic syndrome (Kahn, R., Buse, J., Ferrannini, E., & Stern 2005). The increased prevalence of metabolic disorders in schizophrenia is partly attributed to the antipsychotic treatments (Smith et al. 2008), as they may influence the food intake and glucose and lipid metabolisms

(Reynolds and Kirk 2010). Obesity and other metabolic consequences for patients taking antipsychotic medication increase their risk of developing diabetes (Reynolds and Kirk 2010). Besides, diabetes is usually a long-term consequence; it has also been reported that rapid, non-weight related glucose intolerance and diabetes development can occur on antipsychotic receiving patients (Reynolds and Kirk 2010).

Nowadays, most drugs are prescribed with narrow and inflexible criteria. Since treatment responses can differ among patients, the lack of individualized doses, or a more individualized treatment scheme, promotes the treatment's inefficacy and appearance of ADRs. Differences in the treatment reaction have a multifactorial aetiology and are hard to predict, which hampers the improvement and safety of psychotic disorders treatment.

1.1. Schizophrenia

Schizophrenia has been principally pointed to as a mesolimbic dopamine signal dysfunction, in which the increased capacity of dopamine synthesis and release may lead to psychosis (Yang and Tsai 2017). However, four dopaminergic pathways have been associated with several schizophrenia symptoms (Patel et al. 2014) (Lavretsky 2008):

- Excessive dopamine levels in the **mesolimbic pathway** (from the ventral tegmental area (VTA) to limbic areas) may contribute to schizophrenia positive symptoms.
- Low dopamine levels in the **mesocortical pathway** (from the VTA to the cortex) may lead to negative symptoms and cognitive deficits.
- Low dopamine levels in the **nigrostriatal pathway** (from the substantia nigra to the caudate nucleus) are thought to alter the extrapyramidal system, causing motor complications.
- Decline or blockade of dopamine in the **tuberoinfundibular pathway** (from the hypothalamus to the pituitary gland) results in elevated prolactin levels and consequent galactorrhea, amenorrhea, and reduced libido

Still, evidence has shown that schizophrenic behavioural, social, and cognitive dysfunctions may also involve serotonergic, glutamatergic and gamma-aminobutyric acid (GABA) signalling disparagements (Yang and Tsai 2017).

1.2. Antipsychotic treatments

Current antipsychotics achieve therapeutic effects by acting on D2 like receptors (D2, D3 and D4) (Pan et al. 2016). In 1952, the first antipsychotic, chlorpromazine, was released. Later on, other antipsychotics as haloperidol and fluphenazine, known now as first-generation antipsychotics (FGAs) or typical antipsychotics, were also introduced. Although FGAs showed to be helpful for the treatment of positive symptoms as disturbances, delusions and hallucinations; they showed limited efficacy against negative symptoms like social withdrawal, lack of empathy and self-care (Reynolds and Kirk 2010); and produced extrapyramidal symptoms (EPS), like akathisia, tardive dyskinesia, dystonia and parkinsonism among other side effects (Divac et al. 2014). It has been observed that typical antipsychotics achieve their antipsychotic effect at 60-80% of D2 receptor occupancy, while 75-80% occupancy leads to acute EPS, making it very difficult to avoid the positive and negative occupancy overlap (Divac et al. 2014).

Approximately one-third of the schizophrenic patients are treatment-resistant (Gillespie et al. 2017), being clozapine the only evidence-based antipsychotic drug that displays effectiveness in treatment-refractory schizophrenia (Kane 2011). Although clozapine causes agranulocytosis, a severe side effect, its efficacy and lack of EPS motivated the development of second-generation antipsychotics (SGAs) or atypical antipsychotics, such as olanzapine, risperidone, quetiapine, and more recently ziprasidone and aripiprazole; which are similar to clozapine but with a safer profile (Divac et al. 2014). Atypical antipsychotics bind to multiple receptors (D2, serotonin 5-HT2A, 5-HT2C, muscarinic) (Pan et al. 2016). Their therapeutic effect is attributed to some degree of D2 receptor blockage, but mainly to the antagonism of serotonin receptors, particularly 5-HT2A (Divac et al. 2014). Animal models have suggested that atypical antipsychotics fast binding and dissociating from D2 receptors may be a possible explanation for producing fewer EPS (Kapur and Seeman 2001).

Despite their advantages, SGAs produce endocrine and cardiometabolic side effects, making part of the metabolic syndrome (Riordan et al. 2011). Epidemiological data reveal that the incidence of metabolic disturbances after treatment with SGAs is 20 to 60% (Yang et al. 2019). The relationship between antipsychotic treatment and metabolic syndrome is complicated. It may involve the interaction of adrenergic and muscarinic receptors, dopamine, histamine, orexigenic neuropeptides and failed glucose homeostasis, among other risk factors (Ijaz et al. 2018). SGAs have been shown to increase the fat deposition, macrophage infiltration, expression of cytokines in the hypothalamus and white adipose tissue (WAT), in addition to the induction of brown adipose tissue (BAT) atrophy (Yang et al. 2019). Therefore, the peripheral and central actions account for the weight gain and metabolic disturbances caused

by SGAs (Yang et al. 2019). While some SGAs as ziprasidone, risperidone and aripiprazole are associated with a lower risk of dyslipidemia, some others as quetiapine, olanzapine and clozapine are related to higher risk (Papanastasiou 2013). A summary table of the receptor-binding profile and associated metabolic risks for different antipsychotics is shown in Table 1.

Table 1. Receptor-binding profile and metabolic risk of antipsychotic drugs

	RECEPTOR BINDING PROFILE																				RISK		
	D_1	D_2	D_3	D_4	H_1	H_2	H_3	5-HT_{1A}	5-HT_{1B}	5-HT_{2A}	5-HT_{2B}	5-HT_{2C}	5-HT_6	5-HT_7	M_1	M_3	α_1	α_{2A}	α_{2B}	α_{2C}	Transporter	Weight Gain	Glucose Abn	Lipid Abn
Olanzapine	++	++	++	++	+++	++	+		+	+++	++	++	+++	++	++	++	++	+	++	++		++++	++	++
Zotepine	++	+++	+++	+	+++	+		+	++	+++		+++	+++	++	+	+	+++	+	+++	++	SERT, NET	+++/++++	(LD)	(LD)
Clozapine	+	+	+	++	+++	+		+	+	++	+++	++	++	++	+++	++	+++	++	++	++		+++/++++	++	++
Chlorpromazine	++	+++	+++	+++	+++	+	+			+++	+++	++	+++	+++	++	++	+++	+	++	++		+++/++++	+/++	+/++
Sertindole		+++	+++	+++	+			+	++	++++		+++		++			+++	+	+	+		+++/++++	+/++	+/++
Iloperidone	+	+++	+++	++	+			++	++	+++		++	+	+			+++	+	+	++		+++/++++	+/++	+/++
Risperidone	+	+++	+++	+++	+++	+		+	++	++++	++	++		+++			+++	++	++	+++		+++	+/++	+/++
(Nor)quetiapine	+	+	+		+++			++		++		+	+	++	+	+	++	+	+	++	NET	+++	+/++	++
Paliperidone	+	+++	+++	+++	++	+		+	++	+++		++	+	+++			+++	+++	+++	+++		+++	+/++	+/++
Asenapine	+++	+++	++++	+++	+++	+++		+++	+++	++++	++++	++++	++++	++++			+++	+++	++++	+++		++	+	+
Amisulpride		+++	+++	+++							++			++								++	+	++(LD)
Aripiprazole		+++	+++	+	++			+++	+	++	++++	++	+	++			++	++	++	++	SERT	++	+	+
Brexpiprazole	+	++++	+++	+++	++			++++	++	++++	+++	+	++	+++			+++	++	++	++++	SERT, NET	+(LD)	+(LD)	+(LD)
Cariprazine		++++	++++		++			+++		++	++++	+		+			+					+(LD)	+(LD)	+(LD)
Haloperidol	+	+++	+++	+++		+			+	+				+			++	+	+	+		+	+	+
Lurasidone	+	+++						+++		+++		+		++++			++	++		+++		+	+	+
Ziprasidone	+	+++	+++	++	++			+++	+++	++++	++	++++	++	+++			++	+	++	++	SERT, NET	+	+	+

A. Receptor-binding profile. Antagonism and inverse agonism are indicated by blue colour, whereas partial agonism by yellow. The number of crosses and colour intensity is correlated to binding affinity. B. Metabolic risk. The number of crosses correlates to the risk of weight gain (maximum ++++), glucose and lipid abnormalities (maximum ++). (LD): Limited Data, abn: abnormalities. **Source: (Siafis et al. 2017)**

1.2.1. **Olanzapine**

Olanzapine (2-methyl-4-(4-methyl-1-piperazinyl)-10H-thieno[2,3-b][1,5]benzodiazepine) was introduced in 1996 (Xu and Zhuang 2019). It is a thienobenzodiazepine, structurally similar to clozapine (Figure 1) that is metabolized in the liver by glucuronidation and cytochrome P450 (CYP) oxidation into 10-N-glucuronide and 4'-N-desmethylolanzapine (Alvarez-Herrera et al. 2020). Together with clozapine, they have shown the most significant impact on body weight gain, glucose abnormality, insulin resistance, and hyperlipidemias (Yang et al. 2019). They have also demonstrated the highest relative affinities for the 5-HT2C and histamine H1 receptors, which seem to contribute to satiety control (Reynolds and Kirk 2010). Being obesity an increased risk for the development of diabetes, a meta-analysis with a sample size greater than 270,000 subjects confirmed that the intake of olanzapine and clozapine are associated with a higher risk of developing diabetes (Holt and Peveler 2011). Remarkably, these antipsychotics are also associated with the rapid, non-weight related diabetes onset (JW. 2005), which may be regulated by the peripheral M3 muscarinic receptor antagonism and the central 5-HT2C effects (Reynolds and Kirk 2010).

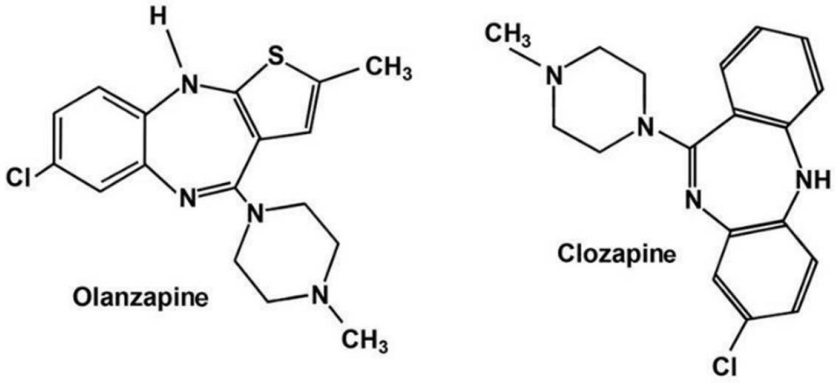

Figure 1. Chemical structures of olanzapine and clozapine
The figure shows the chemical structures of olanzapine and clozapine. Modified from: (Alvarez-Herrera et al. 2020)

1.2.2. **Aripiprazole**

Aripiprazole was introduced in 2002 (Xu and Zhuang 2019). It is a derivative of quinolinone (Figure 2), metabolized in the liver by CYP (CYP2D6 and CYP3A4) through dehydrogenation, hydroxylation, and N-dealkylationIt into dehydro-aripiprazole, an active metabolite (Alvarez-Herrera et al. 2020). It is distinguished from earlier antipsychotics by its partial agonist activity at D2, D3, 5-HT1A, and 5-HT2C receptor targets, which translates to the successful reduction of positive, negative, and cognitive symptoms of schizophrenia while also lowering the risk of weight gain and movement side effects (Lingala and Ghany 2016). Aripiprazole characterizes by its adaptative pharmacological response as a partial agonist, a moderate antagonist or a full antagonist depending on dopamine D2 receptors and the endogenous dopamine signalling and levels (De Bartolomeis, Tomasetti, and Iasevoli 2015). Clinical trial data and real-world data-based analyses support the claim of aripiprazole's favourable safety and tolerability profile and corroborate its metabolic advantages compared to other SGAs as it has a small tendency to cause weight gain, hypercholesterolemia, hyperprolactinemia, cardiovascular abnormalities, or glucose dysregulation (DeLeon, Patel, and Crismon 2004) (Brixner et al. 2006). A study with 31 schizophrenia or schizoaffective disorder patients who were either newly started on aripiprazole (n= 2) or switched from other antipsychotics to aripiprazole (n= 29) showed that after 3 months of aripiprazole treatment, body weight, body mass index, and waist circumference decreased. Moreover, fasting glucose, fasting insulin, insulin resistance index, serum lipids levels (cholesterol, triglycerides, low-density lipoprotein (LDL), LDL/HDL, Chol/HDL, and non-HDL cholesterol), and prolactin levels significantly declined as well. From 7 cases of recent-onset diabetes, the 7 were reverted; and MetS was reverted in 50% of patients (De Hert et al. 2007)

Figure 2. Chemical structure of aripiprazole
The figure shows the chemical structure of aripiprazole. Modified from: (Alvarez-Herrera et al. 2020)

1.3. Mechanisms involved in the induction of metabolic disturbances by SGAs

The Central Nervous System (CSN), Autonomous Nervous System (ANS) and peripheral organs where antipsychotics' receptors are expressed, have neuroendocrine connections that can be altered by antipsychotic action leading to metabolic dysfunctions (Siafis et al. 2017) (Figure 3). A summary of the central and peripheral effects of antipsychotics' pharmacological action is shown in Table 2.

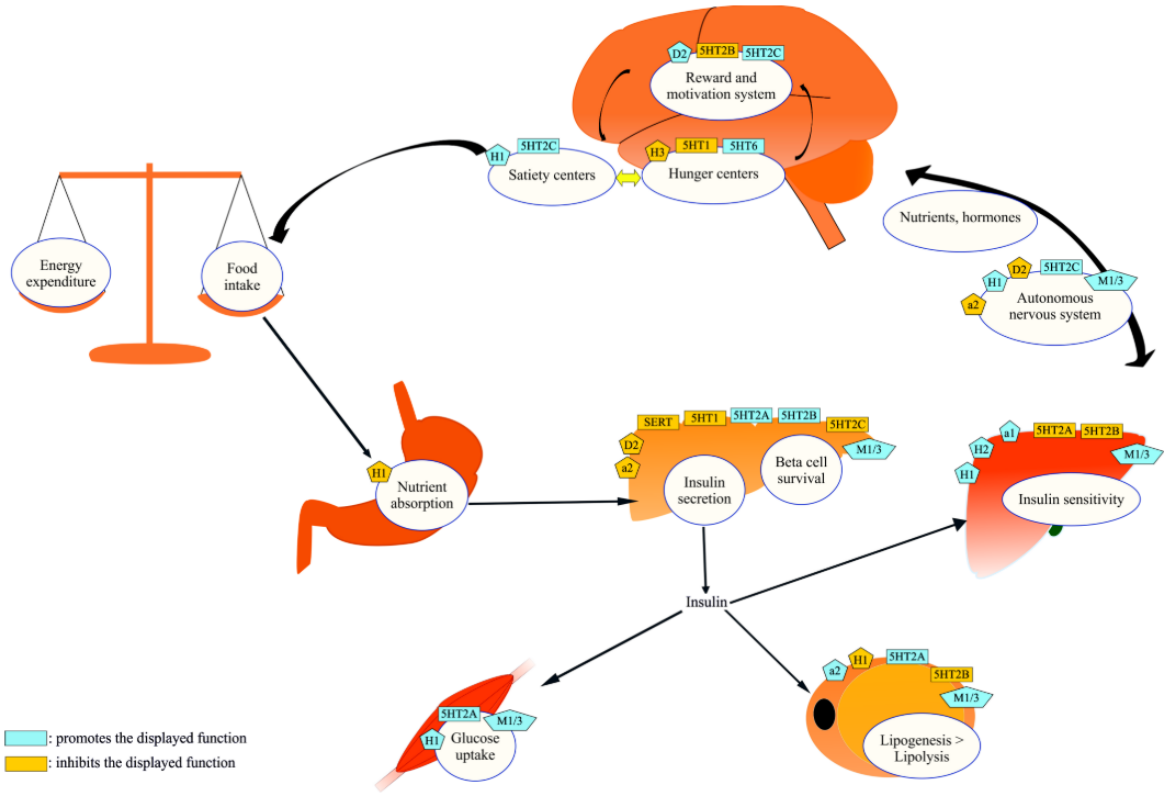

Figure 3. Antipsychotics' receptors and antipsychotic-induced metabolic dysfunctions
CNS, ANS and peripheral organs have antipsychotic-induced receptors, which action can disrupt their neuroendocrine connections. **Source: (Siafis et al. 2017)**

Table 2. Central and peripheral effects of antipsychotics' pharmacological activity

	Central effects	Peripheral effects
$D_{2/3}$ antagonism	↑ Food intake	↑ Insulin secretion
	↑ Hypothalamic AMPK	↑ Proliferation and survival of beta cells
	↑ EPS	Deplete insulin stores (chronic)
	↑Catecholamine release	
	↑ Prolactin	
5-HT_1 partial agonism	↓ Food intake	↓ Insulin secretion
	↓ EPS	↓ Glucose uptake (adipose tissue)
	↓ Prolactin	
5-HT_{2A} antagonism	↓ Food intake	↓ Insulin secretion
	↓ EPS	↑ Hepatic insulin sensitivity
	↓ Prolactin	↓ Glucose uptake (skeletal muscle)
		↓Adipose tissue lipogenesis
5-HT_{2C} antagonism	↑ Food intake	↑ Insulin secretion (?)
	ANS disruption	
H_1 antagonism	↑ Food intake	↓ Hepatic insulin sensitivity
	↑ hypothalamic AMPK	↓ Glucose uptake (adipose tissue, skeletal muscle)
	↑ Sedation	↑ Adipose tissue lipogenesis
	ANS disruption	↑ Fructose absorption
		↑ Atherosclerosis
M_3 antagonism	↑ Food intake	↓ Insulin secretion
	↓ EPS	↓ Adipose tissue lipogenesis
	ANS disruption	↓ Glucose uptake (skeletal muscle)
alpha$_1$ antagonism	↑ Food intake	↓ Hepatic insulin sensitivity
	↑ hypothalamic AMPK	↓ Peripheral vascular resistance
	↑ Sedation	↓ Glucose uptake (adipose tissue, skeletal muscle)
	ANS disruption	
alpha$_2$ antagonism	↓ Food intake	↑ Insulin secretion
		↓Adipose tissue lipogenesis
	↑ Catecholamine release	

Source: (Siafis et al. 2017)

1.3.1. **Weight gain**

SGAs are believed to induce an imbalance of calories intake and energy expenditure (Xu and Zhuang 2019). One proposed mechanism is the induction of hyperphagia through moderate antagonism of serotonin, histamine, or dopamine receptors (Coccurello and Moles 2010):

- Because serotonin (5-HT) promotes satiety, 5-HT2C receptor antagonism prevents it or delays it, increasing meal size. This process is thought to happen through the inhibition of pro-opiomelanocortin neurons (POMC) in the arcuate nucleus (AN) of the hypothalamus (Balt et al. 2011), which reduces αmelanocyte-stimulating hormone (α-MSH) activity. α-MSH is an endogenous agonist of melanocortin 4 receptors (MC4Rs), which results in less food intake. Conversely, MC4R haploinsufficiency constitutes the most common monogenic cause of severe obesity in humans, comprising 5% of the cases (Cone 2005). The inhibition of POMC neurons also leads to disinhibition of the AN neurons' neuropeptide Y (NPY), a potent appetite enhancer. (Balt et al. 2011).
- H1 blockage stimulates AMP-activated protein kinase (AMPK1) activity, which reverses the action of leptin (Kim et al. 2010), a hormone secreted by adipocytes that positively correlate with fat mass and has an anorexigenic action (Coccurello and Moles 2010). Other hormones as adiponectin, secreted by adipose tissue and ghrelin, secreted by the stomach, have opposite effects as leptin promoting food intake (Xu and Zhuang 2019). Olanzapine has been associated with the decrease of adiponectin (Bartoli, Crocamo, et al. 2015). Lower adiponectin levels have been correlated with insulin resistance and increased inflammation in schizophrenic patients treated with SGAS (Sapra et al. 2016). Olanzapine has been observed to boost ghrelin-receptor signalling in cells (Tagami et al. 2016), and when administered chronically, to inhibit the post-prandial ghrelin reduction in rats (Hegedus et al. 2015).
- The dopaminergic system modulates the brain reward circuit (Blum, Thanos, and Gold 2014) through its projections from the ventral tegmental area into the NAc. Other implicated projections are the dorsal striatum, cortical and limbic regions and the lateral hypothalamus (Volkow, Wang, and Baler 2011). The involvement of dopamine in food reward has been associated with its increase in the striatum, linked to the desire to eat food (Volkow et al. 2002). While increased brain dopamine concentration has an anorexigenic effect, drugs that block dopamine D2 receptors lead to increased appetite and weight gain (Chen et al. 2008). Several DRD2 (Dopamine Receptor D2) polymorphisms have been related to drug and nicotine addiction and food disorders. A study in healthy volunteers showed that the availability of the striatal DRD2 was reduced in very obese people (Wang et al. 2001). The dopamine transporter (DAT)

plays a critical role in dopamine neurotransmission by transporting dopamine into the nerve terminal. There is evidence that insulin regulates DAT activity (Owens et al. 2005), therefore modulating the dopaminergic reward pathways (Owens et al. 2005). A study in rats showed that DAT mRNA and activity and dopamine uptake decreased in rats made hypoinsulinemic through fasting (Patterson et al. 1998). Moreover, a significant co-morbidity of drug abuse and eating disorders have been observed (Grigson 2002).

A second mechanism involves the development of adiposity without an increase in the food intake amount. A possible mechanism involves a sedative effect from the antipsychotics, leading to decreased energy expenditure. The antipsychotics, however, may as well have a direct impact on adipocytes promoting lipogenesis (Xu and Zhuang 2019).

1.3.2. **Dyslipidemia**

There is evidence that weight gain and obesity harm serum lipid profiles; consequently, antipsychotics that cause substantial weight gain correlate with a significant effect on serum lipids (Meyer and Koro 2004). Body fat increase is associated with a higher lipolysis rate, promoting free fatty acids (FFAs) mobilization and oxidation in muscle and liver. As FFAs are used as an alternative energy source, the muscles' glucose consumption declines. In contrast, hepatic glucose production rises due to elevated FFA oxidation, resulting in hyperglycemia and disrupted glucose tolerance (Pi-Sunyer 2002).

One mechanism by which antipsychotics disrupt the lipid metabolism is through dysregulation of sterol regulatory element-binding proteins (SREBPs): SREBP-1 and SREBP-2 (Xu and Zhuang 2019). While SREBP-1 is a major regulator of fatty acid synthesis and a molecular connection between lipid metabolism, insulin activity and obesity, SREBP-2 is a key regulator of cholesterol metabolism (Kotzka and Müller-Wieland 2004). Studies in cultured human glial and liver cells demonstrated that their exposure to different antipsychotics activated SREBP transcription factors, leading to upregulation of downstream cholesterol and fatty acid biosynthesis (Raeder et al. 2006) (Fernø et al. 2006). SREBPs are synthesized in the endoplasmic reticulum, where they make a complex with the cleavage activating protein (SCAP) and the insulin-induced gene (INSIG) proteins (INSIG1 and INSIG2) (Le Hellard et al. 2009). Low levels of sterol trigger SREBPs cleavage and its consequent translocation to the nucleus (Rawson 2003), where they bind to several SREBP target genes, thus stimulating lipogenic gene expression (Le Hellard et al. 2009). A study in rats liver (Cai et al. 2015) revealed that clozapine or risperidone enhanced lipogenesis and cholesterogenesis by down-

regulation of PGRMC1/INSIG-2 and up-regulation of SCAP/SREBP expressions. However, the effect was not replicated by the treatment with aripiprazole or haloperidol. Furthermore, the treatment with mifepristone (MIF), a steroid antagonist, reverted the lipid disruptions by up-regulating PGRMC1/INSIG-2 and down-regulating SCAP/SREBP expressions. The authors suggest that lipid metabolism disturbances may occur in an early stage of the treatment with antipsychotics, even before the weight gain. However, they could be reversed by administering a steroid antagonist that may enhance the PGRMC1 pathway.

A second possible mechanism is a deficiency in long-chain omega-3 (LC n-3) fatty acids. Low levels of n-3 fatty acids have been correlated with higher liver triglycerides and their secretion (Xu and Zhuang 2019). Mice with n-3 PUFA depletion showed hypercholesterolemia (total, HDL, and LDL cholesterol) and increased hepatic cholesteryl ester and triglycerides content (Pachikian et al. 2008). However, when the authors analyzed the liver gene expression of key enzymes and nuclear factors involved in lipid metabolism, the results suggested decreased lipogenic enzyme activity (SREBP-1c, FAS, PPARγ) and a higher hepatic β-oxidation capacity (CPT1, PPARα and PGC1α), with no changes in fatty acid esterification (DGAT2, GPAT1), intracellular transport (L-FABP) or secretion (MTTP). Therefore, although steatosis was confirmed in n-3 low mice compared to controls, it occurred independently of lipogenesis and β-oxidation mechanisms. The exact mechanism by which low n-3 enhance triglycerides levels remains unclear. However, clinical studies have shown significantly lower LC n-3 fatty acid content in the liver and erythrocytes of obese and nonalcoholic fatty liver disease (NAFLD) patients (Burrows, Collins, and Garg 2011) (Sertoglu, Kayadibi, and Uyanik 2015). Similar results have been observed in schizophrenic patients receiving atypical antipsychotics compared to healthy controls (Evans et al. 2003). Moreover, supplementing LC n-3 fatty acid through diet has been observed to reduce the elevation of triglycerides in antipsychotic-treated patients (Caniato, Alvarenga, and Garcia-Alcaraz 2006). In conjunction, this data suggests that low n-3 may represent a risk factor for enhanced triglycerides production by antipsychotic treatments, which, however, could be modified through the diet (Xu and Zhuang 2019).

1.3.3. **Inflammation**

Adipose tissue is not just involved in energy expenditure but also in endocrine functions as it produces: pro-inflammatory cytokines such as the tumour necrosis factor-alpha (TNF-α) and interleukin (IL)-6 and IL-1β; chemokines such as the monocyte chemotactic protein-1 (MCP-1) and the C-X-C motif chemokine 5 (CXCL5); and hormones such as leptin and adiponectin (Gonçalves, Araújo, and Martel 2015). In adipose tissue from obese mice and humans with

insulin resistance, these molecules, especially inflammatory cytokines such as TNF-α and IL6, have been found over-expressed, implying a link between obesity, inflammation, and insulin resistance (Hotamisligil and Spiegelman 1994) (Bulló et al. 2003).

There is evidence that atypical antipsychotic treatments alter the peripheral levels of pro-inflammatory, anti-inflammatory and growth factor molecules like IL-1β, IL-6, IL-12, IL-10, TNF-α, interferon (IFN)-γ, C-reactive protein (CRP), among others. Additionally, SGAs modify macrophages (MQs), dendritic cells (DCs), lymphocytes (T and B), neutrophils, and other leukocytes' cell count, function, phagocytosis, Th1-Th2 differentiation, apoptosis and cytokine production and release (Alvarez-Herrera et al. 2020).

The treatment with olanzapine has been associated with decreased numbers of leukocytes and eosinophils and down-regulation of receptors D1, D2, 5-HT2A, and transforming growth factor (TGF)-β mRNA expression in PBMC (Alvarez-Herrera et al. 2020). In a study with schizophrenia, schizophreniform disorder, and schizoaffective disorder patients, pro-inflammatory cytokines: TNF-α, soluble TNF receptor (sTNFR)-2 and soluble interleukin-2 receptors (sIL-2R); and leptin significantly increased since the first week of treatment with olanzapine, but not sTNFR-1 and IL-6 (Kluge et al. 2009). A chronic treatment (46 days) study in rats (Victoriano et al. 2010) produced low-grade inflammation. Low-grade inflammation has been defined as a term for conditions with a 2- to 3-fold increase in systemic concentrations of TNF-α, IL-1, IL-6, IL-1Ra, sTNF-R, and CRP observed (Petersen and Pedersen 2005). In Victoriano et al. 2010 study, low-grade inflammation was characterized by significant infiltration of CD68+ cells (macrophages) in the adipose tissue and a 2-fold increase in TNF-α gene expression. Highly activated macrophages lead the secretion of cytokines (like TNF-α and IL−1β) out of the adipose tissue triggering a decline of insulin sensitivity in insulin target cells (Sobiš et al. 2015). Olanzapine seems to activate TNF-α primarily, while low-grade inflammation during obesity increases the levels of other cytokines such as IL-6, MCP-1, and PAI-1, suggesting that inflammation produced by chronic olanzapine treatment differ from inflammation produced during obesity (Victoriano et al. 2010).

On the other hand, aripiprazole has been associated with an anti-inflammatory profile (Alvarez-Herrera et al. 2020). The treatment with aripiprazole has been observed to decrease the neutrophil count (Felin, Naveed, and Chaudhary 2018) (Lim, Park, and Park 2013) and to alter cytokine secretion by significantly reducing the serum levels of pro-inflammatory cytokines IL−1β, IL-6, TNF-α, IL-12, IL-23 and IFN-γ, and the anti-inflammatory cytokines IL-4 and TGF-β1 (Sobiš et al. 2015). Nevertheless, the levels of the anti-inflammatory cytokine IL-10 significantly raised. IL-10 impedes the secretion of pro-inflammatory mediators from monocytes, macrophages and DCs, hence inhibiting the IFN-γ induced secretion of TNF-α, IL-

1b, IL- 6, IL-8, and IL-12 (Sobiš et al. 2015). IL-10 also inhibits the production of Th1 associated cytokines: IL-2 and IFN-γ; and Th2-associated cytokines: IL-4 and IL-5 (Mosser and Zhang 2008). Moreover, higher levels of IL-10 correlate with insulin sensitivity by counter-regulation of IL-6/TNF-α induced insulin resistance through upregulation of tyrosine kinase activity of the insulin receptor and decreasing lipolysis; therefore, conferring protection against type 2 diabetes and metabolic syndrome (Van Exel et al. 2002).

The anti-inflammatory effect of aripiprazole could be linked to the suppression of inflammatory genes such as cyclooxygenase (COX)-2 and inducible nitric oxide synthase (iNOS), leading to reduced levels of nitric oxide (NO), prostaglandin E2 (PGE2) and TNF-α (Yoo, Kim, and Cho 2018). Aripiprazole may also decrease NO levels in serum through an anti-oxidant activity that regulates reactive oxygen species (ROS) and, therefore, inflammation cytokines, probably by increasing the activity of glutathione peroxidase (GSH-Px) and superoxide dismutase (SOD). Both enzymes have been shown to decrease the concentration of NO in supernatants and TNF-α, IL-1α, IL-2, and IL-10 levels in mice serum (Alvarez-Herrera et al. 2020).

1.3.4. **Mitochondria impairments and Oxidative Stress**

Antipsychotics alter mitochondrial homeostasis, leading to impaired fusion/fission ratios (del Campo et al. 2018). Mitochondria fusion and fission (joining and splitting) may work as an exchange mechanism of content such as proteins, lipids, and mitochondrial DNA (mtDNA) to maintain functional integrity (Koopman et al. 2010). When the fusion/fission ratios become altered, it may lead to an inefficient mitochondrial phenotype, possibly related to the antipsychotics' metabolic side effects (del Campo et al. 2018).

Optic atrophy protein-1 (OPA-1) is a mitochondrial protein involved in mitochondrial membrane fusion and maintenance of the cristae protecting the cells from apoptosis (Caffin et al. 2013), which is stimulated by insulin through the Akt-mTOR-NFkB-Opa-1 signalling pathway, leading to mitochondrial fusion (Parra et al. 2014). It has been observed that olanzapine disrupts insulin signalling by reducing Akt phosphorylation, subsequently modifying the mitochondrial dynamics, which contributes to mitochondrial dysfunction (del Campo et al. 2018). OMA-1 is a mitochondrial zinc metalloprotease that plays a non-redundant role in the processing of OPA-1, causing its functional inactivation under stress conditions. *Oma-1* deficient mice under stress conditions such as a high-fat diet, with consequent functional Opa-1 and a fusion induced state; developed obesity, loss of glucose metabolism improvement, and decreased β-oxidation that led to increased expression of genes of the lipogenic pathway that manifested as significant hepatic steatosis (Quirós et al. 2012).

In a study with lymphoblastoid cell lines (LCLs) from schizophrenic patients (Scaini et al. 2018), reduced mRNA expression of *Mfn-2* and *Drp-1* was observed after treatment with high doses of clozapine and olanzapine. Drp-1 down-regulation promotes mitochondrial fusion, which supports an increase in ROS, leading to damage of respiratory function and mitochondrial transport (Scaini et al. 2018); and a loss of mtDNA, which associates with reduction of cellular ATP, inhibition of cell proliferation and autophagy (Parone et al. 2008). On the other hand, Mfn2 downregulation promotes mitochondrial fission, which associates with reduced mitochondrial membrane potential, glucose oxidation, cell respiration and the expression of oxidative phosphorylation subunits (Bach et al. 2003). The inhibition of enzymes of the respiratory chain complex and blockage of electron transport by clozapine and olanzapine may partially explain the impairment of the oxidative system by these compounds (Scaini et al. 2018).

Overall, this information suggests that distorted mitochondrial fusion/fission dynamics by antipsychotics may contribute to the antipsychotics metabolic side effects.

Mitochondria are virtually present in every human cell. Although they are known for being the primary producers of cellular energy, mitochondria are also involved in other cellular processes such as heat production, breakdown of fatty acids, biosynthesis of heme, ureum, pyrimidines, amino acids, phospholipids and nucleotides, apoptosis signalling, ROS generation, redox homeostasis and calcium signalling (Blanchet et al. 2012). Cell energy is mainly produced by oxidative phosphorylation. Mitochondrial adenosine-triphosphate (ATP) is originated as electrons flow across electron transport chain (ETC) complexes (I to IV). The energy produced in the form of protons re-enters the mitochondrial matrix through ATP synthase (complex V), delivering ATP (Gubert et al. 2013). Altered ETC may reduce NADH oxidation and electrons transfer to ubiquinone, which may expose electrons to molecular oxygen, produce ROS and cause oxidative stress (Gubert et al. 2013).

Cellular membrane pathology due to oxidative stress has been considered in the study of schizophrenia pathophysiology, which is thought to be exacerbated by antipsychotic treatments (Ranjekar et al. 2003). Oxidative stress arises when free radicals overpass the cellular antioxidant capacity causing cell injury (Mahadik and Mukherjee 1996). The body has two antioxidant defences: a) antioxidant enzymes such as superoxide dismutase (SOD), catalase (CAT) and glutathione peroxidase (GPx) and b) dietary supplements such as antioxidant vitamins (A, C, E, Q), b-carotene, quinones, flavones, lycopenes, and uric acid (Ranjekar et al. 2003). In schizophrenic patients, antioxidant enzymes constitutively expressed in all tissues are distorted in erythrocytes (Mahadik and Mukherjee 1996). Reduced membrane polyunsaturated fatty acids (PUFAs) (i.e., reduced incorporation into phospholipids with

increased breakdown) in the brain and plasma membranes of erythrocytes and increased lipid peroxidation products in cerebrospinal fluid and plasma may mediate free radicals CNS injury (Mahadik and Mukherjee 1996) (Khan et al. 2002). The brain is especially vulnerable to damage by free radicals, as its membranes are preferentially enriched in PUFAs, and damaged adult neurons do not recover (Mahadik and Mukherjee 1996). In a study with never medicated, first episode of psychosis schizophrenic patients (Khan et al. 2002), increased lipid peroxides and reduced erythrocyte membrane's PUFAs were observed, supporting that antioxidant imbalance leads to membrane injury. Furthermore, the lipid peroxides and PUFAs levels were significantly lower and higher, respectively, in patients treated with atypical antipsychotics, although not with typical ones, encouraging atypical antipsychotics' contribution to oxidative cellular injury.

1.3.5. **Glucose intolerance and insulin resistance**

The liver response to pancreatic hormones, insulin and glucagon, is central for the whole body glucometabolic control. Insulin regulates blood glucose levels by supporting glucose uptake from the blood into tissues and repressing hepatic glucose production (Saltiel and Kahn 2001). The canonical insulin-signalling pathway initiates by insulin binding and activating the transmembrane insulin receptor (IR) tyrosine kinase, which leads to phosphorylation of intracellular insulin receptor substrate (IRS) 1 and IRS2. Once activated, IRS proteins stimulate phosphatidylinositol 3-kinase (PI3K) and p85 to generate phosphatidylinositol (3,4,5)-triphosphate (PIP3) through the phosphorylation of PIP2. PIP3 increment recruits 3-phosphoinositide-dependent protein kinase-1 (PDK1) and Akt to the plasma membrane where Akt is activated by PDK1-mediated phosphorylation (Copps and White 2012). Akt promotes glucose uptake and glycolysis and inhibits Forkhead Box O1 (FOXO1) and PPAR-γ coactivator-1α (PGC-1α), which is indispensable for gluconeogenesis repression (Collier and Scott 2004).

Peripheral glucose regulation abnormalities and type 2 diabetes are common complications of schizophrenic patients, even before introducing antipsychotic treatments. However, atypical antipsychotic treatment has been associated with impaired glucose metabolism, exacerbation of active type 1 and 2 diabetes, new-onset type 2 diabetes mellitus (T2DM), and diabetic ketoacidosis (Haupt and Newcomer 2001). Type 1 diabetes has been referred to in the past as insulin-dependent or juvenile-onset diabetes. It is characterized by a primary β-cell defect that causes insulin secretion failure and is not generally associated with schizophrenia (Haupt and Newcomer 2001). Type 2 diabetes, also known as insulin-dependent or adult-onset

diabetes, is associated with insulin resistance and a progressive β-cell dysfunction which leads to a relative insulin deficiency (Gavin et al. 2002).

Recent studies suggest that antipsychotics damage glucose regulation by reducing insulin action, producing higher fasting glucose levels and glucose intolerance. Elevated glucose levels could be explained by reduced insulin-mediated glucose uptake or increased hepatic glucose production/output (HGO) (Xu and Zhuang 2019). A study performed in healthy rats (Houseknecht et al. 2007) provided the first in vivo evidence that antipsychotics cause severe acute insulin resistance after a single treatment dose. In the study, constant insulin and somatostatin were infused to produce constant hyperinsulinemia and avoid pancreatic insulin secretion. Glucose was infused at an adjustable-rate to maintain euglycemia. Olanzapine and clozapine were administered, and acute impairment of insulin sensitivity was observed in a dose-dependent manner. Additionally, clozapine produced profound insulin resistance after 5 days of treatment (10 mg/kg/day). Hepatic glucose production increased, while no effect was noted on the glucose uptake. Treatment with risperidone and ziprasidone had no effect. A study in mice treated with atypical antipsychotics: clozapine, desmethylclozapine, quetiapine, and loxapine, and the typical antipsychotic, chlorpromazine, showed a correlation between their ability to inhibit glucose transport and cause hyperglycemia. On the other hand, haloperidol and sulpiride, which have a negligible effect on glucose uptake, did not induce hyperglycemia (Dwyer and Donohoe 2003).

1.4. Transcriptomic studies

A transcriptome refers to the complete set of transcripts in a cell, taking into account their quantity at a specific physiological condition or developmental stage (Wang, Gerstein, and Snyder 2009). As gene expression is a significant determinant of cellular phenotype, biomedical research has exploded genome-wide expression analysis through high-throughput sequencing technology, such as RNA-seq, to obtain insights into the molecular events triggering human biology and disease (Melé et al. 2015). RNA-seq has advantages over its predecessor technology, cDNA microarrays; such as (a) higher reproducibility through lanes and flow-cells, reducing the number of needed technical replicates; (b) identification of isoforms and unknown transcripts, and quantification of their expression; and (c) a dropping cost of the technology as it becomes more popular (Costa-Silva, Domingues, and Lopes 2017).

RNA-seq is useful to perform differential expression analyses between specific conditions (Zhang et al. 2014). In general, RNA samples are fragmented, and complementary DNA (cDNA) is synthesized and sequenced. The generated sequences are mapped to a genome

or transcriptome reference, and the expression levels for each gene or isoform are estimated. Differentially expressed genes (DEGs) are identified through statistical methods and queried against biological databases to identify altered processes (Costa-Silva et al. 2017).

Personalized medicine requires effective non-invasive methods to defeat the difficulties of obtaining target tissue samples (Mohr and Liew 2007). Blood cells express organ-specific genes, such as pancreas' insulin genes and heart's β-myosin heavy chain (Mohr and Liew 2007). Along this line, Liew et al. showed that about 80% of the expression of nine different human tissues was shared with the peripheral blood transcriptome (Liew et al. 2006), making the identification of blood biomarkers a promising alternative for the assessment of individual's health (Mohr and Liew 2007).

2. OBJECTIVES

2.1. General objective

The current project aims to contribute to the evaluation of short- and long-term antipsychotic drug responses and their impact on the development of metabolic diseases. The project focuses on a translational integrative genomic analysis on mice and healthy human volunteers' samples using bioinformatics strategies. We expect that fast changes in metabolic cues, detectable in blood samples after 5 days of drug administration, can identify patients at high risk of developing chronic metabolic diseases.

2.2. Specific objectives

1. Evaluate the peripheral blood transcriptomic changes on healthy volunteers after a 5 days treatment with aripiprazole and olanzapine.
2. Evaluate the transcriptome of pancreatic islets from WT mice treated with aripiprazole and olanzapine compared to the transcriptome of pancreatic islets from untreated mice.
3. Evaluate the short- and long-term liver genetic response to the treatment with aripiprazole and olanzapine on WT, PTP1B KO and PGC-1α KO mice.
4. Compare the transcriptional changes produced among the different models studied.
5. Stratify the volunteers according to their transcriptomic response to the treatment with aripiprazole and olanzapine.
6. Explore by bioinformatics approaches the origin of this transcriptomic stratification and provide insights on its biological and/or pharmacogenomic nature.

3. METHODS

3.1. Experimental design – summary

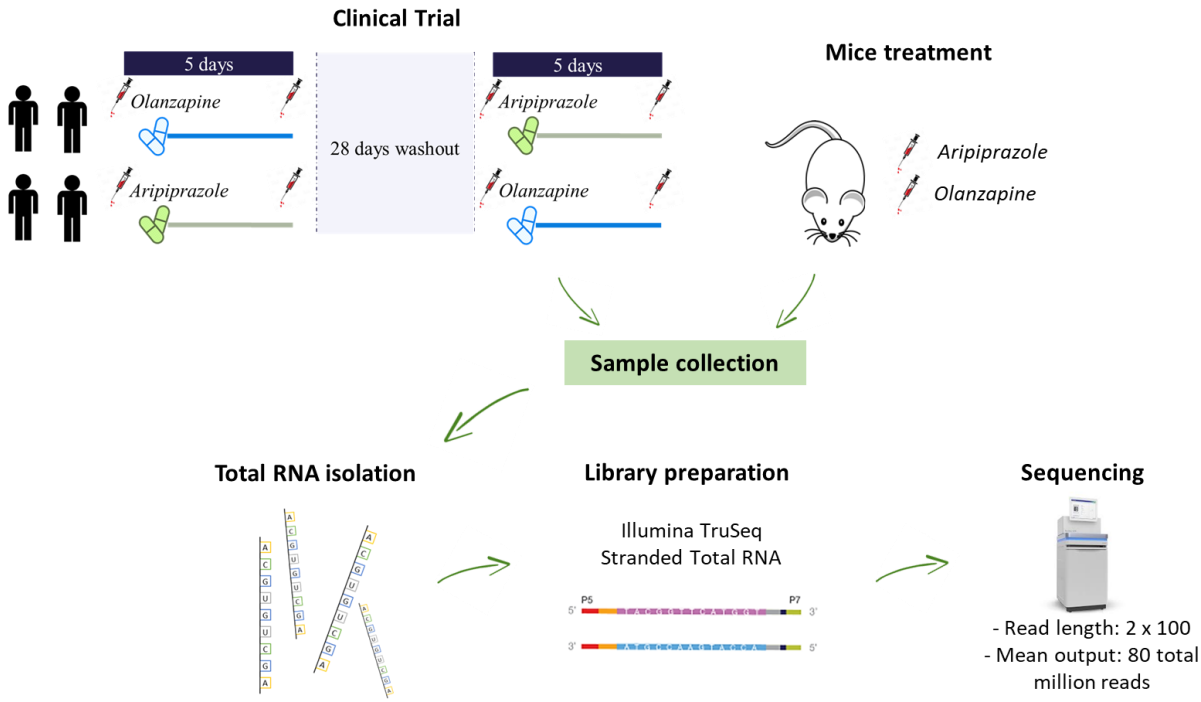

Figure 4. Experimental design.
An open, controlled, randomized, crossover clinical trial in healthy volunteers was carried out to evaluate the short-term effect (5 days) of olanzapine and aripiprazole. Blood samples were collected before and after each treatment making a total of 48 samples. Mice models were treated with short- and long-term aripiprazole and olanzapine schemes. Liver and pancreatic islets were isolated. Total RNA was extracted from the blood and tissue samples and processed with Illumina TruSeq Stranded RNASeq technology. The libraries were sequenced 2 X 100 with a mean output of 40 million reads for the libraries coming from mice samples and 80 million reads for the libraries made from human samples. The reads quality control was assessed with FASTQC and were aligned to a reference genome with Kallisto and HISAT2. The read counting from HISAT2 alignment was achieved with GenomicAlignments package. The samples were preliminarily explored through a PCA. Differential expression analysis was performed with DESeq2 and a Gene Set Enrichment Analysis with GSEA.

3.1.1. Healthy volunteers' study

An open, controlled, randomized, crossover clinical trial in healthy volunteers was carried out at the Clinical Pharmacology Department of the Biomedical Foundation of the University Hospital of La Princesa FIBHUP, in collaboration with Dr Dora Koller and Dr Francisco Abad Santos. Twelve healthy, male and female, human subjects between 18-50 years old were selected to evaluate the effect of multiple doses of olanzapine and aripiprazole. Ten mg/day

aripiprazole tablets or 5 mg/day film-coated olanzapine tablets were administered under fasting conditions daily at 9:00 hrs during 5 consecutive days. The treatment was selected using the block randomization method. After a washout period of 28 days, a second period of the study was carried out, in which the volunteers received the opposite treatment. Blood samples were collected before the beginning of each period and after 5 days of treatment administration.

3.1.2. **Animal studies**

Transcriptomic analyses were performed on pancreatic islets and liver samples from C57/BL6 x 129 sv mice housed at the Institute of Biomedical Research "Alberto Sols" (IIBM) animal facility. Mice were kept at a 12h light/darkness cycle at 22ºC temperature and 45-55% humidity and with *ad libitum* water and food access. Mice were treated with antipsychotics by Dr. Diana Grajales, Vitor Ferreira, Ramazan Yildiz and Gaurang Patel under the supervision of Dr Ángela Valverde and Dr María Monsalve at IIBM. For the animal work, IIBM's teams count on their Research Ethics Committee Approval. Olanzapine, aripiprazole or vehicle was administered to the mice intraperitoneally or through the diet, daily in short- and long-term protocols. Models included wild-type and genetically modified mice (KO) at a critical node of insulin signalling (PTP1B) and a master regulator of oxidative metabolism (PGC-1α). The specific treatment conditions are described in Table 3.

Table 3. Animal model's design

Treatment scheme	Strain	Genotype	Treatment	Sample type	Collaborators
Short treatment scheme (5 days)	C57Bl/6 x129 sv (males)	Wild-type	Intraperitoneally: Vehicle (6 mice) Aripiprazole 5mg/kg (6 mice) Olanzapine 5mg/kg (6 mice)	Liver	Ramazan Yildiz Gaurangkumar Patel Dr María Monsalve
		PGC-1α KO	Intraperitoneally: Vehicle (6 mice) Aripiprazole 5mg/kg (6 mice) Olanzapine 5mg/kg (6 mice)	Liver	
Long treatment scheme (6 months)	C57Bl/6 x129 sv (males)	Wild-type	Diet: Vehicle (2 mice) Aripiprazole (2 mice) Olanzapine (2 mice)	Liver	Vitor Ferreira Dr Ángela Valverde
		PTP1B KO	Diet: Vehicle (2 mice) Aripiprazole (2 mice) Olanzapine (2 mice)	Liver	
Long treatment scheme (6 months)	C57Bl/6 x129 sv (females)	Wild-type	Diet: Vehicle (5 mice, 300 islets) Aripiprazole (7 mice, 300 islets) Olanzapine (5 mice, 400 islets)	Pancreatic islets	Diana Grajales Dr Ángela Valverde

3.2. Samples collection and RNA extraction

Animal tissues were isolated in TRIzol (Ambion, Life Technologies) to preserve the RNA integrity. Once isolated, the liver tissues were lysed and homogenized using the rotor-stator method. In contrast, the pancreatic islets were lysed with a mortar and pestle and homogenized by passing them through a needle. The RNA extraction was performed from the homogenized tissues by PureLink® RNA Mini Kit (Ambion, Life Technologies) according to the manufacturer protocol. During the isolation, a DNase treatment was performed, using the same kit, with an on-column DNase Digestion. Elution of RNA was completed according to the standard protocols.

The human blood samples were collected in PAXgene Blood RNA Tubes (PreAnalytiX GmbH), which intend to stabilize the intracellular RNA. The RNA extraction was performed with the PAXgene Blood RNA Kit (PreAnalytiX GmbH), according to the manufacturer's protocol.

The quality and concentration of the extracted RNA was determined by spectrophotometry using a Nanodrop 2000 (Thermofisher Scientific, Inc.), and by fluorometry using a Qubit fluorometer (Thermofisher Scientific, Inc.). RNA integrity was assessed with the 4200 TapeStation (Agilent Technologies Inc.).

3.3. Library preparation and sequencing

Libraries were prepared with the TruSeq® Stranded Total RNA technology (Illumina, Inc.) in combination with the IDT for illumina TruSeq RNA UD Indexes kit (Illumina, Inc, 96 indexes). The general procedure is illustrated on Figure 5. During the protocol, the Ribo-Zero Globin is used to deplete the globin-encoding mRNA in addition to the rRNA. Once depleted, a reverse transcriptase and random primers are used to produce a first strand cDNA. A second strand cDNA is synthetized using DNA Polymerase I and RNase H. On this strand, dTTP are replaced with dUTP to quenche it during the amplification. An adenine is added to the 3' ends to prevent them from ligating to each other during the adapter ligation. Index adapters are ligated to the ds-cDNA. Strands not containing dUTP become enriched with PCR and purified to obtain the final cDNA library.

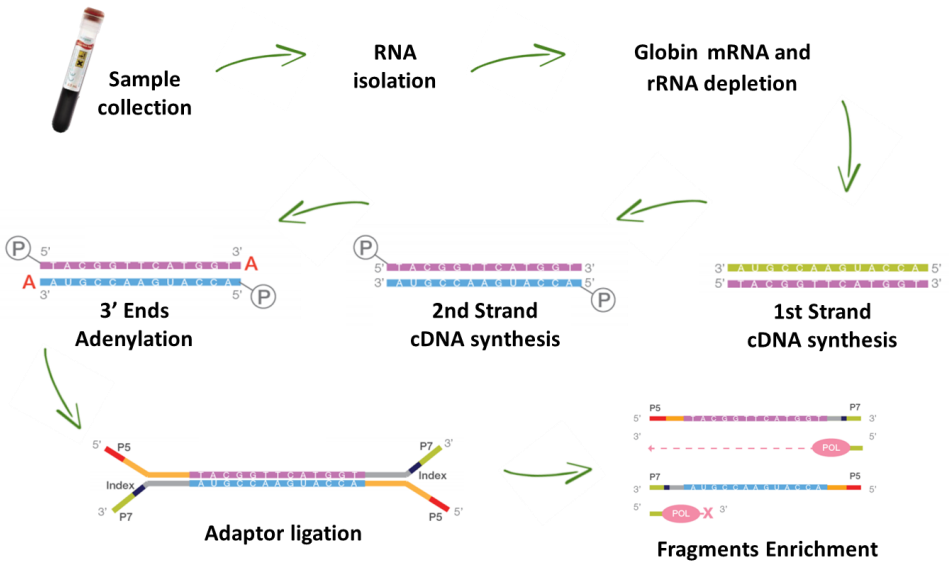

Figure 5. Library preparation procedure
Modified from Illumina Reference Guide #1000000040499 v00 (Illumina 2017)

The libraries were quantified by fluorometry using a Qubit fluorometer (Thermofisher Scientific, Inc.) and by qPCR with the KAPA Library Quantification Kits for Illumina® platforms (Kapa Biosystems, Inc.). The libraries were sequenced in a NovaSeq 6000 sequencer (Illumina, Inc.) 2 X 100 with an intended mean output of 80 million reads for the human samples and 40 million reads for the mice samples. Two runs were performed required to complete the sequencing.

3.4. RNA-Seq Data analysis

The base call (or BCL) files outputted by the sequencer were demultiplexed to fastq files based on their index sequences using Illumina bcl2fastq conversion software. As paired runs were performed, one read 1 (R1) and one read 2 (R2) fastq files were obtained for each sample analyzed. The sequencing quality was assessed with the FastQC tool from the Babraham Institute and merged for their statistical analysis with MultiQC tool. Poly A and poly G tails longer or equal to 10 bp were trimmed from the fastq files with the fastp (S. Chen et al. 2018) tool.

3.4.1. Healthy volunteers' study

The human samples' reads were aligned to an rRNA reference with Bowtie2 (Langmead and Salzberg 2012) aligner to remove the sequences matching ribosomal RNA. The cleaned reads

were kept, and a new quality assessment with FastQC was performed. The remaining reads were aligned to the reference genome (GRCh37/hg19) with HISAT2 (Kim et al. 2019). SringTie (Pertea, M., Pertea, G. M., Antonescu, C. M., Chang, T. C., Mendell, J. T., & Salzberg 2015) and Ballgown (Frazee et al. 2014) were used to generate count matrices.

Genes with less than 1 counts were removed from the analysis. DESeq2 package (Love, Huber, and Anders 2014) was selected for the differential expression analyses. DESeq2 is a count-based statistical method that inputs un-normalized counts matrices (Love et al. 2019). A DESeqDataSet object was built with the **design = ~1**, which shows the data without considering the variables. A variance stabilizing transformation (VST) (Soneson, Love, and Robinson 2015) was applied to the data. Exploratory analyses as hierarchical clustering and Principal Component Analyses (PCA) were performed with R libraries to assess the comparability of the downstream results from both alignments and provide insight on the result's general view. The downstream analyses for the human study were performed with the alignments obtained with HISAT2.

Factors were established to set reference levels for the period, sequencing batch, library batch, treatment, sex and condition: time zero (T0) and 5 days of treatment variables (Figure 6).

```r
sampleTable$Period2 <- factor(sampleTable$Period2, levels = c("P1","P2"))
sampleTable$BatchSecuenciacion <- factor(sampleTable$BatchSecuenciacion, levels = c(1,2))
sampleTable$BatchLibreria <- factor(sampleTable$BatchLibreria, levels = c(1,2,3,4,5,6,7))
sampleTable$Treatment <- factor(sampleTable$Treatment, levels = c("Olanzapine", "Aripiprazole"))
sampleTable$Sex <- factor(sampleTable$Sex, levels = c("Female", "Male"))
sampleTable$Condition <- factor(sampleTable$Condition, levels = c("T0", "T5"))
```

Figure 6. Illustration of the factors established for the different variables in the human experiment design.
The figure shows the reference levels set for the different variables involved in the experimental design. In this case, reference levels were set for the period, sequencing batch, library batch, treatment, sex and condition (understood as T0 and 5 days after the treatment).

The different clusters observed on the PCA were analyzed by colouring the plot according to the different experimental variables: sex, ethnicity, treatment, condition, period, volunteer's number, library batch and sequencing batch.

Differential expression analyses were performed with DESeq2 package, for which the DEGs were described as those with adjPval < 0.1 when performing a Wald test between two conditions and a Benjamini-Hochberg (BH) adjustment. The Deseq2 object was created with the **design = ~ Sex + Treatment.** This design looks into the differences due to the treatment (olanzapine vs aripiprazole) after considering the differences due to the gender.

The volunteers were randomly assigned to be treated with either olanzapine or aripiprazole during the first period of the clinical trial. Their treatment was exchanged for the second period. Figure 7 shows a schema explaining the analysis variables: period, treatment and condition. It was assessed if statistical differences exist between the 2 groups of volunteers at T0 (before administering any treatment). For this, a **contrast = c("Treatment", "Aripiprazole", "Olanzapine")** was studied for all the samples corresponding to T0 of the first period (Figure 7, yellow). The same analysis was performed for the samples taken after the washout period, which corresponded to T0 of the second period (Figure 7, green).

After assessing that no differences exist between the two groups of volunteers at T0 of each period, a Deseq2 object was created with the design = **~ Sex + Period** to study if statistical differences exist between the samples assigned to the same treatment and condition (time point) but from different periods. The 4 comparisons performed are represented by different colours in Figure 8. It was assessed that minimal differences exist between samples under the same conditions (treatment and time point) but from different periods. Therefore all further analyzes were performed with the combined data from the 2 periods.

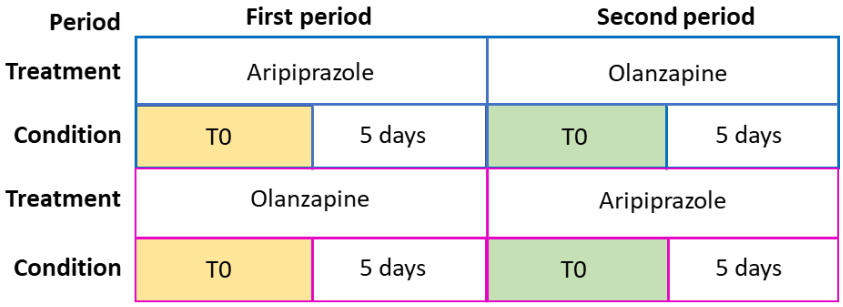

Figure 7. Schematic representation of the meaning assigned to some of the analysis variables and the variables contrasted for the T0 comparisons.
The figure represents the meaning of some of the analysis variables. It is shown that the periods were divided as first and second. The treatment corresponds to the antipsychotic assigned to a person during a specific period of the clinical trial. The condition states if the sample was taken at T0 or after the 5 days of treatment administration. In yellow and green are highlighted the samples compared to assess statistical differences between the treatment groups at T0 for each period.

After these validations, the effect of the treatments on the gene expression was tested by building a Deseq2 object with **design = ~ Sex + Condition**. Comparisons 5 days vs T0 were performed for aripiprazole and olanzapine. The analysis was repeated with only the protein-coding genes. A similar number of dysregulated as for the analysis with all genes was observed.

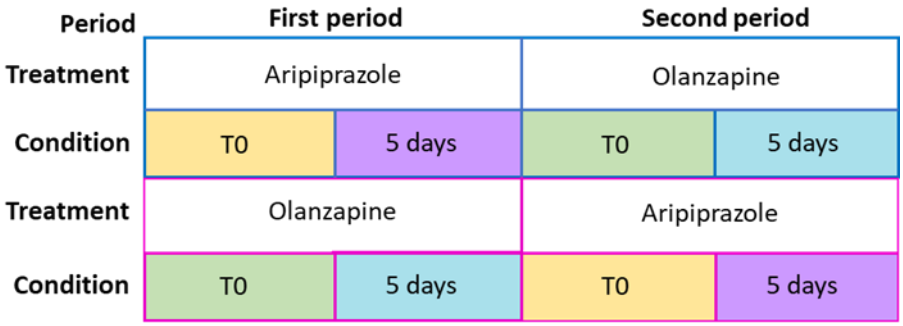

Figure 8. Representation of the variables contrasted between the periods.
The figure represents the contrasted variables to understand if a statistical difference exists between the two periods (period 2 vs period 1). In yellow, the comparison between aripiprazole samples at T0. In green, the olanzapine T0 samples compared. In purple, the aripiprazole samples after 5 days of treatment. In blue, the olanzapine samples after 5 days of treatment.

There was a small number of genes to perform overrepresentation analyzes. Thus, Gene Set Enrichment Analyses (GSEA) were performed with the genes ranked by their Log2FoldChange when comparing "5 days vs T0" for each treatment. The dataset containing all the genes and not just the protein-coding genes was used for this analysis.

3.4.2. **Animal studies**

As a resource-saving method compared with HISAT2, we decided to align the mouse samples' reads with Kallisto (Bray et al. 2016) to a mouse transcriptome reference (Mus_musculus.GRCm38.cdna.all.fa.gz, ENSEMBL). Tximport package (Soneson, Love, and Robinson 2015) and Ensembl annotation were used to read in the transcript abundance estimates and summarize their expression at the gene level. The DESeqDataSet object for the mice analyses was built with the **design = ~ Treatment**. Therefore, the analysis compared the gene expression between mice treated with olanzapine Vs untreated mice and the gene expression of mice treated with aripiprazole Vs untreated mice. Genes with less than 10 counts were removed from the analysis. The VST was applied to the data. PCAs were performed, including all mice samples and analyzed by colouring them according to the type of tissue from which the samples came from, the genetic background of the animals, the treatment administered and the researcher who facilitated the samples. Euclidean and Poisson distances matrices were also computed and compared against the PCA results.

A separate analysis was implemented for each of the tissue types. We performed differential expression analyses to compare pancreatic islets samples from mice treated with aripiprazole Vs pancreatic islets from mice fed with a placebo diet (chow). We also performed a correlative

analysis comparing pancreatic islets from mice treated with olanzapine, Vs those from mice fed the chow diet. We performed PCA of the DEGs and GSEA against the KEGG database with the fold-changes from all genes to assess differentially expressed pathways.

In the same way, we studied the liver differentially expressed genes between WT treated mice (aripiprazole or olanzapine) and the WT mice fed with the chow diet. We performed GSEA analyses against the KEGG and Gene Ontology (GO) databases. What's more, we compared the Log2FoldChange of the dysregulated genes (adjPval < 0.05) produced by the short- and long-term treatments with aripiprazole and olanzapine to understand if the prompt responses maintain or change through time.

We finally analyzed if statistically significant (adjPval < 0.05) differences occur between the gene expression of PGC-1α KO and WT mice after a 5-days treatment with aripiprazole and olanzapine. In addition, a similar comparison was studied between PTP1B KO and WT mice after six months of treatment with the same antipsychotics. Heatmaps of the top significantly dysregulated genes were plotted.

3.5. Healthy volunteers' classification by genetic response to the treatments

The samples' similarity was quantified by computing the Euclidean and Poisson (Witten 2011) distances between each pair of samples to produce sample distances heatmaps that allowed the samples' clustering according to their similarity. We observed a differential response among the volunteers, as some volunteers' samples clustered together, meaning that their gene expression suffered minimal modifications. In contrast, others showed more considerable differences among their samples, therefore clustering apart. Next, we performed an interaction analysis with the **design = ~ Volunteer + Condition + Volunteer:Condition**. In this design, the interaction term "Volunteer:Condition" allows us to know the Log2FoldChanges (T5 Vs T0) difference between each volunteer and a volunteer choose as reference. Volunteer 24 was chosen as reference as its Log2FoldChanges T5 Vs T0 for both aripiprazole and olanzapine were close to zero. We statistically tested each gene's Log2FoldChange difference among the volunteers by performing a likelihood ratio test (LRT) that examines two counts models: a **full model= ~ Volunteer + Condition + Volunteer:Condition**, and a **reduced model = ~ Volunteer + Condition**, in which some terms of the full model are removed to determine if the increased likelihood of the data using the extra terms in the full model is more than expected

if those extra terms are truly zero. We considered genes with statistically differential responses among the volunteers as those with adjPval < 0.1 in the LRT. We performed a PCA with those genes to observe the volunteers distribution. Additionally, we performed an enrichment analysis against several databases with the online tool Enrichr.

We performed single nucleotide variant prediction with VarScan (Koboldt et al. 2012) from BWA alignments, followed by annotation with Annovar (Wang, Li, and Hakonarson 2010). We compared the different polymorphisms observed for the volunteers with varying response levels (high, medium, low). Additionally, volunteers' clinical variables registered during the trial as weight, triglycerides, cholesterol, glucose and insulin were kindly provided by Dr Dora Koller and Dr Francisco Abad Santos. We analyzed them with t-tests to know if statistical differences exist between the response groups low Vs high + medium.

We estimated the transcript-level fragments per kilobase of transcript per million fragments mapped (FPKMs) with Tablemaker software provided by Ballgown package developers (Frazee et al. 2014), which calls Cufflinks (Trapnell et al. 2010) for the estimation. Then we plot the different transcript isoforms for a specific gene by using the plotTranscripts() function from the Ballgown package.

We performed differential expression analyses for the low and high + medium response volunteers separately to understand the effect of the treatments on the different response groups. The high + medium response volunteers were mixed in a group to maintain the sample size of the analysis as high as possible. The DESeq object was built with **design = ~ Sex + Condition**. Enrichment analyses against several databases were performed for the differentially expressed genes (adjPval < 0.5) with the online tool Enrichr.

3.6. Features seleccion

We used Scikit-learn, an open-source machine learning library, to select the minimal number of features out of the genes with statistically significant differential response across the volunteers, which may allow us to distinguish between the low and high response groups. The volunteers included in the low response group are volunteers 13, 15, 20, 21 and 22, whereas the volunteers included in the high response groups are volunteers 11, 16 and 19.

First, we performed some tests to select the best filtering method. On a first approach, we estimated the performance of the nearest neighbour classifier on the dataset using 10-fold cross-validation when all the features are used for prediction. The number of neighbours was

chosen using 3-fold inner cross-validation. To run the pipeline, we designed functions to accomplish the *data standardization*, which includes the data split into train and test; *Hyperparameters_evaluation*, which chooses the best number of neighbours, (1 or 2); and the *model performance evaluation*:

```
def data_standarization(X, y, train_index, test_index):

    X_train, X_test = X[train_index], X[test_index]
    y_train, y_test = y[train_index], y[test_index]

    #Data standarization
    scaler = preprocessing.StandardScaler().fit(X_train)
    X_train_scaled = scaler.transform(X_train)
    X_test_scaled = scaler.transform(X_test)

    return [X_train_scaled , y_train, X_test_scaled, y_test]
```

```
def Hyperparameters_evaluation(pipeline, X_train_scaled, y_train):
    #Specification of the Hyperparameters (number of neighbors to consider)
    N_neighbors = [1, 2]
    param_grid = { 'knn__n_neighbors': N_neighbors }

    #Evaluating the Performance for each Value of the Hyperparameters
    skfold = RepeatedStratifiedKFold(n_splits=3, n_repeats=1, random_state=None)
    gridcv = GridSearchCV(pipeline, cv=skfold, n_jobs=1, param_grid=param_grid, \
    scoring= make_scorer(accuracy_score))
    result = gridcv.fit(X_train_scaled, y_train)

    #Obtain the mean accuracy and the corresponding standard deviation across data splits.
    accuracies = gridcv.cv_results_['mean_test_score']
    std_accuracies = gridcv.cv_results_['std_test_score']

    #Choose the best hyperparameter
    best_reg_param_value = param_grid['knn__n_neighbors'][ np.argmax(accuracies) ]

    return(best_reg_param_value)
```

```
def Model_performance(best_reg_param_value, X_train_scaled , y_train, X_test_scaled, y_test):
    #Computation of the confusion matrix on the test set
    knn = KNeighborsClassifier(n_neighbors = best_reg_param_value)
    knn.fit(X_train_scaled, y_train)

    accuracy= np.mean(knn.predict(X_test_scaled) == y_test)

    return accuracy
```

On a second approach, we estimated the performance of the nearest neighbour classifier when using a feature selection technique based on the F-score (ANOVA), picking up the 10 most relevant features:

```
def Filtering_Fscore(k_features, X_train , y_train, X_test, y_test):

    filtering = SelectKBest(f_classif, k_features)

    filtering.fit(X_train, y_train)
    X_train_vr = filtering.transform(X_train)
    X_test_vr = filtering.transform(X_test)

    return[X_train_vr , y_train, X_test_vr, y_test]
```

Finally, we essayed an initial filtering method based on the F-score to keep only the 20% most promising features and final filtering with a random forest approach to pick up the 10 most relevant features:

```
def Filtering_RandomForest(k_features_rf, X_train_vr , y_train, X_test_vr, y_test):

    rf_selection = SelectFromModel(RandomForestClassifier(n_estimators = 2000, \
    random_state = 0), threshold = 0.0)

    rf_selection.fit(X_train_vr, y_train)
    rf_selection.threshold = -1.0 * \
    np.sort(-1.0 * rf_selection.estimator_.feature_importances_)[ k_features_rf - 1 ]
    X_train_rf = rf_selection.transform(X_train_vr)
    X_test_rf = rf_selection.transform(X_test_vr)

    return[X_train_rf , y_train, X_test_rf, y_test]
```

We observed that the feature selection with F-score + Random Forest performed the best in terms of the generalization error obtained. However, the difference with the F-score alone was slight, and this method ran significantly faster. Therefore we decided to continue the analysis using the F-score method. For the previous essays, we limited the number of features filtered to 10. However, we did not know if this number was optimal. Therefore, we estimated the performance of the nearest neighbour classifier with K=2 using an F-score to filter features from 1 to 200. We used a 10-times 10-fold cross-validation method and plotted the prediction error Vs the number of features used for prediction:

```
ensemble_size = 200

#10-fold cross validation
n_repeats = 10
rkfNNC_4 = RepeatedKFold(n_splits=3, n_repeats = n_repeats, random_state=None)

s = ((3 * n_repeats), ensemble_size)
total_error_NNC_4= np.zeros(s)
split = 0

for train_index, test_index in rkfNNC_4.split(X, y):

    sys.stdout.write('.')
    sys.stdout.flush()

    dataNNC_4 = data_standarization(X, y, train_index, test_index)

    #Defining the Pipeline of Data Transformation and Estimation
    pipelineNNC_4 = Pipeline([ ('knn', KNeighborsClassifier()) ])

    for i in range(ensemble_size):

        #Filtering to pick the most relevant features with the F-score technique
        k_featuresNNC_4 = i+1
        dataNNC_4_vr = Filtering_Fscore(k_featuresNNC_4, dataNNC_4[0],dataNNC_4[1], \
                                        dataNNC_4[2], dataNNC_4[3])

        #Fitting the Final Model and Estimating Its Performance
        total_error_NNC_4[split, i]=(1-(Model_performance(2, dataNNC_4_vr[0],dataNNC_4_vr[1],
                                                          dataNNC_4_vr[2], dataNNC_4_vr[3])))

    split += 1

average_error_NNC_4 = total_error_NNC_4.mean(axis=0)

print('\n',average_error_NNC_4)
```

We repeated that process when the feature selection is done externally to the cross-validation loop using all the available data to compare the prediction error to the previous method.

We determined the slightest prediction error out of the 200 essays to choose the number of features to classify the volunteer groups better.

We performed a heatmap of the volunteer's response and a PCA for the final features selected.

4. OUTCOMES

4.1. Experimental design

The current project was developed in NIMGenetics, a biotechnological company based in Madrid, Spain. When the project started, the RNA-sequencing technique was not yet implemented in the company. Therefore, apart from the scientific goals, the project's development aimed to contribute to the company by searching, troubleshooting and providing insight on key steps of the RNA-sequencing protocols and data analysis. The knowledge acquired is intended to serve as a reference for the company to implement RNA-sequencing as a new service.

Since the project includes two different biological models, tissue mice samples and human blood samples, it was essential to begin the protocol implementation by thinking about each model's most appropriate experimental design. Some of the critical choices were the number of biological and technical replicates and the sequencing depth.

The number of replicates in an RNAseq experiment is influenced by biological variability and technical reproducibility. Although reproducibility is usually high at the sequencing level, previous steps as RNA isolation and library preparation may introduce biases (Conesa et al. 2016). However, it has been shown that, while the library preparation may have the most considerable contribution to the technical variability, this feature may be minimal compared to the biological one (Bullard et al. 2010), resulting in the biological replicates being favoured over the technical ones. Generally, in RNA-seq, each biological replicate is prepared separately. However, alternatively, biological replicates can be pooled before the library preparation (Williams, A. G., Thomas, S., Wyman, S. K., & Holloway 2014). Because humans naturally have higher biological variability than the mice models, it was decided to make individual biological replicates for the human samples. In contrast, some mice samples were pooled before the library preparation to study more conditions as their genetic background is known.

Sequencing depth influence the number of detected transcripts. A larger number of transcripts will be detected with a higher precision as the number of sequences read is increased (Conesa et al. 2016). However, a cost-effective experiment must adjust the number of reads to the experiment's purpose. The ENCODE consortium have provided information about the number of necessary reads to quantify genes with accuracy. They determined that approximately 80% of genes with more than 10 fragments per kilobase of exon per million reads mapped (FPKM) could be quantified with ~36 million mapped reads.

In contrast, genes expressed at lower levels could only be quantified by mapping ~80 million reads (Sims et al. 2014). With these numbers in mind, ~36 million reads would be enough to study changes on abundant genes, for which it was decided to set the coverage for the mice experiments to 40 million reads per sample. The human samples' coverage was set to 80 million reads as more biological variability, and extra technical steps as globin depletion may entail higher accuracy requirements.

4.2. Quality control

RNA was isolated from mice liver and pancreatic islets and human blood samples. The concentration of the isolated RNA was determined through spectrophotometric and fluorometric methods. The average RNA concentration for the human blood samples was 35.1 ng/uL when measured with a Nanodrop, a spectrophotometric method; and 41.6 ng/uL when measured with a Qubit, a fluorimetric method. The average RNA concentration for the animal tissue samples was 48.5 ng/uL with the Nanodrop and 47.3 ng/uL with the Qubit. According to the library preparation protocol, Illumina TruSeq Stranded Total RNA technology has been optimized for an RNA input of 0.1 to 1 ug in a maximum volume of 10 uL. Because all of the samples' RNA concentration ranged between the standardized input concentrations for the library preparation and were close to the middle of the optimized range (500 ng/uL), it was decided to input 10 uL of undiluted RNA as all the isolated samples were between the optimized range. The average 260/280 and 260/230 ratios were 2.2 and 0.8, respectively, for the blood samples, and 1.7 and 1.5 respectively for the tissue samples. RNA integrity was assessed with the 4200 TapeStation (Agilent Technologies Inc.). The average RIN for the blood samples was 7.8, while the tissue samples had an average RIN of 9.4.

The sequencing quality was evaluated with the FastQC tool which provides a Phred score for each of the base positions. The Phred score is a predictor of the sequencing error rate that takes into account the peak resolution, uncalled/called ratio, spacing, among others; and can be defined as (Liao, Satten, and Hu 2017):

$$Q = -10 \log_{10} \Pr(observed\ allede \neq true\ allele)$$

All sequenced reads got a Q > 35, meaning that each base's error rate was < 0.03%, while the average read length was 100 bp (Figure 9). Hence, the data obtained had the necessary quality to be analyzed.

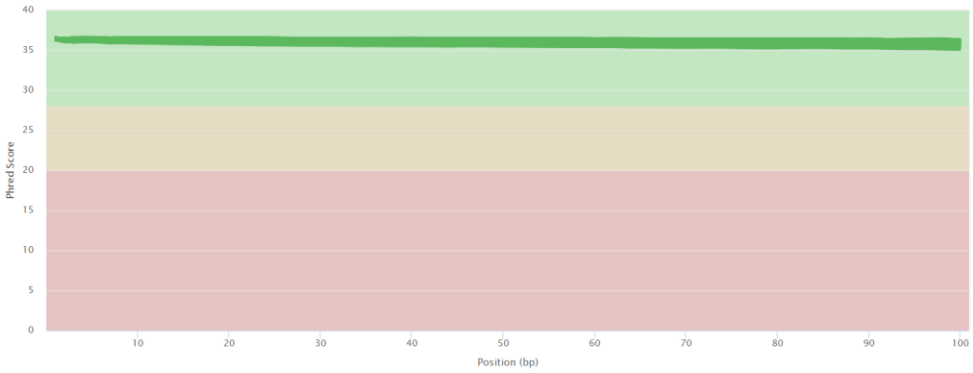

Figure 9. FastQC mean quality scores.
The Phred score for the reads was above 35 for each of the base positions. The read length was, on average, 100 bp.

4.3. Transcriptomic studies

4.3.1. Healthy volunteers' study

We analyzed 48 samples from healthy volunteers to study the transcriptomic changes produced by treatments with aripiprazole and olanzapine. After the sequencing was completed, the ribosomal matching reads were removed, and the remaining reads were aligned to the reference genome (GRCh37/hg19). Count matrices were generated and annotated to read in the transcript abundance estimates and summarize their expression at the gene level.

Some statistical exploratory methods such as PCA work better when the data have similar variance at different means. However, on the count matrices from RNA sequencing, the variance is higher for the most expressed genes; as their counts have the more significant absolute differences between the samples, thus resulting in the set of the genes with larger counts directing or biasing the results of plot and therefore ignoring the information provided by less expressed genes (Love et al. 2019). Trying to minimize this situation, we analyzed the variance stabilizing transformation (VST) to the data to favour an equal contribution from all genes.

We performed PCA from the DESeqDataSet object with design = ~1 (without predictors). The method reduces the original group of variables, which may be related to each other, to a new, smaller and uncorrelated group of variables. In this way, the data set's characteristics that contribute the most to its variance, the main components, are retained, collecting the most relevant information. PCA plots are depicted in Figure 10. In the first panel (Figure 10A), three apparent clusters were observed. The dots were coloured according to the different experimental conditions to assess the causes of clusters' formation. Clear separation by

gender was observed on the horizontal axis; on the upper part of the plot were the samples from females and the samples from males on the bottom. Therefore, the gender-related differences were considered for further analyses. The volunteers included in the study have Caucasian and Latin American ancestries. The 2 Latin American volunteers mixed with the 10 Caucasians, validating that ethnicity does not affect the analysis results (Figure 10B).

Each volunteer received both of the tested treatments (aripiprazole/olanzapine). Figure 10C shows that the global samples' distribution was not affected by the treatment received, as the samples did not cluster according to the treatment administered. The "condition" defined as either T0 or 5 days after the treatment was not ruling the samples' distribution either, as there is no apparent difference among the time points (Figure 10D). When colouring the plot by the clinical trial periods, there is no division either (Figure 10E).

None of the assay variables explains the cluster's separation on the x axis. Therefore, the samples were coloured by volunteer number. We observed that the four samples corresponding to each person, in general, plotted close to each other (Figure 10F). While the sequencing was performed in two rounds, the library preparation was done in several rounds. Subsequently, we performed a PCA plot colouring samples according to the library (Figure 10G) and sequencing (Figure 10H) batches to understand if they correlate with the observed clusters. By seeing the plots, it was possible to establish a correlation between the clusters and the library preparation batch, as all samples from the same batch clustered close to each other. A degree of correlation with the sequencing batch was also observed. Considering an existing technical batch effect, all the samples from the same person were kept in the same batch of library preparation and sequencing to avoid technological noises, making a reasonable approach to compare the samples from the same volunteer to each other within the batches.

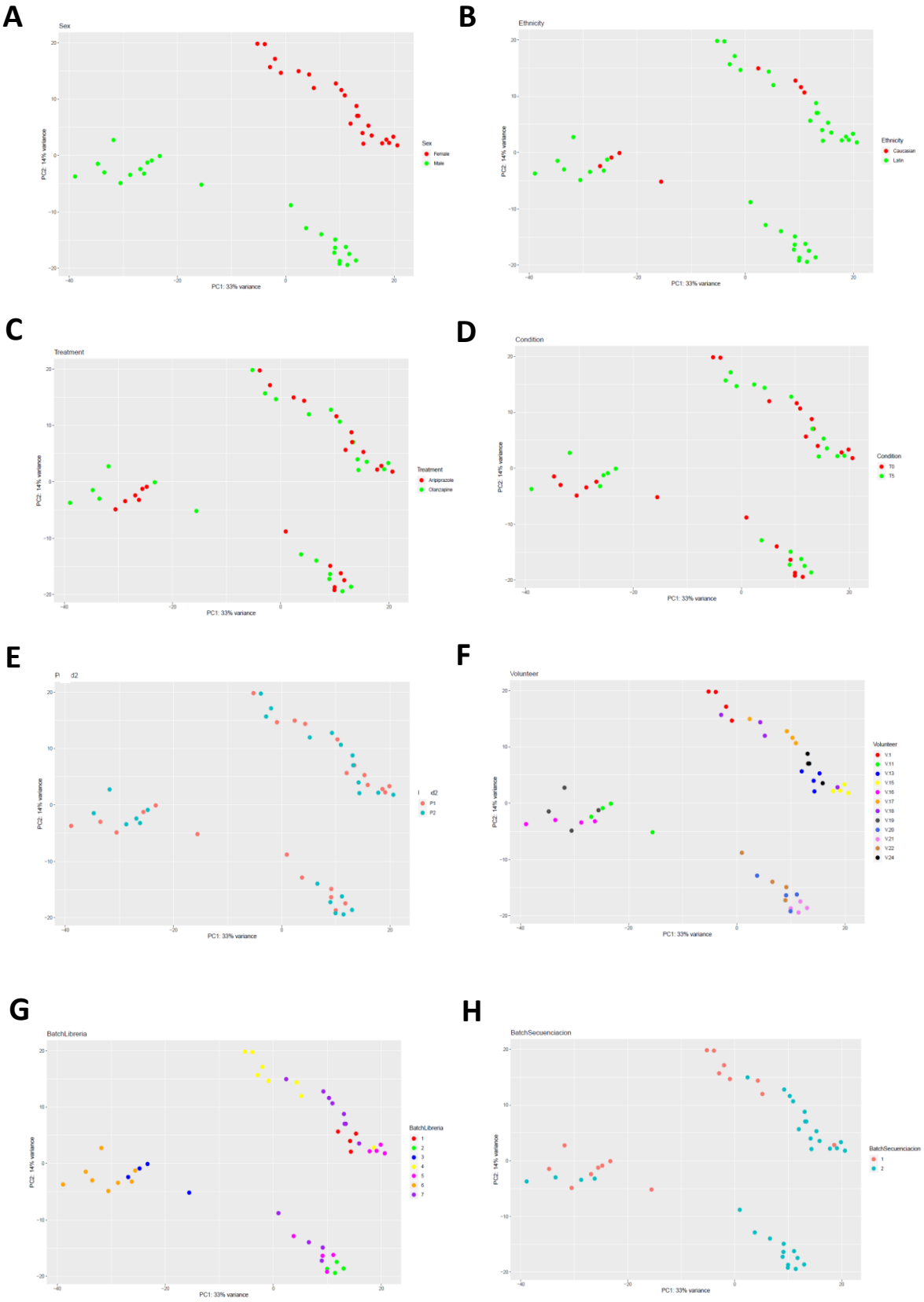

Figure 10. PCA from the healthy volunteers sequencing data.

A PCA was performed on the sequencing results from the 48 samples analyzed from the healthy volunteers. The plot was coloured by the gender (referred to as sex on the plot) (A), treatment (B), ethnicity (C), condition (D), period (E), volunteer (F), library batch (G) and sequencing batch (H).

To further proceed with our analysis, a DESeq2 object was built with the **design = ~ Sex + Treatment** to observe the gene expression differences due to the treatment while adjusting for gender differences. We assessed if statistical differences exist among the treatment groups at T0 for each clinical trial period. A total of zero genes were differentially expressed when comparing aripiprazole vs olanzapine at the T0 of the first period. The same result was observed for the second period. This outcome validated that there are no statistical differences between the two randomly selected groups; therefore, the comparison between treatments will be legit.

Due to the small sample size we decided to analyze together the samples corresponding to the same treatment and time point (condition) even if they were taken during different periods of the clinical trial. To support this approach, a Deseq2 object with the **design = ~ Sex + Period** was built. The contrast, in this case, was "perido2" vs "period1". When analyzing aripiprazole samples at T0, 5 DEGs were pointed out (adjPval < 0.05, Wald test). The analysis for aripiprazole samples after 5 days of treatment, resulted in 1 gene differentially expressed, (adjPval < 0.05, Wald test). The analysis for olanzapine samples produced 3 and 1 differentially expressed genes for T0 and 5 days, respectively (adjPval < 0.05, Wald test). In conclusion, a minimal number of genes showed differential gene expression when comparing the same conditions at different periods. This outcome suggested that it would be safe to combine the data from different periods to increase the sample size. Therefore, all subsequent analyzes were performed with the combined data from the two periods. The DEGs obtained from the periods' contrast were taken into account when performing further analyses.

After completing the previous validations, we tested the treatments' effect on gene expression by creating a DESeq2 object with **design = ~ Sex + Condition.** After the treatment with aripiprazole, 2 genes became dysregulated (adjPval < 0.05, Wald test); while the treatment with olanzapine modified the expression of 5 genes (adjPval < 0.05, Wald test). The time points comparison was repeated with only the protein-coding genes. 3 genes statistically modified their expression after the treatment with aripiprazole (adjPval < 0.05, Wald test), while the treatment with olanzapine modified the expression of 5 genes (adjPval < 0.05, Wald test).

Since the number of dysregulated genes was small to perform overrepresentation analyses efficiently, we next followed a Gene Set Enrichment Analysis (GSEA) strategy as this approach considers all the genes in the data set, ranked by their Log2FoldChange, rather than only the dysregulated genes. GSEA was in first place run against the KEGG database (Figure 11). The top up-regulated gene set by the treatment with aripiprazole was the "Nicotine addiction" gene set with a Normalized Enrichment Score (NES)= 1.83; and a False Discovery Rate (FDR)= 0.02. From the 34 genes in the gene set, 5 had a Log2FoldChange > 1.50 (*GABRR3, GABRB3,*

GRIN2D, GABRG2, CHRNB2). The second more up-regulated pathway was "Maturity onset diabetes of the young" with NES= 1.66 and FDR= 0.16; with 1 gene (HNF4A) with Log2FoldChange > 1.50. Other up-regulated gene sets were: Butanoate metabolism (NES= 1.64), from which *ACSM2B* had a Log2FoldChange > 1.50, while other genes as *GAD1*, *ACSM2A*, *ACSM1*, followed the up-regulation pattern showing a Log2FoldChange >= 1.00; Retinol metabolism (NES= 1.63), from which *CYP1A1*, *AOX1*, *LRAT* and *ADH1B* had a Log2FoldChange > 1.50; Olfactory transduction (NES= 1.61), from which several olfactory receptor family genes had a Log2FoldChange > 1.50; Steroid hormone biosynthesis (NES= 1.55) from which *CYP1A1* and *CYP19A1* had a Log2FoldChange > 1.50; Ovarian steroidogenesis (NES= 1.53), from which *CYP1A1*, *IGF1*, *ADCY1* and *CYP19A1* had a Log2FoldChange > 1.50*;* Breast cancer, from which "hes related family bHLH transcription factor" genes (*HEYL, HEY*2), fibroblast growth factor genes (*FGF17, FGF22*) and insulin-like growth factor 1 (*IGF1*) had a Log2FoldChange > 1.50; and Taurine and hypotaurine metabolism (NES= 1.40) from which no individual genes showed a a Log2FoldChange > 1.50. (Figure 11A).

The hematopoietic cell lineage was the most down-regulated gene set by the treatment with aripiprazole with a NES= -0.65 and FDR= 0.01; being GP1BB (glycoprotein Ib platelet subunit beta) the most down-regulated gene within the set, with a Log2FoldChange= -23.81. Other down-regulated gene sets are: Fructose and mannose metabolism (NES= -1.86), Salmonella infection (NES= -1.85), Staphylococcus aureus infection (NES= -1.78), Bladder cancer (NES= -1.74), Other glycan degradation (NES= -1.73), Chemokine signaling pathway (NES= -1.69), Osteoclast differentiation (NES= -1.68), Legionellosis (NES= -1.67), and the Fc gamma R-mediated phagocytosis gene set (NES= -1.65). Even though the gene sets were as a whole repressed, the majority did not include any gene with a Log2FoldChange< -1.50. However, the Salmonella infection, Chemokine signalling pathway, and Legionellosis gene sets shared the repression of chemokine ligand genes as *CXCL3*, *CCL24* and *CCL22*, with a Log2FoldChange< -1.50.

Regarding the treatment with olanzapine, we observed that the most up-regulated pathway was the Nitrogen metabolism pathway with a NES= 1.55 and an FDR= 0.56. Out of this pathway, *CA12* (carbonic anhydrase 12) had a Log2FoldChange= 2.6, while other family genes were up-regulated with a Log2FoldChange< 1.50. Other up-regulated pathways with FDR> 0.05 were: fat digestion and absorption (NES= 1.55) from which *PLA2G2F* had a Log2FoldChange= 2.47; Nicotinate and nicotinamide metabolism (NES= 1.52) from which *NNMT* had a Log2FoldChange= 2.01; Phototransduction (NES= 1.47) from which *CNGA1* had a Log2FoldChange= 2.06; alpha-Linolenic acid metabolism (NES= 1.42) from which *PLA2G2F*

had a Log2FoldChange= 2.47; Pentose and glucuronate interconversions (NES= 1.40) from which no genes had a Log2FoldChange> 1.50;

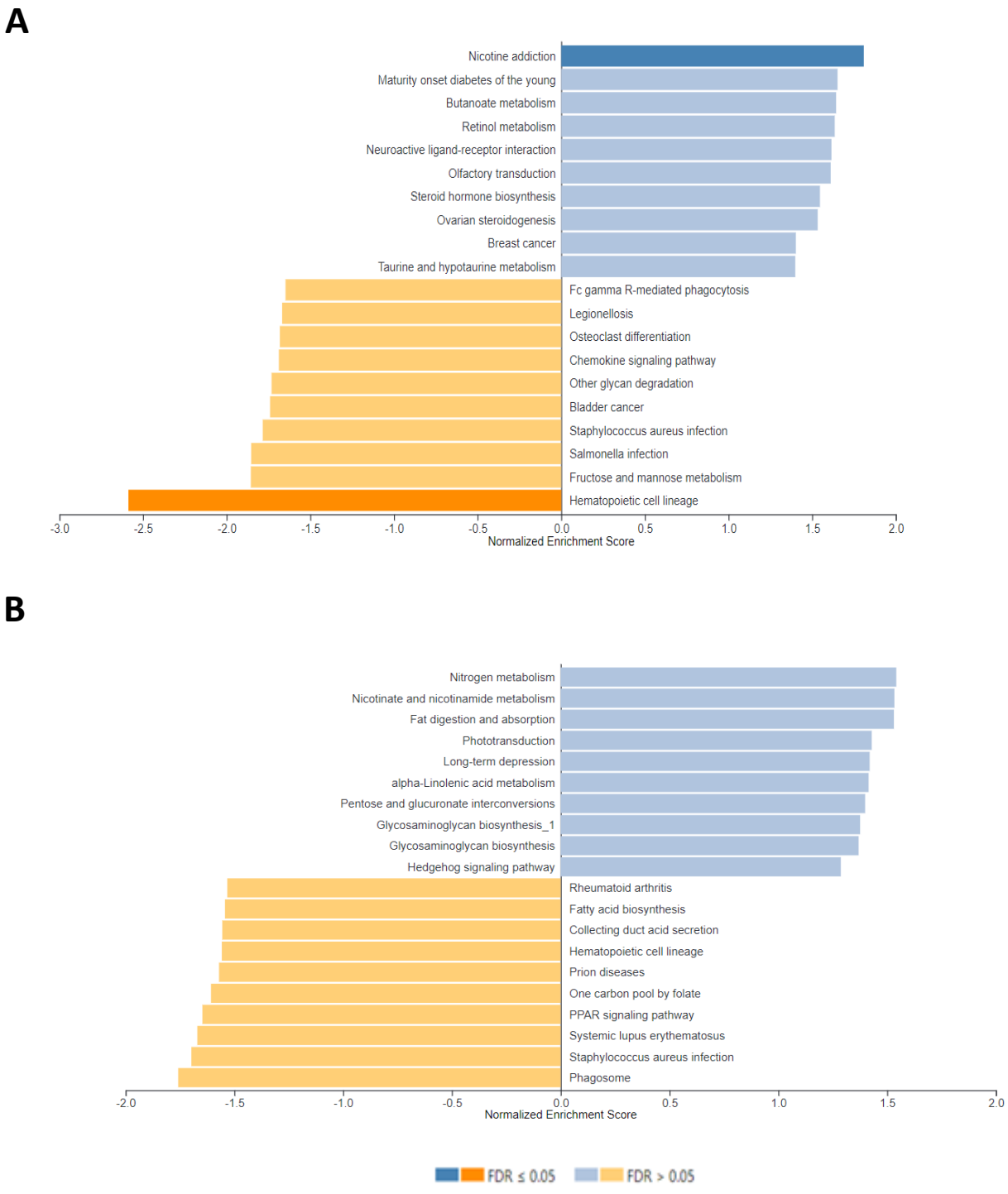

Figure 11. GSEA of the human blood samples against the KEGG database

The figure shows the KEGG pathways dysregulated after the treatment with aripiprazole (A) and olanzapine (B). The "x" axis represents the normalized enrichment score assigned to each pathway. The bars coloured blue represent up-regulated pathways, while the orange bars represent down-regulated ones.

Glycosaminoglycan biosynthesis_1 (NES= 1.38) from which *CHST3* was the only up-regulated gene with a Log2FoldChange= 1.38; Glycosaminoglycan biosynthesis (NES= 1.36) from which *CHST6*, the most up-regulated gene within the set had a Log2FoldChange= 1.01; and Hedgehog signalling pathway (NES= 1.29) from *DHH* gene (desert hedgehog signalling molecule) was up-regulated with a Log2FoldChange= 2.02 (Figure 11).

All down-regulated pathways by the treatment with olanzapine had an FDR> 0.05. The most down-regulated was the Phagosome gene-set with a NES= -1.76. The *HLA-G* (major histocompatibility complex, class I, G) was the most down-regulated gene within the set with a Log2FoldChange= -2.51. Other down-regulated pathways are: Staphylococcus aureus infection (NES= -1.70); Systemic lupus erythematosuswith (NES= -1.67), both with no genes having a Log2FoldChange< -1.50; PPAR signalling pathway (NES= -1.65) from which a group of genes had a Log2FoldChange< -1.50 *PCK1* (-2.22), *ACSBG2* (-2.21), *FABP3* (-2.14) and *ADIPOQ* (-1.72); One carbon pool by folate (NES= -1.61) from which *ALDH1L1* had a Log2FoldChange= -1.67; Prion diseases (NES= -1.57) from which *IL1A* had a Log2FoldChange= -1.31; Hematopoietic cell lineage (NES= -1.56) from which *GP1BB* had a Log2FoldChange= -4.20; Collecting duct acid secretion (NES= -1.56) from which none of the genes had a Log2FoldChange< -1.50; Fatty acid biosynthesis (NES= -1.54) from which *ACSBG2* (acyl-CoA synthetase bubblegum family member 2) had a Log2FoldChange= -2.20; and Rheumatoid arthritis (NES= -1.53) from which none of the genes had a Log2FoldChange< -1.50, although among them, *IL1A* and *IL11* were the most down-regulated genes with a Log2FoldChange of -1.31 and -1.22 respectively.

In summary, while the aripiprazole treatment resulted in an enriched expression from of the "Nicotine addiction" gene set and a dimished expression from the gene involved in the hematopoietc cell lineage; the treatment with olanzapine up-regulated the Nitrogen metabolism pathway and downregulated pathways in a wider and profound range of biological activities such as the coordination of the immune response.

4.3.2. **Mice's study**

Liver and pancreatic islets samples from WT mice treated with aripiprazole, olanzapine or placebo in short or long-term schemes were processed with Illumina TruSeq Stranded RNASeq technology to study the transcriptomic changes due to the different treatments. As a general exploratory resource, we performed PCA from the VST produced from the counts (Figure 12A).

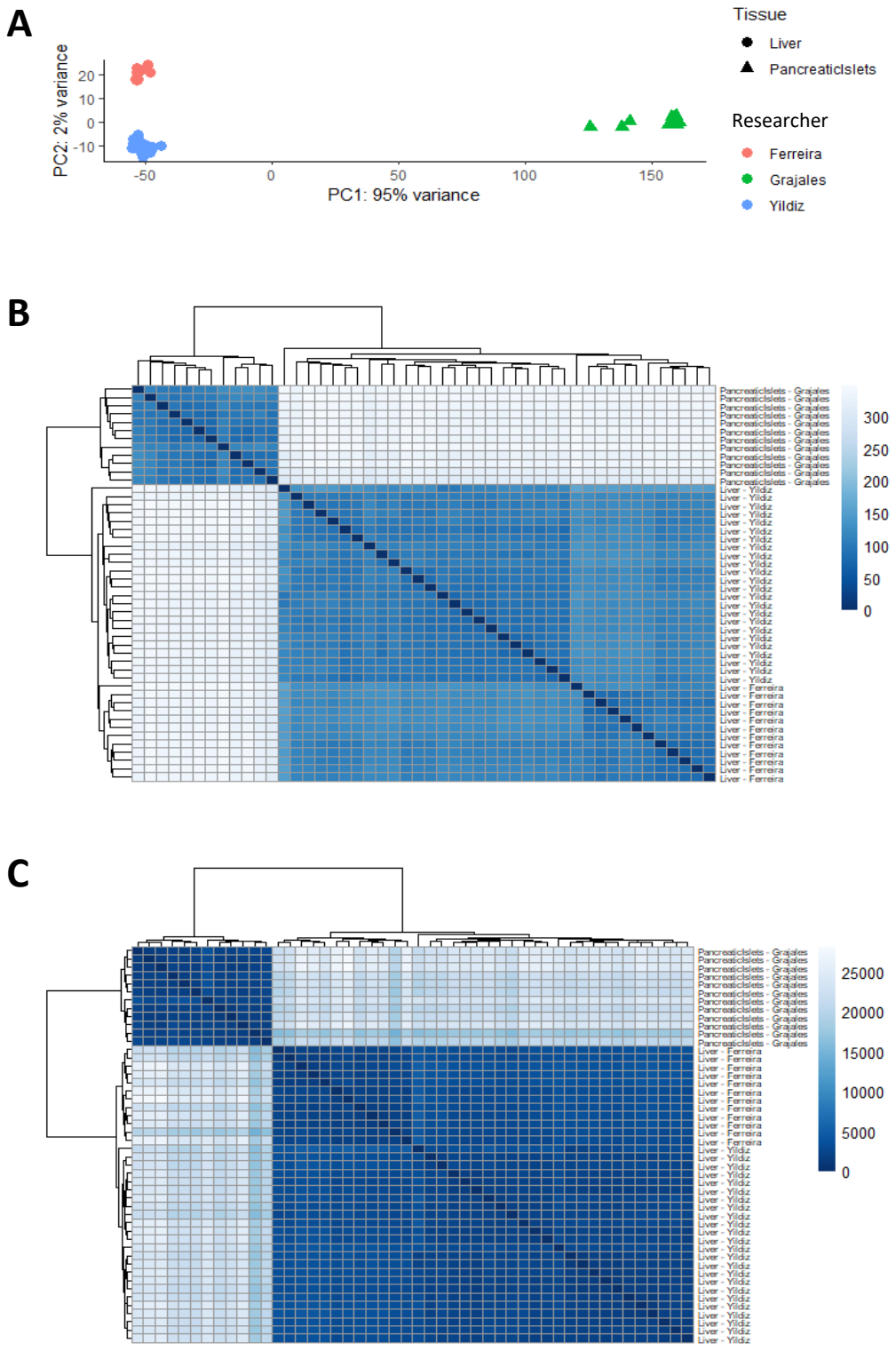

Figure 12. Mice's samples PCA and sample distance matrices

A: PCA plot of all mice samples studies coloured by the researcher who provided the samples (Red: Ferreira, green: Grajales and blue: Yildiz) and with shapes corresponding to the tissue type from which they were collected (Dot: liver, triangle: pancreatic islets). B: Euclidean distance matrix plot. C: Poisson distance matrix plot. For both distance matrices, a dark blue shows a smaller distance between two samples, being the diagonal the comparison between each sample to itself. The lighter the shade of blue symbolizes the more significant distance between the samples compared.

Three clusters formed, two on the left side of the X-axis and one on the right side. By colouring the plots by the researcher who provided the samples and giving them shape according to the type of tissue from which the samples were obtained, it is possible to recognize that while on the X-axis, the samples are divided according to the tissue type (liver or pancreatic islets), on the Y-axis the samples divide according to the researcher who provided them. This outcome is expected as the samples were processed by different people, also confirming that the gene expression is differential among the tissue types.

Euclidean (Figure 12B) and Poisson (Figure 12C) distances matrices were plotted to confirm what was seen on the PCA plot. We observed that all samples processed by the same researcher clustered together, confirming that the three clusters of samples correlate with which laboratory team processed them. However, it is important to notice that the more significant difference could be accounted to the tissue type from which the samples proceed. In fact, the most considerable distances were computed when comparing the pancreatic islets against any liver sample. Taking into account these results, we decided to study the liver and pancreatic islet samples separately.

4.3.2.1 Pancreatic islets samples' analysis

A PCA of the pancreatic islets samples did not produce any clusters (Figure 13), suggesting that the number of dysregulated genes may be small.

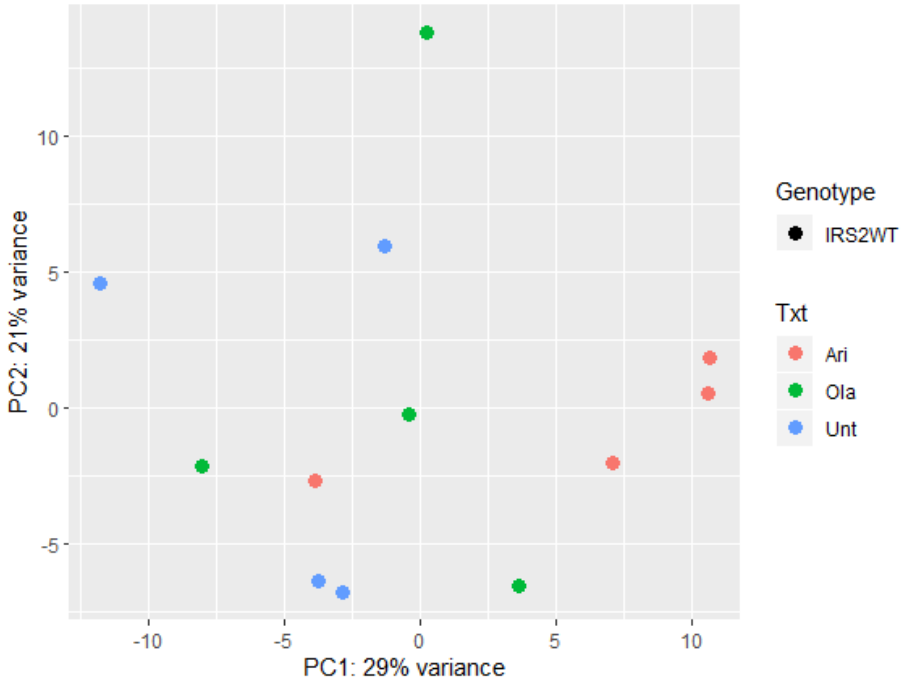

Figure 13. PCA of pancreatic islets from mice treated with aripiprazole, olanzapine or placebo diet

Following a similar approach to the one explored for the human samples, we decided to run a differential expression analysis comparing the gene expression of pancreatic islets from WT mice treated with aripiprazole compared with the gene expression of the mice fed with a placebo diet (Chow). This analysis yielded a total of 143 up-regulated genes and 97 down-regulated. A PCA of the DEGs produced two clusters that separated the samples according to the treatment given to the mice (aripiprazole, chow) (Figure 14A). The results of a GSEA against the KEGG database are shown in Figure 14B.

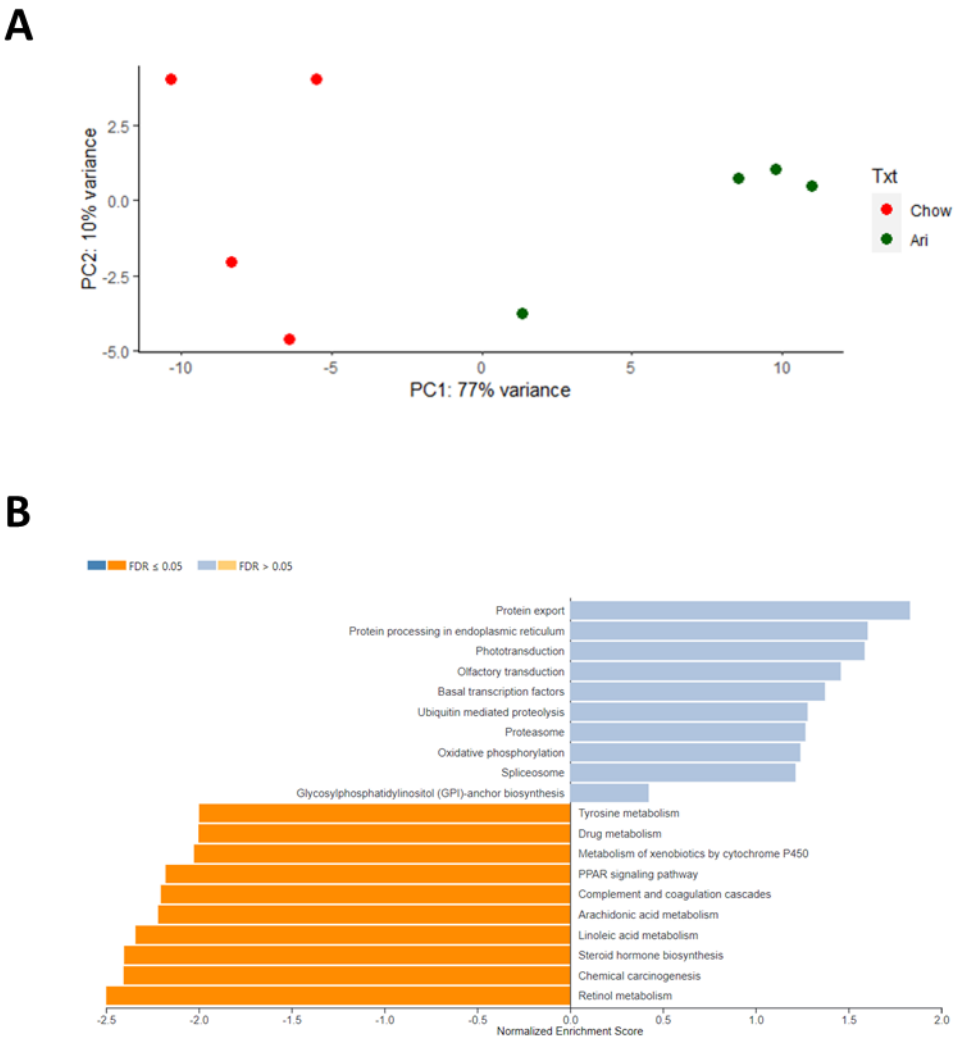

Figure 14. PCA of DEGs and GSEA of pancreatic islets from mice treated with aripiprazazole Vs untreated mice

PCA of the pancreatic islets' DEGs produced by the treatment with aripiprazole (A) KEGG pathways enriched by GSEA. The "x" axis represents the normalized enrichment score assigned to each pathway. The bars coloured blue represent up-regulated pathways, while the orange bars represent down-regulated ones (B).

The treatment with aripiprazole led to the up-regulation of pathways with FDR> 0.05, from which “Protein export” was the most overexpressed one with a NES= 1.83. However, no individual genes within the pathway had a Log2FoldChange> 1.50. Other overexpressed gene sets were: Protein processing in the endoplasmic reticulum (NES= 1.60), with no genes with a Log2FoldChange> 1.50; Phototransduction (NES= 1.59), from which *Calml3* was the top up-regulated gene with a Log2FoldChange= 1.92; Olfactory transduction (NES= 1.46), from which several olfactory receptor genes had a Log2FoldChange> 1.5, being *Olfr1016*, *Olfr584* and *Olfr1051* with Log2FoldChange = 4.21, 3.77 and 3.19, respectively the top up-regulated ones; Basal transcription factors (NES= 1.37), with no genes with a Log2FoldChange> 1.50; Ubiquitin mediated proteolysis (NES= 1.28) from which *Ube2u* and *Gm10705* had Log2FoldChange= 2.64 and 1.71 respectively; Proteasome (NES= 1.27), with no genes with a Log2FoldChange> 1.50; the Oxidative phosphorylation geneset (NES= 1.24) which included cytochrome c oxidase subunit genes as top up-regulated genes: *Cox6b2* (Log2FoldChange= 1.69), *Cox7b2* (Log2FoldChange= 1.46) and *Cox7a1* (Log2FoldChange= 1.39); Spliceosome (NES= 1.22); and Glycosylphosphatidylinositol (GPI)-anchor biosynthesis (NES= 0.42) both with no genes with a Log2FoldChange> 1.50.

The down-regulated pathways by aripiprazole included genesets with FDR> 0.05 as Retinol metabolism (NES= -2.50) from which several cytochrome P450 had a Log2FoldChange> 2. The top 3 were: *Cyp3a41a* (Log2FoldChange= -18.89), *Cyp3a11* (Log2FoldChange= -18.48) and *Cyp2a5* (Log2FoldChange= -16.35); Chemical carcinogenesis (NES= -2.40), which shared *Cyp3a41a* and *Cyp3a11* as top down-regulated genes; Steroid hormone biosynthesis (NES= -2.40), Linoleic acid metabolism (NES= -2.34) and Arachidonic acid metabolism (NES= -2.22) also included several cytochrome P450 genes as top down-regulated genes. Other down-regulated genesets were: Complement and coagulation cascades (NES= -2.20), from which *Kng1* (Log2FoldChange= -19.79), *Fga* (Log2FoldChange= -7.02) and *Fgg* (Log2FoldChange= -6.35) were the top down-regulated genes; PPAR signaling pathway (NES= -2.18), from which the top down-regulated genes included *Cyp4a14* (Log2FoldChange= -4.74), *Fabp1* (Log2FoldChange= -4.74) and Hmgcs2 (Log2FoldChange= -4.70); Metabolism of xenobiotics by cytochrome P450 (NES= -2.03), from which different UDP glucuronosyltransferases and cytochrome P450 genes made up to the top down-regulared genes: *Ugt1a1* (Log2FoldChange= -4.37), *Cyp2f2* (Log2FoldChange= -4.31), *Ugt2b5* (Log2FoldChange= -4.27), among others; Drug metabolism (NES= 2.00) from which the top down-regulated genes included *Ces1c* (Log2FoldChange= -19.16) among some UDP glucuronosyltransferase family genes as *Ugt1a1* (Log2FoldChange= -4.40) and *Ugt2b5* (Log2FoldChange= -4.27); and Tyrosine metabolism, from which *Hpd* (Log2FoldChange= -

19.10), *Aox3* (Log2FoldChange= -3.21) and *Adh4* (Log2FoldChange= -2.70) were the top down-regulated genes.

The differential expression analysis, comparing the pancreatic islets from mice treated with olanzapine against mice treated with the chow diet, produced 12 up-regulated and 3 down-regulated genes. As for aripiprazole, the PCA of the DEGs produced by the treatment with olanzapine separated the samples into two clusters: the samples from mice treated with olanzapine and the mice fed with the chow diet (Figure 15A). The results of a GSEA against the KEGG database are shown in (Figure 15B).

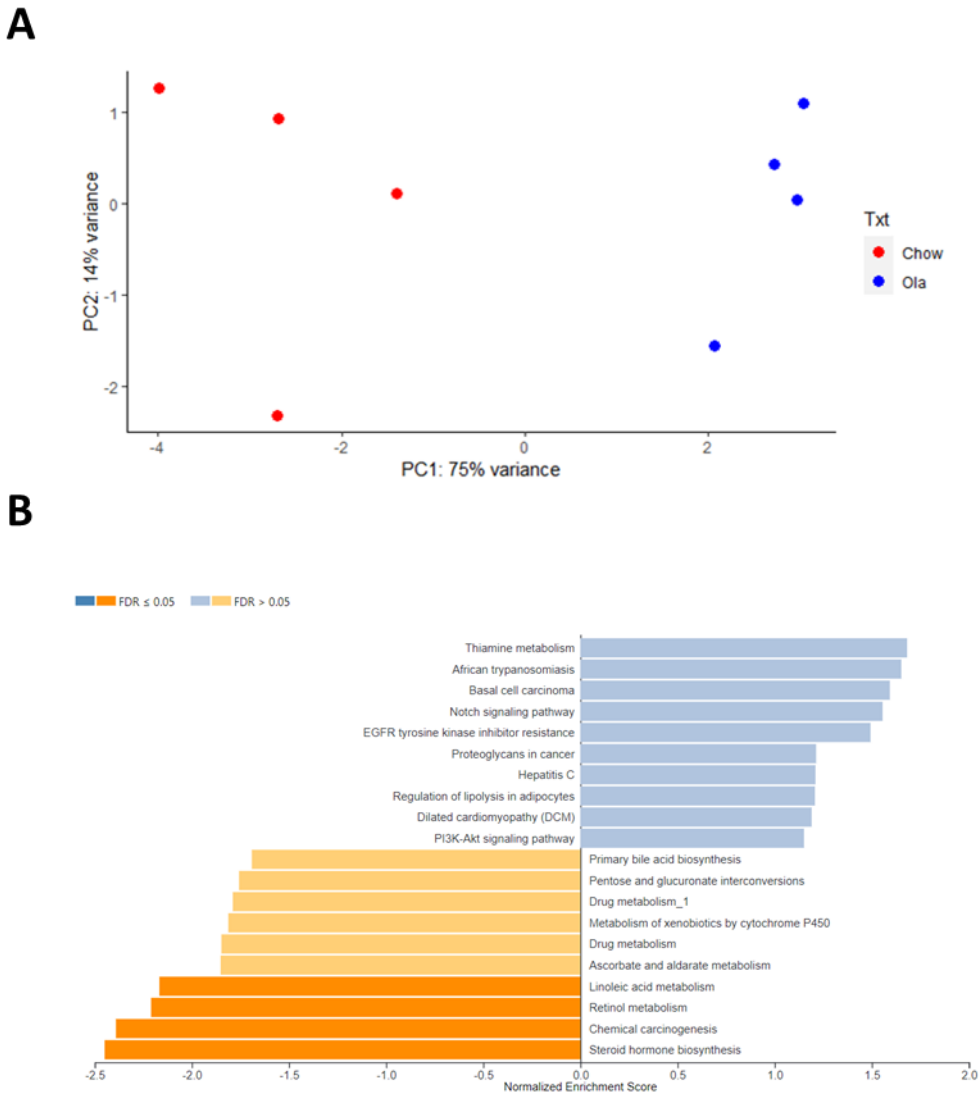

Figure 15. PCA and GSEA of pancreatic islets from mice treated with olanzapine Vs untreated mice

PCA of the pancreatic islets' DEGs produced by the treatment with olanzapine (A) KEGG pathways enriched by GSEA. The "x" axis represents the normalized enrichment score assigned to each pathway. The bars coloured blue represent up-regulated pathways, while the orange bars represent down-regulated ones (B).

The up-regulated genesets had an FDR> 0.05 and included pathways as Thiamine metabolism (NES= 1.49), from which *Alpi* (Log2FoldChange= 4.02) and *Akp3* (Log2FoldChange= 2.76) were represented; EGFR tyrosine kinase inhibitor resistance, from which platelet derived growth factor receptor, alpha polypeptide gene (*Pdgfra*) was the top up-regulated gene with a Log2FoldChange= 2.26; Proteoglycans in cancer (NES= 1.21) from which *Wnt2* (Log2FoldChange= 4.78) and *Dcn* (Log2FoldChange= 1.54) were the top up-regulated genes; Regulation of lipolysis in adipocytes (NES= 1.21), from which the insulin receptor substrate 4 gene (*Irs4*, Log2FoldChange= 2.43) and *Ptgs2* (prostaglandin-endoperoxide synthase 2) (Log2FoldChange= 2.41) were the top up-regulated genes; Dilated cardiomyopathy (DCM) (NES= 1.19) with no genes having a Log2FoldChange> 1.5; and PI3K-Akt signaling pathway (NES= 1.15), from which *Pdgfra* (Log2FoldChange= 2.26) and *Lama1* (Log2FoldChange= 1.52) were the top up-regulated genes within the set.

The analysis produced 4 down-regulated pathways with an FDR< 0.05: Steroid hormone biosynthesis (NES= -2.45) from which several cytochrome P450 family genes and UDP glucuronosyltransferase genes were included. Within the geneset, *Cyp3a41b* (Log2FoldChange= -24.31), *Cyp2c39* (Log2FoldChange= -5.20) and *Hsd17b2* (Log2FoldChange= -3.00) were the top down-regulated genes. *Cyp3a41b* and *Cyp2c39* repeated as top down-regulated for other pathways as Chemical carcinogenesis (NES= -2.39); Retinol metabolism (NES= -2.21) and Linoleic acid metabolism (NES= -2.17) pathways. Other down-regulated genesets with FDR> 0.05 are: Ascorbate and aldarate metabolism (NES= -1.85), that included several UDP glucuronosyltransferase family genes as *Ugt1a5* (Log2FoldChange= -1.94), *Ugt1a9* (Log2FoldChange= -1.77) and *Ugt2b1* (Log2FoldChange= -1.71). Other downregulated genesets included related genes: Drug metabolism (NES= -1.85); Metabolism of xenobiotics by cytochrome P450 (NES= -1.81); and Pentose and glucuronate interconversions (-1.76). Primary bile acid biosynthesis (NES= -1.69) included as top down-regulated genes *Cyp7a1* (cytochrome P450, family 7, subfamily a, polypeptide 1), with a Log2FoldChange= -2.48 and *Baat* (bile acid-Coenzyme A: amino acid N-acyltransferase), with a Log2FoldChange= -1.66.

In summary, the differential expression profile of pancreatic islets from WT mice treated with aripiprazole showed up-regulation of pathways related to protein processing and export and oxidative phosphorylation, and down-regulation of the metabolism of different molecules such as fatty acids and hormones. The profile of pancreatic islets from WT mice treated with olanzapine showed up-regulation of pathways involved in cellular functions and down-regulation of the metabolism of molecules such as fatty acids, vitamins and hormones.

4.3.2.2 Liver tissue samples' analysis

We performed differential expression analyses between liver samples from WT mice treated with aripiprazole or olanzapine Vs untreated mice liver samples for both short- and long-term schemes. There were 169 up-regulated and 95 down-regulated genes with aripiprazole and 832 up-regulated and 775 down-regulated genes with olanzapine for the short-term treatments (5 days). On the other hand, the long-term treatments (6 months) produced 220 up-regulated and 190 down-regulated genes with aripiprazole and 85 up-regulated and 148 down-regulated genes with olanzapine (Figure 16).

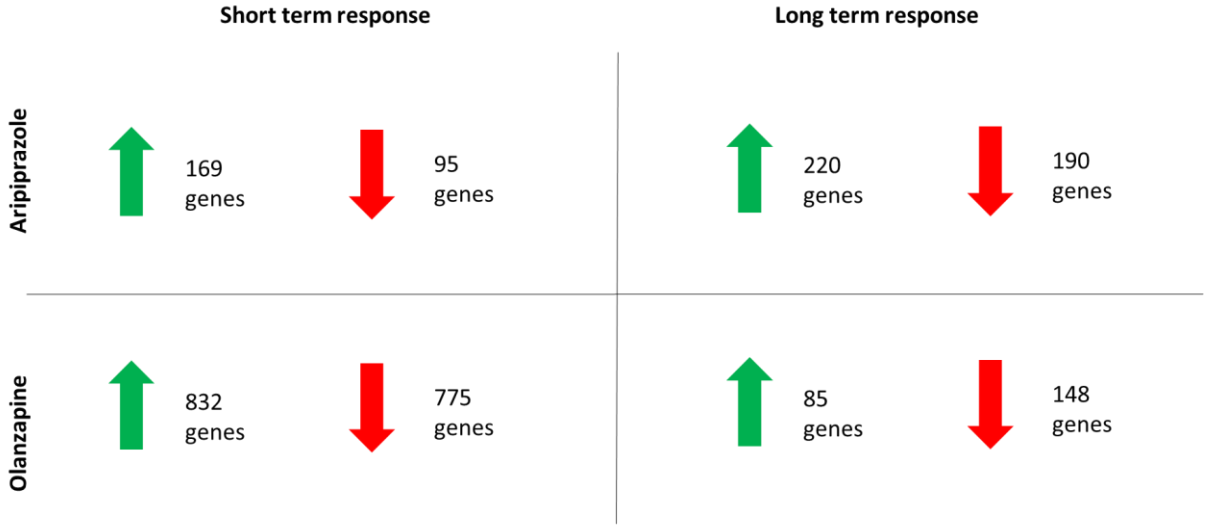

Figure 16. DEGs on liver samples from WT mice treated with aripiprazole and olanzapine after short-term (5 days) and long-term (6 months) treatment schemes.
The green arrows symbolize the up-regulated genes, while the red arrows symbolize the down-regulated ones.

We performed enrichment analyses against the KEGG database for the genes ranked by their fold changes when comparing the short-term treated mice Vs the WT untreated ones (Figure 17). All pathways altered by aripiprazole had an FDR> 0.05. The top up-regulated pathway was the Calcium signalling pathway (NES= 1.85), from which *Tnnc2* was the top up-regulated gene with a Log2FoldChange= 24.76. Other up-regulated genesets that included several up-regulated myosin and calcium channel genes, from which the top one was *Myh2* (Log2FoldChange= 25.62), were the Tight junction (NES= 1.83); Arrhythmogenic right ventricular cardiomyopathy (ARVC) (NES= 1.78); Hypertrophic cardiomyopathy (NES= 1.76); Dilated cardiomyopathy (NES= 1.74); Cardiac muscle contraction (NES= 1.70), from which the top genes also included cytochrome c oxidase genes as *Cox8b* (Log2FoldChange= 7.17); and

Focal adhesion (NES= 1.70), from which the top gene was *Thbs4* (thrombospondin 4, Log2FoldChange= 21.74). Other up-regulated genesets were the Biosynthesis of amino acids (NES= 1.75), that had as top genes *Pgam2* (Log2FoldChange= 3.42); *Asns* (Log2FoldChange= 2.29) and *Bcat1* (Log2FoldChange= 2.11); Phagosome geneset (NES=1.67), from which *Thbs4* was the top gene; and Arginine biosynthesis (NES= 1.63).

The top down-regulated geneset by the short-term treatment with aripiprazole was the olfactory receptor (NES= -1.31), having several olfactory receptor genes with a Log2FoldChange< -1.5. Other down-regulated genesets were the Carbohydrate digestion and absorption (NES= -1.30), from which the top genes were the amylase genes *Amy2a2, Amy2a3* and *Amy2a4*, all of them with a Log2FoldChange= -2.32; Asthma (NES= -1.27), from which *Il4* had a Log2FoldChange= -1.55; mRNA surveillance pathway (NES= -1.25), from which *Pabpc1l* (poly(A) binding protein, cytoplasmic 1-like, Log2FoldChange= -3.71) and *Nxf7* (nuclear RNA export factor 7, Log2FoldChange= -2.22) were the top genes;

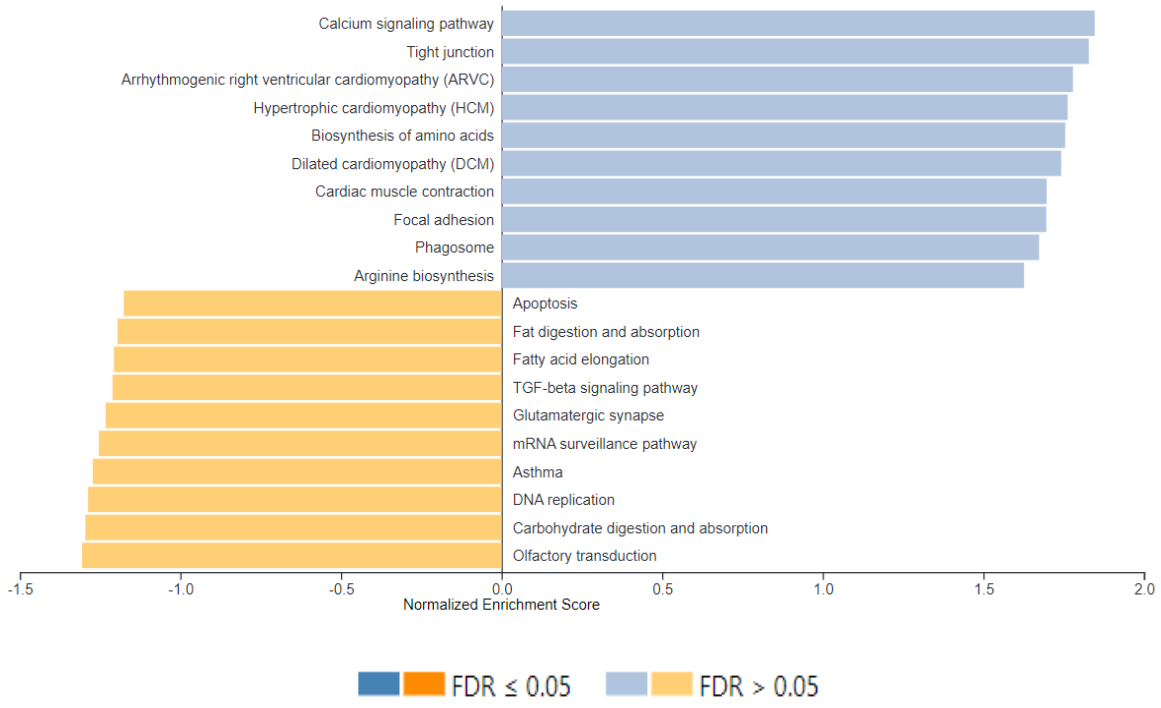

Figure 17. GSEA against the KEGG database of liver samples from mice treated 5 days with aripiprazole Vs untreated mice

The figure shows the KEGG pathways dysregulated after 5 days treatment with aripiprazole. The "x" axis represents the normalized enrichment score assigned to each pathway. The bars coloured blue represent up-regulated pathways, while the orange bars represent down-regulated ones.

Glutamatergic synapse (NES= -1.23), having glutamate receptor genes as *Grm6* (Log2FoldChange= -2.63), *Gria1* (Log2FoldChange= -2.23) and Grin2b (Log2FoldChange= -

1.86) in the top down-regulated genes; TGF-beta signaling pathway (NES= -1.21), from which *Fst* (follistatin, Log2FoldChange= -2.02) and *Id3* (Log2FoldChange= -1.95) were the top genes; Fat digestion and absorption (NES= -3.82) had as top gene *Pnlip* (pancreatic lipase, Log2FoldChange= -1.86). DNA replication (NES= -1.29); Fatty acid elongation (NES= -1.21); and Apoptosis (NES= -1.18) had no genes with a Log2FoldChange< -1.5.

When comparing the liver samples from the mice treated with olanzapine Vs those untreated some pathways resulted enriched with an FDR> 0.05 (Figure 18). Out of them, the most up-regulated was the Systemic lupus erythematosus (NES= 2.06), from which several histone cluster genes had a Log2FoldChange> 1.50. Other up-regulated pathways were Cardiac muscle contraction (NES= 1.96), from which the top up-regulated gene was *Cox6a2* (cytochrome c oxidase subunit 6A2, Log2FoldChange= 17.07), followed by *Actc1* (actin, alpha, cardiac muscle 1, Log2FoldChange= 5.01), *Atp1a4* (ATPase, Na+/K+ transporting, alpha 4 polypeptide, Log2FoldChange= 2.29), *Myl2* (myosin, light polypeptide 2, regulatory, cardiac, slow, Log2FoldChange= 2.23), *Cacng7* (calcium channel, voltage-dependent, gamma subunit 7, Log2FoldChange= 2.07) among others; Staphylococcus aureus infection (NES= 1.71), included as top up-regulated genes *Cfd* (complement factor D (adipsin), Log2FoldChange= 3.12), *Dsg1a* (desmoglein 1 alpha, Log2FoldChange= 2.77) and *H2-Oa* (histocompatibility 2, O region alpha locus, Log2FoldChange= 2.51); which was also included in the Th1 and Th2 cell differentiation geneset (NES= 1.64), from which *Tbx21* was the top up-regulated gene (Log2FoldChange= 2.84); the Intestinal immune network for IgA production (NES= 1.70) and Asthma (NES= 1.66) pathways, shared *H2-Oa* as top up-regulated gene; the alcoholism (NES= 1.67) geneset included several up-regulated histone cluster 1 genes, being *Hist1h3c* the top up-regulated one with a Log2FoldChange= 3.6. The Parkinson disease (NES= 1.64) and Oxidative phosphorylation (NES= 1.60) pathwasy shared *Cox6a2* as top up-regulated gene with a Log2FoldChange= 17.07; the Aldosterone synthesis and secretion (NES= 1.25) included several genes with a Log2FoldChange> 1.5 as *Cacna1h* (calcium channel, voltage-dependent, T type, alpha 1H subunit), *Hsd3b5* (hydroxy-delta-5-steroid dehydrogenase, 3 beta- and steroid delta-isomerase 5), *Atp1a4* (ATPase, Na+/K+ transporting, alpha 4 polypeptide), *Nr4a1* (nuclear receptor subfamily 4, group A, member 1), *Atp1a3* (ATPase, Na+/K+ transporting, alpha 3 polypeptide) and *Dagla* (diacylglycerol lipase, alpha).

The Arginine biosynthesis (NES= -1.52), Alanine, aspartate and glutamate metabolism (NES= -1.57), Biosynthesis of amino acids (NES= -1.52) and 2-Oxocarboxylic acid metabolism (NES= -1.46) were down-regulated by the short-term treatment with olanzapine, sharing *Got1* (glutamic-oxaloacetic transaminase 1, soluble, Log2FoldChange= -2.84) as top down-regulated gene. Several cytochrome P450 family genes were down-regulated leading to the enrichment of the Retinol metabolism (NES= -1.64), Arachidonic acid metabolism (NES= -

1.53) and Chemical carcinogenesis (NES= -1.49); from which *Cyp2a4* (Log2FoldChange= -4.44), *Cyp2b9* (Log2FoldChange= -4.31) and *Cyp2b10* (Log2FoldChange= -4.20), were the top down-regulated genes. Other down-regulared genesets were the Citrate cycle (TCA cycle) (NES= -1.57); the Ubiquinone and other terpenoid-quinone biosynthesis (NES= -1.50); and the Mineral absorption (NES= -1.47).

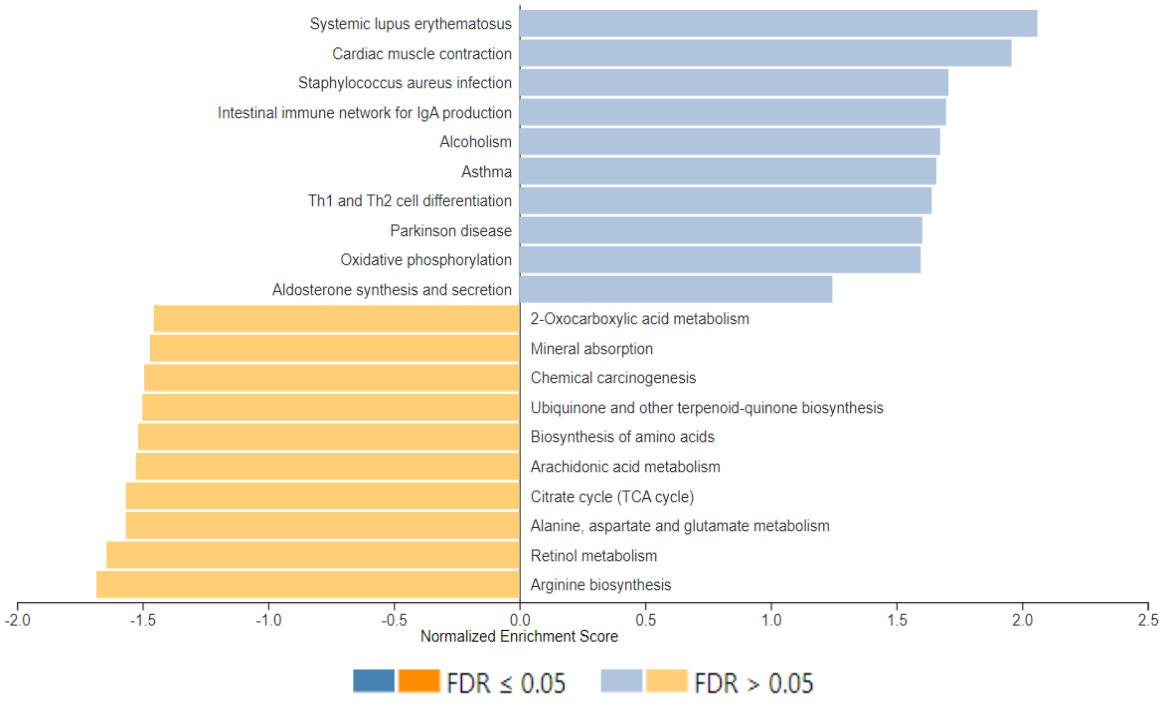

Figure 18. GSEA against the KEGG database of liver samples from mice treated 5 days with olanzapine Vs untreated mice

The figure shows the KEGG pathways dysregulated after 5 days treatment with olanzapine. The "x" axis represents the normalized enrichment score assigned to each pathway. The bars coloured blue represent up-regulated pathways, while the orange bars represent down-regulated ones.

We performed a GSEA against the Gene Ontology (GO) database to observe which biological processes are altered in the mice liver after the 5 days treatment with aripiprazole (Figure 19A) and olanzapine (Figure 19B). Aripiprazole up-regulated 5 biological processes with an FDR< 0.05: the Multicellular organismal movement (GO:0050879, NES= 2.20), Muscle system process (GO:0003012, NES= 2.33), Muscle cell differentiation (GO:0042692, NES= 2.17), Cellular component assembly involved in morphogenesis (GO:0010927, NES= 2.27), Actomyosin structure organization (GO:0031032, NES= 2.17) and Muscle organ development (GO:0007517, NES= 2.06); from which several actin, myosin and troponin genes exhibited Log2FoldChanges> 1.5. Some of the top up-regulated genes within these processes were *Acta1* (Log2FoldChange= 26.22), *Myh2* (Log2FoldChange= 25.62), *Tnnt3* (Log2FoldChange=

25.18), *Tnnc2* (Log2FoldChange= 25.18), *Tnni2* (Log2FoldChange= 24.61), *Myoz1* (Log2FoldChange= 22.05), among others. Other up-regulated genesets with an FDR> 0.05 were the Response to activity (GO:0014823, NES= 1.94, FDR= 0.02); Muscle tissue development (GO:0060537, NES= 1.98, FDR= 1.01); Actin filament-based movement (GO:0030048, NES= 1.90, FDR= 0.05) and Regulation of ATPase activity (GO:0043462, NES= 1.84, FDR= 0.11).

Contrary to the treatment with aripiprazole, the 5 days treatment with olanzapine led to the down-regulation (FDR> 0.05) of some biological processes that were up-regulated for aripiprazole as the Multicellular organismal movement (GO:0050879, NES= -2.03), Muscle system process (GO:0003012, NES= -1.83) and Response to activity (GO:0014823, NES= -1.64). Out of those processes, the top down-regulated genes were *Acta1* (Log2FoldChange= -17.75), *Tnnc2* (Log2FoldChange= -16.60), *Tnnt3* (Log2FoldChange= -16.24), Tnni2 (Log2FoldChange= -16.00), *Myh2* (Log2FoldChange= -17.12) and *Myoz1* (Log2FoldChange= -14.78). Other down-regulated biological processes were the Response to pH (GO:0009268, NES= -1.38), drug catabolic process (GO:0042737, NES= -1.75), Regulation of ATPase activity (GO:0043462, NES= -1.57), Cellular component assembly involved in morphogenesis (GO:0010927, NES= -1.67), Dicarboxylic acid metabolic process (GO:0043648, NES= -1.61) and Tricarboxylic acid metabolic process (GO:0072350, NES= -1.41).

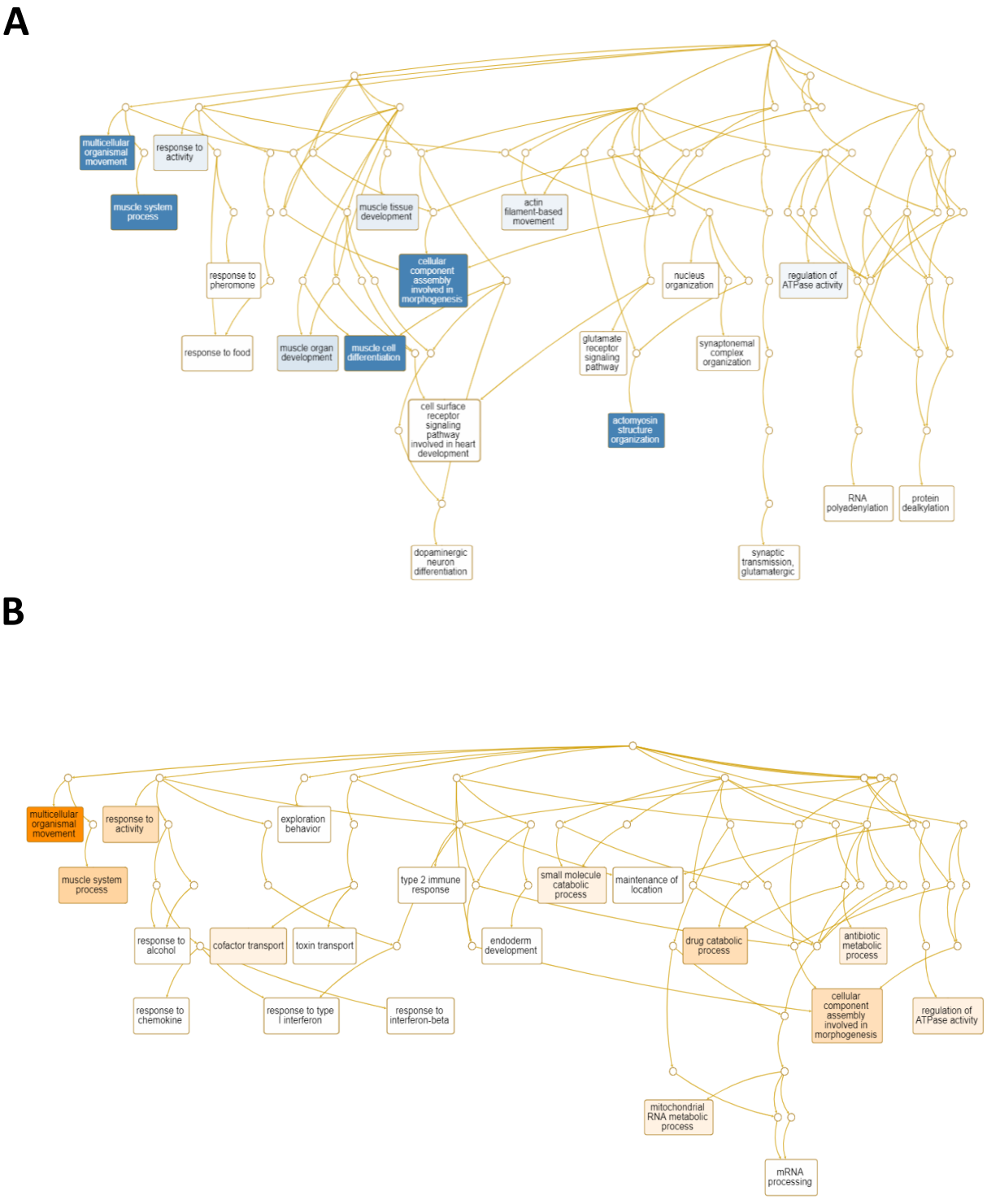

Figure 19. Gene Ontology Directed Acyclic Graphs of Biological Processes altered in mice liver by 5 days treatment with aripiprazole or olanzapine

The figure shows the biological processes dysregulated after the treatment with aripiprazole (A) and olanzapine (B). The boxes coloured blue represent up-regulated pathways, while the orange bars represent down-regulated ones.

We analyzed the effects of the long-term treatment (6 months) with aripiprazole and olanzapine. A GSEA analysis of the liver samples from mice treated with aripiprazole Vs WT mice untreated produced the enrichment of pathways with an FDR> 0.05 (Figure 20). The top up-regulated pathway was the PPAR signalling pathway (NES= 1.74), from which *Cyp4a10* (Log2FoldChange= 2.40) was the top up-regulated gene, followed by *Plin4* (Log2FoldChange= 2.19) and other cytochrome P450 family genes. Other up-regulated pathways included the Nicotine addiction (NES= 1.67) and GABAergic synapse (NES= 1.41) from which the gamma-aminobutyric acid (GABA) A receptor, subunits *Gabre* (Log2FoldChange= 5.14) and *Gabrd* (Log2FoldChange= 3.39) as well as the glutamate receptor Grin2b (Log2FoldChange= 3.72) were the top genes; African trypanosomiasis (NES= 1.63) included haemoglobin and interleukin genes from which *Hba-a1* (Log2FoldChange= 3.10), *Hbb-bs* (Log2FoldChange= 2.31) and *Il10* (Log2FoldChange= 2.14) were the top ones; out of the asthma (NES= 1.57) geneset only *Il10* had a Log2FoldChange> 1.50; beta-Alanine metabolism (NES= 1.56), from which *Gad2* (glutamic acid decarboxylase 2, Log2FoldChange= 2.71), *Aoc3* (amine oxidase, copper containing 3, Log2FoldChange= 1.84) and *Gadl1* (glutamate decarboxylase-like 1, Log2FoldChange= 1.57) were the top genes; the Cocaine addiction (NES= 1.54) included the glutamate receptors *Grin2b*, *Grin2c* (Log2FoldChange= 2.84) and *Grin2d* (Log2FoldChange= 1.50) as top genes; Fatty acid degradation (NES= 1.54), had cytochrome P450 genes: *Cyp4a10*, *Cyp4a14* (Log2FoldChange= 1.86) and *Cyp4a31* (Log2FoldChange= 1.62) as top up-regulated ones; the Arrhythmogenic right ventricular cardiomyopathy (ARVC) (NES= 1.41) included *Tcf7l1* (transcription factor 7 like 1) and *Cacng4* (calcium channel, voltage-dependent, gamma subunit 4) with Log2FoldChange> 2.00; and the Bladder cancer geneset (NES= 1.41) had *Cdkn1a* (Log2FoldChange= 4.49) and *Thbs1* (Log2FoldChange= 1.97) as top up-regulated genes.

The top down-regulated pathway after the six months treatment with aripiprazole was Vitamin B6 metabolism (NES= -1.57), which was enriched by *Aox4* (Log2FoldChange= -2.94), *Pdxp* (Log2FoldChange= -2.03) and *Psat1* (Log2FoldChange= -1.94). Other down-regulated pathways were Nitrogen metabolism (NES= -1.56), which included carbonic anhydrase genes, from which *Car9* (Log2FoldChange= -1.83) and *Car12* (Log2FoldChange= -1.55) were the most down-regulated ones; Systemic lupus erythematosus (NES= -1.51); Viral carcinogenesis (NES= -1.20) and Alcoholism, included several histone cluster 1 genes with Log2FoldChange< -1.50, being Hist1h4k (Log2FoldChange= -5.57) the top one; Steroid biosynthesis (NES= -1.46), with *Cyp27b1* (Log2FoldChange= -3.43) as most altered gene; Hedgehog signaling pathway (NES= -1.39) included *Dhh* (desert hedgehog, Log2FoldChange= -2.74) and *Ptch2* (patched 2, Log2FoldChange= -3.43) as top genes; Ribosome geneset had 2 ribosomal protein genes with Log2FoldChange< -1.50: *Rpl34-ps1* (Log2FoldChange= -5.90) and *Rpl3l*

(Log2FoldChange= -2.50); Olfactory transduction (NES= -1.24) was enriched by several olfactory receptor genes with Log2FoldChange< -1.50, from which *Olfr110* (Log2FoldChange= -4.36) was the most down-regulated one; Nucleotide excision repair (NES= -0.43) did not include any gene with a Log2FoldChange< -1.50.

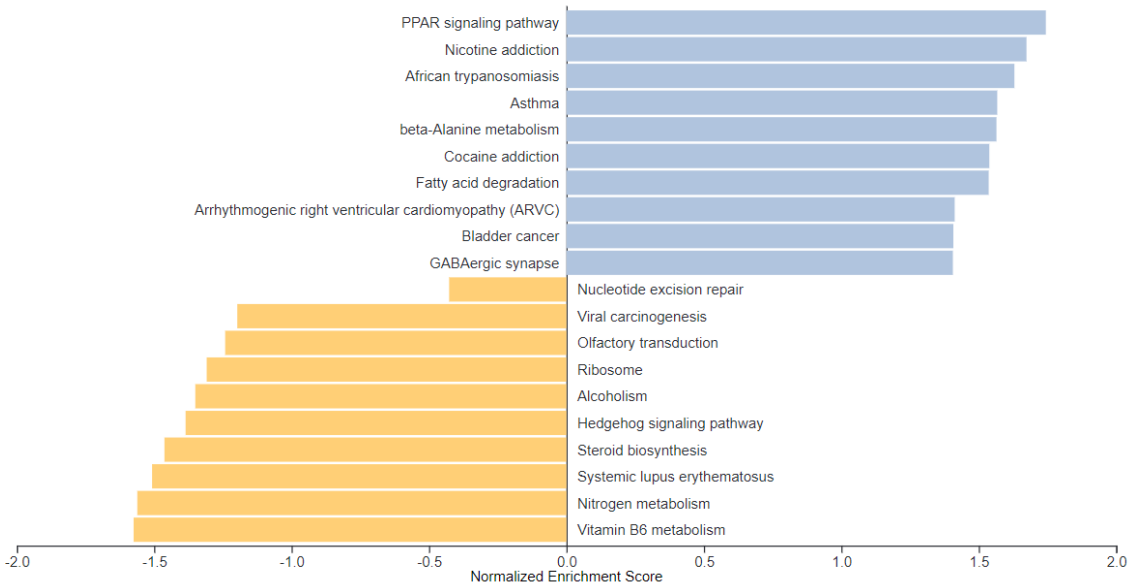

Figure 20. GSEA against the KEGG database of liver samples from mice treated 6 months with aripiprazole Vs untreated mice

The figure shows the KEGG pathways dysregulated after 6 months of treatment with aripiprazole. The "x" axis represents the normalized enrichment score assigned to each pathway. The bars coloured blue represent up-regulated pathways, while the orange bars represent down-regulated ones.

A GSEA analysis of the liver samples from mice treated with olanzapine Vs WT mice untreated produced the enrichment of pathways with an FDR> 0.05 (Figure 21). The top up-regulated pathway was Steroid biosynthesis (NES= 1.71), from which the top up-regulated gene was *Cyp27b1* (Log2FoldChange= 1.68). Other up-regulated pathways are: Malaria (NES= 1.48), which included the haemoglobin alpha genes *Hba-a1* (Log2FoldChange= 2.52), *Hbb-bs* (Log2FoldChange= 2.42) and *Hba-a2* (Log2FoldChange= 1.78) as top up-regulated genes; and the Olfactory transduction (NES= 1.39) pathway, that was enriched by several olfactory receptor genes with a Log2FoldChange> 1.5, from which *Olfr1135* (Log2FoldChange= 3.01) was the top one. Glycosphingolipid biosynthesis (NES= 1.63), Terpenoid backbone biosynthesis (NES= 1.53), Arginine biosynthesis (NES= 1.40), Glycosaminoglycan biosynthesis (NES= 1.32) and Phenylalanine, tyrosine and tryptophan biosynthesis (NES= 1.29) were also up-regulated, although with no genes with a Log2FoldChange> 1.50.

The top down-regulated pathways after 6 months of treatment with olanzapine were the Systemic lupus erythematosus (NES= -1.83) and the Alcoholism (NES= -1.71) genesets; which were enriched by several histone cluster genes, from which *Hist1h2ao* (Log2FoldChange= -4.74) was the most repressed one. Other down-regulated pathways included the PPAR signalling pathway (NES= -1.65), from which the top repressed genes were *Gk2* (Log2FoldChange= -4.27), *Cyp4a31* (Log2FoldChange= -2.11) and *Plin4* (Log2FoldChange= -1.89); Biosynthesis of unsaturated fatty acids (NES= -1.52) that had acyl-CoA thioesterase genes *Acot3* (Log2FoldChange= -2.15) and *Acot1* (Log2FoldChange= -1.55) as the most repressed ones; Oocyte meiosis (NES= -1.48) that included as top genes *Plcz1* (Log2FoldChange= -3.90), *Sgo1* (Log2FoldChange= -2.83), *Bub1* (Log2FoldChange= -2.34), *Ins1* (Log2FoldChange= -2.27), and *Ins2* (Log2FoldChange= -2.04); Asthma (NES= -1.48), from which *Il10* (Log2FoldChange= -2.00) was the most down-regulated gene; Fat digestion and absorption (NES= -1.45), having *Pla2g2d* (Log2FoldChange= -2.36) as top repressed gene; Circadian entrainment (NES= -1.45), which had the glutamate receptor, ionotropic genes *Grin2c* (Log2FoldChange= -3.84), *Grin2d* (Log2FoldChange= -2.63), *Grin2b* (Log2FoldChange= -2.02) and the calcium channel, voltage-dependent gene *Cacna1i* (Log2FoldChange= -2.50) as the most down-regulated genes; Hepatitis C (NES= -1.44) had *Ifit1bl1* (Log2FoldChange= -2.59) as top gene; and beta-Alanine metabolism (NES= -1.42) had *Gadl1* (Log2FoldChange= -1.78).

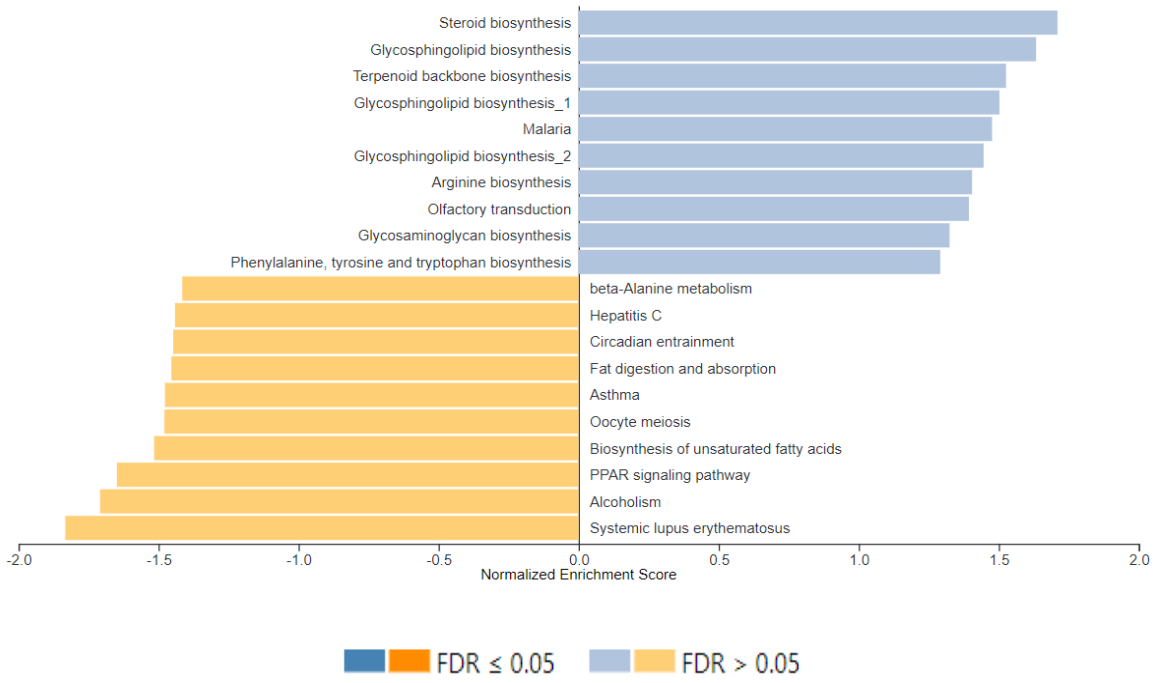

Figure 21. GSEA against the KEGG database of liver samples from mice treated 6 months with olanzapine Vs untreated mice

The figure shows the KEGG pathways dysregulated after 6 months of treatment with olanzapine. The "x" axis represents the normalized enrichment score assigned to each pathway. The bars coloured blue represent up-regulated pathways, while the orange bars represent down-regulated ones.

We made a comparison between the genes that were significantly dysregulated (adjPval < 0.05) between the short- and long-term treatments to understand if the prompt response is maintained or changed through time. The treatments with aripiprazole produced 40 dysregulated genes in both the short- and long-term responses (Table 4). However, while some genes were initially repressed (5 days), after six months, they became up-regulated. The more extreme examples of this case are *Slc34a2* and *Pdk4,* which have 5.17 and 3.52 times overexpression after the long-term treatment compared to the short-term response. On the other hand, *Moxd1*, *Orm2* and *Col6a5* were highly overexpressed by the short-term treatment, but over time, they became highly repressed, having -9.64, -6.63 and -5.76 times response differences, respectively. There was also a group of genes that were not modified by the short-term treatment but by the long-term one, and a group of genes that showed similar responses all over time. Overrepresentation enrichment analyses of the 40 genes returned the enrichment of metabolic pathways as PPAR signalling pathway (*Acsl1, Plin2, Angptl4*), Fatty acid biosynthesis (*Acsl1*), Parathyroid hormone synthesis, secretion and action (*Slc34a2*, *Cdkn1a*), Fatty acid degradation (*Acsl1*); and biological processes as Regulation of lipid metabolic process (*Acsl1, Chd9, G0s2, Plin2, Angptl4*) and Regulation of primary metabolic process (Table 6).

The treatments with olanzapine produced 43 commonly dysregulated genes for both the short- and long-term treatments (Table 5). Similar patterns as with aripiprazole raised. *Sult1e1* and *Ciart* were the most repressed genes by the short treatment, which also became significantly up-regulated after the 6 months, producing a 6.84 and 6.41 times response difference between the time schemes. *Pitx3* and *Gbp10* were the most up-regulated genes initially by olanzapine, which became repressed after the long-term treatment, making a -8.78 and -4.28 times response difference between the schemes. Overrepresentation enrichment analysis of the 43 genes (Table 7) returned the enrichment of KEGG pathways as Fatty acid degradation (*Cpt1a*, *Eci2*, *Acsl3*), PPAR signalling pathway (*Cpt1a*, *Plin4*, *Acsl3*, *Angptl4*), Peroxisome (*Pex11a, Eci2, Crot, Acsl3*), Fatty acid biosynthesis (*Acsl3*), Cholesterol metabolism (*Nceh1, Angptl4*), Insulin resistance (*Cpt1a*, *Ppp1r3b*, *Ppargc1b*), Adipocytokine signalling pathway (*Cpt1a, Acsl3*).

Table 4. Dysregulated genes (adjPval < 0.05) in mice liver after short- and long-term tretment with aripiprazole

Gene	Short term Log2FoldChange	Long term Log2FoldChange	FoldChange
Slc34a2	-1,71	3,46	5,17
Pdk4	-1,15	2,37	3,52
Cdkn1a	1,39	4,49	3,10
Mthfr	-0,69	2,17	2,86
Clstn3	-1,42	1,32	2,74
Slc17a8	-1,16	1,54	2,70
G0s2	-1,29	1,23	2,52
Trmt9b	-0,82	1,59	2,41
Rnf125	-0,99	1,40	2,39
Rell1	-0,85	1,17	2,02
Ypel2	-0,88	1,12	2,00
Efna1	-1,10	0,81	1,91
Net1	-0,54	1,19	1,73
Plin2	-0,61	1,07	1,69
Ces1e	-0,50	0,78	1,28
Acsl1	-0,50	0,54	1,04
Mup2	-1,64	-0,66	0,98
Cnbd2	0,86	1,74	0,88
Angptl4	1,27	1,58	0,31
Chd9	0,88	1,18	0,30
Tedc2	0,86	1,11	0,25
Mfsd2a	1,53	1,69	0,15
Herpud1	1,15	0,93	-0,22
Zbtb16	1,80	1,53	-0,27
Tmem176b	0,49	-0,61	-1,10
Gne	0,71	-0,69	-1,40
Narf	0,70	-0,79	-1,50
Gpcpd1	0,83	-0,75	-1,58
Itih3	1,02	-0,57	-1,60
Coq10b	1,02	-1,16	-2,17
Por	1,03	-1,21	-2,23
Nucb2	1,09	-1,15	-2,24
Smpd3	0,94	-1,49	-2,43
Hpx	1,24	-1,20	-2,45
Cpne8	0,91	-1,62	-2,53
Apcs	0,91	-1,81	-2,72
Upp2	1,65	-1,97	-3,62
Col6a5	3,01	-2,75	-5,76
Orm2	4,34	-2,29	-6,63
Moxd1	3,71	-5,93	-9,64

Table 5. Dysregulated genes (adjPval < 0.05) in mice liver after short- and long-term tretment with olanzapine

Gene	Short term Log2FoldChange	Long term Log2FoldChange	FoldChange
Sult1e1	-3,83	3,00	6,84
Ciart	-4,87	1,54	6,41
Ppargc1b	-1,32	2,04	3,36
Cyp2c40	-1,40	1,36	2,76
Ces1b	-0,52	0,79	1,31
Mfsd2a	-2,62	-1,40	1,22
Txnip	-1,74	-0,57	1,17
Ppp1r3b	0,41	1,07	0,65
Cyp2a5	-2,00	-1,45	0,56
Enho	1,20	1,72	0,52
Plin4	-2,39	-1,89	0,49
Slc25a47	-1,28	-0,82	0,46
Angptl4	-1,75	-1,39	0,37
Acot3	-2,50	-2,15	0,35
Cpt1a	-1,00	-0,71	0,29
Lhpp	-0,82	-0,59	0,22
Cyp2c70	0,49	0,68	0,20
Eci2	-0,83	-0,65	0,18
Nceh1	-0,94	-0,79	0,15
Pex11a	-0,94	-0,81	0,14
Hykk	-0,69	-0,65	0,03
Tuba4a	0,87	0,69	-0,18
C8b	0,80	0,55	-0,24
Cyp4a32	-1,15	-1,41	-0,26
Gnpda1	-0,79	-1,12	-0,33
Tuba1c	1,07	0,70	-0,36
Acsl3	1,65	1,25	-0,39
4833420G17Rik	-0,75	-1,18	-0,42
Chic1	1,44	0,84	-0,61
Avpr1a	1,72	1,10	-0,62
Mup1	1,82	1,14	-0,67
Insig1	1,79	1,01	-0,78
Abtb2	1,74	0,95	-0,79
Lgals4	-1,29	-2,36	-1,07
Stat1	0,62	-0,65	-1,26
Ces1e	0,64	-0,77	-1,41
Crot	0,79	-0,69	-1,48
Paqr7	0,60	-1,03	-1,63
Acaa1b	0,85	-1,12	-1,98
Rtn4rl1	1,04	-1,05	-2,08
Elovl3	1,77	-1,13	-2,90
Gbp6	1,57	-1,94	-3,51
Clstn3	1,95	-1,88	-3,83
Gbp10	2,08	-2,20	-4,28
Pitx3	3,15	-5,62	-8,78

Table 6. Overrepresentation enrichment analysis of commonly dysregulated genes on liver samples from mice treated with aripiprazole in short- and long-term schemes

Index	Name	P-value	Odds Ratio	Combined score
KEGG	PPAR signaling pathway (*Acsl1, Plin2, Angptl4*)	0.0004354	20.27	156.88
KEGG	Fatty acid biosynthesis (*Acsl1*)	0.02570	38.46	140.82
KEGG	Parathyroid hormone synthesis, secretion and action (*Slc34a2, Cdkn1a*)	0.01904	9.43	37.37
KEGG	Fatty acid degradation (*Acsl1*)	0.08441	11.36	28.09
BP	fatty acid transport (GO:0015908) (*Acsl1, Mfsd2a*)	0.0007243	58.31	421.60
BP	Long-chain fatty acid transport (GO:0015909) (*Acsl1, Mfsd2a*)	0.001862	34.96	219.79

Table 7. Overrepresentation enrichment analysis of commonly dysregulated genes on liver samples from mice treated with olanzapine in short- and long-term schemes

Index	Name	P-value	Odds Ratio	Combined score
KEGG	Fatty acid degradation (*Cpt1a, Eci2, Acsl3*)	0.0001322	30.30	270.65
KEGG	PPAR signaling pathway (*Cpt1a, Plin4, Acsl3, Angptl14*)	0.00002293	24.02	256.65
KEGG	Peroxisome (*Pex11a, Eci2, Crot, Acsl3*)	0.00003609	21.42	219.11
KEGG	Fatty acid biosynthesis (*Acsl3*)	0.02887	34.19	121.20
KEGG	Cholesterol metabolism (*Nceh1, Angptl14*)	0.005662	17.78	91.98
KEGG	Insulin resistance (*Cpt1a, PPP1r3b, Ppargc1b*)	0.001843	12.35	77.74
KEGG	Adipocytokine signalling pathway (*Cpt1a, Ascl3*)	0.01055	12.88	58.63

4.3.2.2.1 Knockout mice studies

Trying to gain some further insight in the metabolic effect of the drugs, we studied two different KO mice modes that were available from our collaborators. For the first model, the PGC1α KO, after a five-day treatment with aripiprazole and olanzapine, we compared the gene expression between the KO and the WT mice. Aripiprazole treatment produced statistically significant (adjPval < 0.05) higher expression of 131 genes and lower expression of 124 genes on PGC1α KO mice compared to the WT. Olanzapine treatment, however, only produced 2 up-regulated and 3 down-regulated genes for PGC1α KO compared to the WT mice. A heatmap of the Log2FoldChanges for the most significant genes is shown in Figure 22.

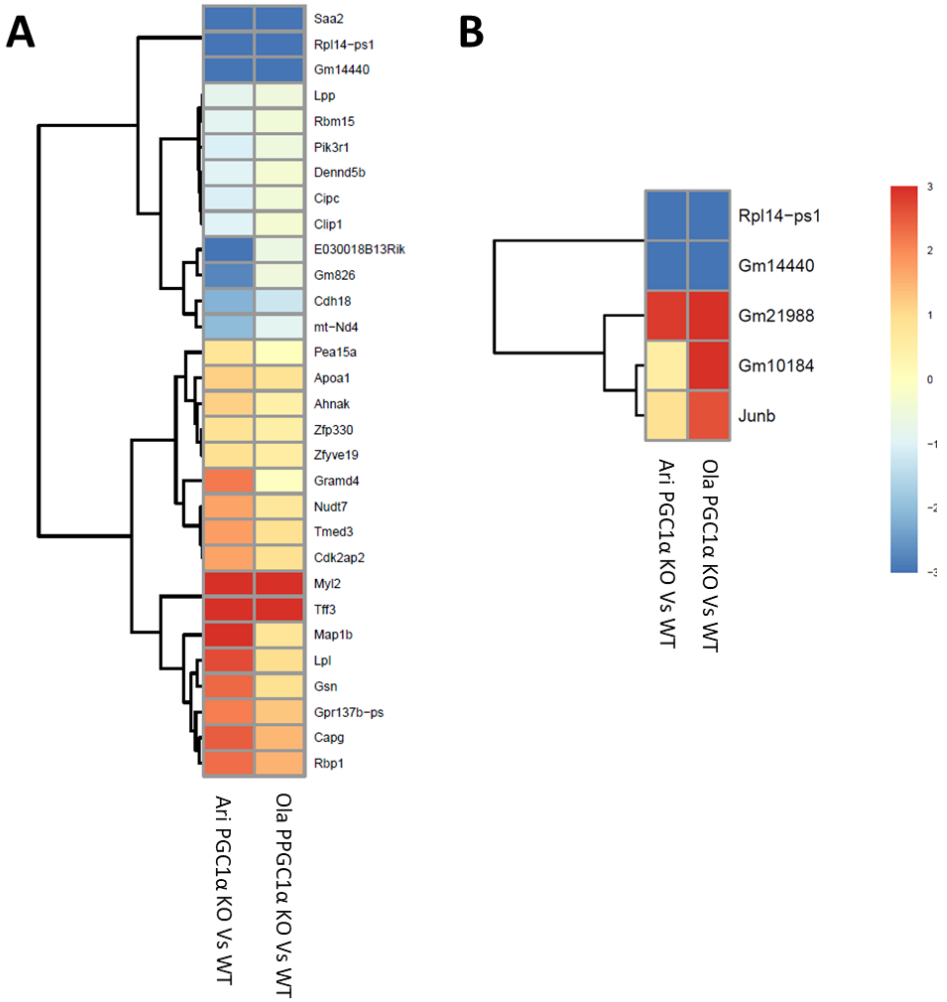

Figure 22. Heatmap of Log2FoldChanges for the top significantly genes when comparing PGC1α KO vs WT mice after a five days treatment with aripiprazole or olanzapine

The figure shows the Log2FoldChanges when comparing PGC1α KO vs WT mice's gene expression after a five days treatment with aripiprazole or olanzapine. The colour scale represents the expression of each gene for PGC1α KO mice compared with WT mice. Therefore, red represents the genes with a higher expression on KO mice than the WT, while blue represents the genes with a lower expression on the KO mice than the WT. Panel **A** shows the 30 genes with the smallest adjPvals after the treatment with aripiprazole and compares the gene expression after the treatment with olanzapine. On the other hand, panel **B** shows the 5 significantly dysregulated genes (adjPvals < 0.05) after the treatment with olanzapine and compares the gene expression after the treatment with aripiprazole.

For the second model, the PTP1B KO mice, we were able to run a six-month treatment approach. We found out that aripiprazole long-term treatement produced 164 genes significantly over-expressed (adjPval < 0.05) on the PTP1B KO mice compared to the WT, and 193 repressed genes. The six-month treatment with olanzapine produced the over-expression of 54 genes and the repression of 91 genes for the PTP1B KO mice compared to the WT. A heatmap of the Log2FoldChanges for the 30 genes with the smallest adjPvals can be seen in Figure 23.

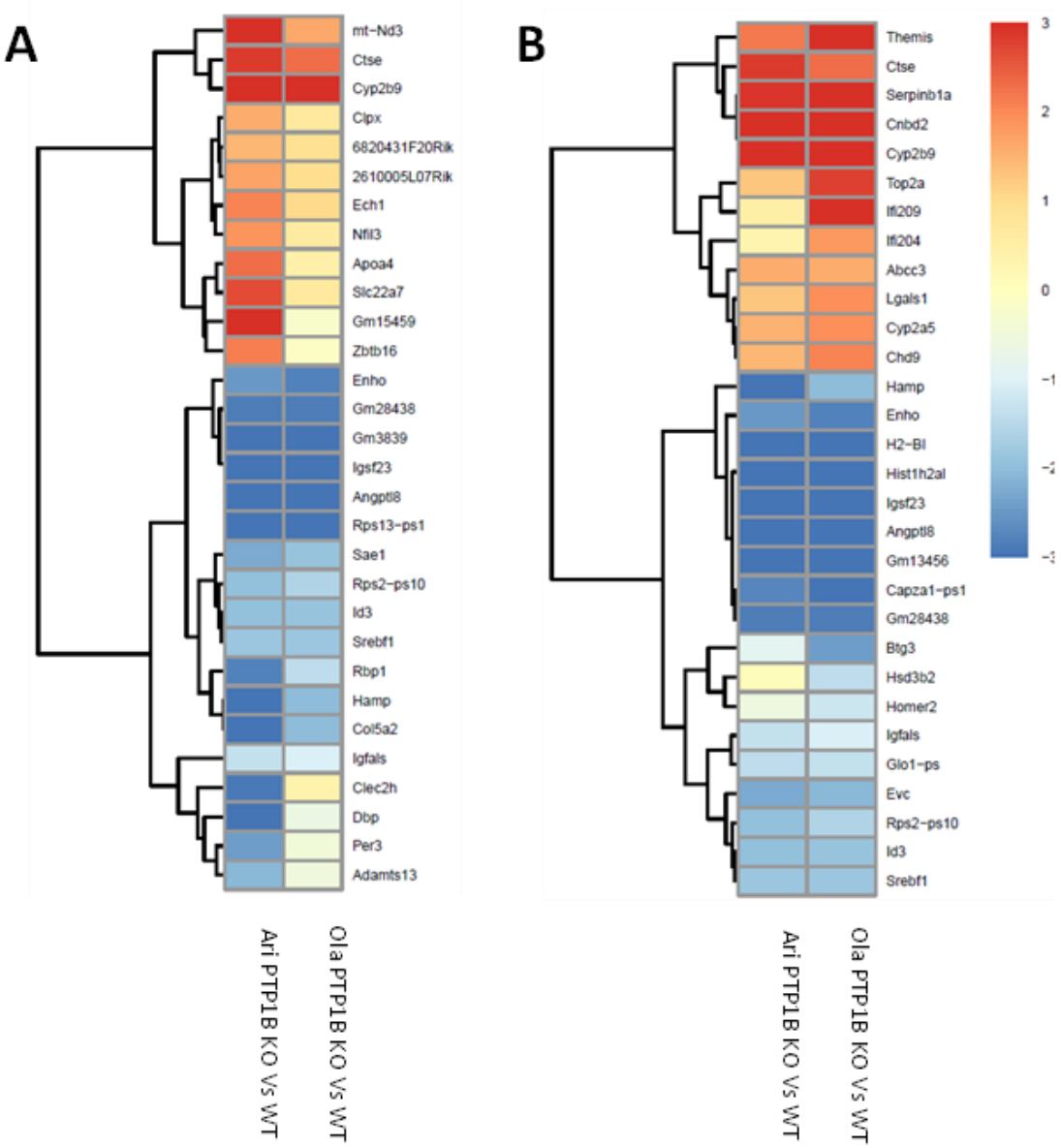

Figure 23. Heatmap of Log2FoldChanges for the top 30 genes with the smallest adjPvals when comparing PTP1B KO vs WT mice after a six months treatment with aripiprazole or olanzapine
The figure shows the Log2FoldChanges when comparing PTP1B KO vs WT mice's gene expression after six months of treatment with aripiprazole or olanzapine. The colour scale represents the expression of each gene for PTP1B KO mice compared with WT mice. Therefore, red represents the genes with a higher expression on KO mice than the WT, while blue represents the genes with a lower expression on the KO mice than the WT. Panel **A** shows the 30 genes with the smallest adjPvals after the treatment with aripiprazole and compares the gene expression after the treatment with olanzapine. On the other hand, panel **B** shows the 30 genes with the smallest adjPvals after the treatment with olanzapine and compares the gene expression after the treatment with aripiprazole.

4.4. Healthy volunteers stratification

We quantitatively tested the similarity among the transcriptomic response of the samples to the two treatments by computing two sample-to-sample distance matrices. One matrix shows euclidean distances between the samples (Figure 24A), and the other one shows Poisson Distances (Figure 24B). The Poisson distance method clustered together more of the volunteers' samples than the Euclidean distance method. For 5/12 (euclidean distance) and 7/12 (poison distance) volunteers, the 4 samples were clustered together, while for 4/12 (euclidean distance) and 3/12 (poison distance) volunteers, at least 3 samples clustered together. RNA-seq data includes only positive counts, modelled better by a discrete count distribution as the negative binomial or Poisson.

Consequently, methods that assume a Gaussian distribution like the Euclidean distance will not perform well with RNA-seq data (Witten 2011). Therefore, it could be safer to assume that the more accurate clustering was obtained using the Poisson distance than the Euclidean distance, although the Euclidean distance method provided similar outcomes. This quantitative clustering correlates with the previous PCA that plotted relatively close to each other, the 4 samples from some volunteers while plotting apart the samples from other volunteers. These results suggest that the volunteers have a differential response to the treatments. While some volunteers showed limited responses, as their samples almost did not modify their gene expression, others had stronger responses, getting their gene expression modified and therefore, their samples clustered apart.

To study the response differences among the volunteers, we did an interaction analysis with the **design= = ~ Volunteer + Condition + Volunteer:Condition**. This model test if the condition effect (Log2FoldChange T5 Vs T0) varies across the volunteers. To statistically test each gene Log2FoldChange difference among the volunteers, we performed a likelihood ratio test (LRT) that examines two counts models: a **full model= ~ Volunteer + Condition + Volunteer:Condition**, and a **reduced model = ~ Volunteer + Condition**, in which some terms of the full model are removed to determine if the increased likelihood of the data using the extra terms in the full model is more than expected if those extra terms are truly zero. Therefore this comparison allows us to understand if differences in the response can be attributed to having different volunteers in the analysis. In practice, LRT is similar to an ANOVA test, allowing us to test multiple interactions between two variables. In this case, we will test if each of the genes response for each volunteer is similar or different from a reference volunteer who we chose to be volunteer 24, which showed small responses to the treatments, according to the sample to sample distance matrices. **The LRT test returned 805 genes with statistically significant differential responses across the volunteers (adjPval < 0.1)**. A

gene with a small p-value on this test will be that one for which one or more volunteers showed a different response to the one had by volunteer 24.

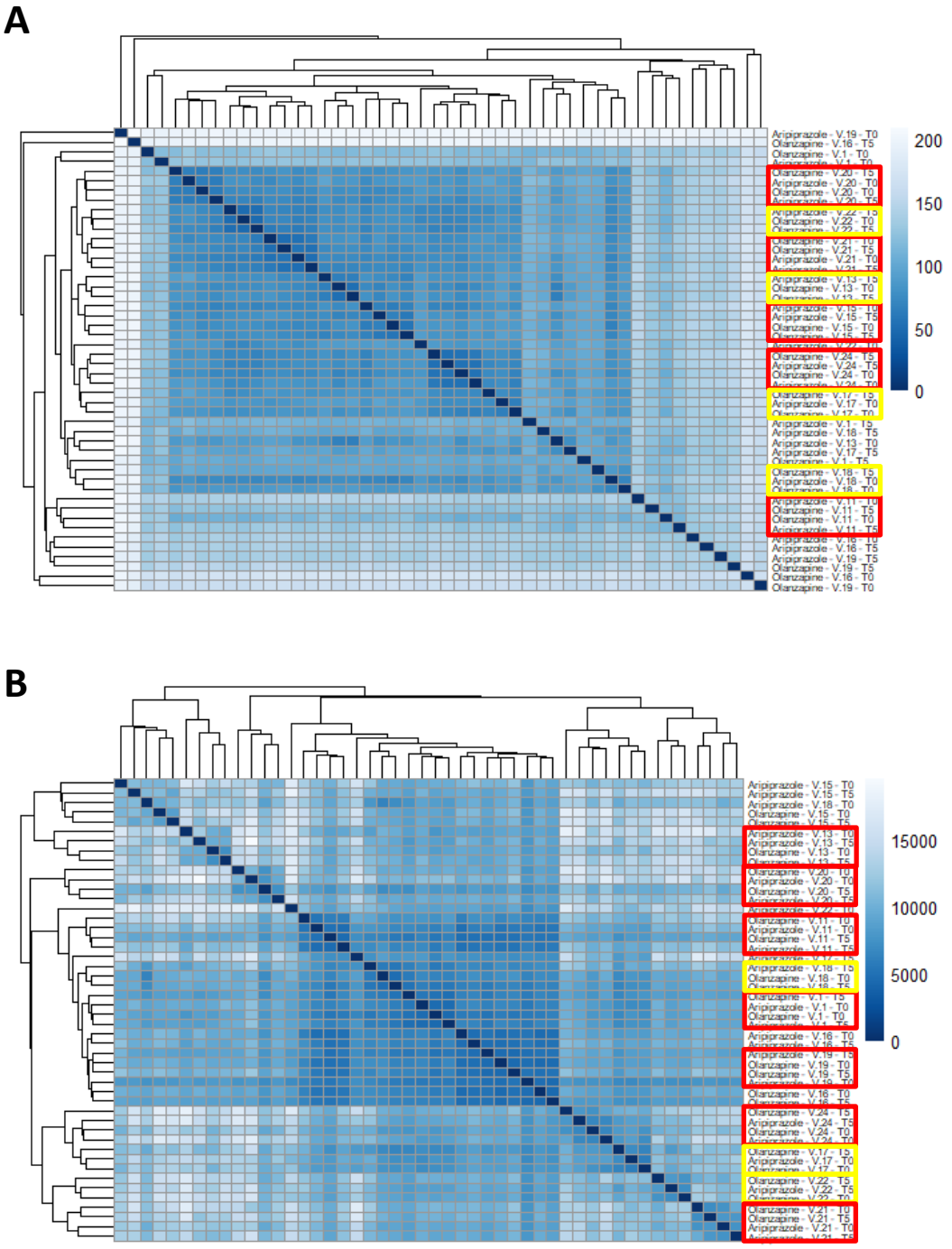

Figure 24. Heatmap of sample-to-sample distances using the variance stabilizing transformed values

The figure shows two sample-to-sample distance matrices. While the first one (A) was constructed with Euclidian distances, the second one (B) was built with Poisson distances. On both cases, 3 or 4 of the samples corresponding to a specific volunteer were clustered together. In red rectangles were highlighted the volunteers for which their 4 samples were clustered together. In yellow rectangles were highlighted the volunteers with 3 samples clustered together. The shades of blue colour correlate with the distance computed when comparing two samples; being dark blue a symbol of large similarity between the samples compared and light blue a symbol of large difference.

A heatmap of the 50 genes with smallests p-adj values can be seen on Figure 25. All of the yellow positions on the map show genes with small responses to the treatments, similar to the volunteer 24 response. The red and blue positions show genes that become either over-expressed or repressed for that specific volunteer, respectively, therefore pointing out to volunteers with stronger reactions to the treatments than others. Just by looking at the plot, it is possible to observe that volunteers 1, 11, 16 and 19 have a larger number of genes with differential responses than the rest of the volunteers, allowing us to think that based on these results it is possible to stratify the volunteers into those with weak and strong responses to the treatmets.

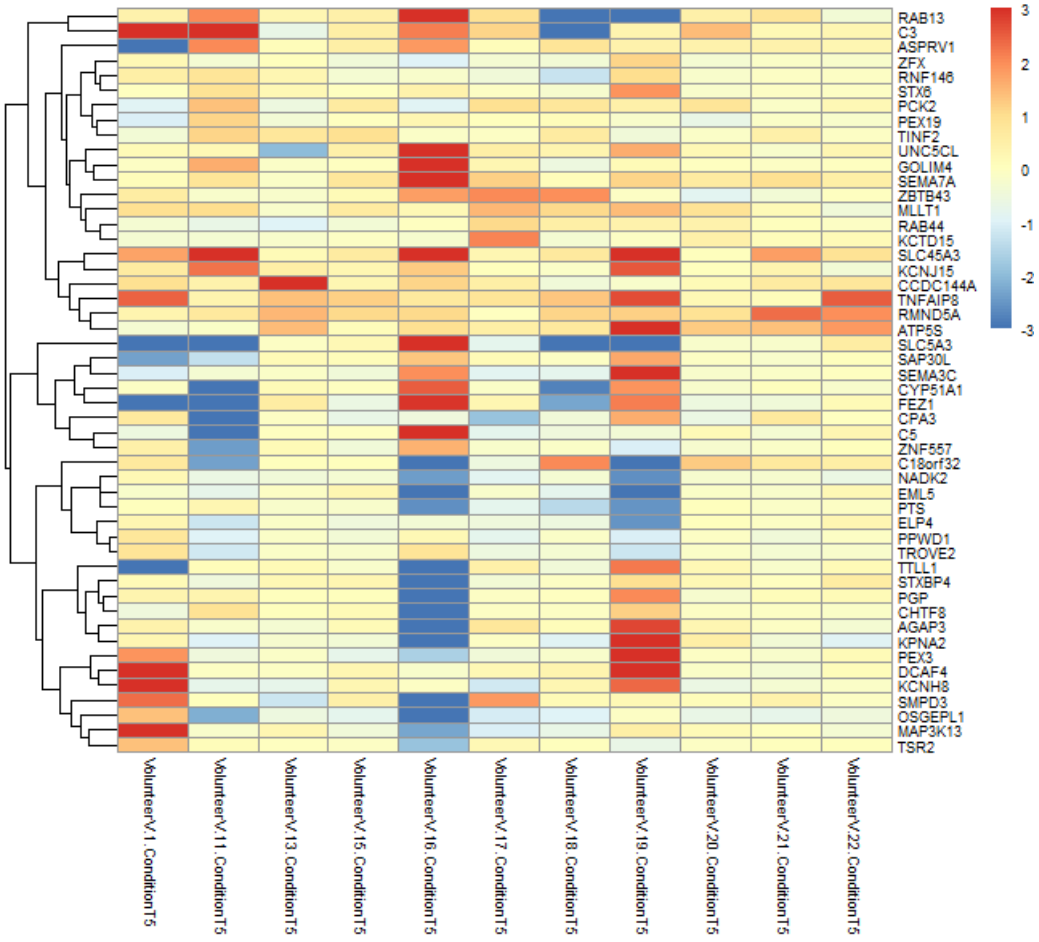

Figure 25. Top 50 genes with a differential response (T5 Vs T0) among volunteers
The figure shows a heatmap of the difference in the response (Log2FoldChange T5 Vs T0) between each volunteer and volunteer 24 who was chosen as reference. The yellow rectangles represent genes with a small difference in the response between the given volunteer and volunteer 24, as volunteer 24 was chosen for having weak responses, it is possible to assume that the volunteers with yellow genes also showed weak responses to the treatments. The red and blue rectangles represent either over-expressed or repressed genes compared to volunteer 24, therefore showing a differential response to the treatments.

A PCA with the 805 differential genes was computed to observe how the volunteers distribute when considering the genes with differential responses among them (Figure 26A).

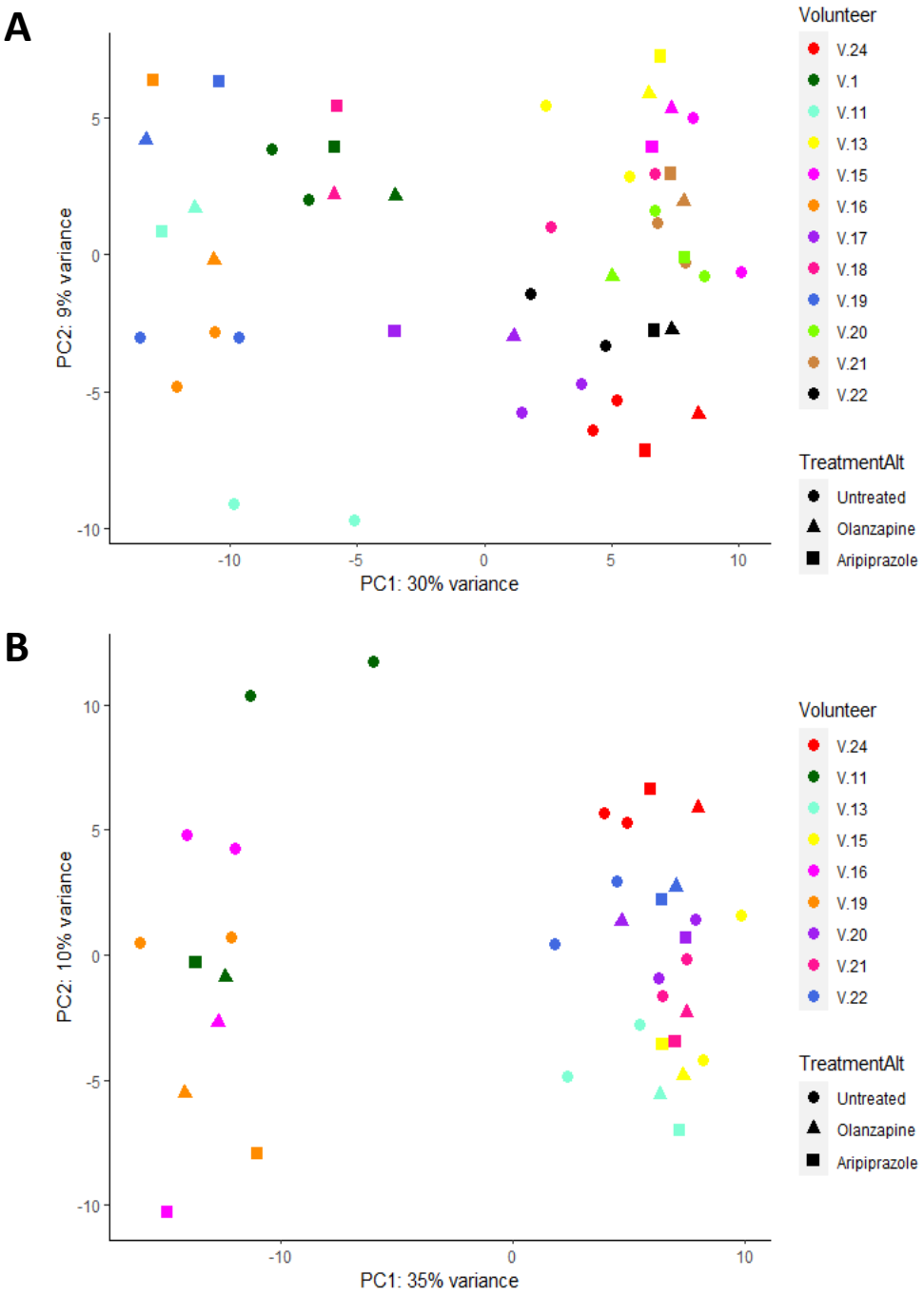

Figure 26. PCA of the volunteers taking into account only the 805 genes with differential responses to the treatments

PCA of the volunteers includes only the 805 genes with differential responses among them (adjPval < 0.1 in the interaction analysis). On **A,** all volunteers are included in the study. It is possible to see that they divided on axis x according to their level of response to the treatments, being on the left side of the plot the volunteers with strong responses and on the right side the volunteers with weak responses. Some volunteers remained in the middle of the plot (1, 17 and 18), for whom it was assumed a medium intensity response. The plot was repeated without the medium response volunteers (B) to observe better the stratification of the low and high response volunteers.

Figure 26A shows that the volunteers distributed along the plot's x-axis according to their response to the treatments. On the right side are the volunteers with weak responses; while on the left side are the volunteers with stronger responses. Besides, for the volunteers with strong responses, the samples split across the y-axis, being the samples from T0 (untreated) on the lower part of the plot and the samples after 5 days of treatment (olanzapine or aripiprazole) on the upper part of the plot. The samples from the volunteers with weak responses did not show a specific distribution across the y-axis. Therefore, it is possible to assume that the intensity of the response drives the clustering of the samples. There are, however, 3 volunteers that did not follow these patterns: volunteers 17 and 18 have samples on both sides of the x-axis, and in the case of volunteer 1, even all of its samples are on the left side of the plot, they remained all together, and the treated and untreated samples did not spread apart. This correlates with the heatmap of the top 50 genes with a differential response (Figure 25), as it is possible to see that volunteers 1, 17 and 18 have an intermediate number of genes with responses to the treatments (red, blue positions), compared to volunteers with a larger number of responding genes and those with a majority of none responding genes. Therefore, we decided to consider these 3 volunteers as having an intermediate intensity response. On a new PCA (Figure 26B) without the intermediate response volunteers (1, 17 and 18) we can observe that the two types of responses, weak and strong, are separated as well as the treated and untreated samples from the strong response volunteers, showing that the stratification of the volunteers according to their response to the treatments is possible.

4.4.1. Analysis of the differential response signal

Enrichment analysis of the 805 differential response genes against the TRANSFAC and JASPAR PWMs database showed the enrichment of peroxisome proliferator-activated receptor gamma (PPARG) by 178 genes with binding motifs at their promoters (pVal = 0.0011): *GHDC, MTCH2, CRTC2, FAAH, SERPINE2, ZFAND3, TUSC2, HDAC11, RORC, PEBP1, EPRS, CHCHD5, ALKBH1, FAM122C, CDK20, ROPN1L, ZNF688, AP1S3, TMEM14A, TBC1D10A, TMEM8B, SLC39A3, TYW3, ATG9B, HGF, SPNS3, NSMCE2, ALG5, IFRD1, MYO7B, TSC2, ARMC8, FAM203A, C1ORF122, CTDNEP1, RBP7, TPST1, PHOSPHO1, MSH3, VDAC3, SPNS1, TSSK4, CLEC4F, FAM8A1, ZNF157, SLC45A3, RAB5C, SHC1, MRPL14, FPR2, DTX3, ACTR3B, FBLN2, NCAPH, CCDC144A, C3, C5, KLC2, CALD1, BLOC1S1, PTPMT1, HLTF, SLC38A7, SERPINH1, TNFRSF17, ZNF425, PSMF1, MARK2, SNX6, TBC1D8B, RAP1GAP2, CPSF4, CADM4, ACBD4, JUP, PMM1, TNFSF14, ZNF382, APOBEC3H, OSGIN2, LSM3, PRRC2A, IBTK, RNF103, CAPRIN1, C16ORF45, MRVI1, COL9A2, AMOTL1, TAB1, FARSA, LRP10, RYR1, ABCD4, DAZAP2, FASTKD1, SPIN3,*

ICA1, SECTM1, HBB, HCCS, EFCAB11, DMKN, MS4A4A, SMPD3, AKAP13, PTBP1, BCL7A, AIFM2, MED10, TOP1MT, HYAL3, ME3, ZNF248, BBS7, CTSF, DLGAP4, TOP3B, IZUMO4, MME, NSUN5, GPX3, TNFRSF18, WDR31, GLRX2, ITFG3, ZFX, GAK, RCN3, PTP4A2, CEACAM1, MYO3B, ZNF239, IFT46, FBP1, KANK2, PPP1R15A, ZNF473, DDX27, DOT1L, HEATR1, C4ORF36, MLLT1, TYMS, AKAP2, DCAF15, RAB20, TP53INP2, CXCR2, NHS, POC1A, FLNB, BRD4, ZNF221, YTHDF2, CMTM3, NUBPL, CYP51A1, MAPK14, SORBS3, NUDT9, PDCL3, RIT1, CD4, LRG1, MYO1C, POLR3A, CENPI, PSAT1, ERCC2, TSR2, CENPL, TRIP10, PNPLA6, SYCP3, CENPQ, CLEC2D, BNIPL.

PPARG and the peroxisome proliferator-activated receptor-gamma co-activator 1 (PPARGC1) family, PPARGC1A and PPARGC1B, play a key role in the development and pathophysiology of T2DM (Zhu et al. 2017). Several studies search the associations between the *PPARGC1A* and *PPARGC1B* polymorphisms and the risk of developing metabolic dysfunctions. Therefore, we performed a single nucleotide variant prediction with VarScan (Koboldt et al. 2012) from BWA alignments, followed by annotation with Annovar (Wang, Li, and Hakonarson 2010). All volunteers previously classified as having a low response have polymorphisms on one or both of *PPARGC1B* and *PPARGC1A*. In contrast, none of the volunteers with medium or high responses had polymorphisms on any of these genes. The variants found on the volunteers with low response can be seen in the suplementary Table 10.

Volunteers' clinical variables registered during the trial as weight, triglycerides, cholesterol, glucose and insulin were kindly provided by Dr Dora Koller and Dr Francisco Abad Santos. We analyzed them with t-tests to know if statistical differences exist between the response groups low Vs high + medium. Only the weight difference between day 15 of the first period of the clinical trial and the weight registered at the initial screening showed to be statistically different between the two groups (pval= 0.0254). Figure 27 shows the graphical representation of the weight difference in kg. It can be observed that, while the volunteers with low response generally gained weight on the first 15 days of the trial, the volunteers with high and medium responses either maintained or reduced their weight. Statistical differences in the volunteers' weight change were not observed at other stages of the trial. These results, however, may correlate with the *PPARGC1* family polymorphisms observed on the low response volunteers, which are in their majority associated with obesity.

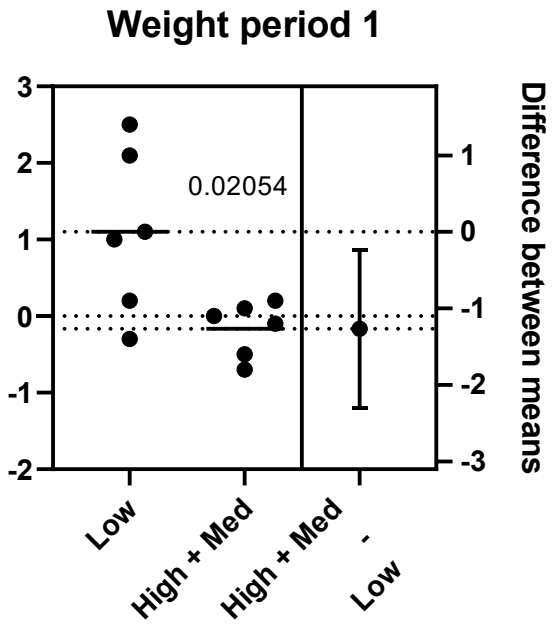

Figure 27. Difference between the weight registered by the volunteers at day 15 of the clinical compared to the weight registered at the initial screening.
The figure shows the difference in kg between the weight registered by each volunteer on day 15 of the clinical trial and the weight registered at the initial screening. The volunteers are grouped by their type of response: low or high and medium. An unpaired t-test showed that statistical differences exist among the groups (pval= 0.02054). On the right side, the plot also shows the difference between the two groups means.

As most polymorphisms were found on *PPARGC1B*, we produced plots to visualise assembled transcripts for *PPARGC1B* with the plotTranscripts function from the Ballgown package (Frazee et al. 2014). Figure 28 shows *PPARGC1B* transcripts abundance in FPKMs for representative high (11), medium (17) and low (24) response volunteers. It was observed that the same transcripts are produced for all volunteers at all time points. However, the abundance of the transcripts in the volunteer with a high response (11) is noticeable higher than for the medium and low response ones. Plots for all volunteers in the study can be seen in supplementary figures. In general, it was observed that, independently of the abundance level at time zero of period 1, volunteers with high response kept or increased their *PPARGC1B* transcripts abundance that did not decrease during the rest of the trial (Figure 31). In the case of medium response volunteers, the abundance remained low in general (Figure 32). For the low response volunteers, the abundance decreased at T5 of period 1 for those volunteers whose starting abundance levels were higher. However, it increased at the end of period 2, ending the trial at a higher abundance level than the one at which they started. Their abundance level, however, never reached high response volunteers' levels (Figure 33).

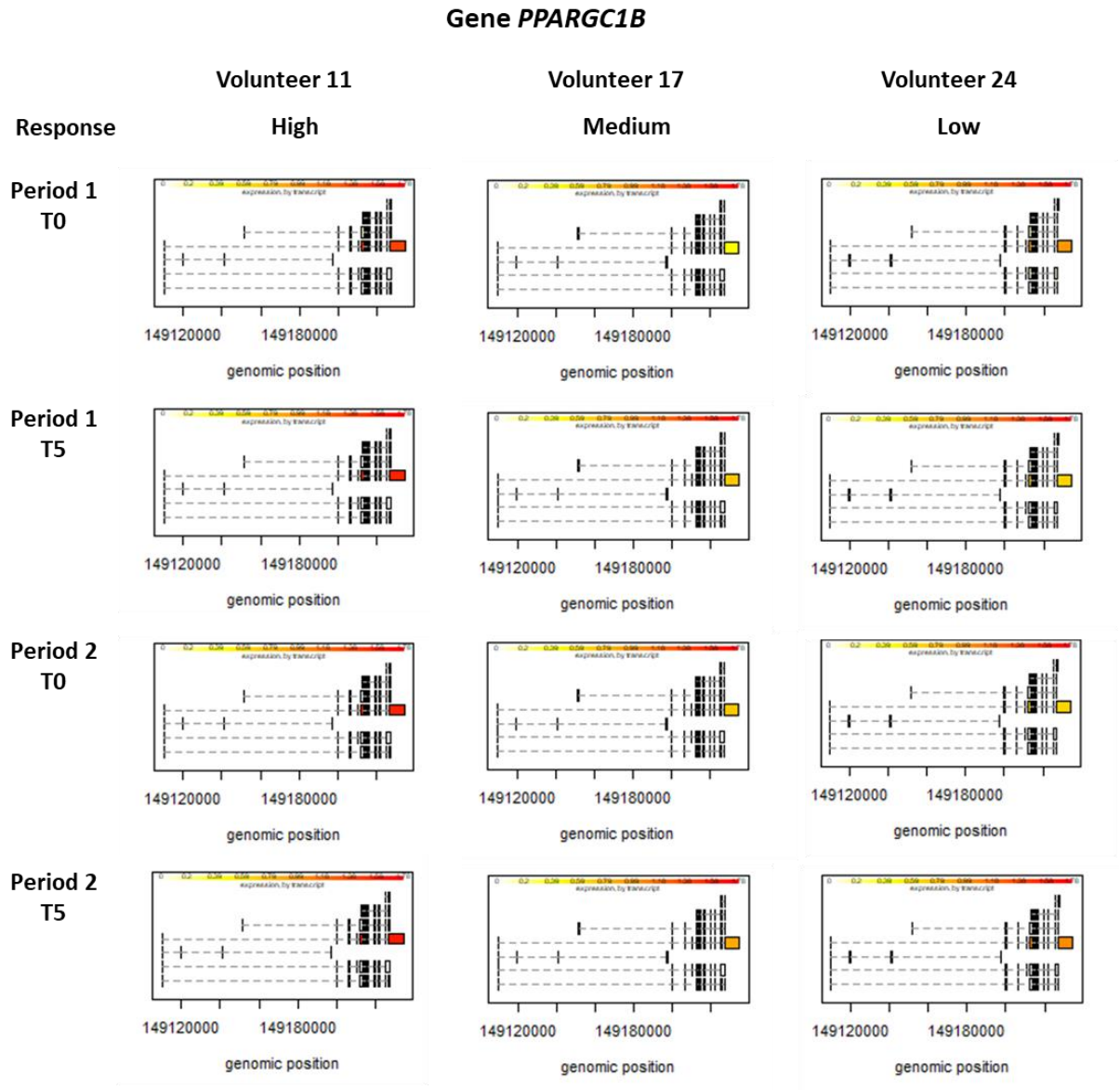

Figure 28. *PPARGC1B* transcripts abundance visualization for high (11), medium (17) and low response (18) volunteers.

The figure shows the abundance of *PPARGC1B* transcripts for a representative volunteer from each response level: high response (volunteer 11), medium response (volunteer 17) and low response (volunteer 24). The colour scale goes from 0 (yellow) to 170 (red) FPKMs.

We performed a differential expression analysis to see the effect of the treatments on the different response groups. We mixed the high + medium response volunteers for one analysis and performed a second one with the low response volunteers to maintain a larger sample size. The DESeq object was built with **design = ~ Sex + Condition**. The comparison T5 Vs T0 yielded 0 and 6 differential genes with aripiprazole and olanzapine, respectively, for the low response volunteers, and 504 and 18 differential genes for the high + medium response volunteers (Table 8).

Table 8. Dysregulated genes by aripiprazole and olanzapine by response groups

Response	Treatment	Number of up-regulated genes	Number of down-regulated genes
High + medium	Aripiprazole	342	162
	Olanzapine	5	13
Low	Aripiprazole	0	0
	Olanzapine	2	4

We performed enrichment analyses against several databases with the online tool Enrichr. Some relevant enriched pathways are described on Table 9.

Table 9. Enriched pathways by the 504 dysregulated genes by aripiprazole treatment on the high + medium response volunteers

Pathway	adjPval	Genes that enriched the pathway	Database
Cytoplasmic Ribosomal Proteins	4.178e-22	*RPL4, RPL5, RPL30, RPL31, RPL34, RPL12, RPLP0, RPL11, RPL36A, RPL9, RPL6, RPL7, RPS17, RPS27A, RPL39, RPS10, RPL17, RPS7, RPL21, RPL23, RPS6, RPL35A, RPSA, RPS3A, RPS25, RPS27, RPS29, RPL27, RPS24*	WikiPathway 2021 Human
IL-3 signalling pathway	5.496e-6	*TGFB1, SRC, INPP5D, STAT3, RAPGEF1, PIK3CD, PTPN6, GAB2, CD69, PRKACA, CBL*	WikiPathway 2021 Human
Osteoclast differentiation	6.104e-5	*LILRA6, CSF1R, SPI1, TGFB1, NCF1, NCF4, PIK3CD, GAB2, TYK2, LILRB2, LILRB3, SIRPB1, FOSL2, MAPK13, SIRPA*	KEGG 2021 Human
Leukocyte transendothelial migration	6.647e-5	*ITGAM, NCF1, ACTN1, TXK, NCF4, PXN, PIK3CD, ITGAL, ICAM1, GNAI2, MAPK13, RAC2, PTK2B, SIPA1*	KEGG 2021 Human
IL-4 signalling pathway	9.475e-4	*INPP5D, STAT3, PIK3CD, STAT6, PTPN6, TYK2, GAB2, CBL, JAK3*	WikiPathway 2021 Human
Estrogen Response Early	1.201e-3	*SVIL, SCARB1, KDM4B, ITPK1, MYOF, GAB2, KLF4, CBFA2T3, IGF1R, NCOR2, SLC7A5, FASN, RARA, RRP12, IL6ST, FKBP5*	MSigDB Hallmark 2020

Chemokine signalling pathway	1.732e-3	*NCF1, PRKCD, PXN, STAT3, WAS, PIK3CD, ARRB2, PIK3R5, GNAI2, PREX1, RAC2, PTK2B, CSK, PRKACB, JAK3*	WikiPathway 2021 Human
Regulatory circuits of the STAT3 signalling pathway	1.967e-3	*CREBBP, CSF3R, SRC, STAT3, TYK2, IL6ST, IL7R, JAK3, IL6R, MAPK13*	WikiPathway 2021 Human
Oncostatin M Signaling Pathway	2.228e-3	*SRC, PRKCD, RPS6, PXN, STAT3, PTK2B, TYK2, IL6ST, JAK3*	WikiPathway 2021 Human
Endocytosis	2.739e-3	*ARF1, IQSEC1, SRC, VTA1, ARAP3, EPS15L1, ARRB2, ARAP1, CBL, IGF2R, IGF1R, CYTH2, CAPZA1, PSD4, PIP5K1C, RAB7A, HSPA1A, SH3GL1*	KEGG 2021 Human
Microglia Pathogen Phagocytosis Pathway	2.774e-3	*ITGAM, NCF1, NCF4, RAC2, PIK3CD, PTPN6, SIGLEC7*	WikiPathway 2021 Human
Interferon type I signalling pathways	2.774e-3	*RPS6, STAT3, RAPGEF1, PIK3CD, PTPN6, TYK2, GAB2, CBL*	WikiPathway 2021 Human
Complement	2.803e-3	*SERPINA1, ITGAM, CR1, LRP1, BRPF3, SRC, GZMA, PRKCD, RHOG, WAS, PIK3R5, GNAI2, TIMP2, TIMP1, HSPA1A*	MSigDB Hallmark 2020
IL-6 signalling pathway	3.530e-3	*CREBBP, PRKCD, STAT3, TIMP1, TYK2, IL6ST, IL6R*	WikiPathway 2021 Human
Interleukin-11 Signaling Pathway	3.530e-3	*TGFB1, SRC, STAT3, RPS6, TYK2, IL6ST, ICAM1*	WikiPathway 2021 Human
IL-6/JAK/STAT3 Signaling	4.113e-3	*CSF3R, TGFB1, STAT3, TYK2, LTBR, IL6ST, CBL, IL17RA, PIK3R5*	MSigDB Hallmark 2020
TNF-alpha Signaling via NF-kB	5.501e-3	*ABCA1, KDM6B, PFKFB3, KLF4, ICAM1, FOSL2, BCL6, TNIP1, GPR183, BCL3, DENND5A, CD69, IL6ST, IL7R*	MSigDB Hallmark 2020

HIF-1 signaling pathway	9.654e-3	*CREBBP, PFKFB3, RPS6, STAT3, PIK3CD, TIMP1, LTBR, IL6R, CAMK2G, IGF1R*	KEGG 2021 Human
IL-2 signalling pathway	1.164e-2	*STAT3, RPS6, PTK2B, GAB2, CBL, JAK3*	WikiPathway 2021 Human
Inflammatory Response	1.395e-2	*ABCA1, CSF3R, SEMA4D, RHOG, ICAM1, PIK3R5, TAPBP, GPR183, STAB1, TIMP1, CD69, IL7R, LY6E*	MSigDB Hallmark 2020
Insulin Signaling	3.301e-2	*MAP3K3, ARF1, PRKCD, STXBP2, RAC2, RAPGEF1, PIK3CD, FLOT2, CBL, IGF1R, MAPK13*	WikiPathway 2021 Human
IL-7 signalling pathway	4.237e-2	*STAT3, PTK2B, IL7R, JAK3*	WikiPathway 2021 Human

4.4.2. **Candidate genes for response groups classification**

We used Scikit-learn to select the genes, which allow us to distinguish better between the low (volunteers 13, 15, 20, 21 and 22) and high response volunteer groups (volunteers 11, 16 and 19). The selection was made from the 805 genes with statistically significant differential response across the volunteers.

To choose the best filtering method, we estimated the performance of the nearest neighbour classifier using 10-fold cross-validation and selecting the number of neighbours by using 3-fold inner cross-validation. We essayed three filtering methods and computed their prediction error:

1) No filtering (prediction error= 0.4000).
2) Feature selection technique based on the F-score (ANOVA), picking up the 10 most relevant features (prediction error= 0.3722).
3) Initial filtering with F-score to keep only the 20% most promising features and final filtering with a random forest approach to pick up the 10 most relevant features (prediction error= 0.3444).

The feature selection with F-score + Random Forest performed the best in terms of the generalisation error obtained. However, the difference with the F-score alone was slight, and this method ran significantly faster. Therefore, we decided to continue the analysis using the

F-score method. For the previous essays, we limited the number of features filtered to 10. However, since we did not know if this number was optimal, we estimated the performance of the nearest neighbour classifier with K=2 using an F-score to filter features from 1 to 200. We used a 10-times 10-fold cross-validation method and plotted the prediction error Vs the number of features used for prediction. We repeated that process when the feature selection is done externally to the cross-validation loop using all the available data to compare the prediction error to the previous method (Figure 29). The classification error when all the data was used for the feature selection is much smaller than the error obtained when only the training set is used, showing that the generalisation error is underestimated when all the data is used to select attributes.

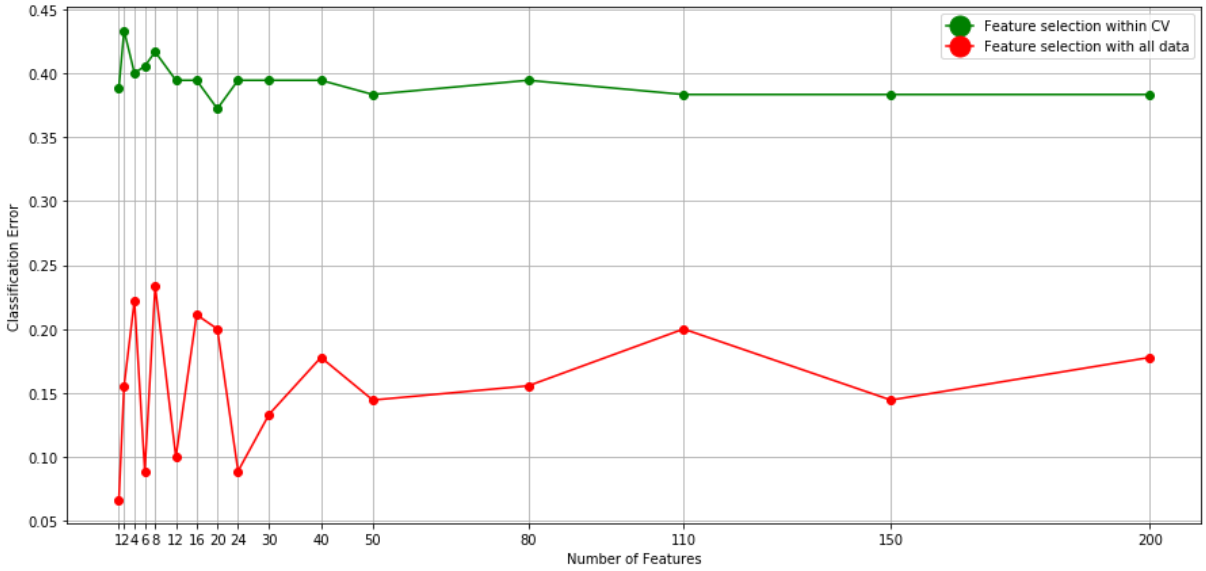

Figure 29. Performance of the nearest neighbour classifier with K=3 as a function of the features used for prediction

Error rate associated with predicting the volunteers' response group (low or high). The feature selection was performed with the F-score method. The classification was done with the nearest neighbor classifier with K=2 as a function of the features used for prediction. 10-times 10-fold cross-validation method is represented with a green line. Feature selection without cross-validation is represented with a red line. Results reported when performing the prediction with 1 to 200 features. The minimum error rate was obtained when selecting 21 features.

For the feature selection with cross-validation, the optimal number of features to use was 21 as that number of features selected produced the smallest classification error. A heatmap of the foldchange T5VsT0 in comparison with the foldchange of volunteer 24 for the 21 genes selected is shown in Figure 30.

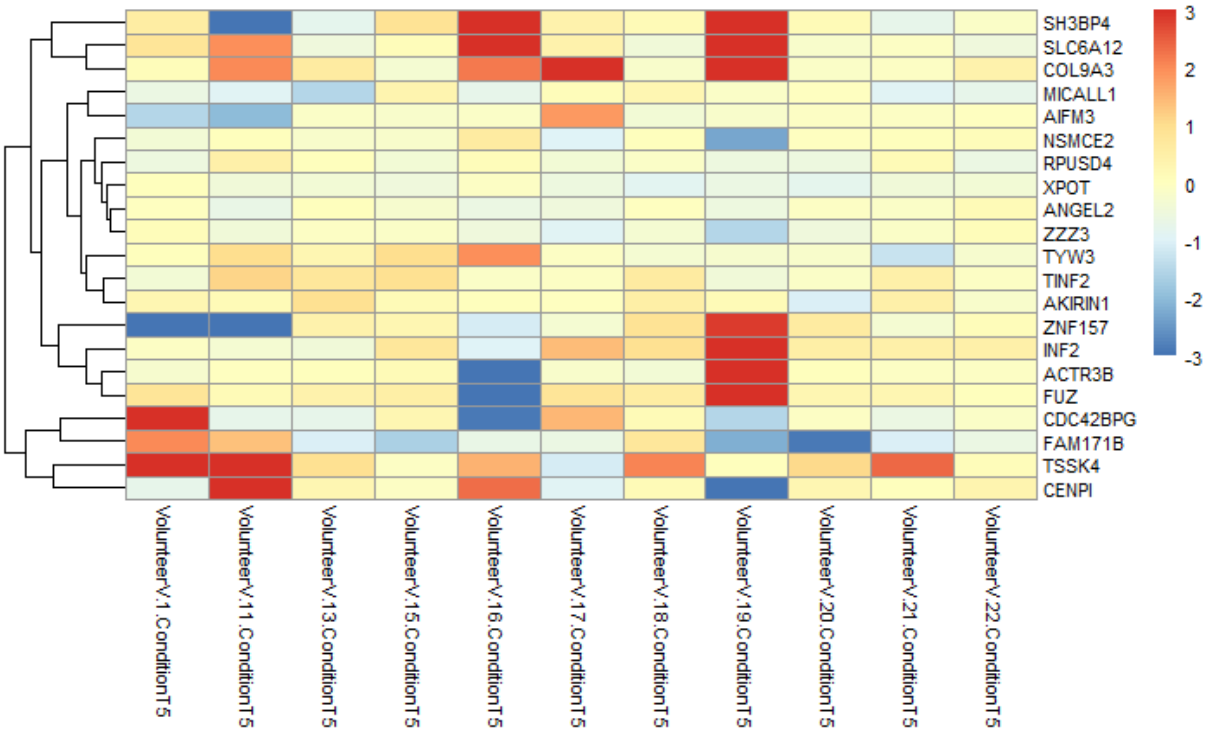

Figure 30. Hierarchical clustering of the candidate genes for response prediction to the treatments

The figure shows a heatmap of the difference in the response (Log2FoldChange T5 Vs T0) between each volunteer and volunteer 24, who was chosen as reference. The yellow rectangles represent genes with a small difference in the response between the given volunteer and volunteer 24. The red and blue rectangles represent either over-expressed or repressed genes, respectively, compared to volunteer 24.

These results are coming from a small sample size therefore precluding any substantial biological hypothesis. However, they provide an interesting piece of information to be confirmed by larger series and, if so, explored with biological models.

5. DISCUSSION

The metabolic syndrome is a leading cause of morbidity and mortality in schizophrenia patients, with a double prevalence rate than for nonpsychiatric populations (Riordan et al. 2011). The increased prevalence of metabolic disorders in schizophrenia is partly attributed to the antipsychotic treatments (Smith et al. 2008), as they may influence the food intake and glucose and lipid metabolisms (Reynolds and Kirk 2010). It has been proposed that the weight gain induced by antipsychotics may be associated with the $5HT_{2C}$, H_1, and D_2 receptors affinity, which is also associated with insulin resistance and reduced glucose uptake (Ho et al. 2014). Olanzapine being a high-affinity $5HT_{2C}$ and H_1 antagonist (Ki = 6.8 and 2 nM for 5HT2C and H1, respectively) (Bába et al. 2019), shows more potent metabolic effects than aripiprazole, which has a considerably weaker affinity to these receptors (Ki = 15 and 61 nM for 5HT2C and H1, respectively) (Bába et al. 2019), and is considered metabolically neutral (Christine Rummel-Kluge et al. 2010).

An open, controlled, randomized, crossover clinical trial in healthy volunteers was carried out to evaluate the short-term effect (5 days) of olanzapine and aripiprazole. Blood samples were collected before and after each treatment. Additionally, mice models were treated with short (5 days) and long-term (6 months) aripiprazole and olanzapine schemes. Liver and pancreatic islets were isolated. Total RNA was extracted from the blood and tissue samples to perform differential expression analyses. The computed Log2FoldChanges were used to perform Gene Set Enrichment Analyses against KEGG and Gene Ontology databases. This strategy allowed us to understand different genesets' general behaviour after the treatment with aripiprazole or olanzapine.

5.1. Effects on schizophrenia symptoms

The treatment with aripiprazole up-regulated the Nicotine addiction gene set with the highest NES in the human blood samples. From the genes included in this set, some of the most up-regulated ones were $GABA_A$ receptor subunits (GABRR3, GABRB3, GABRG2, GRIN2B, GABRR1). Schizophrenia has been primarily associated with dysfunctional synthesis and release of dopamine; therefore, treatments as aripiprazole target dopamine signalling (Yang and Tsai 2017), which regulate G protein-dependent PKA, a D2-like receptor down-stream pathway which in turn regulates $GABA_A$ receptor, that is implicated in the pathophysiology of schizophrenia (Pan et al. 2016). Previous short-term (1 week) studies on rats treated orally with aripiprazole (0.75 mg/kg) showed the effect of aripiprazole on the activation of the PKA

signalling and the up-regulation of mRNA and protein expression of the $GABA_A$ receptor in the nucleus accumbens (NAc) (Pan et al. 2016). These results correlate with what was observed on the volunteers' peripheral blood transcriptome treated for 5 days with aripiprazole, suggesting that the treatment effects are reflected on the blood samples collected.

In the liver from WT mice, six-month aripiprazole treatment up-regulated Nicotine addiction, GABAergic synapse and Cocaine addiction pathways. The top up-regulated genes were the $GABA_A$ receptor subunits Gabre and Gabrd, which correlates with the human findings, and the glutamate receptors Grin2b, Grin2c and Grin2d. Glutamate facilitates most excitatory neurotransmission (Paoletti, Bellone, and Zhou 2013) and participates in several central nervous system (CNS) processes and essential neuronal functions (Ochoa-de la Paz et al. 2021). Therefore, impaired glutamatergic neurotransmission could largely explain nervous system diseases' symptoms and neurocognitive deficits (Yu et al. 2018). The N-methyl-D-aspartate-glutamatergic receptor (NMDAR) is composed of NR1 and NR2 subunits and less frequently of subunit NR3. NR1 subunit is abundantly expressed across the brain, while NR2 subunits vary in their distribution in the CNS (Karolewicz, Stockmeier, and Ordway 2005). NR2 has four isoforms in vertebrates: NR2A, NR2B, NR2C and NR2D, encoded by *GRIN2A, GRIN2B, GRIN2C* and *GRIN2D,* respectively (Fasipe 2017). NR2B has been related to memory, learning, processing and feeding behaviours and several human pathological disorders such as major depressive disorder (MDD). Several post-mortem studies have found changes in the NMDAR subunits expression in MDD patients, probably as compensation to glutamatergic levels changes (Fasipe 2017). For example, in postmortem tissue of MDD patients, NR2B and NR2C subunits have shown increased expression in the locus coeruleus (Chandley et al. 2014). These outcomes correlate with our findings, suggesting that chronic treatment with aripiprazole boosts the expression of NR2 subunits to alleviate glutamatergic neurotransmission impairment in schizophrenic patients.

The Nicotinate and nicotinamide metabolism was one of the top up-regulated genesets by olanzapine in the human samples, being *NNMT*, a target of nicotinic receptors, the top up-regulated gene within the set. Reduced levels of *NNMT* mRNA were observed in the frontal cortex of post-mortem schizophrenic patients, suggesting that NNMT is involved in the aetiology of schizophrenia (Bromberg et al. 2012). The up-regulation of *NNMT* on the volunteers after the treatment with olanzapine compared with the time zero may suggest that olanzapine is compensating for the *NNMT* repression in people with schizophrenia.

5.2. Olanzapine inhibits glyceroneogenesis through PEPCK signalling repression

Different Peroxisome proliferator-activated receptors (PPARs) signaling pathway genes were dysregulated by aripiprazole and olanzapine in the different treated models. PPARs are part of the steroid receptor superfamily and regulate cell differentiation, tissue development, inflammatory response, immune tolerance and metabolic and energy homeostasis, including glucose metabolism, lipid uptake and storage, insulin sensitivity, mitochondrial biogenesis, and thermogenesis (Brunmeir and Xu 2018).

So far 3 isotypes of PPARs have been described: PPARα (NR1C1), PPARβ/δ (NUC1; NR1C2) and PPARγ (NR1C3); encoded by *Ppara*, *Ppard* and *Pparg genes,* respectively (Moraes, Piqueras, and Bishop-Bailey 2006). The 3 isoforms have different although overlapping roles due to their expression profiles in distinct tissues, their sensitivities to agonists and their regulation of target genes. PPARα is highly expressed in tissues with high Fatty acid oxidation (FAO) capacity like kidney, liver, heart, skeletal muscle and BAT, where it regulates fatty acid metabolism in response to nutritional changes such as fasting/feeding through β-oxidative degradation of fatty acids (Chinetti, Fruchart, and Staels 2000) (Brunmeir and Xu 2018). PPARβ/δ is involved in cell differentiation, lipid accumulation, and polarization; and is enriched in tissues related to fatty acid metabolism, like the gastrointestinal tract, fat, kidney, heart, skeletal muscle and skin (Peng et al. 2021) (Brunmeir and Xu 2018). PPARγ has an important role in glucose metabolism, adipogenesis and inflammation (Peng et al. 2021). It is activated by different ligand PUFAs such as oxidized low-density lipoprotein, eicosanoids and fatty acids (Peng et al. 2021). There are 2 isoforms of the protein: PPARγ1, which lacks the 30 first amino acids, is expressed in various cells, including immune and brain cells, while PPARγ2, the full-length protein, is highly enriched in BAT and WAT (Brunmeir and Xu 2018).

PPAR signalling and Fatty acid biosynthesis pathways were down-regulated by olanzapine treatment in healthy human volunteers. Out of the PPAR signalling pathway, *PCK1*, *ACSBG2*, *FABP3* and *ADIPOQ*, were the top down-regulated genes, while for the Fatty acid biosynthesis *ACSBG2*, was the top down-regulated one. At the same time, the fat digestion and absorption geneset was up-regulated, being *PLA2G2F* the most up-regulated gene within the set.

The PPARγ2/RXRα heterodimer, a transcription factor known as ARF6, is an important regulator of *PCK1* in adipose tissue (Tontonoz et al. 1995). *PCK1*, the top down-regulated PPAR signalling gene by olanzapine in the healthy volunteers, encodes PEPCK-C, one of the PEPCK isozymes significantly expressed in proximal tubular epithelia of the kidney, hepatocytes, adipocytes, and intestinal epithelia (Beale, Harvey, and Forest 2007). PEPCK

catalyzes the transformation of oxaloacetate (OAA) into phosphoenolpyruvate (PEP), the rate-limiting stage in gluconeogenesis and glyceroneogenesis. (Tontonoz et al. 1995). The production of PEP from OAA is a cataplerotic reaction during gluconeogenesis as it sustains the metabolic flux through the citric acid cycle (CAC), also known as the TCA cycle or the Krebs cycle, by removing excess OAA (Ko et al. 2018) (Beale et al. 2007).

Although CAC constitutes the central process in energy metabolism, it also contributes to biosynthetic pathways as intermediates of the cycle are removed from it to be converted into non-essential amino acids, glucose, and fatty acids (Owen, Kalhan, and Hanson 2002). It has been suggested that metabolites from CAC impact macrophage inflammatory phenotypes (Ko et al. 2018). For example, citrate, which is exported from mitochondria to the cytosol, is cleaved by citrate lyase into acetyl-CoA and OAA. Acetyl-CoA is used for fatty acid synthesis to meet the requirement of lipids in the proinflammatory state (Infantino et al. 2011). A study with mice having a myeloid cell-specific *Pck1* deletion (Ko et al. 2018) showed that on lipopolysaccharide (LPS) stimulation bone marrow-derived macrophages (BMDM), which promotes the inflammatory phenotype, *Pck1* gene deletion led to pyruvate dihydrogen complex flux reduction, followed by decreased citrate levels and therefore reduced fatty acid synthesis. This suggests an anaplerotic role (replacement of removed anions from the CAC) of *Pck1* in macrophages, as the deletion of Pck1 inhibits the conversion of PEP to OAA to malate to CAC (Ko et al. 2018).

In white adipose tissue, PEPCK1 enhances adipose lipid storage by helping the synthesis of Glyceraldehyde 3-phosphate (G3P) for fatty acid esterification into triglycerides (glyceroneogenesis) (Beddow et al. 2019). In mice, inhibition of *Pck1* expression in adipocytes reduced their adipocytes size and content (Olswang et al. 2002), contributing to adipose tissue dysfunction. This information suggests that glyceroneogenesis was disrupted in the volunteers treated with olanzapine, and is supported by the down-regulation of *ACSBG2A*, an acyl-CoA synthetase gene. Acyl-CoA synthases catalyze the conversion of long-chain and very-long-chain fatty acids into their active acyl-CoAs for oxidation or esterification into complex lipids such as phospholipids, triglycerides and cholesterol esters (Lopes-Marques et al. 2013). Thus, *ACSBG2A* down-regulation supports the theory of disruption of triglycerides synthesis by olanzapine.

PLA2G2F (Phospholipase A2 Group IIF) was up-regulated by olanzapine in the volunteers. *PLA2G2F* is part of the sPLA2 family and has been implicated in several lipid metabolism pathways, such as alpha-linolenic acid metabolism, ether lipid metabolism, linoleic acid metabolism, fat digestion and absorption and pancreatic secretion (Dong et al. 2018). sPLA2s are secreted by the immune and other cells (Jarc and Petan 2020). By similarity with

PLA2G2D, it is thought that *PLA2G2F* has a role in lipid mediator production by providing arachidonic acid to downstream cyclooxygenases and lipoxygenases (The UniProt Consortium 2021). Eicosanoids are derivatives of arachidonic acid and are known for their participation in initiating and perpetuating the inflammatory response (Jarc and Petan 2020). *PLA2G2F* up-regulation may, in consequence, be part of the olanzapine course of action to instate an inflammatory state after its administration.

Olanzapine induces major weight gain/obesity side effects. Toll-like receptor-4 (TLR4) signalling is important in regulating arcuate nucleus (ARC) neurons activity and food intake (Gorina et al. 2011). A study in astrocyte cultures and rats treated with olanzapine (He et al. 2021) showed activation of hypothalamic TLR4 signalling that may be related to olanzapine-induced weight gain and inflammation. Moreover, TLR4 signalling activation was at least in part associated with increased ER stress. TLR4 signalling activation immediately reduces fatty acid synthesis with a subsequent increase in eicosanoid synthesis, linked to the arachidonic acid pathway and sphingolipid and sterol biosynthesis (Dennis et al. 2010). Moreover, it has been reported that TLR4 mediates PEPCK repression in adipocytes during LPS-induced inflammation (Feingold et al. 2012). This correlates with the observed effects of olanzapine in the volunteers, suggesting TLR4 signalling activation contributes to the perpetuation of an inflammatory state by enhancing eicosanoid production, which contributes to PEPCK signalling repression.

As in macrophages, it has also been reported that PEPCK expression is inhibited by inflammation in adipose tissue. A study in mice with chronic inflammation in adipose tissue showed reduced PEPCK activity with a consequent deficiency in glyceroneogenesis (Zhang et al. 2011). In a study performed in rats, olanzapine treatment produced a low-grade inflammatory state associated with a substantial macrophage infiltration to adipose tissue (Victoriano et al. 2010). Consequently, it is possible to suggest that olanzapine is impairing glyceroneogenesis through the onset of an inflammatory phenotype similar to that observed in obese people, in which a significant amount of M1 macrophages accumulate in adipose tissue and liver, where they relieve cytokines that act on insulin target cells to disrupt insulin signalling (Li et al. 2013).

Glyceroneogenesis limits the release of free fatty acid (FFA) into de blood by FFA re-esterification (Vatier et al. 2012). However, it has been observed that glyceroneogenesis is diminished in the adipocytes from overweight people in a BMI dependent manner, which contributes to the systemic rise of FFA (Leroyer et al. 2006). Maintaining triglycerides/FA flux between adipose tissue and liver is essential to maintain glucose and lipid homeostasis, thus preventing insulin resistance (Millward et al. 2010).

Increased FFA flux from adipose tissue to non-adipose tissues has shown to contribute to metabolic disarrangements, characteristic of insulin resistance and T2D, such as dyslipidemia and hepatic steatosis, impaired glucose metabolism and insulin sensitivity, reduced insulin clearance, peripheral tissue hyperinsulinemia, impaired pancreatic β-cell function, among others (Lewis et al. 2002). In a study with mice, adipocyte-specific inactivation of *PCK1* enhanced systemic insulin resistance which was associated to increased circulating FFA (Millward et al. 2010). Another study with liver-specific *Pck1* null fasted mice (Burgess et al. 2004), determined that energy homeostasis was altered as showed by an atypical hepatic redox state, reduced oxygen consumption, lower CAC flux and increased CAC intermediates pool sizes with consequent hepatic steatosis, developed due to the inhibition of fatty acid oxidation.

In correlation with the above exposed, *Cyp7a1* was repressed by olanzapine in pancreatic islets from WT mice. In accordance with our results, a study with apoE null mice (C. H. Chen et al. 2018), reported that treatment with olanzapine produced the down-regulation of CYP7A1, together with other proteins involved in hepatic cholesterol efflux and bile acid metabolism (LXRα, apoAI, ABCA1, ABCG5 and ABCG8). It was concluded that the down-regulation of these proteins led to the accumulation of lipids in the liver, especially total cholesterol, free cholesterol, FA, and glycerol, as de novo lipid synthesis-related proteins were enhanced and cholesterol clearance down-regulated. These outcomes support what was observed in the humans' study, as hepatic steatosis might be induced by olanzapine treatment. However, inhibition of *Cyp7a1 has been related to* an increase in insulin after feeding, which may be the reason why

PTP1B deficient mice are protected against insulin resistance and obesity induced through the diet and are hypersensitive to leptin (Bence et al. 2006). In the PTP1B KO model, one of the genes with the most significant differential response compared to the WT mice after the treatment with aripiprazole was *Dbp*. DBP can transactivate the Cyp7a1 promoter, therefore avoiding the accumulation of lipids in the liver (Inoue et al. 2006). When *Dbp* is repressed, Cyp7a1 is also repressed leading to accumulation of lipids in the liver. *Dbp* expression did not change in the KO mice with olanzapine treatment compared to the WT, probably because PTP1B deficiency prevented *Dbp* repression as a protective action against its adverse effects, which was an expected outcome to happen. However, *Dbp* was significantly repressed in the KO mice treated with aripiprazole. This outcome was not expected as PTP1B KO should represent protection against the *Cyp7a1* repression-induced lipid accumulation, a phenotype that didn't occur with aripiprazole treatment in WT mice. Further analysis would be needed to elucidate the reasoning behind this outcome.

Following the above, Adiponectin (*ADIPOQ*) was also down-regulated by olanzapine treatment in healthy human volunteers. *ADIPOQ* encodes a hormone produced and secreted by adipose tissue with insulin-sensitizing and anti-inflammatory activities (Jassim et al. 2011). It has been proposed that adiponectin stimulates fatty-acid oxidation, boosts glucose uptake, and reduces the activity of gluconeogenesis factors (Kadowaki et al. 2006). Moreover, plasma adiponectin levels negatively correlate with waist circumference and triglycerides concentration (Bartoli, Lax, et al. 2015). Decreased adiponectin plasma levels in the obese rhesus monkey model preceded the onset of diabetes together with reduced insulin sensitivity (Hotta et al. 2001). Similarly, reduced adiponectin plasma levels have also been reported in obese humans (Kadowaki et al. 2006).

Serum adiponectin levels are known to be altered by antipsychotic treatment (Jassim et al. 2011). A study with olanzapine treated patients showed a marked decrease in adiponectin concentrations (Birkenaes et al. 2009). These outcomes correlate with our results, as *ADIPOQ* expression was down-regulated by olanzapine, which may at least partially contribute to olanzapine's treatment reported weight gain and glucose, insulin and lipids metabolism imparements.

Altogether, these outcomes suggest that olanzapine-induced metabolic disarrangements may be explained by increased FFA impairing glucose and lipid homeostasis due to PEPCK signalling repression from low-grade inflammation.

5.3. The glyceroneogenesis inhibition produced by olanzapine treatment may be enhanced by c-Jun enriched expression. Contrastingly, aripiprazole does not modify this signalling

PGC1α is known to protect against hepatic steatosis and insulin resistance through its binding at the promoter region of IL-10 (Wan et al. 2020). IL-10 is a cytokine of type II with anti-inflammatory properties that has a critical role in preventing inflammatory and autoimmune pathologies (Saraiva and O'Garra 2010). In a study with mice, inhibition of IL-10 for 5 days led to an increase in the expression of inflammatory cytokines such as TNF-a, IL6, IL-1b, the deterioration of insulin signalling and the activation of gluconeogenic and lipidogenic pathways (Cintra et al. 2008). In the analysis performed with PGC1α KO mice, the most up-regulated gene by olanzapine in the KO mice compared to WT mice was *Junb*. Interestingly, this gene

was not dysregulated by the treatment with aripiprazole. *Junb* makes part of the transcriptional factor AP-1, a protein complex consisting of proteins belonging to the Jun (c-jun, junB and junD) and Fos (c-Fos, FosB, among others) families (Tapia et al. 2016). Saturated FFAs activate AF-1, which promotes the expression of inflammatory cytokines such as TNF-α and IL-1, which enable an inflammation state (Tapia et al. 2016). In a model of mice, a 12-week high calory diet promoted the development of obesity, insulin resistance, significant hepatic steatosis, inflammation and fibrosis. c-Jun expression was enriched, which was also confirmed in human tissues. Therefore, it was concluded that the abundance of c-Jun in NAFLD eases the development and progression to its advanced form nonalcoholic steatohepatitis (NASH) (Dorn et al. 2014).

The absent metabolic protection conferred by PGC1α in the PGC1α KO mice, allowed us to observe up-regulation of *Junb,* which was specific to the treatment with olanzapine as the *Junb* expression was not modified by aripiprazole. These outcomes suggest that the metabolic disarrangements produced by olanzapine in the different models studied may be at least in part produced by c-Jun enriched expression, causing pro-inflammatory signalling. This signalling, however, was not disrupted by aripiprazole, which may explain the more benign metabolic side effects produced by aripiprazole.

5.4. Olanzapine may disrupt insuline and glucose activities in β-cell through enhancement of Irs4

Olanzapine up-regulated *Irs4* expression in pancreatic islets from WT mice. Irs4 is one of the 4 Insulin receptor substrate (IRS) molecules. It has been observed that IRS4 may negatively regulate the insulin-like growth factor 1 (IGF-1) signalling by suppressing IRS-1 and IRS-2 activity at several steps. While IRS1 null mice have shown reduced body size, insulin resistance and hyperplasia; deletion of IRS2 has caused defective hepatic insulin action, failure to suppress glucose production in the liver and β-cell deficiency caused by compromised IGF-1 mitogenic signalling (González-Rodríguez et al. 2010). This information suggests that olanzapine may impair insulin and glucose activities in β-cell through the enhanced activity of Irs4.

5.5. Muscle fibres turning into a more glycolytic phenotype due to olanzapine treatment lack protection against insulin resistance and glucose intolerance. Aripiprazole favoured an intermediate fast oxidative-glycolytic phenotype

The short-term treatment (5 days) with olanzapine up-regulated *Cox6a2* in mice liver. COX6A is one of the thirteen subunits of the respiratory chain complex IV and, in mammals, is present in two isoforms: COX6A1, liver-type; and COX6A2, heart-type (Quintens et al. 2013). In a study with *Cox6a2* deficient mice, it was observed that *Cox6a2* deficiency is protective against obesity, insulin resistance and glucose intolerance induced by a high-fat diet. This protection was conferred by the skeletal muscle fibres turning into a more oxidative phenotype with consequent increase of ROS production, activation of AMPK, and increased expression of uncoupling proteins, which dissipate energy as heat (Quintens et al. 2013). Because *Cox6a2* was not repressed in the mice treated with olanzapine, this protection is not present, which may contribute to olanzapine metabolic side effects.

The long-term treatment (6 months) with olanzapine down-regulated *Plin4* expression in WT mice liver. It has been reported that PLIN4, one of the 5 perilipin (PLIN) family members, is involved in lipid droplets (LDs) formation in human adipocytes (Nimura et al. 2015). Consequently, olanzapine increases the protein expression of PLIN4 during adipocyte differentiation as it contributes to the initial stage of LD formation. Little is known about PLIN4 activity in the liver, and its over-expression in adipose tissue due to olanzapine treatment contrast our outcomes as we saw olanzapine repressing *Plin4* in the liver. However, it has been observed that PLIN4 is more abundant in type I fibres (oxidative fibres) than in type II (glycolytic fibre) in skeletal muscles (Pourteymour et al. 2015). These outcomes may provide insight into why we observed down-regulation of *Plin4* by olanzapine as it may contribute to fibres turning into a more glycolytic phenotype, thus reducing the abundance of *Plin4* and, as mentioned before, losing their protection against obesity, insulin resistance and glucose intolerance.

Contrary to olanzapine, aripiprazole long-term treatment (6 months) produced up-regulation of *Plin4* in the liver from WT mice. As already mentioned *Plin4* is more abundant in oxidative fibres, suggesting that oxidative fibres are being favoured by aripiprazole, contributing to its protective phenotype against insulin resistance and glucose intolerance. This outcome

correlates with the heavily over-expression of *Myh2* (Log2FoldChange= 25.62) observed in pancreatic islets after the short-term treatment with aripiprazole. Myh2 is present in fibres with an intermediate fast oxidative-glycolytic phenotype; thus, it can be suggested that by avoiding the glycolytic fibres phenotype, aripiprazole maintains its protective state against insulin and glucose impairments.

5.6. Aripiprazole activates *hnf4a* signalling, possibly as a compensatory effect to inflammation

The hematopoietic cell lineage was the most significantly dysregulated pathway by the treatment with aripiprazole, being the glycoprotein Ib platelet subunit beta gene (*GP1BB*), the most repressed gene with a fold change of -23.81. A study of the differentially expressed proteins in obese relative to subjects using PBMCs extracts showed a -1.52 fold-change for GP1BB (Abu-Farha et al. 2013). Other down-regulated genes with a Log2FoldChange< -1.5 were chemokine ligand genes as *CXCL3*, *CCL24* and *CCL22*. Chemokines are cytokines that induce cell migration and inflammation. By homology with the observed with olanzapine, it is possible to sense that the metabolic disturbances produced by aripiprazole may be related to the induction of inflammation.

The above idea is supported by other up-regulated pathways by aripiprazole in the volunteers such as Retinol metabolism, Steroid hormone biosynthesis, and Ovarian steroidogenesis included top up-regulated CYP family genes, such as CYP450 isoform 1A1 (*CYP1A1*). *CYP1A1* is the hallmark of oxidative stress, as it is one of the microsome cytochromes that most strongly generate ROS (He et al. 2015). CYP is a superfamily of hemeproteins mainly found in the endoplasmic reticulum (Fessler and Parks 2011). CYP catalyses the oxidative metabolism of several endogenous and foreign compounds mainly by inserting an oxygen atom in the substrate molecule (Park, Reed, and Backes 2015). Some compounds generated by CYPs can activate an inflammatory response, which can modify the expression and activity of CYPs, reducing or enhancing ongoing drug metabolism and therefore altering its toxicity (Woolbright and Jaeschke 2015).

Maturity-onset diabetes of the young (MODY) gene set was up-regulated on healthy human volunteers by aripiprazole treatment. MODY is a monogenic form of diabetes that results in the dysfunction of pancreatic β-cells and, therefore, insulin production (Heuvel-Borsboom et al. 2016). However, several suspect genes have been implicated in the MODY onset, from which the most common are hepatocyte nuclear factors (*HNF1A*, *HNF4A*, *HNF1B)* and *GCK* genes

(Yahaya and Ufuoma 2020). HNF4A, HNF1A and HNF1B are transcription factors that regulate the insulin gene expression and genes involved in glucose metabolism and transport. Their reduced expression in the β-cells leads to reduced insulin production and release (Heuvel-Borsboom et al. 2016). Out of the MODY gene-set, *HNF4A* was the most up-regulated gene by the treatment with aripiprazole. As HNF4A activates hepatic gluconeogenesis and has been implicated in inflammation, diabetes and lipid metabolism (Santiago and Potashkin 2015).

PPARg coactivator 1α (PGC-1α) is a co-activator for HNF4α to activate target genes such as *Pck1*. The absence of HNF4α in mouse liver leads to steatosis due to altered fatty acid metabolism and transport (Gonzalez 2008), probably as a consequence of its ability to activate PEPCK. Having HNF4A up-regulated in the volunteers after the treatment with aripiprazole may suggest that aripiprazole is activating a compensatory signalling through the up-regulation of HNF4A to avoid the metabolic effects produced by reduced FA synthesis, which could be triggered by an inflammatory state produced by the treatment with aripiprazole.

Genes associated with acyl-CoA metabolism (acyl-CoA synthases, thioesterases, ligases and a co-factor for a desaturase) have been pointed out as putative HNF4A targets (Fang et al. 2012). Among them, *ACSM2B* (acyl-CoA synthetase medium-chain family member 2B) was the most up-regulated gene in humans out of the "Butanoate metabolism" gene-set, followed by other family genes as *ACSM2A,* a mitochondrial enzyme that catalyzes the first step of fatty acid metabolism, fatty acid activation, through the transfer of acyl-CoA [provided by RefSeq, May 2017], suggesting that *HNF4A* up-regulation, subsequently favours the butanoate metabolism through overexpression of acyl-CoA synthetase medium-chain family genes.

Butanoate, also known as butyrate, is a gut microbiota metabolic product (Zhang et al. 2019) that primes the production of acetyl-CoA for entry into the Krebs cycle (Walejko et al. 2018). Short-chain fatty acids (SCFAs) such as acetate, butyrate, and propionate have been thought to have a role in preventing and treating metabolic syndrome (Kasubuchi et al. 2015). Butyrate, for example, increased insulin sensitivity and energy expenditure in obese mice (Gao et al. 2009). It has also shown to protect against obesity-induced through the diet and regulate gut hormones (Lin et al. 2012). It is metabolized by mitochondria to generate ATP. Specifically, butyrate enters the TCA cycle as acetyl-CoA and is converted to citrate and subsequently to OAA (Zhang et al. 2021), impacting energy expenditure and metabolic functions as body weight, insulin sensitivity and glucose homeostasis (Kasubuchi et al. 2015). This information supports the idea of aripiprazole compensating metabolic disturbances as up-regulation of the butanoate metabolism enhances FA synthesis.

In summary, although aripiprazole may be inducing inflammation, it seems to compensate it through activation of *HNF4A* signalling, promoting FA synthesis, and therefore avoiding the adverse effects of excessive FAA production.

Aripiprazole down-regulated *Fabp1* expression in WT mice pancreatic islets after 5 days of treatment. FABP1 is a fatty acid-binding protein (FABP) that is abundant in the liver in mice, although it is also expressed in the small intestine and pancreas. FABP1 belongs to a family of molecules that direct lipid responses in cells. Its principal function is the transport of lipophilic substrates such as long-chain fatty acids. Furthermore, it possesses antioxidant and hepatoprotective properties (Bogdan et al. 2015). It has been reported that repression of FABP1 in the liver decreases hepatic TG accumulation and improves hepatic inflammation and oxidative stress (Mukai et al. 2017). These outcomes suggest that down-regulated *Fabp1* expression may be part of the compensatory effect that aripiprazole showed on human volunteers.

Supporting this idea, aripiprazole also down-regulated *Pnlip* (pancreatic lipase) in pancreatic islets from WT mice after a short-scheme treatment. *Pnlip* is an enzyme secreted by the pancreas to hydrolyzes TG in the small intestine. Repression of Pnlip has been shown to inhibit high-fat diet-induced obesity in mice and aid in losing weight in humans [provided by RefSeq, Jul 2016].

Finally, it was observed that aripiprazole up-regulated the expression of *IL-10* in the liver from WT mice treated for 6 months with aripiprazole. As already mentioned, IL-10 possess anti-inflammatory properties and, therefore, has a critical role in preventing inflammation. This outcome supports all the above mentioned as the over-expression of IL-10 aids to counteract the inflammation produced by the antipsychotic treatment.

5.7. Dysregulated genes by olanzapine maintain their effect over time. On the contrary, aripiprazole showed differential responses after short- and long-term treatments

Genes that were dysregulated by olanzapine at both short- and long treatment schemes (Table 5) in the liver of WT mice enriched lipid and insulin related pathways such as “Fatty acid degradation”, “PPAR signalling pathway”, “Peroxisome”, “Fatty acid biosynthesis”,

“Cholesterol metabolism”, “Insulin resistance” and “Adipocytokine signalling pathway”. The genes that enriched these pathways kept a similar dysregulation at short- and long-term treatment, suggesting that the metabolic impairments observed presented shortly after beginning the treatment with olanzapine (5 days) and remained during the chronic treatment (at least 6 months).

Contrary to olanzapine, most genes dysregulated by aripiprazole in the liver of WT mice showed different responses after the short- and long-term scheme treatments (Table 4). An example of this is the expression of *pdk4,* which after the 5 days treatment was down-regulated (Log2FoldChange= -1,15), while after the 6 months, treatment was up-regulated (Log2FoldChange= 2,37). PDK4 directs glucose and fat consumption. It has been observed that deficiency of Pdk4 in mice contributed to liver regeration by enhancing insulin-signalling sensitivity and FA oxidation and intracellular ATP production (Zhao et al. 2020). These results suggest that down-regulation of *pdk4* during the short-term treatment may answer to one of aripiprazole compensatory mechanisms. However, its up-regulation after 6 months treatment may indicate that not all compensatory mechanisms last during chronic administration, which may be the reason why aripirazole seems to activate different compensatory pathways, as not all responses may last. This reasoning could also explain that even aripiprazole is considered to have a benign metabolic profile due to its reduced amount of metabolic disturbances, it may still impare some pathways when then compensatory mechanisms fail. Further analysis may be done to elucidate aripiprazole’s protective mechanisms timing.

5.8. The volunteers showed differential responses to the treatments; therefore, their stratification to enhance personalized medicine is possible

When performing PCA and sample to sample distance matrices of the healthy human volunteer sample’s, it was observed that the samples were divided into two different clusters. One of the clusters included volunteers for which minor modification by the treatments was observed; on the other cluster, a more significant impact by the treatment occurred as the samples from the same volunteer spread apart, showing a larger distance in the plots among them.

A volunteer for which minimal impact by the treatments was chosen as reference, and differential expression analyses were performed comparing each volunteer against the reference one. A PCA produced fed with the DEGs plotted the volunteers through the X-axis

according to their level of impact by the treatments. The volunteers with weak reactions were plotted on the right side of the axis, while those with stronger reactions were plotted on the left side. A third group with what could be described as an intermediate reaction was placed in the centre of the plot. By removing the genes equally expressed among all volunteers, we were able to keep only the genes with different expression levels among the 3 clusters of volunteers.

The differentially expressed genes were tested against the TRANSFAC, and JASPAR PWMs database showed the enrichment of peroxisome proliferator-activated receptor gamma (PPARG) as 178 out of the 805 DEGs have binding motifs for PPARG at their promoters. These results are encouraging as they support the idea that the split of the volunteers into the three clusters may be related to individual levels of response to PPARG signalling. To test this, we performed a single nucleotide variant prediction with VarScan (Koboldt et al. 2012) from BWA alignments, followed by annotation with Annovar to search for differential polymorphisms among the volunteers' clusters. As a result, all volunteers previously classified as having a low response had polymorphisms on one or both of *PPARGC1B* and *PPARGC1A*. In contrast, none of the volunteers with medium or high responses had polymorphisms on any of these genes. These outcomes suggest that *PPARGC1* may be related to the volunteers differential response to the treatments.

Out of these analyses, we divided the volunteers into low or high + medium responses to test the statistical differences in clinical variables such as weight, glucose, insulin, cholesterol and TG, between the two groups. The only clinical variable that showed the statistical difference was the weight. While the volunteers with low response generally gained weight on the first 15 days of the trial, the volunteers with high and medium responses either maintained or reduced their weight.

As most polymorphisms were found on *PPARGC1B*, we produced plots to visualise assembled transcripts for *PPARGC1B.* It was observed that the same transcripts were produced for all volunteers at all time points. Therefore no alternative splicing on this gene is leading the differential response to the treatments. However, the abundance of the transcripts in the volunteers with a high response was noticeable higher than for the medium and low response ones. *PPARGC1B* plays a key role in the development and pathophysiology of T2DM; therefore, its differential abundance among the different groups of volunteers supports the idea that the volunteers may have actually having a differential response to the treatments because of these differences. We propose that is essential to stratify the patients by their *PPARGC1B* genotype and to continue researching on the topic to gain a better understanding on the pharmacogenomics impact of these polymorphisms regarding the antipsychotic treatments.

We performed differential expression analyses comparing the low response volunteers against the medium + high response groups. Almost all DEGs were obtained for the medium + high response group treated with aripiprazole. Enrichment analysis of these DEGs against different databases showed the enrichment of several pathways, most of them related to inflammatory signalling (Table 9). These outcomes suggest that the treatment with aripiprazole may be inducing the compensatory mechanisms observed in the previous analyses, therefore showing more extensive gene expression changes in the volunteers with high + low response. As these mechanisms are activated through the PPAR signalling, it is reasonable to think that the polymorphisms found in the low response volunteers, which in the majority are related to obesity, may be preventing these volunteers from activating protective mechanisms after the treatment with aripiprazole. This theory correlates with the weight differences observed between the two groups, as the volunteers with low response gained weight during the trial, while the volunteers with high and medium responses either maintained or reduced their weight.

The above outcomes may also explain why even we observed gene expression changes in the analysis of healthy human volunteers, most of these changes were not statistically significant. Moreover, we did not observe changes related to cytokines expression. The inter-personal variability could explain these outcomes as all the volunteers were analyzed together and as seen now, they have differential responses to the treatments, therefore not allowing to reach statistical significance.

By observing the value in classifying the volunteers according to their response to the treatments. We decided to perform features selection to select the genes that better classify the volunteers into the two groups. These procedures is useful as instead of testing the 805 DEGs found, we can only test the 21 selected genes and have an even higher accuracy rate.

The selection must be taken with caution as this list of genes was chosen based on the current volunteers' analyses, which account for a small sample size. Further research with larger sample sizes would be needed to avoid overfitting and generate a list of genes that better classify the general population. However, knowing that the people may have different responses to the antipsychotic treatments and that categorising them according to their response as soon as 5 days after the beginning of a treatment is a big step forward to the highly needed personalized medicine. An example of this would be to identify the people with poor ability to activate compensatory mechanisms after the treatment with aripiprazole to assess a change to a medication that may be more convenient for them.

6. CONCLUSIONS

The conclusions of the present Doctoral Thesis are as follows:

1. Olanzapine-induced metabolic disarrangements may be explained by PEPCK signalling repression from low-grade inflammation that may occur as a result of TLR4 signalling activation. PEPCK repression leads to glyceroneogenesis, which enhances FFA contributing to metabolic disarrangements, such as dyslipidemia and hepatic steatosis, impaired glucose metabolism and insulin sensitivity, reduced insulin clearance, peripheral tissue hyperinsulinemia, impaired pancreatic β-cell function, among others.
2. The glyceroneogenesis inhibition produced by olanzapine treatment may be enhanced by c-Jun enriched expression. Contrastingly, aripiprazole does not modify this signalling.
3. Olanzapine may impair insulin and glucose activities in β-cell through the enhanced activity of Irs4.
4. Muscle fibres turning into a more glycolytic phenotype due to olanzapine treatment may produce a lack of protection against insulin resistance and glucose intolerance. Aripiprazole favoured oxidative and intermediate fast oxidative-glycolytic fibres; thus, it can be suggested that by avoiding the glycolytic fibres phenotype, aripiprazole maintains its protective state against insulin and glucose impairments.
5. Aripiprazole activates hnf4a signalling, possibly as a compensatory effect to inflammation.
6. Dysregulated genes by olanzapine maintain their expression level over time. On the contrary, aripiprazole showed differential responses after short- and long-term treatments. This may be an indicator of aripiprazole's protective mechanisms being limited over time and, from there, the need of achieving this protection through different mechanisms.
7. The volunteers may be stratified according to their response to the treatment as it was observed that *PPARGC1* polymorphisms in some people might prevent them from activating aripiprazole's compensatory mechanisms.
8. Lak of statistical significance in the human study was possibly related to the small size of the series and undoubtedly to the interpersonal variability.

9. To assess the people's response to the antipsychotic treatment shortly after the start would allow taking data-based decision on the convenience of that specific treatment in a particular person.

10. Further analyzes are required to validate the above outcomes.

Altogether, the previous conclusions allow us to propose that the metabolic impact differences between olanzapine and aripiprazole are due to aripiprazole activating compensatory signallings to avoid metabolic disturbances produced by inflammation. In contrast, olanzapine, by lacking these compensatory actions, enhances the development of glyceroneogenesis, which subsequently produces an increase of FFA that finally impacts lipid and glucose metabolisms.

The stratification of the volunteers according to their response to the treatment allowed us to recognize those individuals that we believe cannot activate aripiprazole’s compensatory pathways. This knowledge could be transferred into a predictive test to assess shortly after the beginning of an antipsychotic treatment if any specific patient has a relatively higher risk of developing a metabolic syndrome than other, thus allowing a more precise clinical follow-up.

Finally, although the data and conclusions collected in this work are of great interest, additional validations are required that should include larger series of patients to confirm the data and provide them with clinical utility.

7. CONCLUSIONES

Las conclusiones de la presente Tesis Doctoral son las siguientes:

1. Los trastornos metabólicos inducidos por olanzapina pueden explicarse por la represión de la señalización de PEPCK a partir de una inflamación de bajo grado que puede ocurrir como resultado de la activación de la señalización de TLR4. La represión de PEPCK conduce a la gliceroneogénesis, lo que aumenta los ácidos grasos libres, lo que contribuye a trastornos metabólicos, como dislipidemia y esteatosis hepática, alteración del metabolismo de la glucosa, sensibilidad a la insulina, eliminación reducida de insulina, hiperinsulinemia del tejido periférico, y alteración de la función de las células β pancreáticas, entre otros.
2. La inhibición de la gliceroneogénesis producida por el tratamiento con olanzapina puede ser aumentada mediante la sobreexpresión de *CJUN*. Por el contrario, aripiprazol no modifica esta señalización.
3. Olanzapina puede alterar las funciones la insulina y la glucosa en las células β a través de la sobreexpresión de Irs4.
4. Las fibras musculares que se vuelven más glucolíticas debido al tratamiento con olanzapina pueden producir una falta de protección contra la resistencia a la insulina y la intolerancia a la glucosa. Aripiprazol favoreció las fibras oxidativas y glucolíticas-oxidativas rápidas; por lo tanto, se puede sugerir que al evitar el fenotipo de fibras glucolíticas, aripiprazol mantiene su estado protector contra las alteraciones de insulina y glucosa.
5. Aripiprazol activa la señalización de hnf4a, posiblemente como un efecto compensatorio contra la inflamación.
6. Los genes desregulados por olanzapina mantienen su nivel de expresión a lo largo del tiempo. Por el contrario, aripiprazol mostró respuestas diferenciales después de tratamientos a corto y largo plazo. Esto puede ser un indicador de que los mecanismos protectores de aripiprazol están limitados en el tiempo, lo que crea la necesidad de lograr esta protección a través de diferentes mecanismos.
7. Los voluntarios pueden estratificarse según su respuesta al tratamiento ya que se observó que los polimorfismos en *PPARGC1* en algunas personas podrían impedirles activar los mecanismos compensatorios de aripiprazol.

8. La falta de significancia estadística en el estudio humano posiblemente estuvo relacionada con el pequeño tamaño de la serie e indudablemente con la variabilidad interpersonal
9. Evaluar la respuesta de las personas al tratamiento antipsicótico al poco tiempo de iniciarlo permitiría tomar una decisión basada en datos sobre la conveniencia de ese tratamiento específico en una persona en particular.
10. Se requieren más análisis para validar los resultados anteriores

En conjunto, las conclusiones anteriores nos permiten proponer que las diferencias de impacto metabólico entre olanzapina y aripiprazol se deben a que aripiprazol activa señales compensatorias para evitar alteraciones metabólicas producidas por la inflamación. Por el contrario, olanzapina, al carecer de estas acciones compensatorias, potencia el desarrollo de gliceroneogénesis, que posteriormente produce un aumento de FFA que finalmente impacta el metabolismo de los lípidos y la glucosa.

La estratificación de los voluntarios según su respuesta al tratamiento nos permitió reconocer aquellos individuos con más dificultades para activar las vías compensatorias del aripiprazol. Este conocimiento podría trasladarse a una prueba predictiva para evaluar, poco después del inicio de un tratamiento antipsicótico, si algún paciente específico tiene un riesgo relativamente mayor de desarrollar un síndrome metabólico que otro, permitiendo así un seguimiento clínico más preciso.

Finalmente, aunque los datos y las conclusiones recogidas en este trabajo son de gran interés, se requieren validaciones adicionales que incluyan series de pacientes de mayor tamaño para confirmar los datos y dotarlos de utilidad clínica.

8. BIBLIOGRAPHY

Abu-Farha, Mohamed, Ali Tiss, Jehad Abubaker, Abdelkrim Khadir, Fahad Al-Ghimlas, Irina Al-Khairi, Engin Baturcam, Preethi Cherian, Naser Elkum, Maha Hammad, Jeena John, Sina Kavalakatt, Samia Warsame, Kazem Behbehani, Said Dermime, and Mohammed Dehbi. 2013. "Proteomics Analysis of Human Obesity Reveals the Epigenetic Factor HDAC4 as a Potential Target for Obesity." *PLoS ONE* 8(9):1–17. doi: 10.1371/journal.pone.0075342.

Alvarez-Herrera, Samantha, Raúl Escamilla, Oscar Medina-Contreras, Ricardo Saracco, Yvonne Flores, Gabriela Hurtado-Alvarado, José Luis Maldonado-García, Enrique Becerril-Villanueva, Gilberto Pérez-Sánchez, and Lenin Pavón. 2020. "Immunoendocrine Peripheral Effects Induced by Atypical Antipsychotics." *Frontiers in Endocrinology* 11(April). doi: 10.3389/fendo.2020.00195.

Bába, László István, Melinda Kolcsár, Imre Zoltán Kun, Zsófia Ulakcsai, Fruzsina Bagaméry, Éva Szökő, Tamás Tábi, and Zsolt Gáll. 2019. "Effects of Cariprazine, Aripiprazole, and Olanzapine on Mouse Fibroblast Culture: Changes in Adiponectin Contents in Supernatants, Triglyceride Accumulation, and Peroxisome Proliferator-Activated Receptor-γ Expression." *Medicina (Lithuania)* 55(5). doi: 10.3390/medicina55050160.

Bach, Daniel, Sara Pich, Francesc X. Soriano, Nathalie Vega, Bernhard Baumgartner, Josep Oriola, Jens R. Daugaard, Jorge Lloberas, Marta Camps, Juleen R. Zierath, Rémi Rabasa-Lhoret, Harriet Wallberg-Henriksson, Martine Laville, Manuel Palacín, Hubert Vidal, Francisca Rivera, Martin Brand, and Antonio Zorzano. 2003. "Mitofusin-2 Determines Mitochondrial Network Architecture and Mitochondrial Metabolism: A Novel Regulatory Mechanism Altered in Obesity." *Journal of Biological Chemistry* 278(19):17190–97. doi: 10.1074/jbc.M212754200.

Balt, S. L., G. P. Galloway, M. J. Baggott, Z. Schwartz, and J. Mendelson. 2011. "Mechanisms and Genetics of Antipsychotic-Associated Weight Gain." *Clinical Pharmacology and Therapeutics* 90(1):179–83. doi: 10.1038/clpt.2011.97.

Bartoli, Francesco, Cristina Crocamo, Massimo Clerici, and Giuseppe Carrà. 2015. "Second-Generation Antipsychotics and Adiponectin Levels in Schizophrenia: A Comparative Meta-Analysis." *European Neuropsychopharmacology* 25(10):1767–74. doi: 10.1016/j.euroneuro.2015.06.011.

Bartoli, Francesco, Annamaria Lax, Cristina Crocamo, Massimo Clerici, and Giuseppe Carrà. 2015. "Plasma Adiponectin Levels in Schizophrenia and Role of Second-Generation Antipsychotics: A Meta-Analysis." *Psychoneuroendocrinology* 56:179–89. doi: 10.1016/j.psyneuen.2015.03.012.

De Bartolomeis, Andrea, Carmine Tomasetti, and Felice Iasevoli. 2015. "Update on the Mechanism of Action of Aripiprazole: Translational Insights into Antipsychotic Strategies beyond Dopamine Receptor Antagonism." *CNS Drugs* 29(9):773–99. doi: 10.1007/s40263-015-0278-3.

Beale, Elmus G., Brandy J. Harvey, and Claude Forest. 2007. "PCK1 and PCK2 as Candidate

Diabetes and Obesity Genes." *Cell Biochemistry and Biophysics* 48(2–3):89–95. doi: 10.1007/s12013-007-0025-6.

Beddow, Sara A., Arijeet K. Gattu, Daniel F. Vatner, Lauren Paolella, Abdulelah Alqarzaee, Nedda Tashkandi, Violeta B. Popov, Christopher D. Church, Matthew S. Rodeheffer, Gary W. Cline, John G. Geisler, Sanjay Bhanot, and Varman T. Samuel. 2019. "PEPCK1 Antisense Oligonucleotide Prevents Adiposity and Impairs Hepatic Glycogen Synthesis in High-Fat Male Fed Rats." *Endocrinology* 160(1):205–19. doi: 10.1210/en.2018-00630.

Belbasis, L., C. A. Köhler, N. Stefanis, B. Stubbs, J. van Os, E. Vieta, M. V. Seeman, C. Arango, A. F. Carvalho, and E. Evangelou. 2018. "Risk Factors and Peripheral Biomarkers for Schizophrenia Spectrum Disorders: An Umbrella Review of Meta-Analyses." *Acta Psychiatrica Scandinavica* 137(2):88–97. doi: 10.1111/acps.12847.

Bence, Kendra K., Mirela Delibegovic, Bingzhong Xue, Cem Z. Gorgun, Gokhan S. Hotamisligil, Benjamin G. Neel, and Barbara B. Kahn. 2006. "Neuronal PTP1B Regulates Body Weight, Adiposity and Leptin Action." *Nature Medicine* 12(8):917–24. doi: 10.1038/nm1435.

Birkenaes, Astrid B., Kåre I. Birkeland, Vein Friis, Stein Opjordsmoen, and Ole A. Andreassen. 2009. "Hormonal Markers of Metabolic Dysregulation in Patients with Severe Mental Disorders after Olanzapine Treatment under Real-Life Conditions." *Journal of Clinical Psychopharmacology* 29(2):109–16. doi: 10.1097/JCP.0b013e31819b95fc.

Blanchet, Lionel, Lutgarde M.C. Buydens, Jan A.M. Smeitink, Peter H.G.M. Willems, and Werner J.H. Koopman. 2012. "Isolated Mitochondrial Complex I Deficiency: Explorative Data Analysis of Patient Cell Parameters." *Current Pharmaceutical Design* 17(36):4023–33. doi: 10.2174/138161211798764870.

Blum, Kenneth, Panayotis K. Thanos, and Mark S. Gold. 2014. "Dopamine and Glucose, Obesity and Reward Deficiency Syndrome." *Frontiers in Psychology* 5(AUG):1–11. doi: 10.3389/fpsyg.2014.00919.

Bogdan, Maria, Isabela Silosi, Petra Surlin, Andrei Adrian Tica, Oana Sorina Tica, Tudor Adrian Balseanu, Anne Marie Rauten, and Adrian Camen. 2015. "Salivary and Serum Biomarkers for the Study of Side Effects of Aripiprazole Coprescribed with Mirtazapine in Rats." *International Journal of Clinical and Experimental Medicine* 8(5):8051–59.

Bray, Nicolas L., Harold Pimentel, Páll Melsted, and Lior Pachter. 2016. "Near-Optimal Probabilistic RNA-Seq Quantification." *Nature Biotechnology* 34(5):525–27. doi: 10.1038/nbt.3519.

Brixner, Diana I., Qayyim Said, Patricia K. Corey-Lisle, A. Vickie Tuomari, Gilbert J. L'Italien, William Stockdale, and Gary M. Oderda. 2006. "Naturalistic Impact of Second-Generation Antipsychotics on Weight Gain." *Annals of Pharmacotherapy* 40(4):626–32. doi: 10.1345/aph.1G564.

Bromberg, Anna, Elad Lerer, Madhara Udawela, Elizabeth Scarr, Brian Dean, R. H. Belmaker, Richard Ebstein, and Galila Agam. 2012. "Nicotinamide-N-Methyltransferase (NNMT) in Schizophrenia: Genetic Association and Decreased Frontal Cortex MRNA Levels." *International Journal of Neuropsychopharmacology* 15(6):727–37. doi:

10.1017/S1461145711001179.

Brunmeir, Reinhard, and Feng Xu. 2018. “Functional Regulation of PPARs through Post-Translational Modifications.” *International Journal of Molecular Sciences* 19(6). doi: 10.3390/ijms19061738.

Bullard, James H., Elizabeth Purdom, Kasper D. Hansen, and Sandrine Dudoit. 2010. “Evaluation of Statistical Methods for Normalization and Differential Expression in MRNA-Seq Experiments.” *BMC Bioinformatics* 11(1):1–13. doi: 10.1186/1471-2105-11-94.

Bulló, Monica, Pilar García-Lorda, Isabel Megias, and Jordi Salas-Salvadó. 2003. “Systemic Inflammation, Adipose Tissue Tumor Necrosis Factor, and Leptin Expression.” *Obesity Research* 11(4):525–31. doi: 10.1038/oby.2003.74.

Burgess, Shawn C., Natasha Hausler, Matthew Merritt, F. Mark H. Jeffrey, Charles Storey, Angela Milde, Seena Koshy, Jill Lindner, Mark A. Magnuson, Craig R. Malloy, and A. Dean Sherry. 2004. “Impaired Tricarboxylic Acid Cycle Activity in Mouse Livers Lacking Cytosolic Phosphoenolpyruvate Carboxykinase.” *Journal of Biological Chemistry* 279(47):48941–49. doi: 10.1074/jbc.M407120200.

Burrows, T., C. E. Collins, and M. L. Garg. 2011. “Omega-3 Index, Obesity and Insulin Resistance in Children.” *International Journal of Pediatric Obesity* 6(2–2):532–39. doi: 10.3109/17477166.2010.549489.

Caffin, F., A. Prola, J. Piquereau, M. Novotova, D. J. David, A. Garnier, D. Fortin, M. V. Alavi, V. Veksler, R. Ventura-Clapier, and F. Joubert. 2013. “Altered Skeletal Muscle Mitochondrial Biogenesis but Improved Endurance Capacity in Trained OPA1-Deficient Mice.” *Journal of Physiology* 591(23):6017–37. doi: 10.1113/jphysiol.2013.263079.

Cai, H. L., Q. Y. Tan, P. Jiang, R. L. Dang, Y. Xue, M. M. Tang, P. Xu, Y. Deng, H. D. Li, and J. K. Yao. 2015. “A Potential Mechanism Underlying Atypical Antipsychotics-Induced Lipid Disturbances.” *Translational Psychiatry* 5(10). doi: 10.1038/tp.2015.161.

del Campo, Andrea, Catalina Bustos, Carolina Mascayano, Claudio Acuña-Castillo, Rodrigo Troncoso, and Leonel E. Rojo. 2018. “Metabolic Syndrome and Antipsychotics: The Role of Mitochondrial Fission/Fusion Imbalance.” *Frontiers in Endocrinology* 9(APR):1–7. doi: 10.3389/fendo.2018.00144.

Caniato, Riccardo N., Marlies E. Alvarenga, and Miguel Angel Garcia-Alcaraz. 2006. “Effect of Omega-3 Fatty Acids on the Lipid Profile of Patients Taking Clozapine.” *Australian and New Zealand Journal of Psychiatry* 40(8):691–97. doi: 10.1111/j.1440-1614.2006.01869.x.

Chandley, Michelle J., Attila Szebeni, Katalin Szebeni, Jessica D. Crawford, Craig A. Stockmeier, Gustavo Turecki, Richard M. Kostrzewa, and Gregory A. Ordway. 2014. “Elevated Gene Expression of Glutamate Receptors in Noradrenergic Neurons from the Locus Coeruleus in Major Depression.” *International Journal of Neuropsychopharmacology* 17(10):1569–78. doi: 10.1017/S1461145714000662.

Chen, Chia Hui, Song Kun Shyue, Chiao Po Hsu, and Tzong Shyuan Lee. 2018. “Atypical

Antipsychotic Drug Olanzapine Deregulates Hepatic Lipid Metabolism and Aortic Inflammation and Aggravates Atherosclerosis." *Cellular Physiology and Biochemistry* 50(4):1216–29. doi: 10.1159/000494573.

Chen, Po See, Yen Kuang Yang, Tzung Lieh Yeh, I. Hui Lee, Wei Jen Yao, Nan Tsing Chiu, and Ru Band Lu. 2008. "Correlation between Body Mass Index and Striatal Dopamine Transporter Availability in Healthy Volunteers-A SPECT Study." *NeuroImage* 40(1):275–79. doi: 10.1016/j.neuroimage.2007.11.007.

Chen, Shifu, Yanqing Zhou, Yaru Chen, and Jia Gu. 2018. "Fastp: An Ultra-Fast All-in-One FASTQ Preprocessor." *Bioinformatics* 34(17):i884–90. doi: 10.1093/bioinformatics/bty560.

Chinetti, G., J. C. Fruchart, and B. Staels. 2000. "Peroxisome Proliferator-Activated Receptors (PPARs): Nuclear Receptors at the Crossroads between Lipid Metabolism and Inflammation." *Inflammation Research* 49(10):497–505. doi: 10.1007/s000110050622.

Christine Rummel-Kluge, MD, MD Katja Komossa, Sandra Schwarz, Heike Hunger, Franziska Schmid, MD Werner Kissling, MSc Claudia Asenjo Lobos, MD John M Davis, and MDa Stefan Leucht. 2010. "Head-to-Head Comparisons of Metabolic Side Effects of Second Generation Antipsychotics in the Treatment of Schizophrenia: A Systematic Review and Meta-Analysis." *Schizophrenia Research* 123(2–3):225–33. doi: 10.1016/j.schres.2010.07.012.Head-to-head.

Cintra, Dennys E., José R. Pauli, Eliana P. Araújo, Juliana C. Moraes, Cláudio T. de Souza, Marciane Milanski, Joseane Morari, Alessandra Gambero, Mário J. Saad, and Licio A. Velloso. 2008. "Interleukin-10 Is a Protective Factor against Diet-Induced Insulin Resistance in Liver." *Journal of Hepatology* 48(4):628–37. doi: 10.1016/j.jhep.2007.12.017.

Coccurello, Roberto, and Anna Moles. 2010. "Potential Mechanisms of Atypical Antipsychotic-Induced Metabolic Derangement: Clues for Understanding Obesity and Novel Drug Design." *Pharmacology and Therapeutics* 127(3):210–51. doi: 10.1016/j.pharmthera.2010.04.008.

Collier, James J., and Donald K. Scott. 2004. "Sweet Changes: Glucose Homeostasis Can Be Altered by Manipulating Genes Controlling Hepatic Glucose Metabolism." *Molecular Endocrinology* 18(5):1051–63. doi: 10.1210/me.2003-0357.

Cone, Roger D. 2005. "Anatomy and Regulation of the Central Melanocortin System." *Nature Neuroscience* 8(5):571–78. doi: 10.1038/nn1455.

Conesa, Ana, Pedro Madrigal, Sonia Tarazona, David Gomez-Cabrero, Alejandra Cervera, Andrew McPherson, Michal Wojciech Szcześniak, Daniel J. Gaffney, Laura L. Elo, Xuegong Zhang, and Ali Mortazavi. 2016. "A Survey of Best Practices for RNA-Seq Data Analysis." *Genome Biology* 17(1):1–19. doi: 10.1186/s13059-016-0881-8.

Copps, K. D., and M. F. White. 2012. "Regulation of Insulin Sensitivity by Serine/Threonine Phosphorylation of Insulin Receptor Substrate Proteins IRS1 and IRS2." *Diabetologia* 55(10):2565–82. doi: 10.1007/s00125-012-2644-8.

Costa-Silva, Juliana, Douglas Domingues, and Fabricio Martins Lopes. 2017. "RNA-Seq

Differential Expression Analysis: An Extended Review and a Software Tool." *PLoS ONE* 12(12):1–18. doi: 10.1371/journal.pone.0190152.

DeLeon, Anthony, Nick C. Patel, and M. Lynn Crismon. 2004. "Aripiprazole: A Comprehensive Review of Its Pharmacology, Clinical Efficacy, and Tolerability." *Clinical Therapeutics* 26(5):649–66. doi: 10.1016/S0149-2918(04)90066-5.

Dennis, Edward A., Raymond A. Deems, Richard Harkewicz, Oswald Quehenberger, H. Alex Brown, Stephen B. Milne, David S. Myers, Christopher K. Glass, Gary Hardiman, Donna Reichart, Alfred H. Merrill, M. Cameron Sullards, Elaine Wang, Robert C. Murphy, Christian R. H. Raetz, Teresa A. Garrett, Ziqiang Guan, Andrea C. Ryan, David W. Russell, Jeffrey G. McDonald, Bonne M. Thompson, Walter A. Shaw, Manish Sud, Yihua Zhao, Shakti Gupta, Mano R. Maurya, Eoin Fahy, and Shankar Subramaniama. 2010. "A Mouse Macrophage Lipidome." *Journal of Biological Chemistry* 285(51):39976–85. doi: 10.1074/jbc.M110.182915.

Divac, Nevena, Milica Prostran, Igor Jakovcevski, and Natasa Cerovac. 2014. "Second-Generation Antipsychotics and Extrapyramidal Adverse Effects." *BioMed Research International* 2014:6. doi: 10.1155/2014/656370.

Dong, Qingzhuo, Chengcheng Lv, Gejun Zhang, Zi Yu, Chuize Kong, Cheng Fu, and Yu Zeng. 2018. "Impact of RNA-Binding Motif 3 Expression on the Whole Transcriptome of Prostate Cancer Cells: An RNA Sequencing Study." *Oncology Reports* 40(4):2307–15. doi: 10.3892/or.2018.6618.

Dorn, Christoph, Julia C. Engelmann, Michael Saugspier, Andreas Koch, Arndt Hartmann, Martina Müller, Rainer Spang, Anja Bosserhoff, and Claus Hellerbrand. 2014. "Increased Expression of C-Jun in Nonalcoholic Fatty Liver Disease." *Laboratory Investigation* 94(4):394–408. doi: 10.1038/labinvest.2014.3.

Dwyer, Donard S., and Dallas Donohoe. 2003. "Induction of Hyperglycemia in Mice with Atypical Antipsychotic Drugs That Inhibit Glucose Uptake." *Pharmacology Biochemistry and Behavior* 75(2):255–60. doi: 10.1016/S0091-3057(03)00079-0.

Evans, D. R., V. V. Parikh, M. M. Khan, C. Coussons, P. F. Buckley, and S. P. Mahadik. 2003. "Red Blood Cell Membrane Essential Fatty Acid Metabolism in Early Psychotic Patients Following Antipsychotic Drug Treatment." *Prostaglandins Leukotrienes and Essential Fatty Acids* 69(6):393–99. doi: 10.1016/j.plefa.2003.08.010.

Van Exel, Eric, Jacobijn Gussekloo, Anton J. M. De Craen, Marijke Frölich, Annetje Bootsma Van Der Wiel, and Rudi G. J. Westendorp. 2002. "Low Production Capacity of Interleukin-10 Associates with the Metabolic Syndrome and Type 2 Diabetes: The Leiden 85-plus Study." *Diabetes* 51(4):1088–92. doi: 10.2337/diabetes.51.4.1088.

Fang, Bin, Daniel Mane-Padros, Eugene Bolotin, Tao Jiang, and Frances M. Sladek. 2012. "Identification of a Binding Motif Specific to HNF4 by Comparative Analysis of Multiple Nuclear Receptors." *Nucleic Acids Research* 40(12):5343–56. doi: 10.1093/nar/gks190.

Fasipe, Olumuyiwa John. 2017. "Neuropharmacological Classification of Antidepressant Agents Based on Their Mechanisms of Action." *Archives of Medicine and Health Science*

6(1):81–94. doi: 10.4103/amhs.amhs.

Feingold, Kenneth R., Arthur Moser, Judy K. Shigenaga, and Carl Grunfeld. 2012. "Inflammation Inhibits the Expression of Phosphoenolpyruvate Carboxykinase in Liver and Adipose Tissue." *Innate Immunity* 18(2):231–40. doi: 10.1177/1753425911398678.

Felin, Tricia, Sadiq Naveed, and Amna M. Chaudhary. 2018. "Aripiprazole-Induced Neutropenia: Case Report and Literature Review." *J Psychosoc Nurs Ment Health Serv* 56:21–24.

Fernø, Johan, Silje Skrede, Audun O. Vik-Mo, Bjarte Håvik, and Vidar M. Steen. 2006. "Drug-Induced Activation of SREBP-Controlled Lipogenic Gene Expression in CNS-Related Cell Lines: Marked Differences between Various Antipsychotic Drugs." *BMC Neuroscience* 7:1–11. doi: 10.1186/1471-2202-7-69.

Fessler, Michael B., and John S. Parks. 2011. "Intracellular Lipid Flux and Membrane Microdomains as Organizing Principles in Inflammatory Cell Signaling." *The Journal of Immunology* 187(4):1529–35. doi: 10.4049/jimmunol.1100253.Intracellular.

Frazee, a. C., G. Pertea, a. E. Jaffe, B. Langmead, S. L. Salzberg, and J. T. Leek. 2014. "Flexible Isoform-Level Differential Expression Analysis with Ballgown." *BioRxiv* (March):0–13.

Gao, Zhanguo, Jun Yin, Jin Zhang, Robert E. Ward, Roy J. Martin, Michael Lefevre, William T. Cefalu, and Jianping Ye. 2009. "Butyrate Improves Insulin Sensitivity and Increases Energy Expenditure in Mice." *Diabetes* 58(7):1509–17. doi: 10.2337/db08-1637.

Gavin, James R., K. G. M. M. Alberti, Mayer B. Davidson, Ralph A. DeFronzo, Allan Drash, Steven G. Gabbe, Saul Genuth, Maureen I. Harris, Richard Kahn, Harry Keen, William C. Knowler, Harold Lebovitz, Noel K. Maclaren, Jerry P. Palmer, Philip Raskin, Robert A. Rizza, and Michael P. Stern. 2002. "Report of the Expert Committee on the Diagnosis and Classification of Diabetes Mellitus." *Diabetes Care* 25(SUPPL. 1):5–20. doi: 10.2337/diacare.25.2007.s5.

Gillespie, Amy L., Ruta Samanaite, Jonathan Mill, Alice Egerton, and James H. MacCabe. 2017. "Is Treatment-Resistant Schizophrenia Categorically Distinct from Treatment-Responsive Schizophrenia? A Systematic Review." *BMC Psychiatry* 17(1):1–14. doi: 10.1186/s12888-016-1177-y.

Gonçalves, Pedro, João Ricardo Araújo, and Fátima Martel. 2015. "Antipsychotics-Induced Metabolic Alterations: Focus on Adipose Tissue and Molecular Mechanisms." *European Neuropsychopharmacology* 25(1):1–16. doi: 10.1016/j.euroneuro.2014.11.008.

González-Rodríguez, Águeda, Jose A. Mas Gutierrez, Silvia Sanz-González, Manuel Ros, Deborah J. Burks, and Ángela M. Valverde. 2010. "Inhibition of PTP1B Restores IRS1-Mediated Hepatic Insulin Signaling in IRS2-Deficient Mice." *Diabetes* 59(3):588–99. doi: 10.2337/db09-0796.

Gonzalez, Frank J. 2008. "Regulation of Hepatocyte Nuclear Factor 4α-Mediated Transcription." *Drug Metabolism and Pharmacokinetics* 23(1):2–7. doi: 10.2133/dmpk.23.2.

Gorina, Roser, Miriam Font-Nieves, Leonardo Márquez-Kisinousky, Tomàs Santalucia, and Anna M. Planas. 2011. “Astrocyte TLR4 Activation Induces a Proinflammatory Environment through the Interplay between MyD88-Dependent NFκB Signaling, MAPK, and Jak1/Stat1 Pathways.” *Glia* 59(2):242–55. doi: 10.1002/glia.21094.

Grigson, Patricia Sue. 2002. “Like Drugs for Chocolate: Separate Rewards Modulated by Common Mechanisms?” *Physiology and Behavior* 76(3):345–46. doi: 10.1016/S0031-9384(02)00779-5.

Gubert, Carolina, Laura Stertz, Bianca Pfaffenseller, Bruna Schilling Panizzutti, Gislaine Tezza Rezin, Raffael Massuda, Emilio Luiz Streck, Clarissa Severino Gama, Flávio Kapczinski, and Maurício Kunz. 2013. “Mitochondrial Activity and Oxidative Stress Markers in Peripheral Blood Mononuclear Cells of Patients with Bipolar Disorder, Schizophrenia, and Healthy Subjects.” *Journal of Psychiatric Research* 47(10):1396–1402. doi: 10.1016/j.jpsychires.2013.06.018.

Haupt, Dan W., and John W. Newcomer. 2001. “Hyperglycemia and Antipsychotic Medications.” *Journal of Clinical Psychiatry* 62(SUPPL. 27):15–26.

He, Meng, Kun Qian, Ying Zhang, Xu Feng Huang, Chao Deng, Baohua Zhang, Guanbin Gao, Jing Li, Hao Xie, and Taolei Sun. 2021. “Olanzapine-Induced Activation of Hypothalamic Astrocytes and Toll-Like Receptor-4 Signaling via Endoplasmic Reticulum Stress Were Related to Olanzapine-Induced Weight Gain.” *Frontiers in Neuroscience* 14(January):1–21. doi: 10.3389/fnins.2020.589650.

He, Qin, Jin Ke Li, Fang Li, Ru Gui Li, Guo Qing Zhan, Gang Li, Wei Xing Du, and Hua Bing Tan. 2015. “Mechanism of Action of Gypenosides on Type 2 Diabetes and Non-Alcoholic Fatty Liver Disease in Rats.” *World Journal of Gastroenterology* 21(7):2058–66. doi: 10.3748/wjg.v21.i7.2058.

Hegedus, Csaba, Diána Kovács, Rita Kiss, Réka Sári, József Németh, Zoltán Szilvássy, and Barna Peitl. 2015. “Effect of Long-Term Olanzapine Treatment on Meal-Induced Insulin Sensitization and on Gastrointestinal Peptides in Female Sprague-Dawley Rats.” *Journal of Psychopharmacology* 29(12):1271–79. doi: 10.1177/0269881115602952.

Le Hellard, S., F. M. Theisen, M. Haberhausen, M. B. Raeder, J. Fernø, S. Gebhardt, A. Hinney, H. Remschmidt, J. C. Krieg, C. Mehler-Wex, M. M. Nöthen, J. Hebebrand, and V. M. Steen. 2009. “Association between the Insulin-Induced Gene 2 (INSIG2) and Weight Gain in a German Sample of Antipsychotic-Treated Schizophrenic Patients: Perturbation of SREBP-Controlled Lipogenesis in Drug-Related Metabolic Adverse Effects?” *Molecular Psychiatry* 14(3):308–17. doi: 10.1038/sj.mp.4002133.

De Hert, Marc, Linda Hanssens, Ruud Van Winkel, Martien Wampers, Dominique Van Eyck, Andre Scheen, and Joseph Peuskens. 2007. “A Case Series: Evaluation of the Metabolic Safety of Aripiprazole.” *Schizophrenia Bulletin* 33(3):823–30. doi: 10.1093/schbul/sbl037.

Heuvel-Borsboom, H., H. W. de Valk, M. Losekoot, and J. Westerink. 2016. “Maturity Onset Diabetes of the Young: Seek and You Will Find.” *Netherlands Journal of Medicine* 74(5):193–200.

Ho, Cyrus S. H., Melvyn W. B. Zhang, Anselm Mak, and Roger C. M. Ho. 2014. “Metabolic Syndrome in Psychiatry: Advances in Understanding and Management.” *Advances in Psychiatric Treatment* 20(2):101–12. doi: 10.1192/apt.bp.113.011619.

Holt, Richard I. G., and Robert C. Peveler. 2011. “Metabolic Syndrome and Mental Illness.” *The Metabolic Syndrome: Second Edition* (November):177–93. doi: 10.1002/9781444347319.ch11.

Hotamisligil, G. S., and B. M. Spiegelman. 1994. “Tumor Necrosis Factor Alpha: A Key Component of the Obesity-Diabetes Link.” *Diabetes* 43(11):1271–78. doi: 10.2337/diabetes.43.11.1271.

Hotta, Kikuko, Tohru Funahashi, Noni L. Bodkin, Heidi K. Ortmeyer, Yukio Arita, Barbara C. Hansen, and Yuji Matsuzawa. 2001. “Circulating Concentrations of the Adipocyte Protein Adiponectin Are Decreased in Parallel with Reduced Insulin Sensitivity during the Progression to Type 2 Diabetes in Rhesus Monkeys.” *Diabetes* 50(5):1126–33. doi: 10.2337/diabetes.50.5.1126.

Houseknecht, Karen L., Alan S. Robertson, William Zavadoski, E. Michael Gibbs, David E. Johnson, and Hans Rollema. 2007. “Acute Effects of Atypical Antipsychotics on Whole-Body Insulin Resistance in Rats: Implications for Adverse Metabolic Effects.” *Neuropsychopharmacology* 32(2):289–97. doi: 10.1038/sj.npp.1301209.

Ijaz, Sharea, Blanca Bolea, Simon Davies, Jelena Savović, Alison Richards, Sarah Sullivan, and Paul Moran. 2018. “Antipsychotic Polypharmacy and Metabolic Syndrome in Schizophrenia: A Review of Systematic Reviews.” *BMC Psychiatry* 18(1):1–13. doi: 10.1186/s12888-018-1848-y.

Illumina. 2017. “TruSeq ® Stranded Total RNA Reference Guide.” 42.

Infantino, Vittoria, Paolo Convertini, Liana Cucci, Maria Antonietta Panaro, Maria Antonietta Di Noia, Rosa Calvello, Ferdinando Palmieri, and Vito Iacobazzi. 2011. “The Mitochondrial Citrate Carrier: A New Player in Inflammation.” *Biochemical Journal* 438(3):433–36. doi: 10.1042/BJ20111275.

Inoue, Yusuke, Ai Ming Yu, Hee Yim Sun, Xiaochao Ma, Kristopher W. Krausz, Junko Inoue, Charlie C. Xiang, Michael J. Brownstein, Gösta Eggertsen, Ingemar Björkhem, and Frank J. Gonzalez. 2006. “Regulation of Bile Acid Biosynthesis by Hepatocyte Nuclear Factor 4α.” *Journal of Lipid Research* 47(1):215–27. doi: 10.1194/jlr.M500430-JLR200.

Jarc, Eva, and Toni Petan. 2020. “A Twist of FATe: Lipid Droplets and Inflammatory Lipid Mediators.” *Biochimie* 169:69–87. doi: 10.1016/j.biochi.2019.11.016.

Jassim, G., J. Fernø, F. M. Theisen, M. Haberhausen, A. Christoforou, B. Håvik, S. Gebhardt, H. Remschmidt, C. Mehler-Wex, J. Hebebrand, S. Lehellard, and V. M. Steen. 2011. “Association Study of Energy Homeostasis Genes and Antipsychotic-Induced Weight Gain in Patients with Schizophrenia.” *Pharmacopsychiatry* 44(1):15–20. doi: 10.1055/s-0030-1263174.

JW., Newcomer. 2005. “Second-Generation (Atypical) Antipsychotics and Metabolic Effects: A Comprehensive Literature Review.” *CNS Drugs* 19(1):1–93.

Kadowaki, Takashi, Toshimasa Yamauchi, Naoto Kubota, Kazuo Hara, Kohjiro Ueki, and Kazuyuki Tobe. 2006. “Adiponectin and Adiponectin Receptors in Insulin Resistance, Diabetes, and the Metabolic Syndrome.” *Journal of Clinical Investigation* 116(7):1784–92. doi: 10.1172/JCI29126.

Kahn, R., Buse, J., Ferrannini, E., & Stern, M. 2005. “The Metabolic Syndrome : Time for A.” *He Metabolic Syndrome: Time for a Critical Appraisal. Diabetologia* 48(9):1684–99.

Kane, John. 2011. “Clozapine for the Treatment-Resistant Schizophrenic.” *Archives of General Psychiatry* 45(9):789. doi: 10.1001/archpsyc.1988.01800330013001.

Kapur, S., and P. Seeman. 2001. “Does Fast Dissociation from the Dopamine D2 Receptor Explain the Action of Atypical Antipsychotics?: A New Hypothesis.” *American Journal of Psychiatry* 158(3):360–69. doi: 10.1176/appi.ajp.158.3.360.

Karolewicz, Beata, Craig A. Stockmeier, and Gregory A. Ordway. 2005. “Elevated Levels of the NR2C Subunit of the NMDA Receptor in the Locus Coeruleus in Depression.” *Neuropsychopharmacology* 30(8):1557–67. doi: 10.1038/sj.npp.1300781.Elevated.

Kasubuchi, Mayu, Sae Hasegawa, Takero Hiramatsu, Atsuhiko Ichimura, and Ikuo Kimura. 2015. “Dietary Gut Microbial Metabolites, Short-Chain Fatty Acids, and Host Metabolic Regulation.” *Nutrients* 7(4):2839–49. doi: 10.3390/nu7042839.

Khan, Mohammad M., Denise R. Evans, Vijayasudha Gunna, Russell E. Scheffer, Vinay V. Parikh, and Sahebarao P. Mahadik. 2002. “Reduced Erythrocyte Membrane Essential Fatty Acids and Increased Lipid Peroxides in Schizophrenia at the Never-Medicated First-Episode of Psychosis and after Years of Treatment with Antipsychotics.” *Schizophrenia Research* 58(1):1–10. doi: 10.1016/S0920-9964(01)00334-6.

Kim, Daehwan, Joseph M. Paggi, Chanhee Park, Christopher Bennett, and Steven L. Salzberg. 2019. “Graph-Based Genome Alignment and Genotyping with HISAT2 and HISAT-Genotype.” *Nature Biotechnology* 37(8):907–15. doi: 10.1038/s41587-019-0201-4.

Kim, Sun H., Lilla Nikolics, Fahim Abbasi, Cindy Lamendola, James Link, Gerald M. Reaven, and Steven Lindley. 2010. “Relationship between Body Mass Index and Insulin Resistance in Patients Treated with Second Generation Antipsychotic Agents.” *Journal of Psychiatric Research* 44(8):493–98. doi: 10.1016/j.jpsychires.2009.11.007.

Kluge, Michael, Andreas Schuld, Alexander Schacht, Hubertus Himmerich, Mira A. Dalal, Peter M. Wehmeier, Dunja Hinze-Selch, Thomas Kraus, Ralf W. Dittmann, and Thomas Pollmächer. 2009. “Effects of Clozapine and Olanzapine on Cytokine Systems Are Closely Linked to Weight Gain and Drug-Induced Fever.” *Psychoneuroendocrinology* 34(1):118–28. doi: 10.1016/j.psyneuen.2008.08.016.

Ko, Chih Wei, Daniel Counihan, Jing Wu, Maria Hatzoglou, Michelle A. Puchowicz, and Colleen M. Croniger. 2018. “Macrophages with a Deletion of the Phosphoenolpyruvate Carboxykinase 1 (Pck1) Gene Have a More Proinflammatory Phenotype.” *Journal of Biological Chemistry* 293(9):3399–3409. doi: 10.1074/jbc.M117.819136.

Koboldt, Daniel C., Qunyuan Zhang, David E. Larson, Dong Shen, Michael D. McLellan, Ling Lin, Christopher A. Miller, Elaine R. Mardis, Li Ding, and Richard K. Wilson. 2012. “VarScan 2:

Somatic Mutation and Copy Number Alteration Discovery in Cancer by Exome Sequencing." *Genome Research* 22(3):568–76. doi: 10.1101/gr.129684.111.

Koopman, Werner J. H., Leo G. J. Nijtmans, Cindy E. J. Dieteren, Peggy Roestenberg, Federica Valsecchi, Jan A. M. Smeitink, and Peter H. G. M. Willems. 2010. "Mammalian Mitochondrial Complex I : Biogenesis, Regulation, and Reactive Oxygen Species Generation." *Antioxidants & Redox Signaling* 12(12).

Kotzka, Jorg, and Dirk Müller-Wieland. 2004. "Sterol Regulatory Element-Binding Protein (SREBP)-1: Gene Regulatory Target for Insulin Resistance?" *Expert Opinion on Therapeutic Targets* 8(2):141–49. doi: 10.1517/14728222.8.2.141.

Langmead, Ben, and Steven L. Salzberg. 2012. "Fast Gapped-Read Alignment with Bowtie 2." *Nature Methods* 9(4):357–59. doi: 10.1038/nmeth.1923.

Lavretsky, Helen. 2008. "History of Schizophrenia as a Psychiatric Disorder. Clinical Handbook of Schizophrenia." *Acta Medica Croatica* 73(1):3–12.

Leroyer, Stéphanie N., Joan Tordjman, Geneviève Chauvet, Joëlle Quette, Charles Chapron, Claude Forest, and Bénédicte Antoine. 2006. "Rosiglitazone Controls Fatty Acid Cycling in Human Adipose Tissue by Means of Glyceroneogenesis and Glycerol Phosphorylation." *Journal of Biological Chemistry* 281(19):13141–49. doi: 10.1074/jbc.M512943200.

Lewis, Gary F., André Carpentier, Khosrow Adeli, and Adria Giacca. 2002. "Disordered Fat Storage and Mobilization in the Pathogenesis of Insulin Resistance and Type 2 Diabetes." *Endocrine Reviews* 23(2):201–29. doi: 10.1210/edrv.23.2.0461.

Li, Pingping, Nathanael J. Spann, Minna U. Kaikkonen, Min Lu, Da Young Oh, N. Fox, Gautam Bandyopadhyay, Saswata Talukdar, Jianfeng Xu, William S. Lagakos, David Patsouris, Aaron Armando, Oswald Quehenberger, Edward A. Dennis, M. Steven, Johan Auwerx, Christopher K. Glass, and Jerrold M. Olefsky. 2013. "NCoR Repression of LXRs Restricts Macrophage Biosynthesis of Insulin-Sensitizing Omega 3 Fatty Acids." *Cell* 155(1):200–214. doi: 10.1016/j.cell.2013.08.054.NCoR.

Liao, Peizhou, Glen A. Satten, and Yi Juan Hu. 2017. "PhredEM: A Phred-Score-Informed Genotype-Calling Approach for next-Generation Sequencing Studies." *Genetic Epidemiology* 41(5):375–87. doi: 10.1002/gepi.22048.

Liew, Choong Chin, Jun Ma, Hong Chang Tang, Run Zheng, and Adam A. Dempsey. 2006. "The Peripheral Blood Transcriptome Dynamically Reflects System Wide Biology: A Potential Diagnostic Tool." *Journal of Laboratory and Clinical Medicine* 147(3):126–32. doi: 10.1016/j.lab.2005.10.005.

Lim, Myung Ho, Jong Il Park, and Tae Won Park. 2013. "A Case with Neutropenia Related with the Use of Various Atypical Antipsychotics." *Psychiatry Investigation* 10(4):428–31. doi: 10.4306/pi.2013.10.4.428.

Lin, Hua V., Andrea Frassetto, Edward J. Kowalik, Andrea R. Nawrocki, Mofei M. Lu, Jennifer R. Kosinski, James A. Hubert, Daphne Szeto, Xiaorui Yao, Gail Forrest, and Donald J. Marsh. 2012. "Butyrate and Propionate Protect against Diet-Induced Obesity and Regulate Gut Hormones via Free Fatty Acid Receptor 3-Independent Mechanisms." *PLoS ONE* 7(4):1–

9. doi: 10.1371/journal.pone.0035240.

Lin, Jhih Rong, Ying Cai, Quanwei Zhang, Wen Zhang, Rubén Nogales-Cadenas, and Zhengdong D. Zhang. 2016. “Integrated Post-GWAS Analysis Sheds New Light on the Disease Mechanisms of Schizophrenia.” *Genetics* 204(4):1587–1600. doi: 10.1534/genetics.116.187195.

Lingala, Shilpa MD, and Marc G. MD MHSc Ghany. 2016. “可乐定和右美托嘧啶产生抗伤害协同作用 HHS Public Access.” 25(3):289–313. doi: 110.1016/j.bbi.2017.04.008.

Lopes-Marques, Mónica, Isabel Cunha, Maria Armanda Reis-Henriques, Miguel M. Santos, and L. Filipe C. Castro. 2013. “Diversity and History of the Long-Chain Acyl-CoA Synthetase (Acsl) Gene Family in Vertebrates.” *BMC Evolutionary Biology* 13(1). doi: 10.1186/1471-2148-13-271.

Love, Michael I., Simon Anders, Vladislav Kim, and Wolfgang Huber. 2019. “RNA-Seq Workflow: Gene-Level Exploratory Analysis and Differential Expression.” Retrieved January 15, 2021 (https://master.bioconductor.org/packages/release/workflows/vignettes/rnaseqGene/inst/doc/rnaseqGene.html#the-deseqdataset-object-sample-information-and-the-design-formula).

Mahadik, Sahebarao P., and Sukdeb Mukherjee. 1996. “Free Radical Pathology and Antioxidant Defense in Schizophrenia: A Review.” *Schizophrenia Research* 19(1):1–17. doi: 10.1016/0920-9964(95)00049-6.

Melé, Marta, Pedro G. Ferreira, Ferran Reverter, David S. DeLuca, Jean Monlong, Michael Sammeth, Taylor R. Young, Jakob M. Goldmann, Dmitri D. Pervouchine, Timothy J. Sullivan, Rory Johnson, Ayellet V. Segrè, Sarah Djebali, Anastasia Niarchou, The GTEx Consortium, Fred A. Wright, Tuuli Lappalainen, Miquel Calvo, Gad Getz, Emmanouil T. Dermitzakis, Kristin G. Ardlie, and Roderic Guigó. 2015. “The Human Transcriptome across Tissues and Individuals.” *Science* 348(6235):660–65.

Meyer, Jonathan M., and Carol E. Koro. 2004. “The Effects of Antipsychotic Therapy on Serum Lipids: A Comprehensive Review.” *Schizophrenia Research* 70(1):1–17. doi: 10.1016/j.schres.2004.01.014.

Millward, Carrie A., David DeSantis, Chang Wen Hsieh, Jason D. Heaney, Sorana Pisano, Yael Olswang, Lea Reshef, Michelle Beidelschies, Michelle Puchowicz, and Colleen M. Croniger. 2010. “Phosphoenolpyruvate Carboxykinase (Pck1) Helps Regulate the Triglyceride/Fatty Acid Cycle and Development of Insulin Resistance in Mice.” *Journal of Lipid Research* 51(6):1452–63. doi: 10.1194/jlr.M005363.

Mohr, Steve, and Choong Chin Liew. 2007. “The Peripheral-Blood Transcriptome: New Insights into Disease and Risk Assessment.” *Trends in Molecular Medicine* 13(10):422–32. doi: 10.1016/j.molmed.2007.08.003.

Moraes, Leonardo A., Laura Piqueras, and David Bishop-Bailey. 2006. “Peroxisome Proliferator-Activated Receptors and Inflammation.” *Pharmacology and Therapeutics* 110(3):371–85. doi: 10.1016/j.pharmthera.2005.08.007.

Mosser, David M., and Xia Zhang. 2008. “Interleukin-10: New Perspectives on an Old Cytokine.” *Immunol Rev* 226:205–18. doi: 10.1111/j.1600-065X.2008.00706.x.Interleukin-10.

Mukai, Takako, Miki Egawa, Tamaki Takeuchi, Hitoshi Yamashita, and Tatsuya Kusudo. 2017. “Silencing of FABP1 Ameliorates Hepatic Steatosis, Inflammation, and Oxidative Stress in Mice with Nonalcoholic Fatty Liver Disease.” *FEBS Open Bio* 7(7):1009–16. doi: 10.1002/2211-5463.12240.

Nimura, Satomi, Tomohiro Yamaguchi, Koki Ueda, Karin Kadokura, Toshihiro Aiuchi, Rina Kato, Takashi Obama, and Hiroyuki Itabe. 2015. “Olanzapine Promotes the Accumulation of Lipid Droplets and the Expression of Multiple Perilipins in Human Adipocytes.” *Biochemical and Biophysical Research Communications* 467(4):906–12. doi: 10.1016/j.bbrc.2015.10.045.

Ochoa-de la Paz, Lenin D., Rosario Gulias-Cañizo, Estela D´Abril Ruíz-Leyja, Hugo Sánchez-Castillo, and Jorge Parodí. 2021. “The Role of GABA Neurotransmitter in the Human Central Nervous System, Physiology, and Pathophysiology.” *Revista Mexicana de Neurociencia* 22(2):67–76. doi: 10.24875/rmn.20000050.

Olswang, Yael, Hannah Cohen, Orit Papo, Hanoch Cassuto, Colleen M. Croniger, Parvin Hakimi, Shirley M. Tilghman, Richard W. Hanson, and Lea Reshef. 2002. “A Mutation in the Peroxisome Proliferator-Activated Receptor γ-Binding Site in the Gene for the Cytosolic Form of Phosphoenolpyruvate Carboxykinase Reduces Adipose Tissue Size and Fat Content in Mice.” *Proceedings of the National Academy of Sciences of the United States of America* 99(2):625–30. doi: 10.1073/pnas.022616299.

Owen, M. J., Sawa, A., Mortensen, P. 2016. “Schizophrenia.” *Lancet* 388(10039):86–97. doi: 10.1016/S0140-6736(15)01121-6.Schizophrenia.

Owen, Oliver E., Satish C. Kalhan, and Richard W. Hanson. 2002. “The Key Role of Anaplerosis and Cataplerosis for Citric Acid Cycle Function.” *Journal of Biological Chemistry* 277(34):30409–12. doi: 10.1074/jbc.R200006200.

Owens, W. Anthony, Rajkumar J. Sevak, Ruggero Galici, Xiaoying Chang, Martin A. Javors, Aurelio Galli, Charles P. France, and Lynette C. Daws. 2005. “Deficits in Dopamine Clearance and Locomotion in Hypoinsulinemic Rats Unmask Novel Modulation of Dopamine Transporters by Amphetamine.” *Journal of Neurochemistry* 94(5):1402–10. doi: 10.1111/j.1471-4159.2005.03289.x.

Pachikian, B. D., A. M. Neyrinck, P. D. Cani, L. Portois, L. Deldicque, F. C. De Backer, L. B. Bindels, F. M. Sohet, W. J. Malaisse, M. Francaux, Y. A. Carpentier, and N. M. Delzenne. 2008. “Hepatic Steatosis in N-3 Fatty Acid Depleted Mice: Focus on Metabolic Alterations Related to Tissue Fatty Acid Composition.” *BMC Physiology* 8(1):1–11. doi: 10.1186/1472-6793-8-21.

Pan, Bo, Jiamei Lian, Xu Feng Huang, and Chao Deng. 2016. “Aripiprazole Increases the PKA Signalling and Expression of the GABAA Receptor and CREB1 in the Nucleus Accumbens of Rats.” *Journal of Molecular Neuroscience* 59(1):36–47. doi: 10.1007/s12031-016-0730-y.

Paoletti, Pierre, Camilla Bellone, and Qiang Zhou. 2013. “NMDA Receptor Subunit Diversity: Impact on Receptor Properties, Synaptic Plasticity and Disease.” *Nature Reviews Neuroscience* 14(6):383–400. doi: 10.1038/nrn3504.

Papanastasiou, Evangelos. 2013. “The Prevalence and Mechanisms of Metabolic Syndrome in Schizophrenia: A Review.” *Therapeutic Advances in Psychopharmacology* 3(1):33–51. doi: 10.1177/2045125312464385.

Park, Ji Won, James R. Reed, and Wayne L. Backes. 2015. “The Localization of Cytochrome P450s CYP1A1 and CYP1A2 into Different Lipid Microdomains Is Governed by Their N-Terminal and Internal Protein Regions.” *Journal of Biological Chemistry* 290(49):29449–60. doi: 10.1074/jbc.M115.687103.

Parone, Philippe A., Sandrine Da Druz, Daniel Tondera, Yves Mattenberger, Dominic I. James, Pierre Maechler, François Barja, and Jean Claude Martinou. 2008. “Preventing Mitochondrial Fission Impairs Mitochondrial Function and Leads to Loss of Mitochondrial DNA.” *PLoS ONE* 3(9):1–9. doi: 10.1371/journal.pone.0003257.

Parra, Valentina, Hugo E. Verdejo, Myriam Iglewski, Andrea Del Campo, Rodrigo Troncoso, Deborah Jones, Yi Zhu, Jovan Kuzmicic, Christian Pennanen, Camila Lopez-Crisosto, Fabián Jaña, Jorge Ferreira, Eduard Noguera, Mario Chiong, David A. Bernlohr, Amira Klip, Joseph A. Hill, Beverly A. Rothermel, Evan Dale Abel, Antonio Zorzano, and Sergio Lavandero. 2014. “Insulin Stimulates Mitochondrial Fusion and Function in Cardiomyocytes via the AktmTOR-NFkB-Opa-1 Signaling Pathway.” *Diabetes* 63(1):75–88. doi: 10.2337/db13-0340.

Patel, Krishna R., Jessica Cherian, Kunj Gohil, and Dylan Atkinson. 2014. “Schizophrenia: Overview and Treatment Options.” *P and T* 39(9):638–45.

Patterson, Terrell Ann, Michelle D. Brot, Aryana Zavosh, James O. Schenk, Patricia Szot, Dianne P. Figlewicz, and Dianne Figlewicz Lattermann. 1998. “Food Deprivation Decreases MRMA and Activity of the Rat Dopamine Transporter.” *Neuroendocrinology* 68(1):11–20. doi: 10.1159/000054345.

Peng, Lin, Huixia Yang, Yao Ye, Zhi Ma, Christina Kuhn, Martina Rahmeh, Sven Mahner, Antonis Makrigiannakis, Udo Jeschke, and Viktoria von Schönfeldt. 2021. “Role of Peroxisome Proliferator-Activated Receptors (Ppars) in Trophoblast Functions.” *International Journal of Molecular Sciences* 22(1):1–13. doi: 10.3390/ijms22010433.

Pertea, M., Pertea, G. M., Antonescu, C. M., Chang, T. C., Mendell, J. T., & Salzberg, S. L. 2015. “StringTie Enables Improved Reconstruction of a Transcriptome from RNA-Seq Reads.” *Nature Biotechnology* 33(3):290–95. doi: 10.1038/nbt.3122.StringTie.

Petersen, Anne Marie W., and Bente Klarlund Pedersen. 2005. “The Anti-Inflammatory Effect of Exercise.” *Journal of Applied Physiology* 98(4):1154–62. doi: 10.1152/japplphysiol.00164.2004.

Pi-Sunyer, F. Xavier. 2002. “The Obesity Epidemic: Pathophysiology and Consequences of Obesity.” *Obesity Research* 10(SUPPL. 2). doi: 10.1038/oby.2002.202.

Piotrowski, Patryk, Tomasz M. Gondek, Anna Królicka-Deręgowska, Błażej Misiak, Tomasz

Adamowski, and Andrzej Kiejna. 2017. “Causes of Mortality in Schizophrenia: An Updated Review of European Studies.” *Psychiatria Danubina Review* 29(2):108–20.

Pourteymour, Shirin, Sindre Lee, Torgrim M. Langleite, Kristin Eckardt, Marit Hjorth, Christian Bindesbøll, Knut T. Dalen, Kåre I. Birkeland, Christian A. Drevon, Torgeir Holen, and Frode Norheim. 2015. “Perilipin 4 in Human Skeletal Muscle: Localization and Effect of Physical Activity.” *Physiological Reports* 3(8):1–15. doi: 10.14814/phy2.12481.

Quintens, Roel, Sarvjeet Singh, Katleen Lemaire, Katrien de Bock, Mikaela Granvik, Anica Schraenen, Irene Olga Cornelia Maria Vroegrijk, Veronica Costa, Pieter van Noten, Dennis Lambrechts, Stefan Lehnert, Leentje van Lommel, Lieven Thorrez, Geoffroy de Faudeur, Johannes Anthonius Romijn, John Michael Shelton, Luca Scorrano, Henri Roger Lijnen, Peter Jacobus Voshol, Peter Carmeliet, Pradeep Puthenveetil Abraham Mammen, and Frans Schuit. 2013. “Mice Deficient in the Respiratory Chain Gene Cox6a2 Are Protected against High-Fat Diet-Induced Obesity and Insulin Resistance.” *PLoS ONE* 8(2). doi: 10.1371/journal.pone.0056719.

Quirós, Pedro M., Andrew J. Ramsay, David Sala, Erika Fernández-Vizarra, Francisco Rodríguez, Juan R. Peinado, Maria Soledad Fernández-García, José A. Vega, José A. Enríquez, Antonio Zorzano, and Carlos López-Otín. 2012. “Loss of Mitochondrial Protease OMA1 Alters Processing of the GTPase OPA1 and Causes Obesity and Defective Thermogenesis in Mice.” *EMBO Journal* 31(9):2117–33. doi: 10.1038/emboj.2012.70.

Raeder, Maria Baroy, Johan Fernø, Marte Glambek, Christine Stansberg, and Vidar M. Steen. 2006. “Antidepressant Drugs Activate SREBP and Up-Regulate Cholesterol and Fatty Acid Biosynthesis in Human Glial Cells.” *Neuroscience Letters* 395(3):185–90. doi: 10.1016/j.neulet.2005.10.096.

Ranjekar, Prabhakar K., Ashwini Hinge, Mahabaleshwar V. Hegde, Madhav Ghate, Anvita Kale, Sandhya Sitasawad, Ulhas V. Wagh, Vijay B. Debsikdar, and Sahebarao P. Mahadik. 2003. “Decreased Antioxidant Enzymes and Membrane Essential Polyunsaturated Fatty Acids in Schizophrenic and Bipolar Mood Disorder Patients.” *Psychiatry Research* 121(2):109–22. doi: 10.1016/S0165-1781(03)00220-8.

Rawson, Robert B. 2003. “Control of Lipid Metabolism by Regulated Intramembrane Proteolysis of Sterol Regulatory Element Binding Proteins (SREBPs).” *Biochemical Society Symposium* (70):221–31. doi: 10.1042/bss0700221.

Reynolds, Gavin P., and Shona L. Kirk. 2010. “Metabolic Side Effects of Antipsychotic Drug Treatment - Pharmacological Mechanisms.” *Pharmacology and Therapeutics* 125(1):169–79. doi: 10.1016/j.pharmthera.2009.10.010.

Ringen, P. Andreas, John A. Engh, Astrid B. Birkenaes, Ingrid Dieset, and Ole A. Andreassen. 2014. “Increased Mortality in Schizophrenia Due to Cardiovascular Disease - a Non-Systematic Review of Epidemiology, Possible Causes and Interventions.” *Frontiers in Psychiatry* 5(SEP):1–11. doi: 10.3389/fpsyt.2014.00137.

Riordan, Henry J., Paola Antonini, and Michael F. Murphy. 2011. “Atypical Antipsychotics and Metabolic Syndrome in Patients with Schizophrenia: Risk Factors, Monitoring, and Healthcare Implications.” *Am Health Drug Benefits* 4(5):292–302.

Saltiel, Alan R., and C. Ronald Kahn. 2001. “Insulin Signalling and the Regulation of Glucose and Lipid Metabolism.” *Nature* 414(6865):799–806. doi: 10.1038/414799a.

Santiago, Jose A., and Judith A. Potashkin. 2015. “Network-Based Metaanalysis Identifies HNF4A and PTBP1 as Longitudinally Dynamic Biomarkers for Parkinson’s Disease.” *Proceedings of the National Academy of Sciences of the United States of America* 112(7):2257–62. doi: 10.1073/pnas.1423573112.

Sapra, Mamta, Donna Lawson, Ali Iranmanesh, and Anjali Varma. 2016. “Adiposity-Independent Hypoadiponectinemia as a Potential Marker of Insulin Resistance and Inflammation in Schizophrenia Patients Treated with Second Generation Antipsychotics.” *Schizophrenia Research* 174(1–3):132–36. doi: 10.1016/j.schres.2016.04.051.

Saraiva, Margarida, and Anne O’Garra. 2010. “The Regulation of IL-10 Production by Immune Cells.” *Nature Reviews Immunology* 10(3):170–81. doi: 10.1038/nri2711.

Scaini, Giselli, João Quevedo, Dawn Velligan, David L. Roberts, Henriette Raventos, and Consuelo Walss-Bass. 2018. “Second Generation Antipsychotic-Induced Mitochondrial Alterations: Implications for Increased Risk of Metabolic Syndrome in Patients with Schizophrenia.” *European Neuropsychopharmacology* 28(3):369–80. doi: 10.1016/j.euroneuro.2018.01.004.

Sertoglu, Erdim, Huseyin Kayadibi, and Metin Uyanik. 2015. “A Biochemical View: Increase in Polyunsaturated Fatty Acid ω-6/ω-3 Ratio in Relation to Hepatic Steatosis in Patients with Non-Alcoholic Fatty Liver Disease.” *Journal of Diabetes and Its Complications* 29(1):157. doi: 10.1016/j.jdiacomp.2014.10.005.

Siafis, Spyridon, Dimitrios Tzachanis, Myrto Samara, and Georgios Papazisis. 2017. “Antipsychotic Drugs: From Receptor-Binding Profiles to Metabolic Side Effects.” *Current Neuropharmacology* 16(8):1210–23. doi: 10.2174/1570159x15666170630163616.

Sims, David, Ian Sudbery, Nicholas E. Ilott, Andreas Heger, and Chris P. Ponting. 2014. “Sequencing Depth and Coverage: Key Considerations in Genomic Analyses.” *Nature Reviews Genetics* 15(2):121–32. doi: 10.1038/nrg3642.

Smith, M., D. Hopkins, R. C. Peveler, R. I. Holt, M. Woodward, and K. Ismail. 2008. “First- v. Second-Generation Antipsychotics and Risk for Diabetes in Schizophrenia: Systematic Review and Meta-Analysis.” *British Journal of Psychiatry* 192(6):406–11. doi: 10.1192/bjp.bp.107.037184.

Sobiš, Jarosław, Monika Rykaczewska-Czerwińska, Elzbieta ̄więtochowska, and Piotr Gorczyca. 2015. “Therapeutic Effect of Aripiprazole in Chronic Schizophrenia Is Accompanied by Anti-Inflammatory Activity.” *Pharmacological Reports* 67(2):353–59. doi: 10.1016/j.pharep.2014.09.007.

Soneson, Charlotte, Michael I. Love, and Mark D. Robinson. 2015. “Differential Analyses for RNA-Seq: Transcript-Level Estimates Improve Gene-Level Inferences.” *F1000Research* 4(2):1521. doi: 10.12688/f1000research.7563.1.

Tagami, Keita, Yohei Kashiwase, Akinobu Yokoyama, Hitomi Nishimura, Kanako Miyano, Masami Suzuki, Seiji Shiraishi, Motohiro Matoba, Yuichiro Ohe, and Yasuhito Uezono.

2016. “The Atypical Antipsychotic, Olanzapine, Potentiates Ghrelin-Induced Receptor Signaling: An in Vitro Study with Cells Expressing Cloned Human Growth Hormone Secretagogue Receptor.” *Neuropeptides* 58(January 2019):93–101. doi: 10.1016/j.npep.2015.12.010.

Tapia, G. S., D. González-Mañán, A. D’Espessailles, and C. G. Dossi. 2016. “N-3 LCPUFA in the Reversal of Hepatic Steatosis: The Role of ACOX and CAT-1.” *Grasas y Aceites* 67(2):1–8. doi: 10.3989/gya.0886152.

The UniProt Consortium. 2021. “UniProt: The Universal Protein Knowledgebase in 2021.” *Nucleic Acids Research* 49(D1):D480–89. doi: 10.1093/nar/gkaa1100.

Tontonoz, P., E. Hu, J. Devine, E. G. Beale, and B. M. Spiegelman. 1995. “PPAR Gamma 2 Regulates Adipose Expression of the Phosphoenolpyruvate Carboxykinase Gene.” *Molecular and Cellular Biology* 15(1):351–57. doi: 10.1128/mcb.15.1.351.

Trapnell, Cole, Brian A. Williams, Geo Pertea, Ali Mortazavi, Gordon Kwan, Marijke J. Van Baren, Steven L. Salzberg, Barbara J. Wold, and Lior Pachter. 2010. “Transcript Assembly and Quantification by RNA-Seq Reveals Unannotated Transcripts and Isoform Switching during Cell Differentiation.” *Nature Biotechnology* 28(5):511–15. doi: 10.1038/nbt.1621.

Vatier, C., S. Kadiri, A. Muscat, C. Chapron, J. Capeau, and B. Antoine. 2012. “Visceral and Subcutaneous Adipose Tissue from Lean Women Respond Differently to Lipopolysaccharide-Induced Alteration of Inflammation and Glyceroneogenesis.” *Nutrition and Diabetes* 2(DECEMBER):e51-7. doi: 10.1038/nutd.2012.29.

Victoriano, Montserrat, Renaud De Beaurepaire, Nadia Naour, Michèle Guerre-Millo, Annie Quignard-Boulangé, Jean François Huneau, Véronique Mathé, Daniel Tomé, and Dominique Hermier. 2010. “Olanzapine-Induced Accumulation of Adipose Tissue Is Associated with an Inflammatory State.” *Brain Research* 1350:167–75. doi: 10.1016/j.brainres.2010.05.060.

Volkow, N. D., G. J. Wang, and R. D. Baler. 2011. “Reward, Dopamine and the Control of Food Intake: Implications for Obesity.” *Trends in Cognitive Sciences* 15(1):37–46. doi: 10.1016/j.tics.2010.11.001.Reward.

Volkow, Nora D., Gene Jack Wang, Joanna S. Fowler, Jean Logan, Millard Jayne, Dinko Franceschi, Cristopher Wong, Samuel J. Gatley, Andrew N. Gifford, Yu Shin Ding, and Naomi Pappas. 2002. “‘Nonhedonic’ Food Motivation in Humans Involves Dopamine in the Dorsal Striatum and Methylphenidate Amplifies This Effect.” *Synapse* 44(3):175–80. doi: 10.1002/syn.10075.

Walejko, Jacquelyn M., Jeremy P. Koelmel, Timothy J. Garrett, Arthur S. Edison, and Maureen Keller-Wood. 2018. “Multiomics Approach Reveals Metabolic Changes in the Heart at Birth.” *American Journal of Physiology - Endocrinology and Metabolism* 315(6):E1212–23. doi: 10.1152/ajpendo.00297.2018.

Wan, Xingyong, Xudong Zhu, Hu Wang, Ye Feng, Weihua Zhou, Peihao Liu, Weiyan Shen, Lingling Zhang, Leiming Liu, Tangliang Li, Daojun Diao, Fan Yang, Qi Zhao, Li Chen, Jian Ren, Sheng Yan, Jing Li, Chaohui Yu, and Zhenyu Ju. 2020. “PGC1α Protects against

Hepatic Steatosis and Insulin Resistance via Enhancing IL10-Mediated Anti-Inflammatory Response." *FASEB Journal* 34(8):10751–61. doi: 10.1096/fj.201902476R.

Wang, G. J., N. D. Volkow, J. Logan, and N. R. Pappas. 2001. "ScienceDirect.Com - The Lancet - Brain Dopamine and Obesity." *The Lancet* 357:354–57.

Wang, Helen H., Dong Ki Lee, Min Liu, Piero Portincasa, and David Q. H. Wang. 2020. *Novel Insights into the Pathogenesis and Management of the Metabolic Syndrome*. Vol. 23.

Wang, Kai, Mingyao Li, and Hakon Hakonarson. 2010. "ANNOVAR: Functional Annotation of Genetic Variants from High-Throughput Sequencing Data." *Nucleic Acids Research* 38(16):1–7. doi: 10.1093/nar/gkq603.

Wang, Zhong, Mark Gerstein, and Michael Snyder. 2009. "RNA-Seq: A Revolutionary Tool for Transcriptomics." *Nature Reviews Genetics* 10(1):57–63.

Williams, A. G., Thomas, S., Wyman, S. K., & Holloway, A. K. 2014. "RNA‐seq Data: Challenges in and Recommendations for Experimental Design and Analysis." *Current Protocols in Human Genetics* 83(1):11–13. doi: 10.1038/jid.2014.371.

Witten, Daniela M. 2011. "Classification and Clustering of Sequencing Data Using a Poisson Model." *Annals of Applied Statistics* 5(4):2493–2518. doi: 10.1214/11-AOAS493.

Woolbright, Benjamin L., and Hartmut Jaeschke. 2015. "Xenobiotic and Endobiotic Mediated Interactions between the Cytochrome P450 System and the Inflammatory Response In the Liver." *Advances in Pharmacology* 74:131–61. doi: 10.1016/bs.apha.2015.04.001.Xenobiotic.

Xu, Haiyun, and Xiaoyin Zhuang. 2019. "Atypical Antipsychotics-Induced Metabolic Syndrome and Nonalcoholic Fatty Liver Disease: A Critical Review." *Neuropsychiatric Disease and Treatment* 15:2087–99. doi: 10.2147/NDT.S208061.

Yahaya, Tajudeen O., and Shemishere B. Ufuoma. 2020. "Genetics and Pathophysiology of Maturity-Onset Diabetes of the Young (MODY): A Review of Current Trends." *Oman Medical Journal* 35(3):1. doi: 10.5001/omj.2020.44.

Yang, Albert C., and Shih Jen Tsai. 2017. "New Targets for Schizophrenia Treatment beyond the Dopamine Hypothesis." *International Journal of Molecular Sciences* 18(8). doi: 10.3390/ijms18081689.

Yang, Ching Ping, Ya Yu Wang, Shih Yi Lin, Yi Jheng Hong, Keng Ying Liao, Sheng Kuo Hsieh, Ping Ho Pan, Chun Jung Chen, and Wen Ying Chen. 2019. "Olanzapine Induced Dysmetabolic Changes Involving Tissue Chromium Mobilization in Female Rats." *International Journal of Molecular Sciences* 20(3):15. doi: 10.3390/ijms20030640.

Yoo, Sulgi, Mi Yeon Kim, and Jae Youl Cho. 2018. "Syk and Src-Targeted Anti-Inflammatory Activity of Aripiprazole, an Atypical Antipsychotic." *Biochemical Pharmacology* 148:1–12. doi: 10.1016/j.bcp.2017.12.006.

Yu, Yanjie, Yingni Lin, Yuto Takasaki, Chenyao Wang, Hiroki Kimura, Jingrui Xing, Kanako Ishizuka, Miho Toyama, Itaru Kushima, Daisuke Mori, Yuko Arioka, Yota Uno, Tomoko

Shiino, Yukako Nakamura, Takashi Okada, Mako Morikawa, Masashi Ikeda, Nakao Iwata, Yuko Okahisa, Manabu Takaki, Shinji Sakamoto, Toshiyuki Someya, Jun Egawa, Masahide Usami, Masaki Kodaira, Akira Yoshimi, Tomoko Oya-Ito, Branko Aleksic, Kinji Ohno, and Norio Ozaki. 2018. “Rare Loss of Function Mutations in N-Methyl-d-Aspartate Glutamate Receptors and Their Contributions to Schizophrenia Susceptibility.” *Translational Psychiatry* 8(1). doi: 10.1038/s41398-017-0061-y.

Zhang, Jin, Tara M. Henagan, Zhanguo Gao, and Jianping Ye. 2011. “Inhibition of Glyceroneogenesis by Histone Deacetylase 3 Contributes to Lipodystrophy in Mice with Adipose Tissue Inflammation.” *Endocrinology* 152(5):1829–38. doi: 10.1210/en.2010-0828.

Zhang, Lin, Chudan Liu, Qingyan Jiang, and Yulong Yin. 2021. “Butyrate in Energy Metabolism: There Is Still More to Learn.” *Trends in Endocrinology and Metabolism* 32(3):159–69. doi: 10.1016/j.tem.2020.12.003.

Zhang, Wen Qian, Ting Ting Zhao, Ding Kun Gui, Chen Lin Gao, Jun Ling Gu, Wen Jun Gan, Wei Huang, Yong Xu, Hua Zhou, Wei Ni Chen, Zhi Long Liu, and You Hua Xu. 2019. “Sodium Butyrate Improves Liver Glycogen Metabolism in Type 2 Diabetes Mellitus.” *Journal of Agricultural and Food Chemistry* 67(27):7694–7705. doi: 10.1021/acs.jafc.9b02083.

Zhang, Zong Hong, Dhanisha J. Jhaveri, Vikki M. Marshall, Denis C. Bauer, Janette Edson, Ramesh K. Narayanan, Gregory J. Robinson, Andreas E. Lundberg, Perry F. Bartlett, Naomi R. Wray, and Qiong Yi Zhao. 2014. “A Comparative Study of Techniques for Differential Expression Analysis on RNA-Seq Data.” *PLoS ONE* 9(8). doi: 10.1371/journal.pone.0103207.

Zhao, Yulan, Melanie Tran, Li Wang, Dong Ju Shin, and Jianguo Wu. 2020. “PDK4-Deficiency Reprograms Intrahepatic Glucose and Lipid Metabolism to Facilitate Liver Regeneration in Mice.” *Hepatology Communications* 4(4):504–17. doi: 10.1002/hep4.1484.

Zhu, Li, Zhiqiang Xie, Jianping Lu, Qiu Hao, Mingqiang Kang, Shuchen Chen, Weifeng Tang, Hao Ding, Yu Chen, Chao Liu, and Haojie Wu. 2017. “TCF7L2 Rs290481 T > C Polymorphism Is Associated with an Increased Risk of Type 2 Diabetes Mellitus and Fasting Plasma Glucose Level.” *Oncotarget* 8(44):77000–8. doi: 10.18632/oncotarget.20300.

9. APPENDIX

9.1. Supplementary tables

Table 10. *PPARGC1* family polymorphisms found on the low response volunteers

Volunteer	Gene	Nomenclature	RSid	Ref	Alt	Mutation effect	Exon/Intron	MAF (%)	Associated diseases
13	PPARGC1B	5:149119803	rs56393712	T	G	intron variant	1/11	70	Obesity
		5:149127672	rs143650068	C	T	intron variant	1/11	58	Obesity
		5:149128442	rs12654427	G	A	intron variant	1/11	25	Obesity
		5:149137624	rs4705371	C	A	intron variant	1/11	58	Obesity
		5:149138111	rs2012522	T	C	intron variant	1/11	100	Obesity
		5:149138825	rs4705372	G	A	intron variant	1/11	65	Obesity
		5:149139683	rs55954911	C	T	intron variant	1/11	58	Obesity
		5:149139809	rs17711388	G	C	intron variant	1/11	38	Obesity
		5:149219653	rs150637009	G	A	missense variant	9/12	69	Obesity
		5:149230745	rs1549186	T	C	3 prime UTR variant	12/12	50	Obesity
		5:149230787	rs1549187	C	T	3 prime UTR variant	12/12	53	Obesity
		5:149231190	rs397711386 rs397884301 rs5872148	T	TC	3 prime UTR variant	12/12	23	Obesity
		5:149231218	rs201667455	GT	G	3 prime UTR variant	12/12	29	Obesity
		5:149231332	rs26123	G	T	3 prime UTR variant	12/12	57	Obesity
		5:149231519	rs26122	C	T	3 prime UTR variant	12/12	33	Obesity
		5:149231786	rs1107344	G	A	3 prime UTR variant	12/12	47	Obesity

		5:149231830	rs26121	A	G	3 prime UTR variant	12/12	62	Obesity
		5:149233110	rs7712296	C	A	3 prime UTR variant	12/12	39	Obesity
15	PPARGC1A-MIR573	4:24513421	rs73246461	A	G	intergenic region	.	55	.
		4:24515547	rs1810015	T	C	intergenic region	.	100	.
		4:24513421	rs73246461	A	G	intergenic region	.	55	.
		4:24515547	rs1810015	T	C	intergenic region	.	100	.
	PPARGC1B	5:149128158	.	A	G	intron variant	1/11	25	Obesity
		5:149140262	rs6895698	A	G	intron variant	1/11	59	Obesity
		5:149140300	rs6895980	C	T	intron variant	1/11	67	Obesity
		5:149219613	.	C	T	synonymous_variant	9/12	37	Obesity
		5:149228648	rs26124	C	T	3 prime UTR variant	12/12	38	Obesity
		5:149230730	rs25846	T	C	3 prime UTR variant	12/12	100	Obesity
		5:149230732	rs30883	G	A	3 prime UTR variant	12/12	62	Obesity
		5:149231332	rs26123	G	T	3 prime UTR variant	12/12	57	Obesity
		5:149231519	rs26122	C	T	3 prime UTR variant	12/12	63	Obesity
		5:149231830	rs26121	A	G	3 prime UTR variant	12/12	48	Obesity
		5:149232213	rs26120	C	T	3 prime UTR variant	12/12	67	Obesity
		5:149233137	rs62383789	G	A	3 prime UTR variant	12/12	33	Obesity
20	PPARGC1A-MIR573	4:24514934	rs3857112	T	C	intergenic region	.	100	.
	PPARGC1B	5:149173134	rs10875551	A	G	intron variant	1/11	50	Obesity

		5:149173282	rs4705379	G	A	intron variant	1/11	73	Obesity
		5:149230730	rs25846	T	C	3 prime UTR variant	12/12	100	Obesity
		5:149230732	rs30883	G	A	3 prime UTR variant	12/12	47	Obesity
		5:149231332	rs26123	G	T	3 prime UTR variant	12/12	48	Obesity
		5:149231519	rs26122	C	T	3 prime UTR variant	12/12	32	Obesity
		5:149231830	rs26121	A	G	3 prime UTR variant	12/12	59	Obesity
		5:149232213	rs26120	C	T	3 prime UTR variant	12/12	35	Obesity
21	PPARGC1B	5:149230730	rs25846	T	C	3 prime UTR variant	12/12	100	Obesity
		5:149234501	rs11167486	C	T	3 prime UTR variant	12/12	46	Obesity
22	PPARGC1A-MIR573	4:24515547	rs1810015	T	C	intergenic region	.	100	.
24	PPARGC1A-MIR573	4:24516521	rs113904646	C	T	intergenic region	.	47	.
	PPARGC1B	5:149128442	rs12654427	G	A	intron variant	1/11	56	Obesity
		5:149208768	rs10491361	A	G	intron variant	3/11	55	Obesity
		5:149230532	rs139454626	C	A	3 prime UTR variant	12/12	57	Obesity
		5:149230730	rs25846	T	C	3 prime UTR variant	12/12	60	Obesity
		5:149230745	rs1549186	T	C	3 prime UTR variant	12/12	40	Obesity
		5:149230787	rs1549187	C	T	3 prime UTR variant	12/12	56	Obesity
		5:149231332	rs26123	G	T	3 prime UTR variant	12/12	44	Obesity

		5:149231519	rs26122	C	T	3 prime UTR variant	12/12	42	Obesity
		5:149231786	rs1107344	G	A	3 prime UTR variant	12/12	48	Obesity
		5:149231830	rs26121	A	G	3 prime UTR variant	12/12	41	Obesity
		5:149233110	rs7712296	C	A	3 prime UTR variant	12/12	48	Obesity

9.2. Supplementary figures

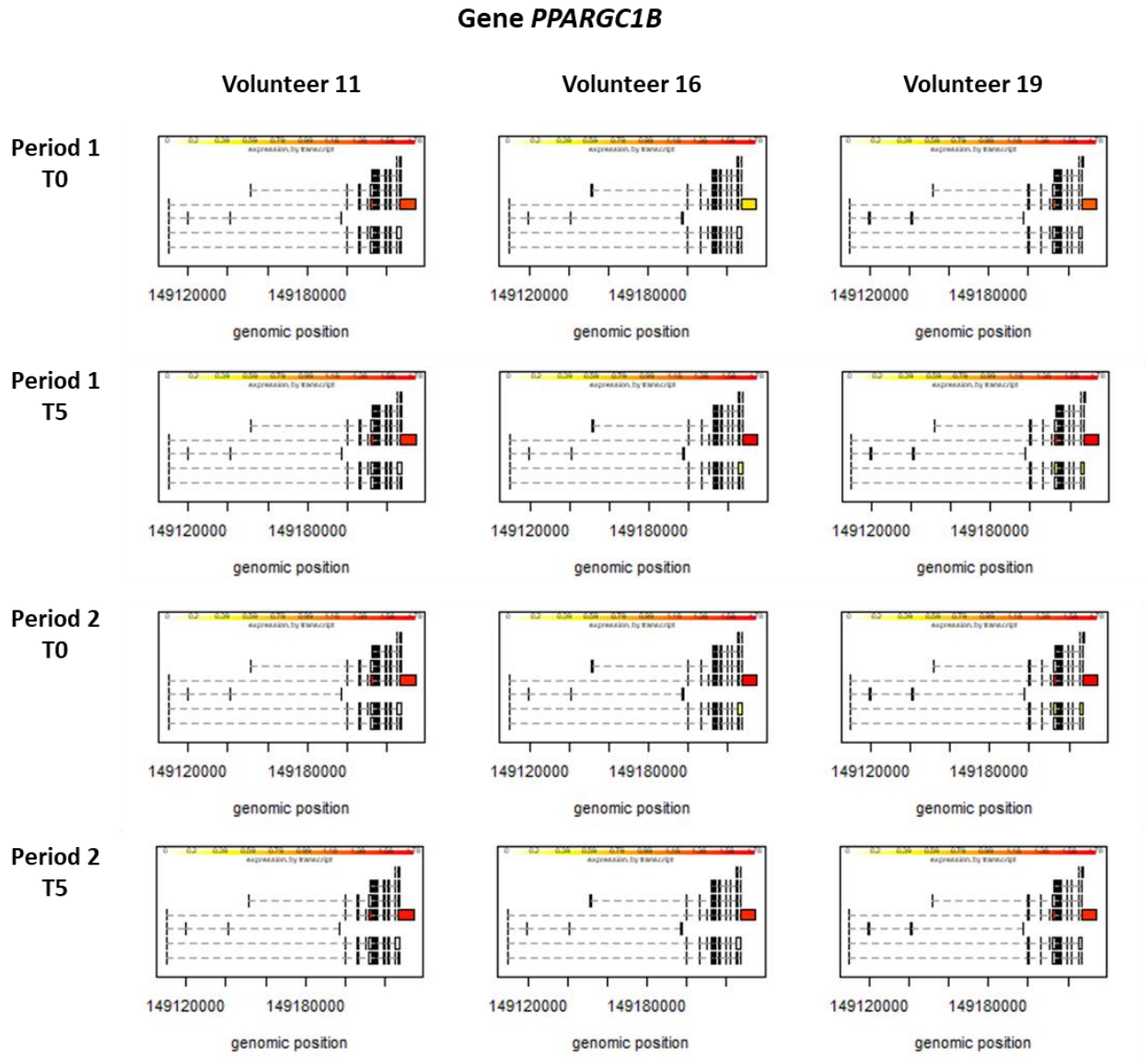

Figure 31. *PPARGC1B* transcripts abundance visualization for high response volunteers. The figure shows the abundance of *PPARGC1B* transcripts for high response volunteers. The colour scale goes from 0 (yellow) to 170 (red) FPKMs.

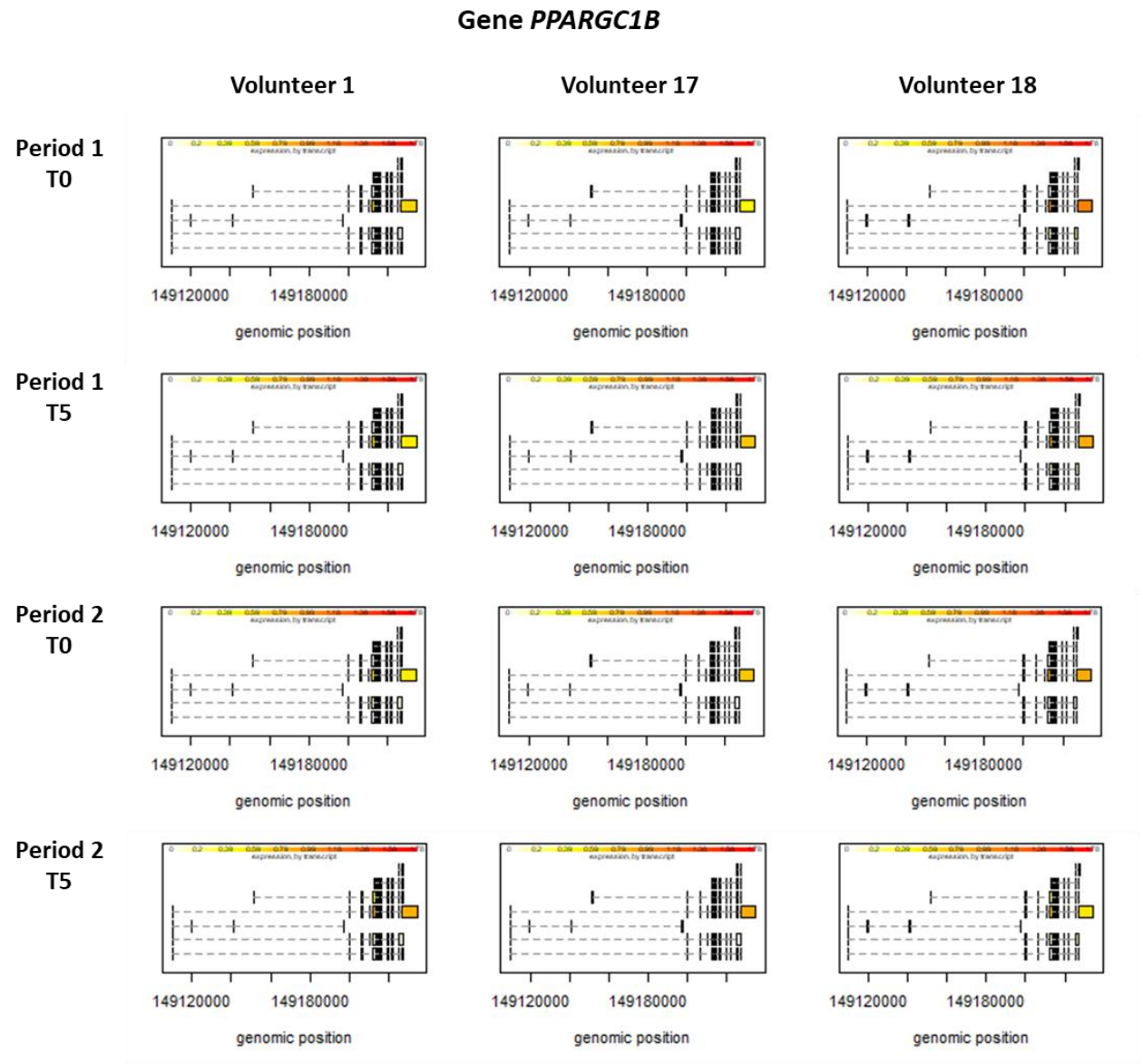

Figure 32. *PPARGC1B* transcripts abundance visualization for medium response volunteers. The figure shows the abundance of PPARGC1B transcripts for medium response volunteers. The colour scale goes from 0 (yellow) to 170 (red) FPKMs.

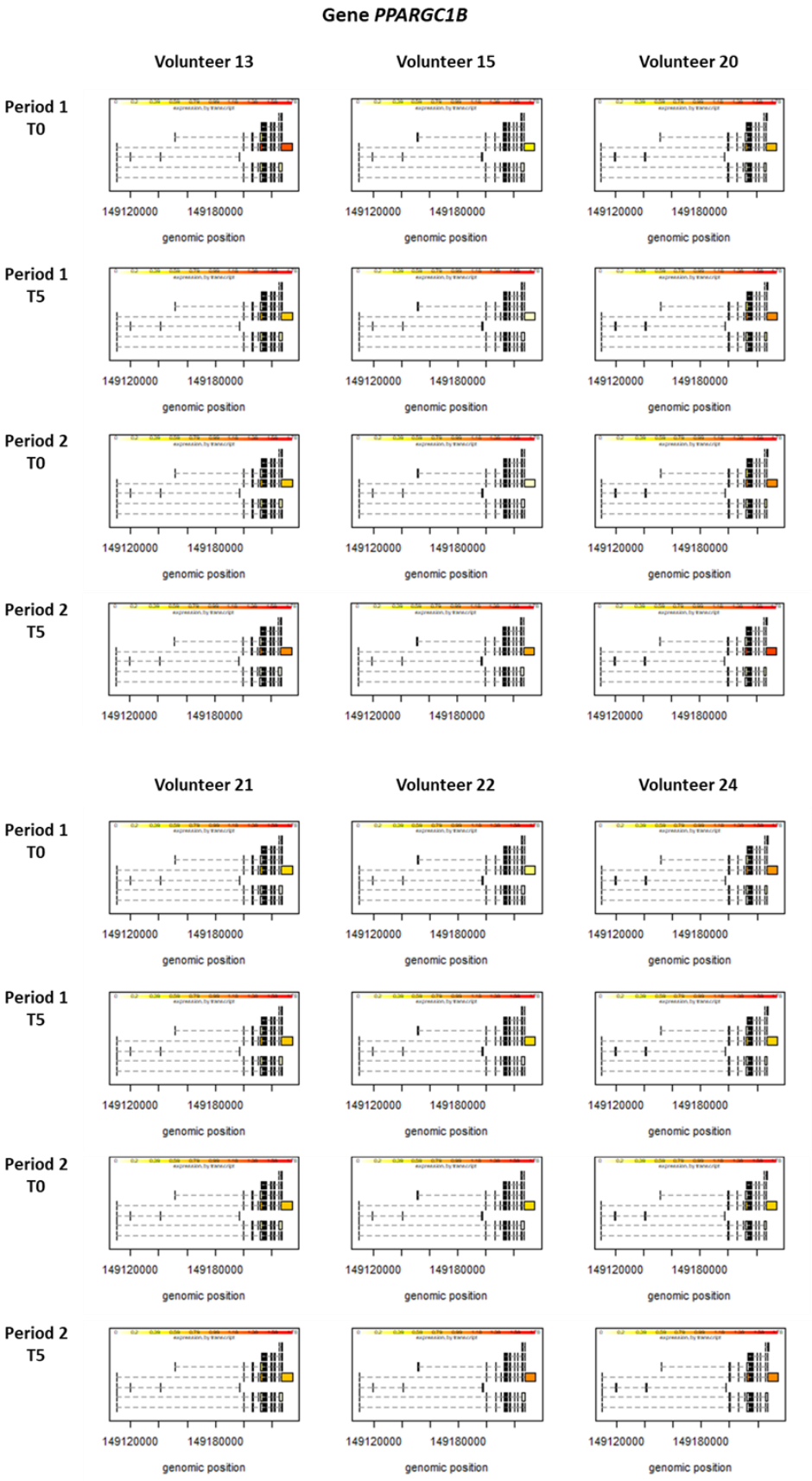

Figure 33. *PPARGC1B* transcripts abundance visualization for low response volunteers. The figure shows the abundance of PPARGC1B transcripts for medium response volunteers. The colour scale goes from 0 (yellow) to 170 (red) FPKMs.

9.3. Publications related to the Doctoral Thesis

Grajales, D., Vázquez, P., **Ruíz-Rosario, M**., Tudurí E., Mirasierra M., Ferreira V., Hitos A.B., Koller D., Zubiaur P., Cigudosa J. C., Abad-Santos F., Vallejo M., Quesada I., Tirosh B., Leibowitz G., Valverde A. M. The second-generation antipsychotic drug aripiprazole modulates the serotonergic system in pancreatic islets and induces beta cell dysfunction in female mice. *Diabetologia* (2021). https://doi.org/10.1007/s00125-021-05630-0

Diabetologia
https://doi.org/10.1007/s00125-021-05630-0

ARTICLE

The second-generation antipsychotic drug aripiprazole modulates the serotonergic system in pancreatic islets and induces beta cell dysfunction in female mice

Diana Grajales[1,2] · Patricia Vázquez[1,2] · Mónica Ruíz-Rosario[3] · Eva Tudurí[2,4] · Mercedes Mirasierra[1,2] · Vítor Ferreira[1,2] · Ana B. Hitos[1,2] · Dora Koller[5] · Pablo Zubiaur[5] · Juan C. Cigudosa[3] · Francisco Abad-Santos[5] · Mario Vallejo[1,2] · Iván Quesada[2,4] · Boaz Tirosh[6] · Gil Leibowitz[7] · Ángela M. Valverde[1,2]

Received: 12 January 2021 / Accepted: 5 October 2021

Abstract

Aims/hypothesis Second-generation antipsychotic (SGA) drugs have been associated with the development of type 2 diabetes and the metabolic syndrome in patients with schizophrenia. In this study, we aimed to investigate the effects of two different SGA drugs, olanzapine and aripiprazole, on metabolic state and islet function and plasticity.

Methods We analysed the functional adaptation of beta cells in 12-week-old B6;129 female mice fed an olanzapine- or aripiprazole-supplemented diet (5.5–6.0 mg kg^{-1} day^{-1}) for 6 months. Glucose and insulin tolerance tests, in vivo glucose-stimulated insulin secretion and indirect calorimetry were performed at the end of the study. The effects of SGAs on beta cell plasticity and islet serotonin levels were assessed by transcriptomic analysis and immunofluorescence. Insulin secretion was assessed by static incubations and Ca^{2+} fluxes by imaging techniques.

Results Treatment of female mice with olanzapine or aripiprazole for 6 months induced weight gain ($p<0.01$ and $p<0.05$, respectively), glucose intolerance ($p<0.01$) and impaired insulin secretion ($p<0.05$) vs mice fed a control chow diet. Aripiprazole, but not olanzapine, induced serotonin production in beta cells vs controls, likely by increasing tryptophan hydroxylase 1 (TPH1) expression, and inhibited Ca^{2+} flux. Of note, aripiprazole increased beta cell size ($p<0.05$) and mass ($p<0.01$) vs mice fed a control chow diet, along with activation of mechanistic target of rapamycin complex 1 (mTORC1)/S6 signalling, without preventing beta cell dysfunction.

Conclusions/interpretation Both SGAs induced weight gain and beta cell dysfunction, leading to glucose intolerance; however, aripiprazole had a more potent effect in terms of metabolic alterations, which was likely a result of its ability to modulate the serotonergic system. The deleterious metabolic effects of SGAs on islet function should be considered while treating patients as these drugs may increase the risk for development of the metabolic syndrome and diabetes.

Keywords Beta cell dysfunction · Beta cell mass · Insulin secretion · Islets · Schizophrenia · Second-generation antipsychotics · Type 2 diabetes

✉ Ángela M. Valverde
avalverde@iib.uam.es

[1] Instituto de Investigaciones Biomédicas Alberto Sols, Consejo Superior de Investigaciones Científicas (CSIC), Madrid, Spain

[2] CIBER de Diabetes y Enfermedades Metabólicas Asociadas (CIBERDEM), Instituto de Salud Carlos III, Madrid, Spain

[3] NIMGenetics, Madrid, Spain

[4] Instituto de Investigación, Desarrollo e Innovación en Biotecnología Sanitaria de Elche (IDiBE), Universidad Miguel Hernández, Elche, Spain

[5] Clinical Pharmacology Department, Hospital Universitario de La Princesa, Instituto de Investigación Sanitaria La Princesa, Madrid, Spain

[6] The Institute of Drug Research, The Hebrew University of Jerusalem, Jerusalem, Israel

[7] Endocrinology and Metabolism Service, Department of Medicine, Hadassah-Hebrew University Medical Center, Jerusalem, Israel

Published online: 21 December 2021

Research in context

What is already known about this subject?

- Second-generation antipsychotic (SGA) drugs are the first-line treatment for schizophrenia because of their clinical efficacy and reduced extrapyramidal side effects
- SGAs have been associated with severe metabolic alterations, including impairment of whole-body glucose homeostasis and body weight gain, which can increase the risk of type 2 diabetes
- Some SGAs are more diabetogenic than others, i.e. olanzapine or clozapine, while others, such as aripiprazole, are considered to be less diabetogenic

What is the key question?

- How does SGA treatment affect pancreatic beta cell function and islet plasticity?

What are the new findings?

- In mice, both olanzapine and aripiprazole induced glucose intolerance and reduced insulin secretion
- Aripiprazole modulates the serotonergic system in mouse islets, inducing mechanistic target of rapamycin (mTOR)/S6 phosphorylation, tryptophan hydroxylase 1 (TPH1) expression and serotonin production in beta cells
- The effects of olanzapine on insulin secretion seem to be independent of the serotonergic system

How might this impact on clinical practice in the foreseeable future?

- A better understanding of the mechanisms by which SGAs induce beta cell dysfunction could pave the way for preventing type 2 diabetes in patients with schizophrenia who are administered these drugs

Abbreviations

D2R	Dopamine D2 receptor
D3R	Dopamine D3 receptor
D4R	Dopamine D4 receptor
DEGs	Differentially expressed genes
EE	Energy expenditure
ΔF	Change in fluorescence
F_{basal}	Basal fluorescence
GSIS	Glucose-stimulated insulin secretion
H_1R	Histamine H_1 receptor
5-HT	5-Hydroxytryptamine
iWAT	Inguinal white adipose tissue
M1R	Muscarinic M1 receptor
M5R	Muscarinic M5 receptor
mTOR	Mechanistic target of rapamycin
mTORC1	Mechanistic target of rapamycin complex 1
ORA	Over-representation analysis
p-adj	Adjusted *p* value
PCA	Principal component analyses
PCPA	4-Chloro-DL-phenylalanine
RER	Respiratory exchange ratio
RNA-seq	RNA-sequencing
RT-qPCR	Quantitative real-time PCR
SGA	Second-generation antipsychotics
TEM	Transmission electron microscopy
TPH1	Tryptophan hydroxylase 1
WAT	White adipose tissue

Introduction

In recent years, an increased incidence of type 2 diabetes in patients taking chronic pharmacological treatment has been reported [1]. In patients receiving second-generation antipsychotic (SGA) drugs [2, 3], the first-line treatment for schizophrenia, the increase in incidence varies between 10% and 20%. SGAs induce metabolic alterations, including weight gain, hyperglycaemia, insulin resistance and dyslipidaemia, which increase the risk for cardiovascular disease [2]. In a large cohort of drug-naive individuals with schizophrenia, the incidence of type 2 diabetes was augmented in those prescribed the SGA olanzapine [4]. Rajkumar et al reported that the SGAs olanzapine and aripiprazole doubled the risk for developing type 2 diabetes, whereas the first in class antipsychotic, clozapine, increased the risk by fourfold [5]. Female individuals are more susceptible to the metabolic side effects of SGAs and, therefore, preclinical studies are often performed on female rodents [6].

SGAs act through a broad range of receptors, including dopamine D1– D4 receptors (D1R– D4R), serotonin receptors (5-hydroxytryptamine [5-HT])$_{1A}$, 5-HT_{2A}, 5-HT_{2C}, 5-HT_3, 5-HT_6 and 5-HT_7), histamine H_1 receptor (H_1R) or muscarinic M1–M5 receptors (M1R–M5R) [7]. Several studies have tested SGA drug-induced effects on whole-body glucose homeostasis [8]; however, their impact on beta cell function remains unclear [9]. Beta cells express different serotonergic receptors

and synthesise, store and release serotonin in response to glucose, but the effects of SGAs on serotonin biosynthesis and signalling in islets and their impact on insulin secretion are not clear [10]. As reviewed previously [8], olanzapine has higher antagonistic activity against serotonin 5-HT_{2A} receptors and the dopamine receptor D2R, but is also antagonistic against D3R and D4R, 5-HT_3 and 5-HT_6 receptors, H_1R, α1-adrenergic receptors and M1R–M5R. On the other hand, aripiprazole has partial agonistic activity for the dopamine receptors D2R, D3R and D4R, 5-HT_{1A} and 5-HT_{2C} receptors, and α1-adrenergic receptors, and also exhibits 5-HT_{2A} and 5-HT_7 receptor antagonism.

Herein, we used the chemically unrelated SGAs, olanzapine (a commonly prescribed SGA that is highly diabetogenic) and aripiprazole (the metabolic side effects of which are less well-known) to study the effects of prolonged treatment with SGAs on blood glucose levels, islet morphometry and beta cell function in female mice.

Methods

Animals Animal experiments were approved by the Animal Ethics Committees of the Spanish National Research Council and Comunidad de Madrid in accordance with Spanish (RD 53/2013) and European Union (63/2010/EU) legislation (PROEX 037/17).

Details of the B6;129 mice used in this study have been previously reported [11]. Mice were housed in a pathogen-free facility in temperature-, humidity- and light-controlled rooms (with a 12 h light–dark cycle), with free access to food and water. Ninety female mice, aged 12 weeks, were randomly allocated into three experimental groups; mice received a standard chow diet (SAFE A04; Scientific Diets [SAFE], France), or the same diet supplemented with olanzapine (GP8311; Glentham Life Sciences, UK) or aripiprazole (AC457990010; ACROS Organics, ThermoFisher Scientific, USA) (both 40 mg/kg chow diet). Dosage (5.5–6.0 mg kg^{-1} day^{-1}) was calculated considering daily food intake. After 6 months on the diet, mice were euthanised by cervical dislocation and pancreatic islets, whole pancreases, white adipose tissue (WAT) depots (epididymal WAT [eWAT] and inguinal WAT [iWAT]) and blood were collected and processed for analysis. As a positive control for serotonin expression in islets we used 12-day pregnant B6 female mice, aged 16 weeks, bred in-house with B6 male mice.

Analysis of olanzapine and aripiprazole in plasma A simple and sensitive LC-MS/MS method (Agilent Technologies, Spain) was used for simultaneous determination of aripiprazole and olanzapine levels in plasma, as reported previously [12] and detailed in the electronic supplementary material (ESM) Methods.

Food intake measurement Food intake was measured manually using KERN PCB2500-2 scales (KERN, Germany) during the first month of treatment in mice housed in group cages and the mean food intake per mouse and per day was calculated.

Metabolic assays After 6 months on the diets, metabolic assays were performed, including i.p. GTT, i.p. ITT, glucose-stimulated insulin secretion (GSIS) and indirect calorimetry (see ESM Methods). In brief, for GTT and GSIS analysis, after 16 h of fasting, D-(+)-Glucose (2 g/kg body weight; G8270; Sigma-Aldrich, USA) was injected into mice and tail vein blood samples were collected at 0–120 min post-injection. For ITTs, after 4 h of fasting, human recombinant insulin (Actrapid; 0.75 U/kg body weight; Novo Nordisk, Denmark) was injected into mice and tail vein blood samples were collected at 0–90 min post-injection. Plasma glucose and insulin levels were measured via glucometer (Accu-Check Aviva; Roche Diagnostics, Switzerland) and ELISA (10-1247-01; Mercodia, Sweden), respectively. Indirect calorimetry analysis was carried out during light and dark cycles using the TSE Phenomaster monitoring system (TSE Systems, Germany). Oxygen consumption and CO_2 release were measured, and respiratory exchange ratio (RER) was determined as $\dot{V}CO_2/O_2$. Energy expenditure (EE) was calculated as EE = (3.185 + 1.232 × RER) × $\dot{V}O_2$. Total locomotor activity was simultaneously measured using an infrared photocell beam interruption method, carried out using the TSE Phenomaster, as described previously [13]. Analysis was performed using the TSE Phenomaster Mouse software V5.1.7 (TSE Systems).

Pancreatic islet isolation and culture Islets were isolated by collagenase P (11215809103; Roche, Germany) digestion (13.5 U/ml in cold Hank's buffer), as described previously [14]. For ex vivo experiments, islets were recovered overnight at 37°C and 5% CO_2 in complete RPMI-1640 medium (2 mmol/l L-glutamine, 1 mmol/l sodium pyruvate, 50 μmol/l β-mercaptoethanol, 10 mmol/l HEPES and 10% [vol./vol.] FBS) containing 5.6 mmol/l glucose. The next day, islets were pooled, randomised and incubated with 6 μmol/l olanzapine or aripiprazole (dissolved in DMSO; D8418; Sigma-Aldrich), 1–500 μmol/l serotonin (14927; Sigma-Aldrich) (1–24 h incubation) or 10 μmol/l 4-Chloro-DL-phenylalanine (PCPA; C6506; Sigma-Aldrich). Control islets were treated with 0.01% (vol./vol.) DMSO.

Static incubations For each individual mouse, 3–6 groups of three islets matched by size were placed in each well of a 96-well plate. Islets were pre-incubated for 1 h at 37°C and 5% CO_2 in KRB containing 2.8 mmol/l glucose, 115 mmol/l NaCl, 5 mmol/l KCl, 1.2 mmol/l $NaHCO_3$, 1.1 mmol/l $MgCl_2$, 1.2 mmol/l NaH_2CO_4, 2.5 mmol/l $CaCl_2$, 25 mmol/l

HEPES and 0.25% (wt/vol.) BSA. Incubations were then performed using 2.8 mmol/l or 16.7 mmol/l glucose at 37°C, 5% CO_2 for 1 h. Insulin levels were determined by ELISA (Mercodia) and values were normalised to islet number.

Insulin content Insulin was extracted from 20 islets/mice using glycine/NP-40 lysis buffer (200 mmol/l glycine, 0.5% NP-40; pH 8.8) and measured by ELISA.

Intracellular Ca^{2+} imaging Islets treated ex vivo with SGAs were pre-incubated with Fura-2 AM (F11212; ThermoFisher Scientific) and perfused with KRB containing glucose (2.8 mmol/l or 16.7 mmol/l). Fluorescence measurements were obtained at excitation wavelengths of 340 nm and 380 nm with an Axiovert 200 inverted microscope (Zeiss, Germany) with appropriate filters. Data acquisition was performed with the Aquacosmos 2.6 software (Hamamatsu Photonics, Japan). Recordings were expressed as the ratio of fluorescence at 340 nm and 380 nm (F340/380).

Immunohistochemistry Pancreases were fixed in Bouin's solution (HT10132; Sigma-Aldrich) overnight at 4°C. Paraffin embedding and tissue sectioning were performed as described previously [15]. Longitudinal pancreatic sections of 6 μm thickness, generated every 80 μm, were hydrated and pre-treated by boiling for 20 min in a microwave in antigen-retrieval solution containing 100 mmol/l sodium citrate dehydrate (pH 6; W302600; Sigma-Aldrich) supplemented with 0.05% (vol./vol.) Tween-20. Insulin and glucagon expression was analysed by immunohistochemistry staining using primary antibodies against insulin and glucagon, and secondary biotinylated antibodies diluted in PBS (ESM Table 1). Pancreatic sections were then processed for diaminobenzidine (DAB)-immunoperoxidase staining (SK-4100; Vector Laboratories, USA) and counterstained with Mayer's Hematoxylin (H3136; Sigma-Aldrich). Images were examined using a Axiophot Zeiss light microscope and captured with a DP70 digital camera (Olympus, Japan). Insulin and glucagon staining and total pancreatic area were quantified by ImageJ software version 1.52a (NIH, USA). Morphometric analysis of the pancreas is described further in ESM Methods.

Immunofluorescence of pancreatic sections and islets Pancreatic sections were processed as described above using antibodies against insulin, glucagon, serotonin, p-S6 and Ki67, and secondary Alexa-Fluor conjugated antibodies (see ESM Methods for further details). For in toto islet immunostaining, 20 islets were handpicked, placed in μ-Slide 8-well plates (80826; Ibidi, Germany) and processed for insulin and serotonin immunostaining, as detailed in ESM Methods. Antibody details are listed in ESM Table 1. Immunofluorescence was examined using an epifluorescence microscope (Nikon 90i; Olympus) and images were taken with a digital camera (Nikon DS-2Mv, Japan). The percentage of beta cells co-expressing insulin and Ki67, p-S6 or serotonin was obtained by dividing the number of positive cells for each staining by the total number of insulin-positive cells in each islet.

Ultrastructural analysis by transmission electron microscopy For transmission electron microscopy (TEM) analysis, pools of 300 pancreatic islets from three mice per condition were processed as described in ESM Methods. Tissue sections were examined using a Zeiss Libra 120 transmission electron microscope and TEM images were taken with an electron multiplying charge coupled device (EMCCD) camera (Albert Tröndle, Germany). The number and type of the secretory granules in beta cells (n = 10 beta cells from three independent mice/group) were assessed using ImageJ software (NIH). Insulin granules from beta cells were classified into four categories: mature (with an electron-dense core); immature (with a less electron-dense core); empty (lacking the core); and atypical (insulin granules with an irregular shape).

Serotonin measurement Supernatants collected from static incubation experiments were used for the measurement of serotonin levels using the ELISA Fast Track kit (BA E-8900; LDN, Germany). Values were normalised to islet number.

Transcriptomic analysis of islets from treated mice by RNA-sequencing Islets were isolated in TRIzol (15596026; ThermoFisher Scientific) and total RNA was extracted using the PureLink RNA Mini Kit (Invitrogen, USA). Total RNA expression was analysed using Illumina TruSeq Stranded RNASeq technology (Illumina, USA). The libraries were sequenced (2 × 100 bp) with a mean output of 40 million reads in a NovaSeq 6000 sequencer (Illumina). After a quality control check with FastQC (www.bioinformatics.babraham.ac.uk/projects/fastqc, access date 27 May 2019), the reads were aligned to reference transcripts with the Kallisto algorithm [16], which provides a matrix of estimated counts per transcript as the output. Exploratory analyses included principal component analysis (PCA) and hierarchical clustering (HC). Transcriptomic analyses were performed with the DESeq2 package [17], for which differentially expressed genes (DEGs) were described as those with an adjusted p value (p-adj) of <0.1 when performing a Wald test between two conditions and a Benjamini–Hochberg adjustment. Over-representation analyses (ORAs) of the DEGs were completed with the WEB-based GEne SeT AnaLysis Toolkit (WebGestalt) [18].

Western blotting Protein levels were assessed in pancreatic islets using antibodies against IRS-2, mechanistic target of rapamycin (mTOR), p-mTOR (Ser2448), S6K1, p-S6K1 (Thr389), p-S6 ribosomal protein, tryptophan hydroxylase 1

(TPH1) and vinculin (ESM Table 1). Immunoreactivity was detected by chemiluminescence, using Clarity Western ECL Substrate (1705061; Bio-Rad, Germany). Densitometric analysis of the bands was performed using ImageJ software (NIH). The protocol is fully described in ESM Methods.

Quantitative real-time PCR Gene expression was determined by quantitative real-time PCR (RT-qPCR) using Power SYBR Green PCR Master Mix (4367659; ThermoFisher Scientific) and 7900HT Fast Real-Time PCR System (ThermoFisher Scientific), as described in ESM Methods. Primer sequences are shown in ESM Table 2.

Statistical analysis Statistical analysis was performed using Prism 8 (Graph software, USA). Datasets were first analysed for normal distribution. For data with parametric distributions, unpaired Student's *t* test was used to compare mean differences between two groups, and for three or more groups, one-way ANOVA with Bonferroni post hoc test was used. For data with non-parametric distributions, differences between groups were examined with Mann–Whitney *U* test for two groups, or Kruskal–Wallis test for three or more groups. Two-way ANOVA was employed to compare two different categorical, independent variables. Where other statistical analyses have been used, this has been indicated in the figure legends. Data are expressed as mean ± SEM. Tests were two-sided and $p<0.05$ was considered statistically significant. Mice and islets were randomly and blindly distributed for the treatments by experimenters. Experimenters were not blind in outcome assessment.

Results

Alterations in body weight, adiposity, energy balance and glucose metabolism in female mice fed an antipsychotic drug-supplemented diet Female mice were fed an olanzapine- or aripiprazole-supplemented diet (40 mg/kg) for 6 months. Figure 1a,b shows plasma drug levels at the end of the treatment. Olanzapine-treated mice gained 8.70 ± 0.88 g of body weight compared with a 4.90 ± 0.47 g gain in controls fed a chow diet ($p<0.01$). Aripiprazole-treated mice also gained more weight than the controls over the treatment period ($p<0.05$) but, as body weight stabilised in the last month of the treatment in this group, there was less body weight gain compared with olanzapine-treated mice ($p>0.05$) (Fig. 1c,d). Both olanzapine- ($p<0.01$) and aripiprazole-treated ($p<0.001$) mice had a significant increase in visceral adiposity and showed a slight, but not significant, increase in iWAT/body weight ratio vs controls (Fig. 1e,f).

We further studied the effects of the two SGAs on food intake. Consistent with a previous report [19], food consumption was higher in the olanzapine-treated group compared with the control group ($p<0.05$; Fig. 1g), whereas no differences were found between aripiprazole-treated mice vs control or olanzapine-treated groups. EE and spontaneous locomotor activity were lower in the dark phase in olanzapine- and aripiprazole-treated mice vs control mice, although this difference was only statistically significant for the aripiprazole-treated group vs controls ($p<0.05$; Fig. 1h,i).

Fed and fasting blood glucose levels did not differ between groups (Fig. 1j, ESM Fig. 1b). However, fed plasma insulin levels were higher in mice receiving the olanzapine- ($p<0.01$) or aripiprazole-supplemented diet ($p<0.05$; Fig. 1k), whereas fasting insulin was similar between groups (ESM Fig. 1c), suggesting increased insulin resistance or impairment of insulin clearance with SGA treatment. We further assessed the effects of SGAs on glucose tolerance and insulin sensitivity. The GTT showed that olanzapine- and aripiprazole-fed mice developed glucose intolerance (Fig. 1l). The ITT revealed that, although insulin sensitivity was reduced in both groups of treated mice, only the difference between the aripiprazole-treated and control groups was statistically significant ($p<0.01$; Fig. 1m). Collectively, these findings suggest that both SGAs induce alterations in glucose homeostasis, despite the fact that aripiprazole treatment was associated with less weight gain.

Olanzapine and aripiprazole impaired beta cell function and altered islet morphology in female mice Olanzapine and aripiprazole treatment markedly impaired GSIS in vivo (AUC $p<0.05$; Fig. 2a), indicating impaired beta cell function. Consistently, ex vivo static incubations showed that GSIS was inhibited in islets of both olanzapine- ($p<0.01$) and aripiprazole-treated animals ($p<0.05$), as compared with islets from chow-diet-fed mice (Fig. 2b), without affecting islet insulin content (Fig. 2c).

To determine the mechanism underlying beta cell dysfunction in response to SGA treatment, islet morphometry was analysed (Fig. 2d–i). Islet size markedly increased in mice treated with olanzapine ($p<0.01$) or aripiprazole ($p<0.001$) vs controls (Fig. 2f). Beta cell mass was increased by twofold in aripiprazole-treated mice compared with chow-fed mice ($p<0.01$), but this effect was not observed in olanzapine-treated mice (Fig. 2g). Interestingly, alpha cell mass was twofold higher in olanzapine-treated mice than in the controls (Fig. 2h), which was associated with a non-significant increase in alpha cell area without changes in islet cell composition (ESM Fig. 2). Comparative analysis of islet size distribution among groups confirmed the increased number of larger sized islets in mice treated with SGAs vs controls ($p<0.001$, analysed by χ^2 test; Fig. 2i). Ultrastructural TEM analysis showed smaller numbers of mature insulin granules ($p=0.09$) and more empty granules ($p=0.09$) in beta cells from olanzapine-treated mice vs controls (ESM Fig. 2f).

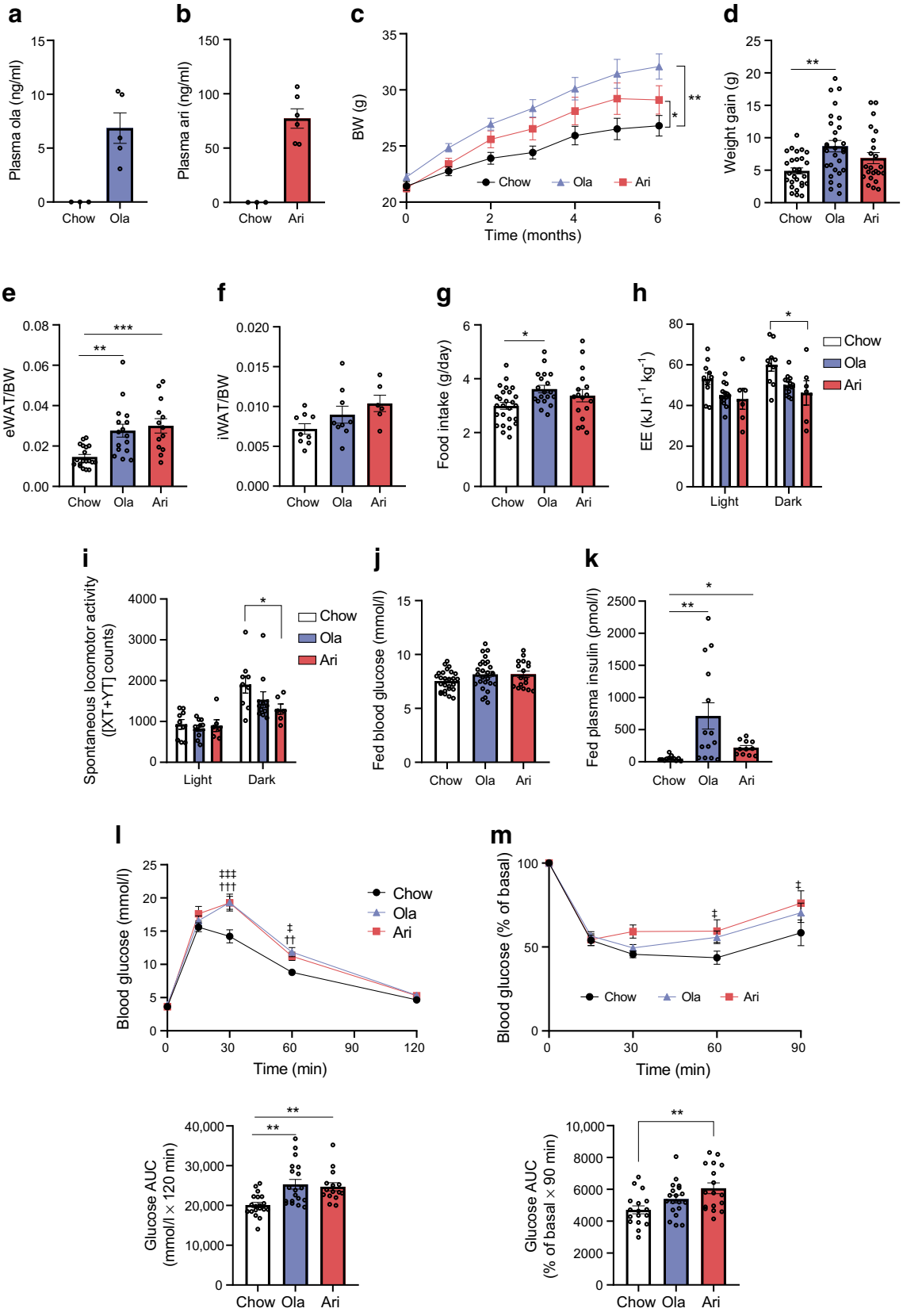

Effects of antipsychotic drug-supplemented diet on beta cell proliferation and size in female mice Consistent with a report in adult animals [20], beta cell proliferation, assessed by Ki67 immunostaining, was low and no differences were found

◀ **Fig. 1** Effects of olanzapine (ola)- and aripiprazole (ari)-supplemented diet on body weight (BW), adiposity, energy balance and glucose metabolism in female mice. (**a**, **b**) Plasma levels of ola (**a**) and ari (**b**) in mice after 6 months of treatment with antipsychotic drug-supplemented diets (n=3–6 mice/group). (**c**) BW monitored monthly and (**d**) BW gain in the last month of the treatment in mice fed an ari- or ola-supplemented diet (n=28 control mice, n=29 ola-treated mice, n=23 ari-treated mice) (**e**) Epididymal WAT (eWAT) and (**f**) iWAT normalised to BW (n=6–19 mice/group). (**g**) Food intake during the first month of treatment (n=17–26 mice/group). (**h**) EE and (**i**) locomotor activity (presented as [XY+YT] counts, indicating the total number of times mice cross the infrared sensors that border the measuring cage on the X and Y planes) measured at the end of the treatment period by indirect calorimetry (n=6–13 mice/group). Light cycle: 08:00–20:00 hours; dark cycle: 20:00–08:00 hours. (**j**) Fed blood glucose (mmol/l) and (**k**) fed plasma insulin (pmol/l) levels (n=11–27 mice/group). (**l**) i.p. GTT and the respective AUC (n=15–19 mice/group). The AUC was calculated from 0 to 120 min, according to the trapezoidal rule. (**m**) i.p. ITT and the respective AUC (n=17–19 mice/group). The AUC was calculated from 0 to 90 min, according to the trapezoidal rule. All data are presented as mean±SEM. p values were determined by one-way (**d**, **e**, **f**, **g**, **j**, **k**, **l** (lower), **m** (lower)) or two-way (**c**, **h**, **i**, **l** (upper), **m** (upper)) ANOVA and Bonferroni post hoc test. *p<0.05, **p<0.01, ***p<0.001 vs mice fed a chow diet; $^{\dagger\dagger}p$<0.01, $^{\dagger\dagger\dagger}p$<0.001, ola-treated mice vs mice fed a chow diet; $^{\ddagger}p$<0.05, $^{\ddagger\ddagger\ddagger}p$<0.001, ari-treated mice vs mice fed a chow diet

between groups (Fig. 3a,b). Notably, beta cell size was increased in both olanzapine- and aripiprazole-treated mice (p<0.05; Fig. 3c). mTOR complex 1 (mTORC1), a key regulator of cell size, plays an important role in beta cell compensation under stress conditions [21]. Immunostaining with an antibody against phosphorylated ribosomal protein S6, a downstream mTORC1 target, showed increased mTORC1 activity in beta cells from aripiprazole-treated mice (p<0.05), but not from mice receiving olanzapine (Fig. 3d,e). Thus, mTORC1 might have a role in mediating beta cell compensation in aripiprazole-treated mice. Islets were then treated ex vivo with aripiprazole for 16 h and mTORC1 activity was assessed by western blotting for mTOR, S6K1 and S6 phosphorylation. Treatment with aripiprazole increased mTOR/S6K1/S6 phosphorylation (Fig. 3f), indicating stimulation of the mTORC1 signalling pathway.

Ex vivo treatment of pancreatic islets with olanzapine and aripiprazole impairs GSIS Ex vivo GSIS analyses showed that both olanzapine and aripiprazole used at 6 μmol/l reduced insulin secretion in islets without affecting insulin content (Fig. 4a,b), suggesting direct inhibitory effects of these drugs on insulin secretion.

We next analysed Ca^{2+} signalling in islets exposed ex vivo to olanzapine or aripiprazole for 24 h. Islets treated with olanzapine showed a similar pattern of Ca^{2+} oscillations compared with control islets and no differences were found in the AUC/min, change in fluorescence (ΔF), basal fluorescence (F_{basal}) or response time to high glucose (time islets take to respond to change in glucose concentration by opening voltage-gated Ca^{2+} channels) vs controls (Fig. 4c,d,f, ESM Fig. 3a,c). By contrast, aripiprazole-treated islets exhibited attenuated Ca^{2+} entry, as reflected by decreased ΔF and AUC/min, and delayed response to high glucose vs controls, while F_{basal} was similar between groups (Fig. 4e,g, ESM Fig. 3b,d). These data suggest that aripiprazole interferes with Ca^{2+} signalling in beta cells.

Transcriptomic analysis in pancreatic islets from female mice fed an olanzapine- or aripiprazole-supplemented diet To identify the transcriptomic profile of mouse islets from SGA-treated mice we conducted RNA-sequencing (RNA-seq). PCA showed differential gene expression in islets from mice under SGA treatment (Fig. 5a,b). DEGs were identified by DESeq2 and classified as genes with p-adj<0.1 as assessed using a Wald test between two conditions with Benjamini–Hochberg adjustment. Fifteen genes were differentially expressed in islets from olanzapine-treated mice and 244 genes were dysregulated in islets from aripiprazole-treated mice (ESM Table 3, ESM Table 4). Islets from mice receiving a chow diet were used to identify baseline gene levels.

We conducted ORA to address the specific genetic signatures associated with olanzapine or aripiprazole treatment. However, because 15 DEGs (in the case of olanzapine) is a small number of genes for ORA, the analysis was performed with all genes with a fold change ≤ −1.5 or ≥1.5 and a p value <0.05, as assessed by the Wald test between two conditions, and relevant findings were further validated by RT-qPCR. A total of 289 genes dysregulated by aripiprazole and 136 by olanzapine were included in the ORA (data not shown). We found that the top-five upregulated pathways in the aripiprazole arm appeared to be related to serotonin biosynthesis (Fig. 5d). The heatmap of serotonin biosynthetic processes (gene set accession no.: GO:0042427, http://amigo.geneontology.org/amigo/term/GO:0042427/?q=DDC; access date 22 July 2019) shows that genes encoding the serotonin-synthetising enzymes *Tph1* and *Tph2* were upregulated in islets from aripiprazole-treated mice, whereas the gene encoding the *Htr3a* receptor was downregulated in islets of olanzapine-treated mice (Fig. 5e). Notably, transcriptional profiling showed no significant alterations in other genes related to islet function with SGA treatment (ESM Table 3, ESM Table 4). Figure 5f shows the RT-qPCR analysis of common islet genes.

Effects of olanzapine and aripiprazole treatment on the expression of serotonin-related genes and serotonin levels in islets In agreement with RNA-seq data, RT-qPCR showed that aripiprazole increased *Tph1* and *Tph2* expression vs controls (p<0.01 and p<0.05, respectively; Fig. 6a), along with an apparent increase in TPH1 protein levels (Fig. 6b). In addition, the expression of the serotonin receptor *Htr3a* was

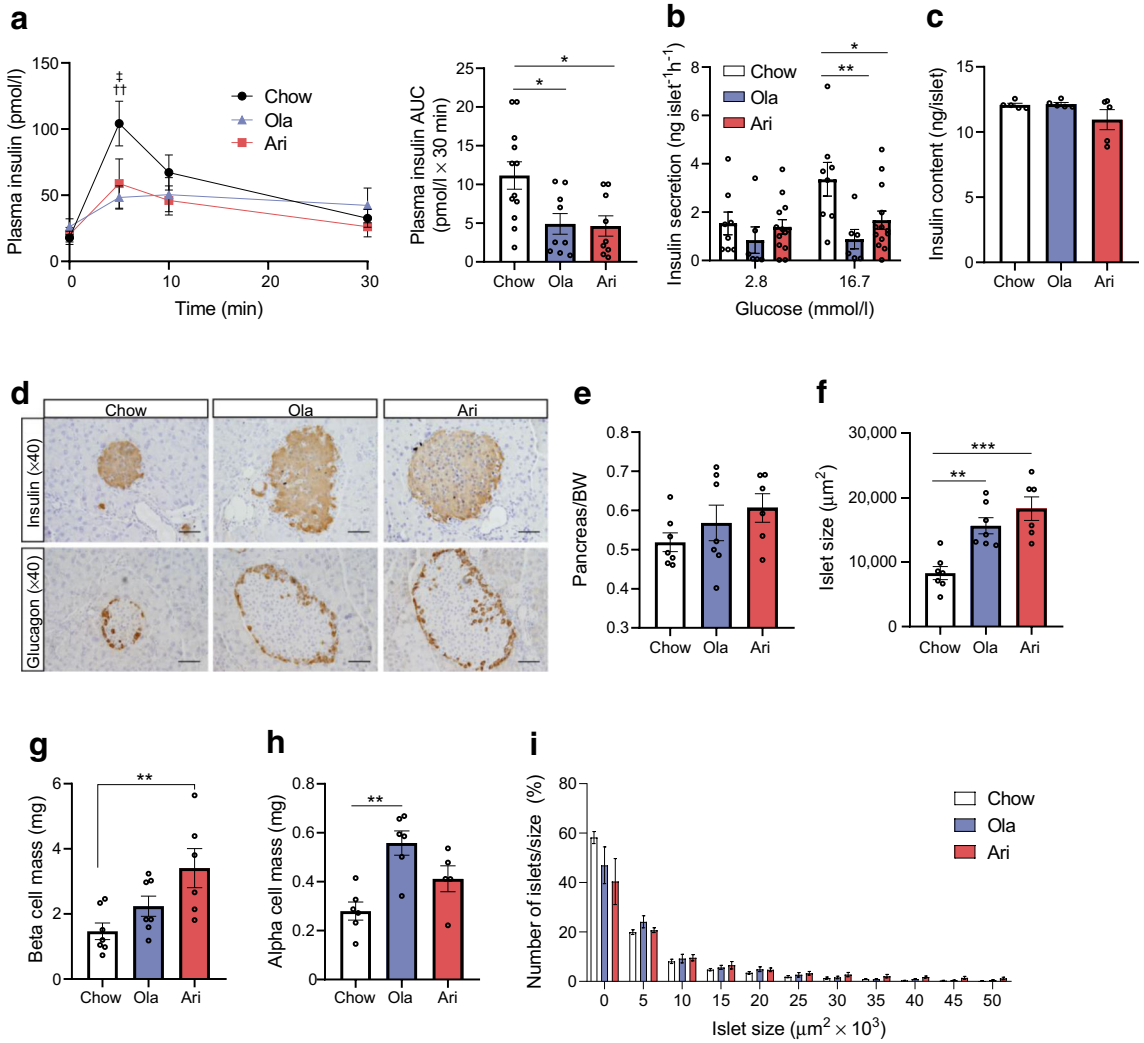

Fig. 2 Effects of olanzapine (ola)- or aripiprazole (ari)-supplemented diet on GSIS and islet morphology in female mice. (**a**) In vivo GSIS and the respective AUC, calculated from 0 to 30 min values, according to the trapezoidal rule (n=9–12 mice/group). (**b**) Ex vivo GSIS, performed using 3–6 technical replicates for each condition and mouse (n=6–13 mice/group). Insulin secretion was corrected for islet number. (**c**) Insulin content in islets. Twenty islets per mouse were lysed and the insulin content was normalised to islet number (n=5 mice/condition). (**d**) Representative images of pancreatic islets stained with insulin and glucagon; scale bars, 50 μm; magnification ×40. (**e**) Pancreas weight normalised to body weight (BW). (**f**) Islet size (μm^2). (**g**) Beta cell mass (mg) (n=7 control, n=7 ola-treated mice, n=6 ari-treated mice) and (**h**) alpha cell mass (mg) (n=6 control, n=6 ola-treated mice, n=5 ari-treated mice). (**i**) Islet size distribution (n=7 control, n=7 ola-treated mice, n=6 ari-treated mice). Between 8 and 12 pancreatic sections per mouse, generated every 80 μm, were analysed. At least 300 islets per mice were counted for determination of islet size. The differences between the distribution of islet size in ola- and ari-treated mouse samples were significant vs the distribution of islet size in samples from mice fed a chow diet (p<0.001, by χ^2 test). All data are presented as mean±SEM. *p<0.05, **p<0.01, ***p<0.001 vs mice fed a chow diet, by one-way ANOVA and Bonferroni post hoc test for the AUC graph in (**a**, right) and in (**c**, **e**, **f**, **g**, **h**) or by two-way ANOVA in (**a**, left, **b**); $^{\dagger\dagger}p$<0.01, ola vs chow; $^{\ddagger}p$<0.05, ari vs chow

reduced in the olanzapine-treated group vs controls (p<0.05; Fig. 6c).

Serotonin has been implicated in beta cell compensation during pregnancy [22, 23]. Ex vivo experiments showed higher serotonin secretion in islets from aripiprazole-treated mice, both with 2.8 mmol/l and 16.7 mmol/l glucose treatment, with findings being significant following exposure to 16.7 mmol/l glucose (p<0.05; Fig. 6d). Immunofluorescence images confirmed higher serotonin levels in islets from mice that received aripiprazole compared with control mice (p<0.01; Fig. 6e,f). In fact, we observed that serotonin levels in islets from aripiprazole-treated mice appeared to be comparable with islets of pregnant mice (Fig. 6e). Overall, our findings indicate that aripiprazole treatment increased serotonin synthesis and secretion in islets.

Aripiprazole increases serotonin generation and induces TPH1 expression in pancreatic islets In light of the in vivo findings showing that aripiprazole treatment increased *Tph1* mRNA (p<0.01) and that there was an apparent increase in

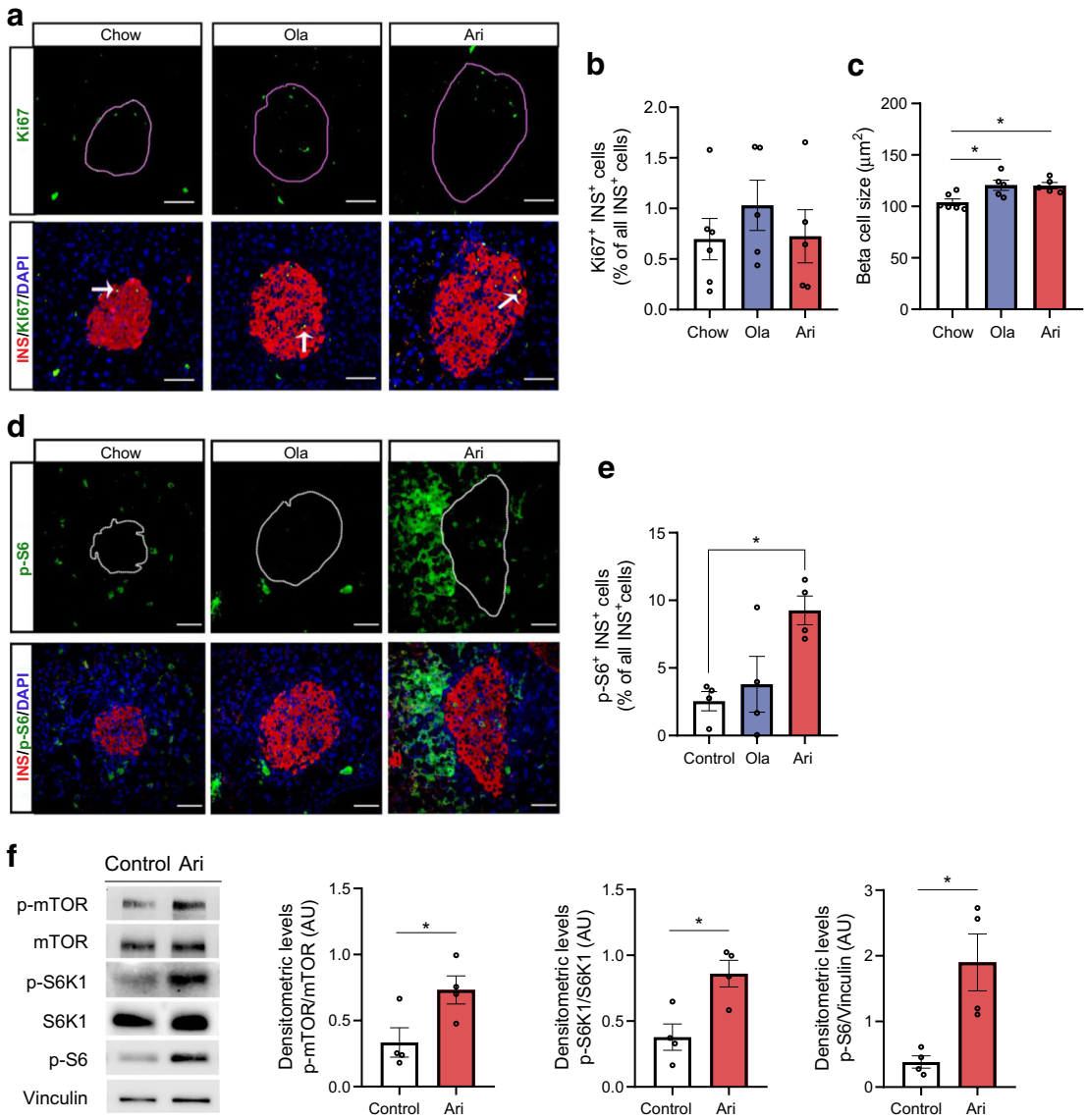

Fig. 3 Analysis of beta cell proliferation and size and phosphorylation of S6 ribosomal protein in islets from female mice after 6 months of treatment with an antipsychotic drug-supplemented diet. (**a**) Confocal images of Ki67 (green) immunofluorescence. Ki67 co-localisation with insulin (INS)$^+$ cells (red) is indicated (white arrows); scale bars, 50 µm; magnification ×40. (**b**) Percentage of Ki67$^+$INS$^+$ cells and (**c**) beta cell size (µm^2). A total of 43.85 ± 4.83 islets were analysed for Ki67 expression and beta cell size (n=5–6 mice/group). (**d**) Confocal microscopy images of islets double immunostained with antibodies against p-S6 (green) and INS (red); scale bars, 50 µm; magnification ×40. (**e**) Percentage of p-S6$^+$INS$^+$ cells. All islets within two pancreatic sections per mouse (n=4 mice/group) were analysed, with each section being generated every 200 µm. A total of 22.83 ± 1.98 islets were quantified for p-S6 staining. (**f**) Islets were incubated with 6 µmol/l aripiprazole (ari) or vehicle (0.01% DMSO [control]) for 16 h and phosphorylation levels of mTOR, S6K1 and S6 were analysed by western blot. Representative blots of mTOR, S6K1 and S6 phosphorylation levels in independent pools of 200–300 islets isolated from n=4–6 mice are shown. Quantification of protein levels is also shown (n=4 independent experiments). Data are presented as mean±SEM. AU, arbitrary units; ola, olanzapine. *p<0.05 vs mice fed a chow diet, analysed by one-way ANOVA test and Bonferroni post hoc test in (**b**, **c**), by Kruskal–Wallis test and Bonferroni post hoc test in (**e**), or unpaired Student's t test in (**f**)

THP1 protein levels, along with increased serotonin secretion (p<0.05) vs controls (Fig. 6a,b,d–f), we studied its direct effects on the serotonergic system in isolated islets. As shown in Fig. 7a,b, treatment with aripiprazole for 24 h appeared to increase serotonin and TPH1 protein levels vs controls.

Finally, we studied whether serotonin mediates the effects of aripiprazole on mTORC1 activity and beta cell function. Our findings suggest that treatment with serotonin (100 µmol/l) for 1 h increased mTORC1 activity, as reflected by apparent increases in mTOR, S6K1 and S6 phosphorylation vs controls (Fig. 7c). Moreover, treatment of islets with serotonin for 24 h inhibited GSIS vs controls (Fig. 7d), as previously reported [24, 25]. Importantly, co-treatment with aripiprazole and the TPH1 inhibitor PCPA prevented the negative effect of

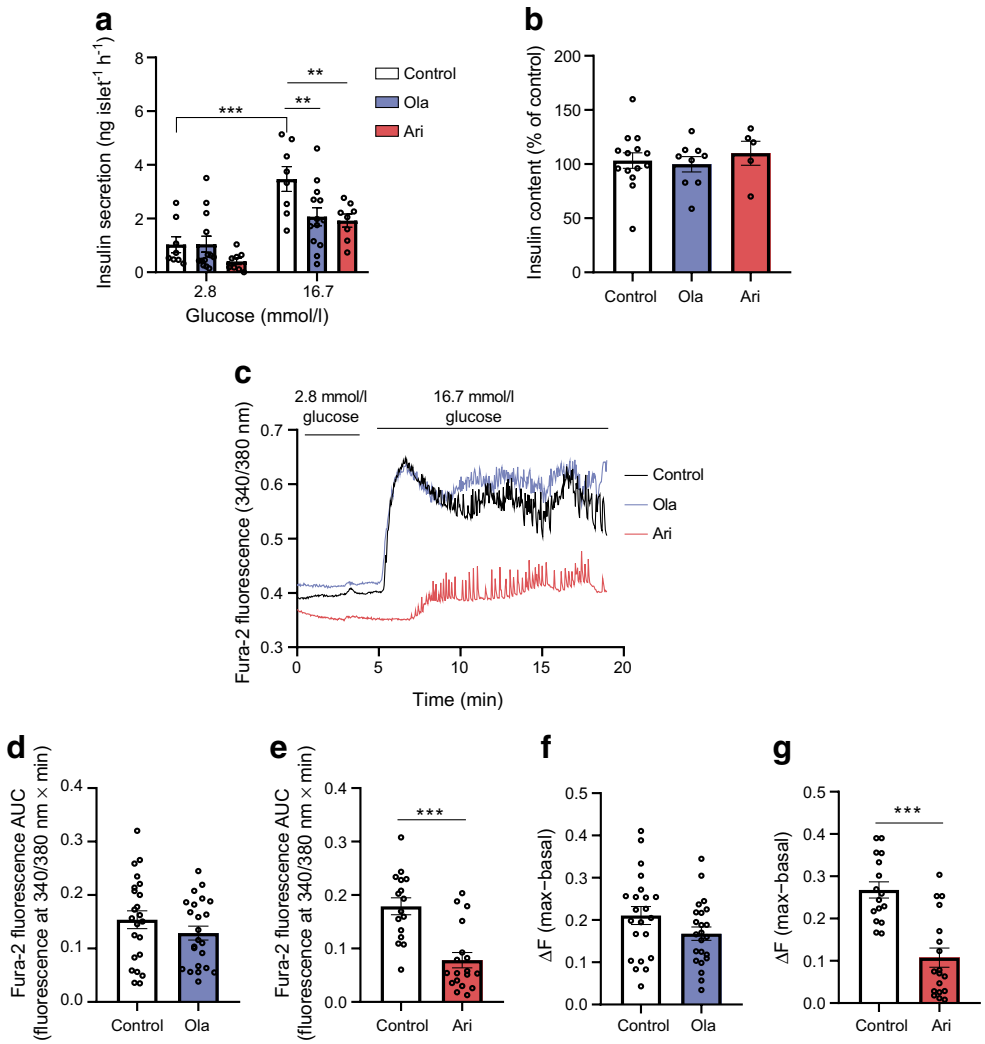

Fig. 4 Effect of ex vivo treatment of pancreatic islets with olanzapine (ola) or aripiprazole (ari) on insulin secretion and Ca^{2+} signalling. (**a**) GSIS analysis performed in islets treated with either ola or ari (6 μmol/l) or vehicle (0.01% DMSO [control]) for 24 h. We performed 3–6 technical replicates for each condition and mouse (n=8–13 mice/group). (**b**) Insulin content in islets. Twenty islets per condition were lysed and the insulin content was measured and normalised to insulin content in control islets. Statistically significant differences were not observed between groups, as determined by one-way ANOVA (n=5–14 mice/group). (**c**) Representative recordings of Fura-2 Ca^{2+} fluorescence in beta cells from islets in response to high glucose concentrations (16.7 mmol/l) under treatment with vehicle (0.01% DMSO [control]), 6 μmol/l ola or 6 μmol/l ari. (**d**, **e**) Quantification of the AUC of Fura-2 Ca^{2+} fluorescence per min in vehicle-treated islets vs islets treated with ola (**d**) or ari (**e**). (**f**, **g**) ΔF (maximum [max] – F_{basal}) in control islets vs islets treated with ola (**f**) or ari (**g**). In (**d**–**g**) a total of 16–25 islets from n=6 mice were used in each condition. Data are presented as mean±SEM. $^{**}p<0.01$, $^{***}p<0.001$ vs control, by two-way ANOVA and Bonferroni post hoc test in (**a**), Student's t test in (**d**, **f**, **g**) or Mann–Whitney U test in (**e**)

aripiprazole on insulin secretion (Fig. 7e). Collectively, we suggest that aripiprazole increases serotonin biosynthesis and secretion in islets and mediates mTORC1 activation and, probably, beta cell hypertrophy, while impairing insulin secretion.

Discussion

This study provides novel findings on the effect of the SGAs olanzapine and aripiprazole in inducing glucose intolerance and reducing insulin secretion. We demonstrate that aripiprazole modulates the serotonergic system in islets, increasing mTOR/S6 phosphorylation, as well as elevating TPH1 expression and serotonin production in beta cells. By contrast, the effects of olanzapine on insulin secretion seem to be independent of the serotonergic system. Since type 2 diabetes develops gradually through life, and chronic medication is needed to tackle schizophrenia, we analysed the metabolic disturbances in female mice treated with these two chemically unrelated SGAs via supplementation in the diet over 6 months. To our knowledge, this is the first preclinical study in rodents to report the metabolic outcomes of long-term administration of olanzapine and aripiprazole that focuses on islet function.

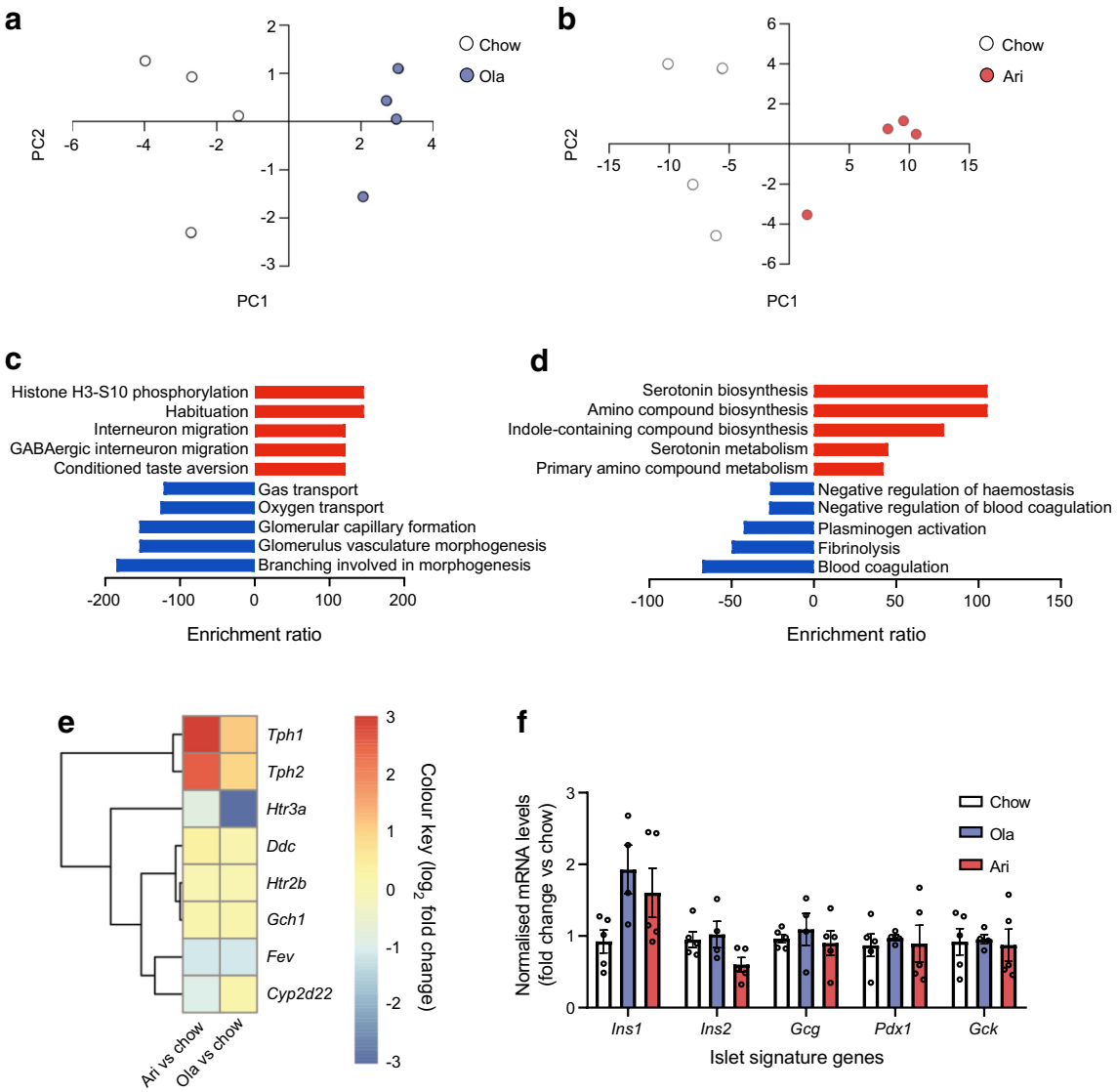

Fig. 5 Transcriptomic analysis in pancreatic islets from female mice fed an olanzapine (ola)- or aripiprazole (ari)-supplemented diet. (**a**, **b**) PCA of samples from mice treated with ola (**a**) or ari (**b**) vs chow-fed mice. Each sample contained a pool of 500 islets from *n*=4 mice (*n*=4 samples/group). (**c**, **d**) ORA of ola-associated (**c**) and ari-associated (**d**) DEGs. (**e**) Heatmap of serotonin biosynthetic processes The $\log_2$ fold change in gene expression in islets treated with ari or ola vs islets from mice fed a chow diet is shown, with downregulated genes shown in blue and upregulated genes shown in red. (**f**) Analysis of common islet-related genes by RT-qPCR. Expression was normalised to the mean C_t values of two housekeeping genes (*Actb* and *Gapdh*). Each sample contained a pool of 500 islets from *n*=4 mice (*n*=4–5 samples/group). Data are presented as mean±SEM. Statistical significance differences were not observed in (**f**), as analysed by the Kruskal–Wallis test, or one-way ANOVA and Bonferroni post hoc test. GABA, γ-aminobutyric acid; PC, principal component

Olanzapine treatment induced weight gain by increasing food intake; this finding is in agreement with previous studies that also demonstrated that this effect was mediated by the 5-HT_{2C} [26] and H_1R receptors in the hypothalamus [27]. Conversely, aripiprazole treatment results in less weight gain and this was not associated with increased food intake, but rather with reduced physical activity and EE during the dark phase, an effect likely contributing to weight gain. Moreover, the effects of olanzapine on EE and physical activity were small, contrary to previous findings [28]. Of clinical relevance, olanzapine-induced weight gain has been reported in patients treated for longer than 12 months, but this has not been the case for aripiprazole [29]. Yet, recent findings point to a mean 6–7% gain in body weight in young people receiving aripiprazole [30]. Remarkably, visceral adiposity was increased in mice treated with either drug, although the effect with aripiprazole treatment was more robust. In studies of olanzapine therapy, increased adiposity has been reported both concomitantly with [31], and also independently from [32] weight gain. Altogether, our results suggest that both olanzapine and aripiprazole increase adiposity, irrespective of the degree of weight gain. Of note, as schizophrenia, per

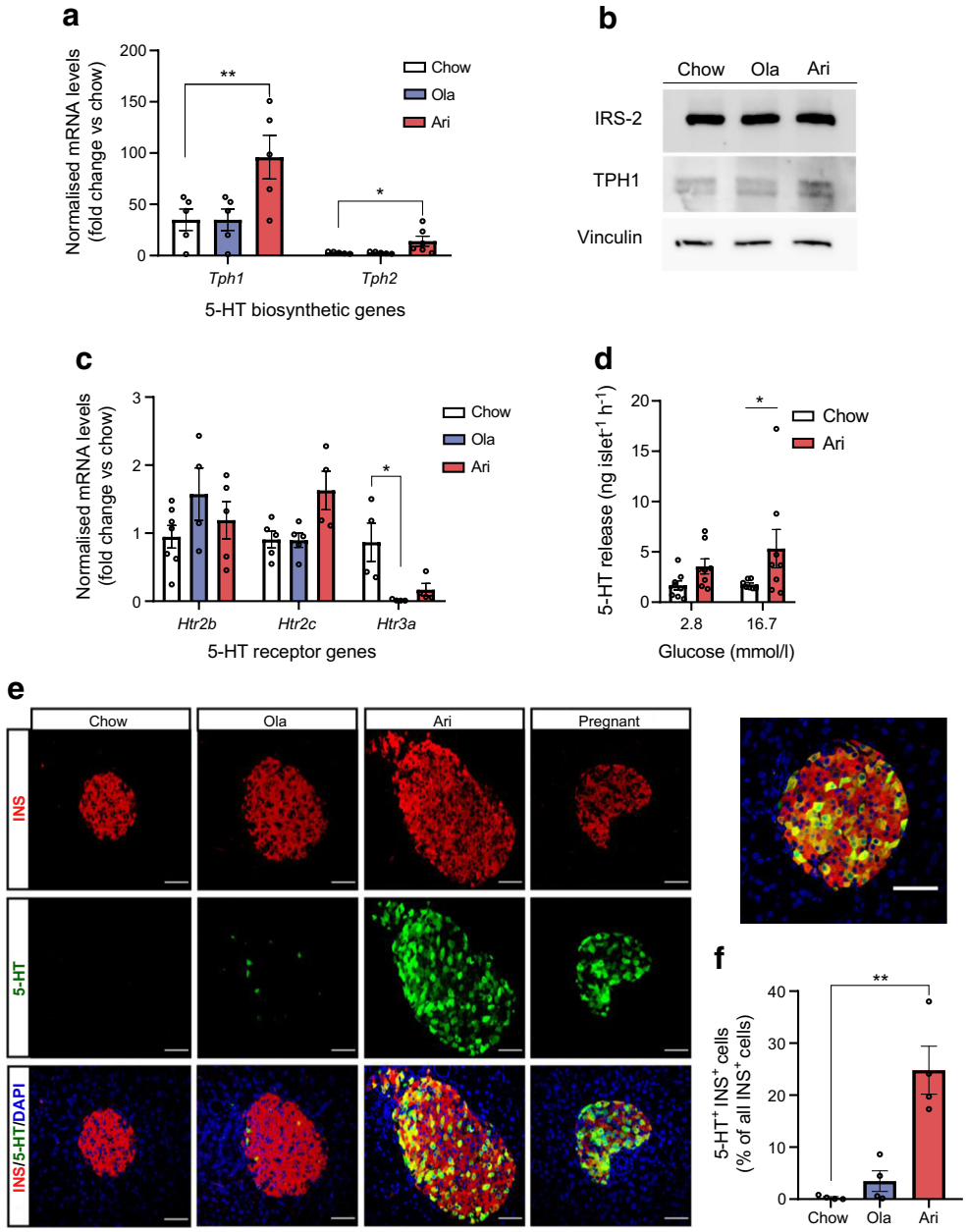

Fig. 6 Effect of olanzapine (ola) or aripiprazole (ari) treatment on the expression of serotonergic system-related genes and serotonin (5-HT) levels in islets from female mice after 6 months of treatment with antipsychotic drug-supplemented diets. (**a**) RT-qPCR analysis of 5-HT-related biosynthetic gene expression normalised against median C_t values of two housekeeping genes (*Actb* and *Gapdh*). Each sample contained a pool of 500 islets from *n*=4 mice (*Tph1* analysis: *n*=5 samples/group; *Tph2* analysis: *n*=5 samples for control, *n*=5 samples for ola-treated mice and *n*=6 samples for ari-treated mice). (**b**) TPH1 protein expression by western blot. Each sample contained a pool of 500 islets from *n*=3 mice/group (control mice, or mice treated with ola or ari for 6 months). Vinculin and IRS-2 were used as loading controls. (**c**) mRNA expression of 5-HT receptor genes, analysed by RT-qPCR. Each sample contained a pool of 500 islets from *n*=4 mice (*n*=4–7 samples/group). (**d**) 5-HT release was measured by ELISA in the culture medium of islets previously challenged with 16.7 mmol/l glucose (*n*=8 mice/group). (**e**) Representative images of pancreatic islets expressing insulin (INS; red) and 5-HT (green), captured with confocal microscopy; scale bars, 50 μm; magnification ×40. A higher magnification of an islet co-expressing INS and 5-HT after ari treatment is also shown; scale bar, 50 μm; magnification ×40. (**f**) Percentage of $5\text{-HT}^+\text{INS}^+$ cells. All islets within two pancreatic sections per mouse (*n*=4 mice/group) were analysed, with each section being generated every 200 μm. A total of 26.25 ± 3.28 islets were quantified for 5-HT expression. Data are presented as mean±SEM. **p*<0.05, ***p*<0.01 vs mice fed a chow diet, analysed by one-way ANOVA and Bonferroni post hoc test in (**a**, **c**), two-way ANOVA and Bonferroni post hoc test in (**d**) or Kruskal–Wallis test (**f**)

se, concurs with metabolic derangements [33], the metabolic side effects of SGAs are likely to be more severe in the context of this disease. Also, although female patients are more susceptible to changes in glucose metabolism following

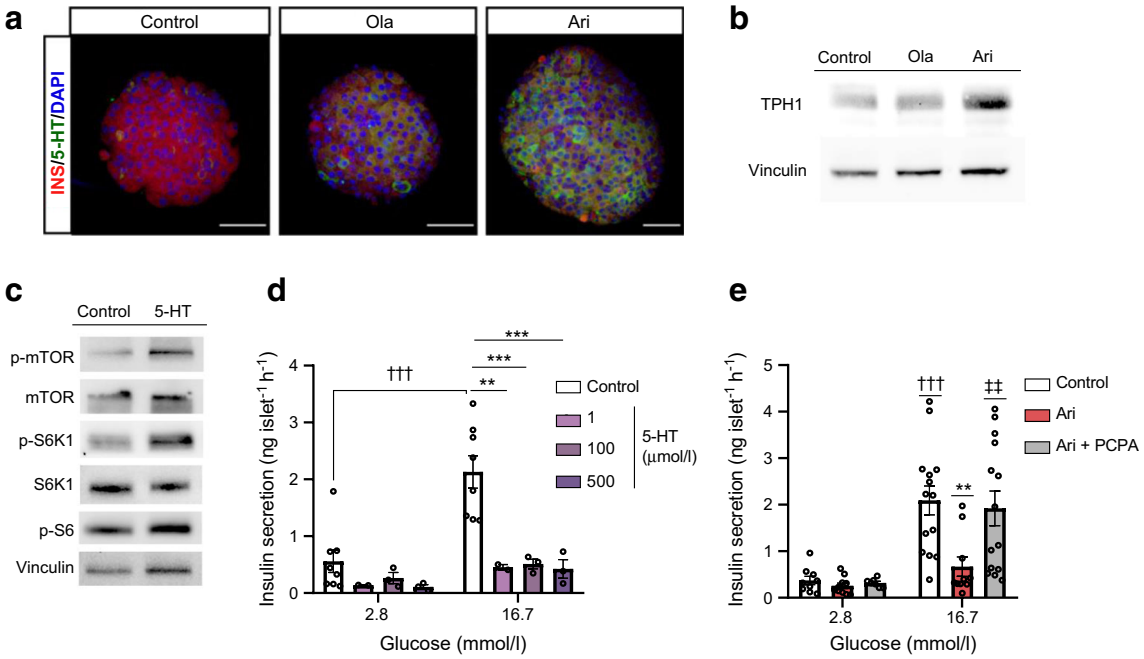

Fig. 7 Effect of ex vivo treatment of pancreatic islets with olanzapine (ola) or aripiprazole (ari) on serotonin (5-HT) expression. (**a**) In toto islets were immunostained for insulin (INS; red) and 5-HT (green) after ex vivo treatment with ola or ari for 24 h. Images were captured by confocal microscopy; scale bar, 50 μm; magnification ×40. (**b**) TPH1 protein expression analysed by western blot (using vinculin as a loading control) after ex vivo treatment of islets with ola or ari for 24 h. Each sample (control [untreated islets], or islets treated ex vivo with ola or ari) contained a pool of 500 islets from n=12 mice. (**c**) Islets were incubated with 100 μmol/l 5-HT for 1 h and phosphorylation levels of mTOR, S6K1 and S6 were analysed by western blot. Each sample (control [untreated islets] or islets treated ex vivo with 5-HT) contained a pool of 200 islets from n=6 mice. (**d**) Ex vivo GSIS in pancreatic islets after 24 h of treatment with 5-HT. We performed 3–6 technical replicates for each condition and mouse (n=2–3 mice for serotonin, n=8 mice for control). (**e**) Ex vivo GSIS in pancreatic islets after 24 h of treatment of ari (6 μmol/l) and PCPA (10 μmol/l). Experiments were performed with at least 3–6 technical replicates per condition in pools of islets from n=10–14 mice (n=3 independent experiments). $^{**}p<0.01$, $^{***}p<0.001$ vs control islets stimulated with 16.7 mmol/l glucose; $^{\dagger\dagger\dagger}p<0.001$ vs control islets stimulated with 2.8 mmol/l glucose; $^{\ddagger\ddagger}p<0.01$ vs islets treated with ari and stimulated with 16.7 mmol/l glucose; analysed by two-way ANOVA and Bonferroni post hoc test

SGA exposure [6], the current study is a single-sex study, a limitation that needs to be considered for its translatability.

Female mice treated with olanzapine or aripiprazole developed glucose intolerance that was associated with insulin resistance in aripiprazole-treated mice. However, we cannot exclude that longer treatments or more sensitive assays to assess insulin sensitivity, such as the euglycaemic–hyperinsulinaemic clamp, would reveal greater effects on blood glucose levels and insulin sensitivity. A step further, this is the first study to unravel a unique effect of aripiprazole in interfering with glucose-regulated Ca^{2+} signalling, whereas olanzapine likely inhibits insulin secretion through a mechanism distal to Ca^{2+} entry into the beta cell. Of interest, while the GSIS test addresses insulin secretion exclusively, we cannot exclude alterations in hepatic insulin clearance or the beta cell insulin-degrading enzyme, both of which impair insulin secretion [34].

Notably, mice treated with the SGAs had larger islets, particularly the aripiprazole-treated group, in which beta cell mass was twofold higher than that of the control group. In obesity and pregnancy, beta cell expansion is associated with enhanced insulin secretion, which compensates for insulin resistance. On the contrary, aripiprazole impairs insulin secretion despite beta cell expansion, indicating that increased beta cell mass, per se, is not sufficient to overcome beta cell dysfunction. The apparent paradoxical effects on mass and function were more prominent in aripiprazole-treated mice in which doubling of beta cell mass was associated with blunted insulin response.

Treatment with SGAs did not affect beta cell proliferation, which remained low, as previously reported in middle-aged mice [20]. However, a compensatory proliferative response might be expected at an earlier stage of the treatment. On the contrary, we found increased beta cell size in islets from both groups of SGA-treated mice, as compared with controls, which might explain the islet size expansion observed at the end of the treatment. Activation of mTORC1 signalling, which increases islet hypertrophy, has been suggested to be involved in the compensatory beta cell expansion during insulin resistance [35]. Our results showed islet hypertrophy in

aripiprazole-treated mice together with increased p-S6 staining in beta cells, an effect reinforced by increased phosphorylation of mTOR and its downstream targets S6K1 and S6 in islets treated ex vivo with this SGA. Thus, the increased islet size and beta cell mass by aripiprazole might be mediated via mTORC1/S6. By contrast, S6 phosphorylation was not increased by olanzapine. At the molecular level, the differential ability of each drug to induce mTORC1/S6 activity or, alternatively, other mechanisms, such as the Hippo pathway [36], might also be implicated in the islet hypertrophy observed with olanzapine. Also, lower mTORC1 activation in olanzapine-treated mice could be due to a more subtle (non-significant) increase in insulin intolerance. It is noteworthy that we found greater (although not significant) differences in insulin granule maturation in olanzapine-treated mice vs the control group, manifested by a decrease and increase in mature and empty granules, respectively (both p=0.09), which deserves further investigation. Additionally, olanzapine-treated mice had higher alpha cell mass, pointing to potential pancreatic alterations beyond beta cells.

The complexity of the dopaminergic and serotonergic systems in pancreatic islets, which regulate insulin secretion [10, 37], together with the broad spectrum of dopamine/serotonin receptors targeted by SGAs, makes it difficult to determine whether a specific receptor mediates the effects of a particular SGA or if the final outcome results from signalling pathways activated by multiple receptors. Transcriptomic analysis of pancreatic islets did not show changes in genes related to dopamine signalling, but revealed changes in genes regulating serotonin synthesis. Aripiprazole upregulated *Tph1* and *Tph2* genes, and the induction of *Tph1* mRNA and TPH1 protein levels (the rate-limiting isoform for serotonin biosynthesis) was associated with increased serotonin content and release in islets from aripiprazole-treated mice. These results were supported by: (1) the ex vivo treatment of islets with aripiprazole, which similarly resulted in increased TPH1 expression; (2) the decrease in insulin secretion in islets treated with serotonin that, like aripiprazole, activated mTORC1/S6 signalling; (3) and the recovery of GSIS in islets treated ex vivo with aripiprazole together with a TPH1 inhibitor, pointing to serotonin-mediated inhibition of insulin secretion by this SGA. Our findings are in agreement with a recent study showing that Sirtuin 3 deficiency in beta cells increased *Tph1* expression, along with impairment of GSIS in obese mice [38].

Transcriptomic analysis also showed that olanzapine downregulated the expression of *Htr3a*, which encodes a serotonin receptor, in islets, potentially playing a role in the impairment of insulin secretion by this SGA, as previously reported [39, 40]. Notably, changes in serotonin receptor expression were found in *db/db* mice, which exhibited increased expression of *Htr2c* [41]. So far, the role of serotonin signalling in beta cell expansion has been described only in pregnancy [22, 23] and the perinatal period [42]. Recent studies suggest that increased serotonin production could affect whole-body glucose homeostasis and adiposity [43]. In the context of tumour growth, serotonin increases mTORC1 activity in hepatocellular carcinoma [44], reinforcing a possible link between serotonin and mTORC1/S6 signalling. Because serotonin is also a strong paracrine regulator of alpha cell activity [45], additional effects of aripiprazole on alpha cells functionality cannot be ruled out.

In summary, we have identified alterations in islet plasticity and insulin secretion in female mice treated with the SGAs olanzapine and aripiprazole, with important translational implications. In the case of aripiprazole, in which the serotonergic system was activated, specific TPH1 inhibitors that do not cross the blood–brain barrier could be used to prevent intra-islet and peripheral serotonin dysregulation without affecting serotonin levels in the brain [46].

Supplementary Information The online version contains peer-reviewed but unedited supplementary material available at https://doi.org/10.1007/s00125-021-05630-0.

Acknowledgements The authors would like to thank M. Belinchón (IIBm, CSIC, Madrid, Spain) for the technical assistance with confocal microscopy. We also acknowledge all members of ÁMV's laboratory for helpful discussions. Some of the data were presented as an abstract at the 55th EASD Annual Meeting in 2019.

Data availability Data presented in this manuscript are available upon request from the corresponding author.

Funding Open Access funding provided thanks to the CRUE-CSIC agreement with Springer Nature. This work was funded by H2020 Marie Sklodowska-Curie ITN-TREATMENT (Grant Agreement 721236, European Commission). We also acknowledge grants RTI2018-094052-B-100/ AEI/10.13039/501100011033 (Ministerio de Ciencia e Innovación y Fondo Europeo de Desarrollo Regional [FEDER]) and S2017/BMD-3684 (Comunidad de Madrid, Spain), and grants from Fundación Ramón Areces (Spain) and CIBERDEM (ISCIII, Spain).

Authors' relationships and activities The authors declare that there are no relationships or activities that might bias, or be perceived to bias, their work.

Contribution statement The study was designed by DG and ÁMV. Islet isolation, data acquisition, and analysis and interpretation of batch incubations were performed by DG. Immunohistochemistry, immunofluorescence and TEM analyses were performed by DG and PV. Gene expression analysis was performed by MRR, JCC and DG. Ca^{2+} experiments and analysis were performed by DG, ET and IQ. MM, ABH, MV and BT assisted with islets studies and data interpretation. GTTs, in vivo GSIS and ITTs were performed and analysed by DG, ÁMV and VF. Concentrations of antipsychotic drugs in plasma were determined and analysed by DK, PZ and FAS. DG, PV and ÁMV wrote the first draft of the manuscript. MRR, ET, MM, VF, ABH, DK, PZ, JCC, FAS, MV, IQ and BT critically revised the manuscript for important intellectual content. GL co-designed the study, collected and interpreted the data and critically revised the manuscript. All authors gave final approval of

the manuscript and gave consent to its publication. ÁMV coordinated the study and is the guarantor of this work.

References

1. Liu MZ, He HY, Luo JQ et al (2018) Drug-induced hyperglycaemia and diabetes: pharmacogenomics perspectives. Arch Pharm Res 41(7):725–736. https://doi.org/10.1007/s12272-018-1039-x
2. Vancampfort D, Wampers M, Mitchell AJ et al (2013) A meta-analysis of cardio-metabolic abnormalities in drug naïve, first-episode and multi-episode patients with schizophrenia versus general population controls. World Psychiatry 12(3):240–250. https://doi.org/10.1002/wps.20069
3. Vancampfort D, Correll CU, Galling B et al (2016) Diabetes mellitus in people with schizophrenia, bipolar disorder and major depressive disorder: a systematic review and large scale meta-analysis. World Psychiatry 15(2):166–174. https://doi.org/10.1002/wps.20309
4. Nielsen J, Skadhede S, Correll CU (2010) Antipsychotics associated with the development of type 2 diabetes in antipsychotic-naive schizophrenia patients. Neuropsychopharmacology 35(9):1997–2004. https://doi.org/10.1038/npp.2010.78
5. Rajkumar AP, Horsdal HT, Wimberley T et al (2017) Endogenous and Antipsychotic-Related Risks for Diabetes Mellitus in Young People With Schizophrenia: A Danish Population-Based Cohort Study. Am J Psychiatry 174(7):686–694. https://doi.org/10.1176/appi.ajp.2016.16040442
6. Castellani LN, Costa-Dookhan KA, McIntyre WB et al (2019) Preclinical and Clinical Sex Differences in Antipsychotic-Induced Metabolic Disturbances: A Narrative Review of Adiposity and Glucose Metabolism. J Psychiatr Brain Sci 4(4):e190013. https://doi.org/10.20900/jpbs.20190013
7. Mauri MC, Paletta S, Di Pace C et al (2018) Clinical Pharmacokinetics of Atypical Antipsychotics: An Update. Clin Pharmacokinet 57(12):1493–1528. https://doi.org/10.1007/s40262-018-0664-3
8. Grajales D, Ferreira V, Valverde AM (2019) Second-Generation Antipsychotics and Dysregulation of Glucose Metabolism: Beyond Weight Gain. Cells 8(11):1336. https://doi.org/10.3390/cells8111336
9. Melkersson K, Khan A, Hilding A, Hulting AL (2001) Different effects of antipsychotic drugs on insulin release in vitro. Eur Neuropsychopharmacol 11(5):327–332. https://doi.org/10.1016/S0924-977X(01)00108-0
10. Cataldo Bascuñan LR, Lyons C, Bennet H, Artner I, Fex M (2019) Serotonergic regulation of insulin secretion. Acta Physiol 225(1):e13101. https://doi.org/10.1111/apha.13101
11. Gonzalez-Rodriguez A, Santamaria B, Mas-Gutierrez JA et al (2015) Resveratrol treatment restores peripheral insulin sensitivity in diabetic mice in a sirt1-independent manner. Mol Nutr Food Res 59(8):1431–1442. https://doi.org/10.1002/mnfr.201400933
12. Koller D, Zubiaur P, Saiz-Rodríguez M, Abad-Santos F, Wojnicz A (2019) Simultaneous determination of six antipsychotics, two of their metabolites and caffeine in human plasma by LC-MS/MS using a phospholipid-removal microelution-solid phase extraction method for sample preparation. Talanta 198:159–168. https://doi.org/10.1016/j.talanta.2019.01.112
13. Ribas-Aulinas F, Ribo S, Parra-Vargas M et al (2021) Neonatal overfeeding during lactation rapidly and permanently misaligns the hepatic circadian rhythm and programmes adult NAFLD. Mol Metab 45:101162. https://doi.org/10.1016/j.molmet.2021.101162
14. Carter JD, Dula SB, Corbin KL, Wu R, Nunemaker CS (2009) A Practical Guide to Rodent Islet Isolation and Assessment. Biol Proced Online 11(1):3. https://doi.org/10.1007/s12575-009-9021-0
15. Téllez N, Montanya E (2020) Determining Beta Cell Mass, Apoptosis, Proliferation, and Individual Beta Cell Size in Pancreatic Sections. Methods Mol Biol 2128:313–337. https://doi.org/10.1007/978-1-0716-0385-7_21
16. Bray NL, Pimentel H, Melsted P, Pachter L (2016) Near-optimal probabilistic RNA-seq quantification. Nat Biotechnol 34(5):525–527. https://doi.org/10.1038/nbt.3519
17. Love MI, Huber W, Anders S (2014) Moderated estimation of fold change and dispersion for RNA-seq data with DESeq2. Genome Biol 15(12):550. https://doi.org/10.1186/s13059-014-0550-8
18. Liao Y, Wang J, Jaehnig EJ, Shi Z, Zhang B (2019) WebGestalt 2019: gene set analysis toolkit with revamped UIs and APIs. Nucleic Acids Res 47(W1):W199–W205. https://doi.org/10.1093/nar/gkz401
19. Liu X, Feng X, Deng C, Liu L, Zeng Y, Hu C-H (2020) Brown adipose tissue activity is modulated in olanzapine-treated young rats by simvastatin. BMC Pharmacol Toxicol 21(1):48. https://doi.org/10.1186/s40360-020-00427-0
20. Rankin MM, Kushner JA (2009) Adaptive beta-cell proliferation is severely restricted with advanced age. Diabetes 58(6):1365–1372. https://doi.org/10.2337/db08-1198
21. Riahi Y, Israeli T (2018) Inhibition of mTORC1 by ER stress impairs neonatal β-cell expansion and predisposes to diabetes in the Akita mouse. eLife 7:e38472. https://doi.org/10.7554/eLife.38472
22. Kim H, Toyofuku Y, Lynn FC et al (2010) Serotonin regulates pancreatic beta cell mass during pregnancy. Nat Med 16(7):804. https://doi.org/10.1038/nm.2173
23. Schraenen A, Lemaire K, de Faudeur G et al (2010) Placental lactogens induce serotonin biosynthesis in a subset of mouse beta cells during pregnancy. Diabetologia 53(12):2589–2599. https://doi.org/10.1007/s00125-010-1913-7
24. Cataldo LR, Mizgier ML, Bravo Sagua R et al (2017) Prolonged activation of the Htr2b serotonin receptor impairs glucose stimulated insulin secretion and mitochondrial function in MIN6 cells. PLoS One 12(1):e0170213. https://doi.org/10.1371/journal.pone.0170213
25. Zawalich WS, Tesz GJ, Zawalich KC (2004) Effects of prior 5-hydroxytryptamine exposure on rat islet insulin secretory and phospholipase C responses. Endocrine 23(1):11–16. https://doi.org/10.1385/ENDO:23:1:11
26. Wang Y, Wang D, Chen Y, Fang X, Yu L, Zhang C (2020) A Novel Synthetic Interfering Peptide Tat-3L4F Attenuates Olanzapine-Induced Weight Gain Through Disrupting Crosstalk Between Serotonin Receptor 2C and Protein Phosphatase and Tensin Homolog in Rats. Int J Neuropsychopharmacol. https://doi.org/10.1093/ijnp/pyaa001
27. Chen X, Yu Y, Zheng P et al (2020) Olanzapine increases AMPK-NPY orexigenic signaling by disrupting H1R-GHSR1a interaction

in the hypothalamic neurons of mice. Psychoneuroendocrinology 114:104594. https://doi.org/10.1016/j.psyneuen.2020.104594
28. Lord CC, Wyler SC, Wan R et al (2017) The atypical antipsychotic olanzapine causes weight gain by targeting serotonin receptor 2C. J Clin Invest 127(9):3402–3406. https://doi.org/10.1172/jci93362
29. Pillinger T, McCutcheon RA, Vano L et al (2020) Comparative effects of 18 antipsychotics on metabolic function in patients with schizophrenia, predictors of metabolic dysregulation, and association with psychopathology: a systematic review and network meta-analysis. Lancet Psychiatry 7(1):64–77. https://doi.org/10.1016/s2215-0366(19)30416-x
30. Shymko G, Grace T, Jolly N et al (2021) Weight gain and metabolic screening in young people with early psychosis on long acting injectable antipsychotic medication (aripiprazole vs paliperidone). Early Interve Psychiatry 15(4):787–793. https://doi.org/10.1111/eip.13013
31. Horska K, Ruda-Kucerova J, Babinska Z et al (2016) Olanzapine-depot administration induces time-dependent changes in adipose tissue endocrine function in rats. Psychoneuroendocrinology 73:177–185. https://doi.org/10.1016/j.psyneuen.2016.07.218
32. Minet-Ringuet J, Even PC, Valet P et al (2007) Alterations of lipid metabolism and gene expression in rat adipocytes during chronic olanzapine treatment. Mol Psychiatry 12(6):562–571. https://doi.org/10.1038/sj.mp.4001948
33. Pillinger T, Beck K, Gobjila C, Donocik JG, Jauhar S, Howes OD (2017) Impaired Glucose Homeostasis in First-Episode Schizophrenia: A Systematic Review and Meta-analysis. JAMA Psychiatry 74(3):261–269. https://doi.org/10.1001/jamapsychiatry.2016.3803
34. Fernández-Díaz CM, Merino B, López-Acosta JF et al (2019) Pancreatic β-cell-specific deletion of insulin-degrading enzyme leads to dysregulated insulin secretion and β-cell functional immaturity. Am J Phys Endocrinol Metab 317(5):E805–e819. https://doi.org/10.1152/ajpendo.00040.2019
35. Fraenkel M, Ketzinel-Gilad M, Ariav Y et al (2008) mTOR inhibition by rapamycin prevents beta-cell adaptation to hyperglycemia and exacerbates the metabolic state in type 2 diabetes. Diabetes 57(4):945–957. https://doi.org/10.2337/db07-0922
36. Ardestani A, Maedler K (2018) The Hippo Signaling Pathway in Pancreatic β-Cells: Functions and Regulations. Endocr Rev 39(1):21–35. https://doi.org/10.1210/er.2017-00167
37. Farino ZJ, Morgenstern TJ, Maffei A et al (2019) New roles for dopamine D2 and D3 receptors in pancreatic beta cell insulin secretion. Mol Psychiatry 25:2070–2085. https://doi.org/10.1038/s41380-018-0344-6
38. Ming X, Chung ACK, Mao D et al (2021) Pancreatic Sirtuin 3 Deficiency Promotes Hepatic Steatosis by Enhancing 5-Hydroxytryptamine Synthesis in Mice With Diet-Induced. Obesity 70(1):119–131. https://doi.org/10.2337/db20-0339
39. Ohara-Imaizumi M, Kim H, Yoshida M et al (2013) Serotonin regulates glucose-stimulated insulin secretion from pancreatic β cells during pregnancy. Proc Natl Acad Sci 110(48):19420–19425
40. Kim K, Oh C-M, Ohara-Imaizumi M et al (2015) Functional role of serotonin in insulin secretion in a diet-induced insulin-resistant state. Endocrinology 156(2):444–452. https://doi.org/10.1210/en.2014-1687
41. Zhang Q, Zhu Y, Zhou W, Gao L, Yuan L, Han X (2013) Serotonin receptor 2C and insulin secretion. PLoS One 8(1):e54250. https://doi.org/10.1371/journal.pone.0054250
42. Moon JH, Kim YG, Kim K et al (2020) Serotonin Regulates Adult β-Cell Mass by Stimulating Perinatal β-Cell Proliferation. Diabetes 69(2):205–214. https://doi.org/10.2337/db19-0546
43. Choi W, Moon JH, Kim H (2020) Serotonergic regulation of energy metabolism in peripheral tissues. J Endocrinol 245(1):R1–r10. https://doi.org/10.1530/joe-19-0546
44. Soll C, Jang JH, Riener MO et al (2010) Serotonin promotes tumor growth in human hepatocellular cancer. Hepatology 51(4):1244–1254. https://doi.org/10.1002/hep.23441
45. Almaça J, Molina J, Menegaz D et al (2016) Human Beta Cells Produce and Release Serotonin to Inhibit Glucagon Secretion from Alpha Cells. Cell Rep 17(12):3281–3291. https://doi.org/10.1016/j.celrep.2016.11.072
46. Betari N, Sahlholm K, Ishizuka Y, Teigen K, Haavik J (2020) Discovery and biological characterization of a novel scaffold for potent inhibitors of peripheral serotonin synthesis. Future Med Chem 12(16):1461–1474. https://doi.org/10.4155/fmc-2020-0127